UNIVERSITE DE LIEGE
FACULTE DE MEDECINE VETERINAIRE
DEPARTEMENT DES MALADIES INFECTIEUSES ET PARASITAIRES
IMMUNOLOGIE - VACCINOLOGIE

Etude de la pathogénie du *Cyprinid herpesvirus 2* chez son hôte naturel et dans un modèle de laboratoire

Illumination of *Cyprinid herpesvirus 2* pathogenesis in both its natural host and a laboratory model

Bo He

THESE PRESENTEE EN VUE DE L'OBTENTION DU GRADE DE DOCTEUR EN SCIENCES VETERINAIRES

ANNEE ACADEMIQUE 2024-2025

欲穷千里目，更上一层楼。

——　王之涣

Desiring to fathom a thousand miles, ascend another floor for a grander view.

——　Wang Zhihuan

Acknowledgements

Liège, 02 July 2024

Time seems to have slipped through my fingers like a fleeting moment. Six years ago, I embarked on a journey from Beijing to Liège, carrying both aspirations and apprehensions about the world of science and the uncertainties that lay ahead. From the moment I set foot on this unfamiliar land, a sense of caution accompanied me. It was a realm filled with countless unknowns and challenges. Yet, as I navigated this new world, I discovered warmth in unexpected places-within the soil of this land, and the embrace of this city. Reflecting on these moments never fails to stir a profound warmth within my heart.

The person I am most profoundly grateful for in my six-year journey of study is my supervisor, Alain F C Vanderplasschen. Undoubtedly, he is an exceptional scientist in the fields of virology and vaccinology. As I came to know him more intimately, I discovered that he is not only an outstanding scientist but also a guiding light in life. Always emanating warmth, tolerance, and wisdom, he has been more than a supervisor; he's been a life mentor. I am deeply thankful for the invaluable guidance and direction I received from him. His words have been a constant wellspring of inspiration and motivation. Phrases like 'Never give up,' 'We will win,' and 'Enjoy science' are etched in my memory. Much like the Star of Bethlehem atop a Christmas tree, he has consistently illuminated my path forward.

I extend my heartfelt thanks to my co-supervisor, Owen Donohoe, who has not only been a colleague but also a cherished 'bro' throughout my six-year doctoral journey. His unwavering support has been instrumental in every aspect of my academic endeavors—from project design and data analysis to paper writing and results reporting. Undoubtedly, he stands as the anchor of our research group, providing invaluable guidance and structure. Beyond his professional contributions, Owen approaches both scientific research and life with an infectious optimism, always ready to lend a helping hand to others. His remarkable qualities serve as a beacon for me, shaping him into a role model from whom I continue to learn.

I believe that teamwork forms the bedrock of successful scientific research. My heartfelt appreciation extends to every member of our collaborative team, including Yuan Gao, Arun Sridhar, Haiyan Zhang, Natacha Delrez, Yunlong Hu, Noah Bernard, Cindy Streiff, Maxime Boutier, Sophie Fourny, Sébastien Pirotte, Lisa Conti, Laurie Conti, Mamadou Diallo, and Elizabeth Goya-Jorge. Your collective contributions have been invaluable, creating a wonderful and supportive atmosphere. Working alongside each of you has been an honor, and I am deeply grateful for the unity and camaraderie that defines our team.

In my journey, the unwavering support from our secretaries and technicians has been indispensable. I extend my sincere thanks to Christina Espert Sanchez, Loréne Dams, Caroline Deketelaere,

Aurélie Vanderlinden, Justine Javaux, Celine D'Alessandro, Alice Lucas, Stéphane Hinant, and Rémy Sandor for their dedicated assistance-a crucial prerequisite for the progress of our team. My appreciation also extends to the cell imaging team and the zebrafish team at GIGA for their invaluable support. Together, your collective efforts have played a vital role in our achievements, and for each contribution, I am truly grateful. Special thanks also go to Laurent Gillet, Benjamin Dewals, and Bénédicte Machiels, along with their dedicated teams, for their seamless collaboration.

Financial support has been paramount on this journey, and I extend my heartfelt gratitude to the China Scholarship Council (CSC) and the University of Liège for providing the doctoral scholarship that turned my dream of studying abroad into a reality. Thank you, Motherland, for enabling this opportunity!

I am immensely grateful to my parents; their unwavering encouragement and support have given me the courage to face the unknown. I appreciate everything they have done for me. A special thanks goes to my girlfriend, Yixin, who has been a constant presence when I needed her most. Together, we've shared both pain and joy, standing firmly by each other's side, bringing the comforting warmth of love to every moment. I am because you are.

Embarking on a Ph.D. journey is a profound practice in life, a continuous evolution. In conclusion, I want to express that the most deserving recipient of my gratitude is myself!

Abbreviations

aa	Amino acid
Abb	Abbreviation
ABRA	Actin-binding Rho-activating protein
AciHV-1	Acipenserid herpesvirus 1
AciHV-2	Acipenserid herpesvirus 2
AER	Apical ectodermal ridge
AlHV-1	Alcelaphine herpesvirus 1
AngHV-1	Anguillid herpesvirus 1
Anguilla anguilla	European eel
Anguilla japonica	Japanese eel
Anguilla rostrata	American eel
ANOVA	Analysis of variance
APS	Astragalus polysaccharide
Ar	Anal fin ray
Ara-C	Cytosine-β-arabinofuranoside
Asb	Anterior swim bladder
BBH	Berberine hydrochloride
BH	Benjamini–hochberg
BoHV-1	Bovine herpesvirus 1
BoHV-4	Bovine herpesvirus 4
BP3	Benzophenone-3
BPA	Bisphenol A
BPL	B-propiolactone
C genotype	China genotype
Carassius auratus	Goldfish
Carassius carassius	Crucian carp
Carassius gibelio	Gibel carp (Prussian carp)
CCB	Common carp brain
CHIKV	Chikungunya virus
CHSE-214	Chinook salmon embryos
CHX	Cycloheximide
CMC	Carboxymethylcellulose
CMV	Human cytomegalovirus
copGFP	Copepod GFP
CPE	Cytopathic effect
Cr	Caudal fin ray
CsA	Cyclosporine A
CyHV-1	*Cyprinid herpesvirus 1 (Cyvirus cyprinidallo 1)*
CyHV-2	*Cyprinid herpesvirus 2 (Cyvirus cyprinidallo 2)*
CyHV-3	*Cyprinid herpesvirus 3 (Cyvirus cyprinidallo 3)*
CyHV-3 Luc	CyHV-3 FL BAC revertant ORF136 Luc strain
Cyprinus carpio	Common carp
Cyprinus carpio koi	Koi carp
Danio rerio	Zebrafish
DEGs	Differentially expressed genes
Dex	Dexamethasone
dpf	Days post-fertilization
dpi	Days post-infection
Dr	Dorsal fin ray
dsDNA	Double stranded DNA
dsRB	Double stranded RNA-binding domains
E gene	Early gene

EF-1α	Elongation factor 1 alpha
EGCG	Epigallocatechin-3-gallate
EK-1	Eel kidney 1
EPC	Papule epithelioma carp
F0 generation	Founder embryos
Fcf	Forked caudal fin
FCS	Foetal calf serum
FDR	False discovery rate
FEP	Fluorinated ethylene–propylene
FHM	Fathead minnow
FISH	Fluorescence in situ hybridization
HHV-1	Human herpesvirus 1
HHV-4	Human herpesvirus 4
HHV-6	Human herpesvirus 6
hpi	Hours post-infection
HSV-1	Herpes simplex virus type 1
HVHN	Herpesviral haematopoietic necrosis
HVHND	Herpesviral hematopoietic necrosis disease
Ich	Ichthyophthirius multifiliis
IcHV-1	Ictalurid herpesvirus 1
ICS	Immunochromatography test strip
ICTV	International Comity for Taxonomy of Viruses
IE gene	Immediate early gene
IFNs	Induced interferons
IHC	Immunohistochemistry
IP	Intraperitoneal
IRS	Inverted repeat
ISGs	Interferon stimulated genes
IVIS	*In vivo* imaging system
J genotype	Japan genotype
KO	Knock-out
kpb	Kilobase pair
L gene	Late gene
LAMP	Loop-mediated isothermal amplification
LFD	Lateral flow Device
Luc2	Luciferase 2
mA	Marker A
mAb	Monoclonal antibody
miRNA	MicroRNA
MOI	Multiplicity of infection
MPTP	1-methyl-1,2,3,6-tetrahydropyridine
MS	Marker sizes
MuHV-1	Murine herpesvirus 1
NCBI	National Center for Biotechnology Information
NES	Normalized enrichment score
NF-κB	Nuclear factor-κB
NLR	Leucine-rich-repeat-containing
NNV	Nervous necrosis virus
NPY	Neuropeptide-Y
ORF	Open reading frame
PAA	Phosphonoacetic acid
pAbs	Polyclonal antibodies
PAF	Paraformaldéhyde
PAMPs	Pathogen-associated molecular patterns

Pb	Pelvic fin bud
PBL	Peripheral blood leukocytes
PCR	Polymerase chain reaction
PFU	Plaque forming unit
Photinus pyralis	Firefly
PKR	Protein kinase R
PKZ	Protein kinase containing Z-DNA binding domains
poly I:C	Polyinosinic-polycytidylic acid
Pr	Pelvic fin ray
Prot	Protruding mouth
PRRs	Pathogen recognition receptors
PRV	Pseudorabies virus
Psb	Posterior swim bladder
RFLP	Restriction fragment length polymorphism
RIN	RNA integrity
RLR	RIG-I-like receptor
RM	Repeated measures
ROI	Region of interest
ROS	Reactive oxygen species
RPA	Recombinase polymerase amplification
RPS	Relative percentage survival
RT	Room temperature
RTG-2	Rainbow trout gonad
RT-like	Reverse transcriptase-like
RT-PCR	Reverse transcriptase polymerase chain reaction
RyuF-2	Ryukin goldfish fin cell line
SalHV-1	Salmonid herpesvirus 1
SalHV-2	Salmonid herpesvirus 2
SalHV-3	Salmonid herpesvirus 3
SARS-CoV-2	Severe acute respiratory syndrome coronavirus 2
SD	Standard deviation
sgRNA	Single guide rnas
SGs	Stress granules
SHVV	Snakehead fish vesiculovirus
SL	Standard length
SNVs	Single nucleotide variants
SVCV	Spring viraemia of carp virus
TeHV-3	Testudinid herpesvirus 3
TEM	Transmission electron microscopy
TiLV	Tilapia lake virus
TK	Thymidine kinase
TNF	Tumour Necrosis factor
TNFR	Tumour Necrosis Factor receptor
TO-2	Tilapia ovary
TR(S)	Terminal repeat(s)
UDG	Uracil DNA glycosylase
UL	Long unique region
US	Short unique region
UT	Third unique region
WT	Wild type
ZF4	Zebrafish embryonic fibroblast
Zfpv	Zebrafish picornavirus
ZNIRE	Zebrafish Non-coding Infection Response Element

Zα	Z-DNA/RNA binding domains
6-FAM	6-carboxyfluorescein

Table of contents

Résumé - Summary

Résumé

Le *Cyprinid herpesvirus 2* (CyHV-2) est un virus à ADN double brin linéaire appartenant au genre *Cyprinivirus,* de la famille des *Alloherpesviridae*. Cet agent pathogène cause une maladie associée à des mortalités élevées chez le poisson rouge (*Carassius auratus*) et d'autres espèces apparentées d'importance économique. Au début de cette thèse, la compréhension de la pathogénie du CyHV-2 souffrait d'un manque d'information sur plusieurs aspects. Aucune étude n'avait été publiée sur la susceptibilité et la permissivité de l'hôte du CyHV-2 aux différents stades de son développement. De même la porte d'entrée du virus n'était pas connue. Contrairement à des virus apparentés, le potentiel d'utilisation du modèle de laboratoire le poisson-zèbre (*Danio rerio*) pour l'étude de la pathogénie du CyHV-2 n'avait pas été investigué. Enfin, malgré l'isolement et le séquençage complet de plusieurs souches de CyHV-2, aucune souche capable d'induire une infection mimant l'infection naturelle n'était disponible au début de cette thèse (infection par immersion dans de l'eau contenant le virus et induction d'une maladie se propageant de sujet à sujet).

Pour combler ces lacunes, nous avons mené trois études interconnectées, correspondant aux trois sections expérimentales de cette thèse. Dans la première étude, nous avons démontré que le poissons rouge présente différents niveaux de sensibilité et de permissivité au virus CyHV-2 aux différents stades de son développement. Nous avons également identifié la porte d'entrée principale du CyHV-2 chez son hôte naturel. Cela a été réalisé en produisant une souche recombinante de CyHV-2 exprimant des gènes rapporteurs. Malheureusement, la souche parentale utilisée n'étant pas pleinement virulente, la souche recombinante produite n'exprimait qu'une faible virulence peu représentative des souches de terrain. Deux actions ont été menées en parallèle pour tenter de développer des modèles d'infection plus représentatifs de la virulence observée sur le terrain. Premièrement, dans la deuxième étude expérimentale, nous avons exploré la possibilité d'utiliser le poisson-zèbre sauvage ou modifié génétiquement comme modèle d'infection par le CyHV-2. A cette fin trois lignées génétiquement modifiées de poisson-zèbre ont été produites et testées quant à leur sensibilité et permissivité au CyHV-2. Deuxièmement, dans la troisième étude expérimentale, nous avons tenté d'identifier de nouvelles souches de CyHV-2 hautement virulentes au sein d'isolats de terrain. De courts résumés de ces trois études sont présentés ci-dessous.

Section Expérimentale 1 : étude par imagerie *in vivo* de la sensibilité et de la permissivité du poisson rouge à l'infection par le CyHV-2 aux différents stades de son développement. Afin de pouvoir étudier la pathogénie du CyHV-2 par imagerie *in vivo,* nous avons produit une souche recombinante exprimant un gène rapporteur codant pour une protéine bioluminescente et une protéine fluorescente. L'infection par immersion de poissons rouges avec cette souche recombinante et l'utilisation de diverses techniques d'imagerie *in vivo*, nous ont permis d'étudier des aspects spatio-temporels de la réplication du CyHV-2 aux stades larvaire, juvénile et adulte. Bien que les larves étaient moins sensibles à l'infection par rapport aux stades ultérieurs de développement, elles présentaient la plus grande

permissivité à la réplication du CyHV-2, entraînant une infection systémique rapide et une mortalité élevée. Une décroissance de la sensibilité et de la permissivité à l'infection a été observée avec le développement de l'hôte. Point très important, à tous les stades de développement, la peau a été identifiée comme le tissu le plus sensible et le plus permissif à l'infection, suggérant qu'elle sert de porte d'entrée principale au virus. Les résultats de cette étude représentent des informations fondamentales précieuses pour comprendre la pathogénie et l'épidémiologie du CyHV-2 chez son hôte naturel ainsi que pour comparer l'évolution de virus apparentés des poissons.

Section Expérimentale 2 : sensibilité et permissivité des larves de poisson-zèbre aux infections par trois cyprinivirus. Le poisson-zèbre est un organisme modèle de laboratoire utilisé dans de multiples domaines de la recherche scientifique dont la virologie. De manière étonnante, ce modèle s'est révélé utile pour l'étude de virus variés dont certains infectant l'homme. Un grand avantage du modèle poisson-zèbre est qu'il est relativement facile de produire des sujets transgéniques très utiles pour l'étude des interactions virus-hôte. Dans le second chapitre de cette thèse, un modèle de poisson-zèbre a été testé pour déterminer sa sensibilité et sa permissivité au CyHV-2 mais également à deux autres virus appartenant également au genre *Cyprinivirus.* Notre étude a révélé que les larves de poisson-zèbre n'étaient pas sensibles à ces virus lorsqu'elles étaient inoculées par immersion. Néanmoins, des infections par le CyHV-2 et le CyHV-3 ont pu être établies en culture de cellules et même *in vivo* à la suite d'inoculation des larves par micro-injection intrapéritonéale. Cependant, ces infections étaient transitoires, avec une élimination rapide du virus corrélée à une mort cellulaire de type apoptotique des cellules infectées.

Section Expérimentale 3 : caractérisation *in vitro* et *in vivo* de nouvelles souches de CyHV-2 isolés aux Pays-Bas. Malgré l'isolement et le séquençage complet de plusieurs souches de CyHV-2, aucune souche disponible au début de cette thèse n'exprimait une virulence comparable à celle observée sur le terrain. L'accès à ce type de souche virulente est essentiel pour étudier la pathogénie du CyHV-2 et pour tester les propriétés des candidats vaccins produits. Dans la troisième et dernière étude de cette thèse, nous avons analysé *in vitro* et *in vivo* les propriétés d'isolats de terrain du CyHV-2 issus des Pays-Bas. Dans cette étude, nous avons testé trois nouvelles souches de CyHV-2. Ces isolats appelés NL-1, NL-2 et NL-3 ont également été séquencés. Les analyses phylogénétiques réalisées ont révélé que ces nouvelles souches sont distinctes des souches connues antérieurement. Les trois souches ont également montré des différences significatives en termes de cinétique de croissance *in vitro*, la souche NL-2 présentant un passage stable et une meilleure multiplication en culture de cellule. Il est important de noter que l'inoculation de la souche NL-2 à des poissons rouges Shubunkin adultes par immersion (2000 PFU/mL) a induit une mortalité moyenne d'environ 40%, alors que les expériences réalisées en parallèle avec la souche de référence CyHV-2 ST-J1 n'ont induit aucune mortalité. En résumé, cette étude a révélé que la souche NL-2 est compatible avec une multiplication en culture de cellule, et qu'elle exprime une grande virulence capable d'induire une mortalité chez les poissons rouges Shubunkin adultes

inoculés par immersion. Cela a abouti à la description d'un nouveau modèle d'infection pour le CyHV-2 représentatif des conditions de l’infection naturelle sur le terrain.

Summary

Cyprinid Herpesvirus 2[1] (CyHV-2), is a linear double-stranded DNA virus that belongs to the genus *Cyprinivirus*[1] within the family *Alloherpesviridae*. This pathogenic agent is responsible for causing high mortality infectious disease in goldfish (*Carassius auratus*), and other economically important *Carassius spp.* Despite its prevalence, a comprehensive investigation into host susceptibility and permissivity at various developmental stages remains elusive, and the primary portal of viral entry into the host organism remains unclear. Also, unlike related viruses, the potential exploitation of zebrafish infection models, has not been explored. Furthermore, despite several CyHV-2 strains being isolated and fully sequenced, there is a lack of detailed characterization and consistent information on strains that exhibit high virulence in adult goldfish through viral challenge by immersion, particularly in the context of European host populations. This last point limits the study of CyHV-2 pathogenesis in the useful biological contexts most relevant to disease mitigation and control.

In order to address these knowledge gaps, we conducted a series of three interconnected studies, corresponding to Experimental Sections 1, 2 and 3 in this thesis. In the first study, we demonstrated that goldfish exhibit different levels of susceptibility and permissivity to the CyHV-2 virus at various developmental stages and identified the primary portal for CyHV-2 entry into the host. This was achieved using a recombinant CyHV-2 strain expressing reporter genes. However, due to the parental strain for which the recombinant was derived from, it did not cause clinical disease in adult hosts when challenged by immersion, and thus it was not representative of highly pathogenic CyHV-2 strains responsible for high mortality outbreaks in the same host populations in the field. Therefore, in order to potentially establish alternative CyHV-2 *in vivo* infection models, we explored two avenues in parallel. Firstly (Experimental Section 2) we explored the possibility of establishing, through genetic engineering, new zebrafish strains, with increased susceptibility and permissively to CyHV-2. Secondly (Experimental Section 3) we sought to identify novel CyHV-2 strains that were highly virulent and capable of inducing CyHV-2 related mortality in European sourced adult goldfish when challenged via immersion. These three studies are summarized as follows in the format of short abstracts:

Experimental Section 1: *In Vivo* Imaging Sheds Light on the Susceptibility and Permissivity of *Carassius auratus* to CyHV-2 According to Developmental Stage. There has been a lack of comprehensive studies regarding CyHV-2 host susceptibility and permissivity across different developmental stages, and the primary portal of viral entry into the host remains unclear. To address these knowledge gaps, we engineered the first recombinant strain of CyHV-2 expressing bioluminescent and fluorescent reporter genes. Infection of goldfish hosts with this recombinant strain through immersion enabled us to utilize various *in vivo* imaging techniques to elucidate the spatiotemporal aspects of CyHV-2 replication during larval, juvenile, and adult developmental stages. Although larvae were less susceptible compared to later developmental stages, they exhibited the highest permissivity to CyHV-2 replication, resulting in rapid systemic infection and high mortality. Permissivity to CyHV-2 decreased

as development progressed, with adults being the least permissive and consequently experiencing the lowest mortality rates. Throughout all developmental stages, the skin was identified as the most susceptible and permissive organ to infection during the early stages post-infection, suggesting that it serves as the primary portal of entry into these hosts. These findings collectively offer valuable fundamental insights into CyHV-2 pathogenesis and epidemiology in *Carassius auratus*, with significant relevance to other economically important virus-host models within the same genus.

Experimental section 2: Susceptibility and Permissivity of Zebrafish (*Danio rerio*) Larvae to Cypriniviruses. The zebrafish (*Danio rerio*) has emerged as a useful model organism in virology, facilitating the study of various viruses. Notably, it has proven to be valuable in studying a wide variety of viruses. Furthermore, it can easily be genetically manipulated, making it a valuable tool in studying virus-host interaction. In this study, a zebrafish model was tested to determine its susceptibility and permissivity to CyHV-2 relative to other viruses in the genus *Cyprinivirus*. Our investigation revealed that zebrafish larvae were not susceptible to these viruses when challenged by immersion. Nevertheless, infections with CyHV-2 and CyHV-3 could be established using artificial infection models both *in vitro* (utilizing zebrafish cell lines) and *in vivo* (via microinjection of larvae). However, these infections were transient, with rapid viral clearance correlated with apoptosis-like death of infected cells.

Experimental Section 3: *In vitro* and *In vivo* Characterization of novel CyHV-2 Strains from The Netherlands. Despite several CyHV-2 strains being isolated and fully sequenced, there is a lack of detailed characterization and consistent information on strains that exhibit high virulence in adult goldfish via challenge by immersion, particularly in the context of European host populations. These kinds of strains are much more compatible with experimental designs that are representative of natural infection. In this study, we isolated three novel strains of CyHV-2 originating from high mortality outbreaks in The Netherlands, which we refer to as NL-1, NL-2, and NL-3. Genome sequencing and phylogenetic analyses revealed that these newly isolated strains are distinct from known strains and from each other. The three strains also exhibited significant differences in terms of *in vitro* growth kinetics, with NL-2 exhibiting stable passaging and superior fitness *in vitro*. Importantly, the challenge of adult Shubunkin goldfish with the NL-2 strain via immersion (2000 PFU/mL) induced an average mortality of ~40%, while parallel experiments with the CyHV-2 reference strain ST-J1 resulted in no mortality. In summary, this study revealed that the NL-2 strain is *(i)* compatible with stable passaging *in vitro*, with acceptable replication kinetics in this environment, and *(ii)* highly virulent and capable of inducing CyHV-2 related mortality in adult Shubunkin goldfish when challenged via immersion. This resulted in the description of a new CyHV-2 *in vivo* infection model, much more compatible with experimental designs that are required to be representative of natural infection.

[1.] Recently *Cyprinid Herpesvirus 2* was renamed *Cyvirus cyprinidallo 2* and the genus *Cyprinivirus* was renamed *Cyvirus* by the International Committee on Taxonomy of viruses (ICTV). This occurred before this present Ph.D. project was completed. Consequently, for consistency with the nomenclature used in publications arising from this study (which were published before these nomenclature changes), in this thesis, we retain the use the previous nomenclature.

Preamble

Preamble

Cyprinid Herpesvirus 2 (CyHV-2) is a linear double-stranded DNA virus belonging to the genus *Cyprinivirus* in the family *Alloherpesviridae*. Since it was initially reported as the causative agent of epizootics in goldfish (*Carassius auratus*) in Japan, this virus has become globally prevalent. Despite its global distribution and economic importance, there are significant knowledge gaps regarding the pathogenesis of CyHV-2, which we address throughout this study.

The thesis begins with an introduction section which was divided into three subsections. The first subsection section focuses on goldfish, the main host species for CyHV-2, which was also utilized in this study. The second subsection focuses on viruses belonging to the order *Herpesvirales*, and with a specific focus on viruses in the family *Alloherpesviridae*, which infect fish and amphibian hosts. This subsection is mainly adapted from the review published by the host lab in fish and amphibian Alloherpesviruses in the *4th edition of the Encyclopedia of Virology*. Finally, the last subsection of the introduction consists of an up-to-date literature review of CyHV-2, the main subject of this thesis. The objectives of the thesis are then described, followed by the experimental sections. The experimental section consists of three subsections: The first describes a study on the susceptibility and permissivity of goldfish to CyHV-2 at different developmental stages, and identification of the major portal of entry of CyHV-2. This study has been published in the journal *Viruses*. The second chapter describes a study comparing the ability of different cypriniviruses (including CyHV-2) to infect zebrafish cell lines and zebrafish larvae. My contribution to this study consisted of the CyHV-2 infection work. This study has also been published in the journal *Viruses*. The third chapter describes a study on the genomic and biological characterization and comparison of three newly isolated CyHV-2 strains, leading to the identification of a strain capable of inducing CyHV-2 related mortality in adult Shubunkin goldfish through inoculation by immersion, thus representing a very valuable new CyHV-2 infection model.

There is a clear, coherent and logical connection between the three experimental sections. While the first study successfully addressed critical questions related to the pathogenesis of CyHV-2, as the CyHV-2 *in vivo* infection model did not result in severe disease or mortality in adult subjects when challenged by immersion, it was not entirely representative of highly pathogenic CyHV-2 strains responsible for high mortality outbreaks in the field. As this may limit future studies into different aspects of CyHV-2 pathogenesis and other aspects relevant to disease mitigation and control with this recombinant, we investigated the potential establishment of alternative CyHV-2 *in vivo* infection models. Firstly (Experimental Section 2) we explored the possibility of establishing, through genetic engineering, new zebrafish strains, with increased susceptibility and permissively to CyHV-2. Secondly (Experimental Section 3) we sought to identify novel CyHV-2 strains that were highly virulent and capable of inducing CyHV-2 related mortality in adult goldfish when challenged via immersion. Finally, in the last section of this thesis, the main findings are discussed collectively, with the added benefit of hindsight and retrospective insights with additional future perspectives arising from this Ph.D. study.

Introduction

1. The goldfish

Fish, constituting the oldest, largest, and most diverse class of vertebrates, encompass approximately 48% of identified species within the subphylum *Vertebrata*. Exhibiting adaptability to a broad spectrum of habitats ranging from freshwater to saltwater, cold polar seas to warm tropical reefs, and shallow surface waters to the profound pressures of ocean depths, fishes serve as an invaluable subject for investigating both physiological and molecular evolution, owing to their evolutionary standing among vertebrates (Helfman et al., 2009). Among the myriad varieties of fish, goldfish stand out for their wide array of forms, and it has become one of the most popular ornamental animals in the world. Furthermore, owing to their distinctive evolutionary processes and physiological structures, goldfish have garnered significance in biological research fields, emerging as a useful complement to mammalian disease models (Blanco and Unniappan, 2022). In this chapter, we will succinctly explore various facets of goldfish, including their origin, historical background, taxonomy, evolutionary trajectory, developmental processes, anatomical characteristics, applications in scientific research scenarios, and prevalent threats they face.

1.1 Origin and brief history

The goldfish (*Carassius auratus*), native to South China, is a domesticated cyprinid teleost fish derived from crucian carp (*Carassius carassius*), belonging to the family *Cyprinidae* within the order *Cypriniformes*. Known for being one of the most popular domesticated animal species, goldfish are commonly housed as a companion animal in indoor aquariums (Chen et al., 2020; Omori and Kon, 2019). The origin of ornamental goldfish dates back almost 2000 years. Historically, various species of fish have been bred and reared for human consumption for thousands of years in East Asia. Some of the normally gray or silver crucian carp species were observed to produce red, orange, or yellow color varieties, with this phenomenon being first recorded during the Chinese Jin Dynasty (AD 265 to 420) (Hervey, 1950). During the Tang Dynasty (AD 618–907), the practice of cultivating fish in ornamental ponds and water gardens gained popularity. Selective breeding of goldfish with preferred phenotypes in ponds or other water bodies began during this period (Chen, 1956). In the Song Dynasty (AD 960 to 1279), the selective domestication of goldfish was gradually improved. Because the golden color of goldfish is very special and is a symbol of royalty, people outside the imperial family were forbidden to keep goldfish of the gold (yellow) variety. During the Ming dynasty (AD 1368–1644), goldfish also began to be raised indoors, which allowed mutants that could not survive in outdoor environments to be retained. In fact, much of the variation in goldfish occurred in these internal environments in the second half of this dynasty. It was also during this period, that several prototypic phenotypes, including the twin-tail, long fin and short bodied variety, were established. Artificial selection through breeding began at the beginning of the Qing dynasty (AD 1644–1912), with the varieties exhibiting traits such as including the telescope-eye, transparent scales and dorsal fin loss, were likely established during this period (Chen, 1956; Smartt, 2001).

The international export of goldfish originated in East Asia, with the first known import to Japan from China in the early 17th century. Japanese enthusiasts further developed numerous varieties during the Edo period, providing a foundation for subsequent cross-breeding (Matsui, 1935). Concurrently, the evolving international transportation networks facilitated the spread of goldfish to Europe, where they gained widespread popularity (Blanco and Unniappan, 2022; Komiyama et al., 2009; Smartt, 2001; Wang et al., 2013). Subsequently goldfish were first introduced to North America around 1850, rapidly becoming a highly sought-after pet in this region (Brunner, 2005; Mulertt, 1883).

1.2 Taxonomy and variety of goldfish

The genus *Carassius*, encompassing the goldfish, exhibits a wide distribution across the Eurasian continent, with a notable prevalence in East Asia (Takada et al., 2010). Historically, there has been considerable debate over the taxonomy of goldfish. In earlier studies, it was thought that goldfish were morphologically closer to the common carp. However, later, goldfish became regarded as being closer to Crucian carp than the common carp. With the advent of modern research tools, specifically the analysis of mitochondrial DNA, the genetic relationship between carp, crucian carp and goldfish has been clarified. The results indicated that the common carp and Crucian carp were clearly different from each other, and that goldfish originated from specific sub-populations of Crucian carp (Komiyama et al., 2009; Podlesnykh et al., 2015; Wang et al., 2013). The designation of goldfish as *C. auratus* dates back to 1758 when the Swedish botanist, zoologist, and physician Carl Linnaeus documented it in his book Systema Naturae, 10th Edition (Blanco and Unniappan, 2022). Within the same genus, five other species are recognized: *Carassius carassius* (Crucian carp), *Carassius cuvieri* (Japanese white crucian carp), *Carassius gibelio* (Gibel carp or Prussian carp), *Carassius langsdorfii* (Ginbuna) and *Carassius praecipuus* (Knytl et al., 2022; Rylková et al., 2013). The current comprehensive taxonomic classification of the goldfish is presented in Table 1.

Table 1 - Taxonomic classification of the goldfish (*Carassius auratus*).

Kingdom	*Metazoa (Animalia)*
Superphylum	*Deuterostomia*
Phylum	*Chordata*
Subphylum	*Vertebrata (Craniata)*
Infraphylum	*Gnathostomata*
Superclass	*Osteichthyes (Euteleostomi)*
Class	*Actinopterygii*
Subclass	*Neopterygii*
Infraclass	*Teleostei*
Supercohort	*Clupeocephala*
Cohort	*Otomorpha*
Subcohort	*Ostariophysi*
Superorder	*Cypriniphysae*
Order	*Cypriniformes*

Suborder	*Cyprinoidei*
Family	*Cyprinidae*
Subfamily	*Cyprininae*
Genus	*Carassius*
Species	*auratus*

From Blanco *et al.* (Blanco and Unniappan, 2022)

On the other hand, the evolution of goldfish species represents a highly intricate and temporally extensive process. Historically, in response to diverse human preferences and aesthetic inclinations, enthusiasts persistently engage in artificial hybridization to introduce novel species, fostering a dynamic co-evolution of goldfish alongside human culture. Currently, goldfish represent one of the most morphologically diverse fish species, with a spectrum of over 300 distinct varieties, each characterized by unique external morphological features (Smartt, 2001). However, broadly speaking, goldfish breeds can be assigned to one of three groups, referred to as Grass-goldfish, Egg-goldfish, and Wen-goldfish (three-breed taxonomy system) (Wang et al., 2013). Notably, considering the common goldfish as a wild type and comparing it to other various strains reveals that the majority of phenotypic variety occurs in eyes, hoods, nasal septa, operculum, skeletal features, fins, body coloration, and scales (Omori and Kon, 2019). Surveys show that the main types of goldfish are Common goldfish, Fantail goldfish, Comet goldfish, Ranchu goldfish, Oranda goldfish, Shubunkin goldfish, Celestial eye goldfish, Telescope goldfish and Bubble-eye goldfish (Komiyama et al., 2009). The appearance and evolutionary relationships of partial divergent strains are shown in Fig. 1.

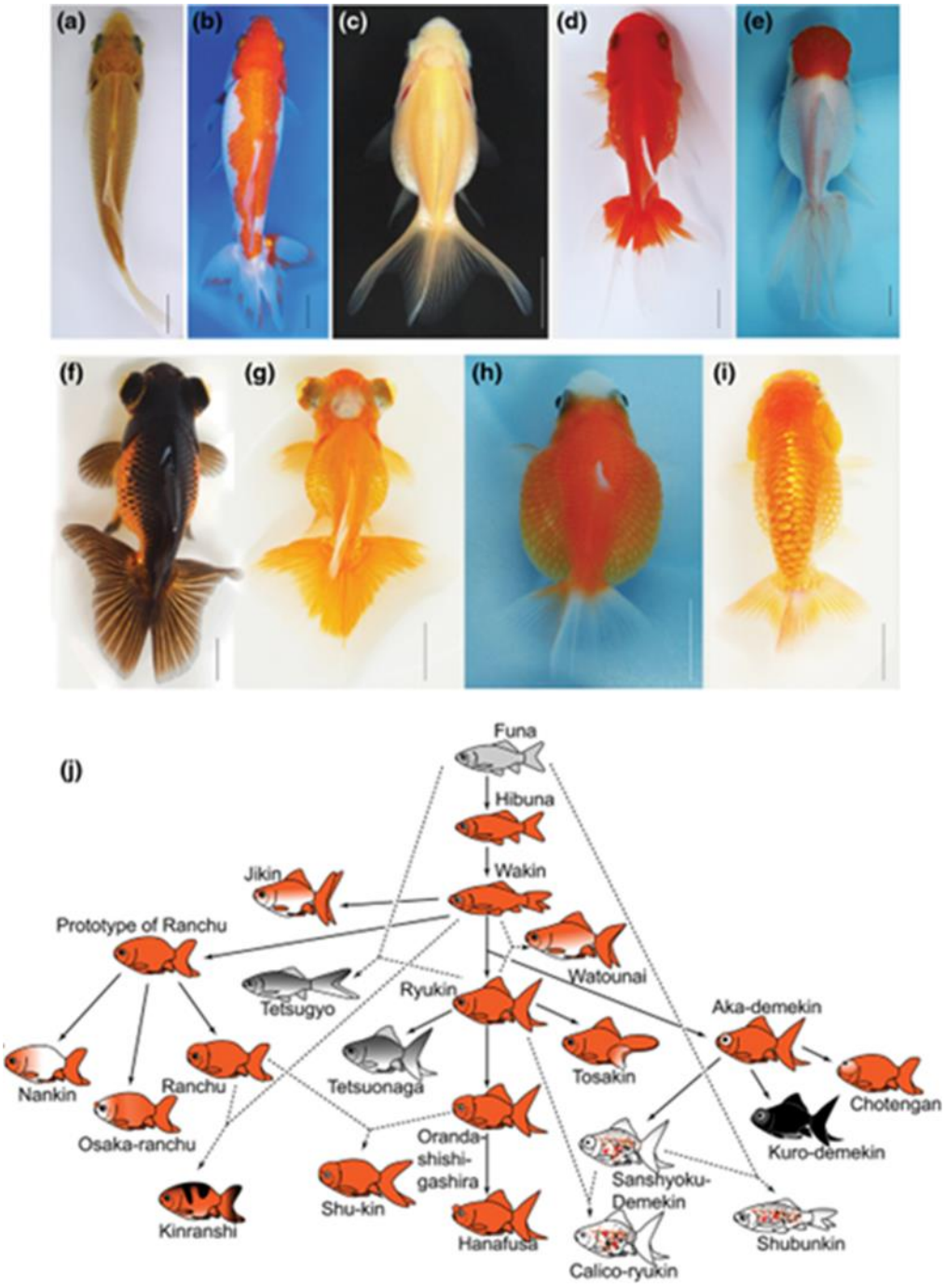

Figure 1 - Variation of goldfish strains. (a–i) Dorsal views of nine different goldfish strains: (a) the single fin Wakin; (b) duplicated caudal fin Wakin; (c) Ryukin; (d) Oranda; (e) Redcap Oranda; (f) Telescope (the 'black moutan' strain); (g) Telescope (butterfly tail); (h) red-color-telescope; and (i) Ranchu. (j) Illustration of Matsui's genealogical diagram. From (Ota and Abe, 2016).

1.3 Development and anatomy of goldfish

The evolution of ornamental goldfish captivated early researchers, precipitating the publication of numerous initial reports elucidating the embryonic and post-embryonic developmental processes specific to this species (Kajishima, 1960; Otani et al., 2002; Sharma and Ungar, 1980; Yamaha et al., 1999). The large amount of information on embryonic and post-embryonic development of goldfish has

culminated in the development of reliable staging tables for normal goldfish development, such as those described by Tsai *et al.* (Tsai et al., 2013) and Li *et al*. (I.-J. Li et al., 2015) which comprehensively describe the developmental process of single-tail common goldfish. In short, the embryonic stage has been categorized into seven periods, including zygote, cleavage, blastula, gastrula, segmentation, pharyngula, and hatching periods. The post-embryonic stage consists of three periods, including larval, juvenile, and adult periods. Given that the research in this Ph.D. project was only concerned with the postembryonic developmental stages of goldfish, we will confine our descriptions to these stages in Table 2.

Table 2 - Description of various developmental stages of goldfish.

Stage name (Abbreviation)	Descriptions (SL and dpf onset)
Protruding mouth (Prot)	Extended mouth, yolk, all fin folds remain; straight notochord at the caudal fin level (5 mm and 3 dpf)
Posterior swim bladder (Psb)	Inflation of the posterior swim bladder; lower jaw extension (5.6-5.7 mm and 5.7 - 5.8 dpf)
Caudal fin ray (Cr)	More than four visible caudal fin rays, snout length longer than Psb, slightly bended caudal fin; this stage can be divided into sub-stages based on the number of fin rays (6.1-6.3 mm and 7.5-7.8 dpf)
Forked caudal fin (Fcf)	Appearance of a largely concaved point in the caudal fin, evident anal and dorsal fin condensation; slightly reduced dorsal and post-anal fin rays (6.8-7.0 mm and 13.6-13.8 dpf)
Anterior swim bladder (Asb)	Inflation of anterior swim bladder; enlarged anal and dorsal fin condensation (7.0-7.3 mm and 12.8-14.8 dpf)
Dorsal fin ray (Dr)	Dorsal fin ray appearance; larger anterior swim bladder lobe than Asb stage (7.5-7.8 mm and 18.0-20.0 dpf)
Anal fin ray (Ar)	Anal fin ray appearance; lack of the dorsal fin fold at the anal fin level, anterior swim bladder is larger than posterior swim bladder; curved triangle shape-like dorsal fin (8.2-8.4 mm and 22.3-24.0 dpf)
Pelvic fin bud (Pb)	Pelvic fin bud being visible from lateral side and equipping AER (8.7-9.0 mm and 26.0-27.0 dpf)
Pelvic fin ray (Pr)	Pelvic fin ray appearance; elongated most posterior dorsal and anal fin rays; trapezium shape dorsal and anal fins (11.0-11.2 mm and 31.0-31.1 dpf)
Juvenile	Complete loss of the fin fold; incomplete squamation; posterior serrations at the anterior dorsal and anal fin ray; this stage can be divided into two sub-stages based on squamation patterns (17.0-17.6 mm and 45.2-49.2 dpf)
Adult	Produce matured eggs and sperms; SL onset, 5 cm

Adapted from (Li et al., 2015).

The anatomy of goldfish has been extensively characterized, taking the common goldfish as an example, its body exhibits a relatively concise and compact shape, characterized by five sets of fins

conforming to the typical arrangement observed in most members of the family *Cyprinidae*. These fins include the dorsal fin along the back, the caudal (tail) fin, the anal fin, the ventral or pelvic fins, and the pectoral fins (Fig. 2A–B). Notably, the scales are large, maintaining a consistent size and shape, arranged in an orderly pattern of overlap. The positioning of the eyes on both sides of the head limits their mobility, rendering goldfish short-sighted; they heavily rely on alternative senses for locating food and detecting potential threats. Each side of the head features a rigid bony flap known as the operculum, which is open at the back for water release, serving to shield and safeguard the gills. Goldfish exhibit a continuous lateral line canal system comprising supraorbital, infraorbital, operculomandibular, and supratemporal commissural canals on the head, complemented by a trunk canal extending the length of the trunk. The goldfish lateral line exhibits remarkable sensitivity, proficient in detecting motion, current, pressure, temperature, and sound (Blanco et al., 2018; Puzdrowski, 2008; Smartt, 2001).

The internal anatomy of the goldfish encompasses homologs of all the essential organs found in vertebrates, as illustrated in Fig. 2B–C. The intricately organized brain is a pivotal component, featuring distinct regions dedicated to regulating various physiological and behavioral functions (Rupp et al., 1996). Situated below the brain is the pituitary gland, or hypophysis, which morphologically consists of two principal regions-the adenohypophysis and the neurohypophysis. The teleost adenohypophysis is further divided into three conserved lobes: the proximal *pars distalis*, the rostral *pars distalis*, and the neurointermediate lobe (Blanco et al., 2018). The goldfish heart adheres to the typical vertebrate structure, comprising four chambers—sinus venosus, atrium, ventricle, and bulbus arteriosus. Additionally, it includes an atrio-ventricular region and a muscularized conus arteriosus supporting the conus valves (Garofalo et al., 2012). Within the abdominal cavity of the goldfish, the predominant occupant is the gastrointestinal tract an elongated, relatively undifferentiated tube. A distinctive feature is the absence of a stomach, replaced instead by an enlarged section of the intestine known as the intestinal bulb. The digestive tract can be partitioned into mouth, buccal cavity, pharynx, esophagus, intestinal bulb, intestine, and rectum (Sarbahi, 1951). Goldfish liver is diffused and formed by narrow right and left hepatic lobes, extending on each side of the intestinal bulb (Blanco et al., 2018). The spleen, primarily composed of red pulp, elongates along the serosal lining of the intestine (Katakura et al., 2015). The goldfish kidney, resembling that of many other fish, is a bilobed organ comprising a cranial and a caudal kidney. The cranial or head kidney serves as an immune and endocrine organ, containing hematopoietic and endocrine tissue, positioned around the posterior cardinal vein (Reimschuessel, 2001; Sampour, 2008). Lastly, the gonads of goldfish, akin to those of other teleosts, lack medullary tissue, corresponding solely to the cortex observed in other vertebrates. Morphologically, male gonads (testes) manifest as elongated paired organs affixed to the dorsal body wall. In females, the ovary comprises oogonia, oocytes, surrounding follicle cells, supporting tissue or stroma, and vascular and nervous tissue (Blanco et al., 2018; Nagahama, 1983).

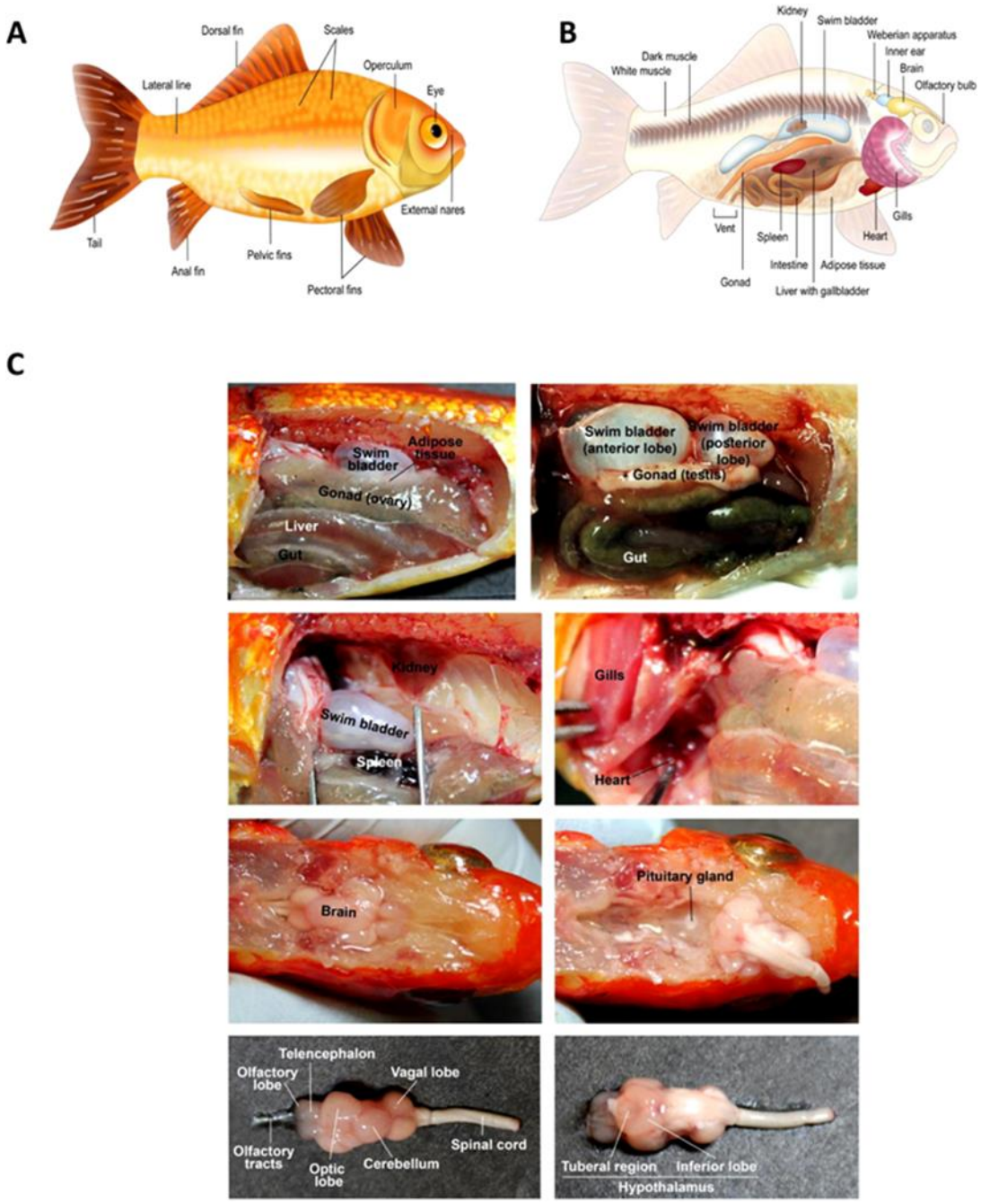

Figure 2 - (A) An artist's rendering of the external anatomy of goldfish. B shows an artist's rendering of the internal organs in goldfish. C shows photographs of the external and internal anatomy of goldfish. Individual organs and brain regions are labelled. Female and male fish are shown separately to mark ovary and testis. From (Blanco et al., 2018).

1.4 Goldfish applications in scientific research

Goldfish, selected as experimental subjects in various biological domains, offer practical advantages in handling and breeding due to their physiological and developmental characteristics (Blanco and Unniappan, 2022). Dating back to 1901, WL Underwood's pioneering description in scientific literature highlighted their role in consuming mosquito larvae (Underwood, 1901). Over a century of ongoing exploration has solidified goldfish's significant role in biological research, particularly in fields

such as endocrinology (Blanco et al., 2018; Chang et al., 2009; Popesku et al., 2008), developmental biology (Omori and Kon, 2019; Ota and Abe, 2016), pharmacology (Kaneko et al., 1991; Mora-Ferrer and Neumeyer, 2009; Nightingale and Gibaldi, 1971), and more, which will be described in this section.

Research on endocrinology using goldfish has predominantly centered on discerning the central or peripheral impacts of hormones and neuropeptides on food intake and metabolic processes. Simultaneously, considerable attention has been devoted to investigating the synthesis and secretion of hormones that regulate physiological processes. For instance, Marchant *et al.* (Marchant et al., 1989) demonstrated the dual role of Gonadotropin-Releasing Hormone as a Growth Hormone-Releasing Factor in goldfish. Further, Peng *et al.* (Peng et al., 1993) identified multiple neuropeptide-Y (NPY) receptors in the goldfish pituitary, with NPY exerting effects on both pituitary cells and nerve terminals. In addition, it was indicated that goldfish exhibit olfactory sensitivity to dopamine and epinephrine, along with their 3-O-methoxy derivatives, metadrenaline, and 3-O-methoxytyramine. This discovery raises the intriguing possibility that catecholamines and/or their metabolites may play a role in external chemical communication (Hubbard et al., 2003). These instances underscore that the highly conserved structure and functions of many hormones, receptors, and bioactive peptides make goldfish a valuable model organism in hormone research. The insights gained from studying this organism hold potential applications across diverse vertebrates.

Similarly, biological investigations related to vertebrate development and disease development often use goldfish as a model. For example, Dawson *et al.* (Dawson and Meyer, 2008) utilized *in vivo* imaging techniques to analyze the dynamic behavior and morphology of regenerating axons in the goldfish optic tectum. This exploration of axon dynamics in systems with inherent regenerative abilities holds promise for uncovering insights applicable to promoting regeneration in humans. In addition, researchers have successfully developed methods for isolating and culturing specific brain cell types, such as astrocytes and microglia-like cells (Houalla and Levine, 2003; Sivron et al., 1993). These approaches contribute valuable knowledge to the understanding of brain homeostasis maintenance, neuronal protection, and control of neuronal proliferation. Notably, Xing *et al.* (Xing et al., 2017) using the goldfish model found that aromatase, and by implication endogenous estrogens, have important roles in glial reaction in response to the neurotoxin 1-methyl-1,2,3,6-tetrahydropyridine (MPTP). Goldfish are also frequently used as models in research on neurodegenerative diseases. It has been shown that the advanced metabolomics approach could be used in goldfish models of Parkinson's disease (Lu et al., 2014; Pollard et al., 1993). Collectively, the aforementioned examples strongly endorse the use of goldfish as a model organism for advancing our understanding of developmental biology and human disease.

Furthermore, goldfish have proven to be valuable models in research aimed at understanding the adverse pharmacological and toxic effects of various medicines and compounds. For example, goldfish have been used to gain insights into the functional organization of the retina in terms of color vision, motion detection, and temporal resolution both before and after intra-ocular injection of various

neuropharmaca with known effects on retinal neurons. The conclusions drawn from this study highlight the distinct and parallel processing of L-cone contribution to different visual functions. Additionally, goldfish have been used to several neurotransmitters, including dopamine, acetylcholine, glycine, and GABA, on motion vision, color vision, and temporal resolution (Mora-Ferrer and Neumeyer, 2009). Zhang *et al.* (2020) used goldfish to establish that exposure to benzophenone-3 (BP3) affects the activity of multiple proteases in goldfish, leading to accumulation in the liver, intestine, and brain. The same team also demonstrated that this accumulation results in inhibited growth performance, histopathological damage in the liver and intestine, and alterations in microbial community abundance. In a separate study, Wang *et al.* (Wang et al., 2019b, 2019a) used goldfish as models to reveal that Bisphenol A (BPA) disrupts testis maturation by inducing apoptosis in germ cells and Leydig cells, consequently reducing 11-KT levels and disrupting spermatogenesis. Additionally, the researchers also demonstrated that BPA induces neurotoxicity, disrupts dopaminergic processes, and damages cerebral blood vessels. Given the well-characterized physiological systems of goldfish, this species represents an extremely useful model in pharmacology and toxicology research.

Overall, goldfish will continue to be a useful model organism for research across many fields globally. Its notable features, including a relatively large body size, the capacity for collecting substantial blood samples, and well-characterized body systems, render this species highly accessible for scientific investigation. However, it is essential to acknowledge that the presence of genome duplication and the resulting duplicated genes imposes limitations in certain studies, for example those that involve gene knockout.

1.5 Disease in goldfish

Healthy goldfish exhibit physical features vibrant, even coloration, glossy and pristine scales with a reflective sheen, clear eyes, upright fins, and an absence of cracks or tears. They also swim gracefully, consume food regularly and eagerly, and exhibit rapid responsiveness to vibrations and changes in light. Deviations from these indicators may signal potential health issues, allowing for prompt diagnosis and appropriate treatment. Notably, inadequate water quality is a common source of fish ailments, underscoring the essential role of maintaining a healthy aquatic environment for disease prevention. Moreover, in diverse breeding scenarios, various pathogens, including parasites, bacteria, fungi and viruses, also pose significant threats to goldfish health.

1.5.1 Parasitic infections

Common parasitic diseases that occur in goldfish farming can be categorized as follows: (i) *Ichthyophthirius multifiliis*, commonly known as "Ich" is a parasitic ciliate responsible for causing Ich spot disease, the most prevalent ailment affecting goldfish in freshwater aquaria (Sharma et al., 2012; Thilakaratne et al., 2003). This disease typically arises due to factors such as poor water quality, overcrowded aquarium conditions, or sudden temperature fluctuations. Manifestations include fish clamping their fins, the presence of small white spots on the body, fins, and gills, as well as observable

irritation and inflammation, prompting affected goldfish to itch against the sides of the tank. A recent study demonstrated that cMOS significantly enhances the mucosal immune response in the skin and gills of goldfish, thereby improving their resistance to *Ichthyophthirius multifiliis* infection (Huang et al., 2022) (Fig. 3). (ii) Anchor worms (*Lernaea spp.)* are external copepod parasites that affix themselves under the scales of fish (Thilakaratne et al., 2003). The introduction of infected fish or plants carrying larvae is a common cause of this disease. Infected goldfish typically exhibit signs of discomfort, such as itching and flashing, followed by the visible presence of parasites attached to their bodies. (iii) Flukes are monogenean parasites that commonly affect freshwater fish, including goldfish (Mayer and Donnelly, 2013). The genera *Dactylogyrus* and *Gyrodactylus* are frequently implicated in infestations. *Dactylogyrus* primarily affects the gills, while *Gyrodactylus* is more commonly found on the skin. Symptoms of fluke infestation in goldfish include flashing, the presence of tiny red spots or yellow dusting, excessive mucus production, shedding of the slime coat, and clumped fins. When infestations impact the gills, respiratory signs such as increased opercular rate, piping, and respiratory distress may also be observed. (iv) Fish lice, belonging to the genus *Argulus*, are branchiuran crustaceans that parasitize both marine and freshwater fishes (Wafer et al., 2015). Similar to anchor worms and flukes, the typical causes of fish lice infestation are the introduction of new, unquarantined fish or plants into the aquarium. Infected fish commonly exhibit itching, and visible parasites can be observed moving around the fish, often in protected areas such as behind the fins, near the eyes, or gills. (v) Goldfish velvet disease, also known as "Rust Dust" or "Gold Dust" disease, is caused by tiny parasites of the genera *Oodinium* that give the fish a dusty, slimy look (Sin et al., 1992). Introduced to tanks by unquarantined infected new goldfish, this disease is highly contagious and can be easily spread via contaminated tanks, fish, or tools. Symptoms include a fine rusty yellowish film on the skin, slime shedding, clamped fins, and scratching. Understanding these classifications is crucial for effective disease management and prevention.

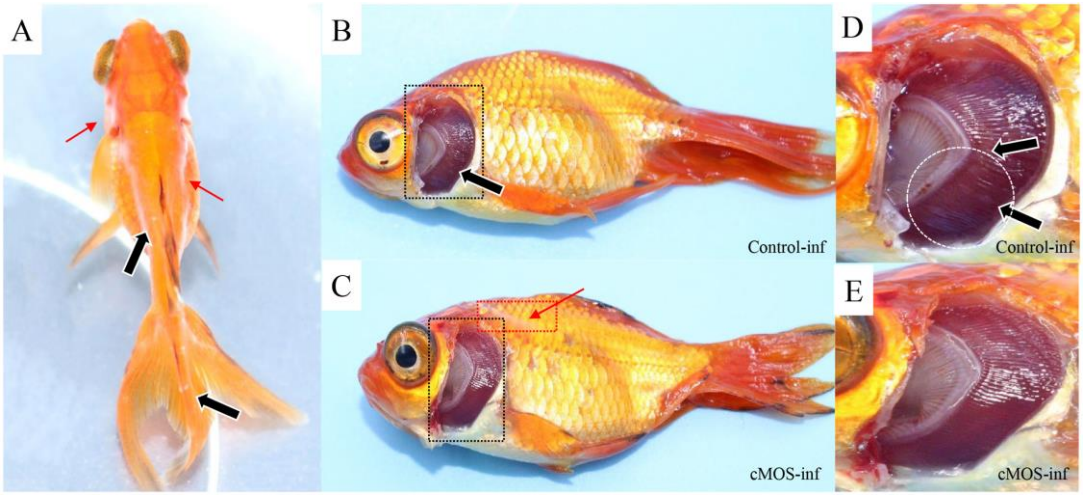

Figure. 3 - Clinical signs and symptoms of goldfish after *Ichthyophthirius multifiliis* challenge in control-inf group and cMOS-inf group. (A) Visible white spots (black arrows) and abundant mucus (red arrows) appeared on the surface of the goldfish; (B) The control-inf goldfish had some visible white spots (black arrows) on the gill; (C) The surface of goldfish

in cMOS-inf group secreted mucus (red arrows, red dotted box); (D) Local amplification of gill in control-inf group, trophont occurred (white dotted circle, black arrows); (E) Local amplification of gill in in cMOS-inf group, almost no trophont. From (Huang et al., 2022).

1.5.2 Bacterial infections

Bacterial infections pose a formidable threat to the aquaculture industry, resulting in significant economic repercussions annually. The pathogenicity of bacteria is particularly pronounced during the growth phase of fish, especially when they are physiologically compromised, nutritionally deficient, or experiencing stressors such as water contamination and overstocking (Vanamala et al., 2022). In the context of goldfish farming, prevalent bacterial infections encompass Fin rot, Mouth rot, Dropsy, and Pop eye. Fin rot, a commonly encountered ailment, is primarily attributed to *Aeromonas, Pseudomonas, Flovobacterium*, or *Vibrio*, with sporadic instances caused by specific fungal strains (Sharma et al., 2012). The principal catalyst for fin rot is suboptimal water quality, although factors like overcrowding, rough handling, aggression, or low temperatures can also precipitate the disease. Manifesting as split and frayed fins with red streaks and a white periphery, fin rot is emblematic of compromised fish health. Mouth rot, typically induced by *Flavobacterium* in conditions of tank overcrowding and poor water quality, manifests as initial redness in the mouth, followed by lip separation and potential collapse, resulting in a distinctive oral aperture (Loch and Faisal, 2015). Dropsy, characterized by an abnormal accumulation of fluid in the body cavity or tissues, serves as a symptomatic indicator rather than an autonomous disease (Conroy, 1961). However, systemic infections by *Aeromonas* bacteria are a prevailing cause of dropsy, presenting with a swollen body, raised scales resembling a pinecone configuration, and often culminating in fatality. Pop eye, or exophthalmia, denotes the abnormal swelling and protrusion of one or both eyes in fish. Analogous to dropsy, pop eye is symptomatic of an underlying problem, frequently associated with bacterial infections, predominantly by *Aeromonas* or *Pseudomonas* spp. Afflicted individuals exhibit visible eye swelling, potential cloudiness, and, in severe instances, eye rupture (Brenden and Huizinga, 1986; Hossain et al., 2018).

1.5.3 Fungal infections

Fungal infections in fish are typically considered secondary issues arising from underlying factors such as water quality problems, poor environmental conditions, trauma (from rough handling or attacks), bacterial diseases, or parasitic infestations. The term "cotton wool" is commonly used to describe fungal infections in aquarium settings. While several fungal species can cause infections in fish, *Saprolegnia* and *Achyla* spp. are among the most prevalent (Yanong, 2003). In healthy fish, fungal infections are uncommon, as they naturally protect themselves by producing mucous layers. Fungi tend to appear on fish that are weakened by stress, illness, or injury. When goldfish are infected by fungi, characteristic symptoms include the development of white, cottony growth on the body and fins (Iqbal et al., 2012; Shaheena et al., 2015). Monitoring and addressing the underlying stressors or health issues are essential for the effective prevention and treatment of fungal infections in fish.

1.5.4 Viral infections

Currently there is an incomplete understanding of what viruses can naturally or primarily infect goldfish. There is some evidence that goldfish can be naturally infected with viruses in the genus *Lymphocystivirus*, leading to a disease referred to as lymphocystis (Joardar, 2018), which a common viral ailment affecting both freshwater and saltwater fish (MacLachlan and Dubovi, 2011). This virus infects fish, transforming fibroblasts of the skin and gills, as well as internal connective tissue, resulting in significant hypertrophy of affected cells known as lymphocysts. Clinical symptoms include the presence of white, pearl-like lesions on the edges of fins or on the body. There is only a single virus that is known to primarily infect goldfish and other species with in the genus *Carassius*, this is *Cyprinid herpesvirus 2* (Thangaraj et al., 2021), which is a member of the family *Alloherpesviridae* in the family *Herpesvirales.* This virus affects the skin and hematopoietic organs and results in high mortality rates within aquaculture facilities (Fig. 4). Furthermore, as this is a herpesvirus, it is likely that it in hosts that survive infection, the virus undergoes long periods of dormancy (referred to as latency) and followed by periodic reactivation throughout their lifetime. This virus is the focus of this thesis, and a comprehensive introduction to the order *Herpesvirales*, the family *Alloherpesviridae* and *Cyprinid herpesvirus 2* will be provided in the subsequent sections of this introduction.

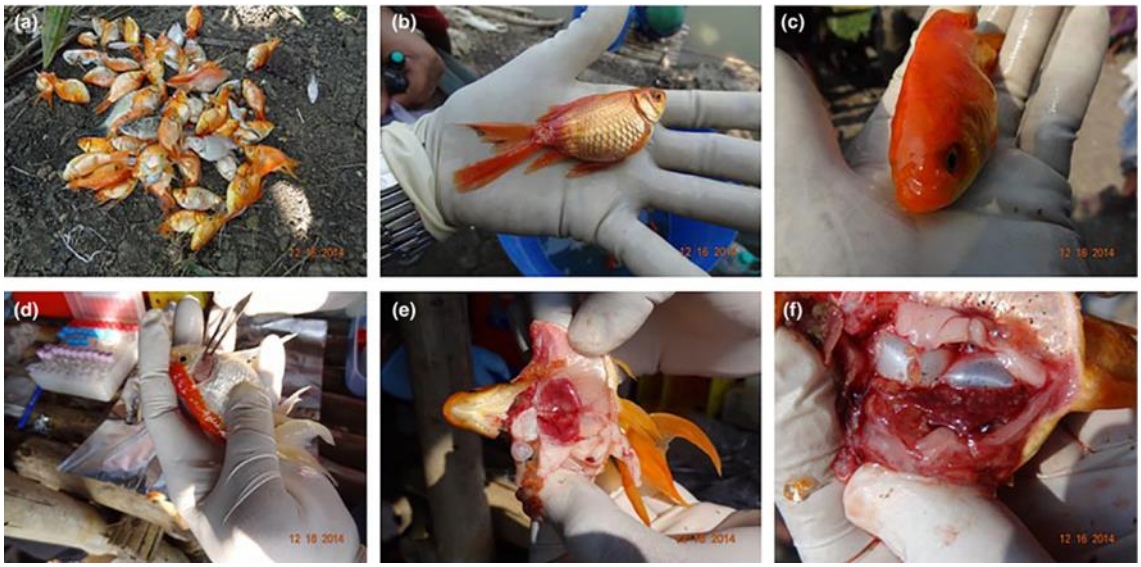

Figure 4 - *Cyprinid herpesvirus 2* (CyHV-2) infection in goldfish (*Carassius auratus*). (a) Mass mortality of goldfish in a polyculture pond in a farm in India during 2014; (b) External clinical signs of CyHV-2 affected goldfish (*Carassius auratus*) including haemorraghes on the body, ascites and protrusion of scales on the body surface; (c) CyHV-2 affected goldfish showing *enophthalmia* (sunken eyes); (d) Inflamed and swollen gills in CyHV-2 affected goldfish; (e) swollen and enlarged kidney in CyHV-2 affected goldfish; (f) enlarged liver with white necrotic foci in CyHV-2 affected goldfish. From (Thangaraj et al., 2021).

2. The order *Herpesvirales*

2.1 General description

The order *Herpesvirales* consists of a large group of viruses, that share similar structural, genetic, and biological characteristics. Phylogenetically, the order *Herpesvirales* is split into three related families that infect a wide variety of host species (Pellett et al., 2011). Recently, the International Comity for Taxonomy of Viruses (ICTV) has updated the nomenclature of herpesviruses to present a more rational structure (ICTV, 2023; Lefkowitz et al., 2018) In this thesis, we use the former nomenclature to maintain the consistency with earlier publications from this thesis. The family *Herpesviridae*, (recently renamed *Orthoherpesviridae* by the ICTV), encompasses herpesviruses that infect mammals, birds, and reptiles. This family is the most significant in terms of both the number of identified members, our understanding of their biology and virus-host interactions (King et al., 2012a). Conversely, the family *Malacoherpesviridae* is much smaller, currently comprising only two species of herpesviruses that infect molluscs (Davison et al., 2009; Renault, 2016). Finally, the family *Alloherpesviridae* includes herpesviruses infecting fish and amphibians. Notably, species within the latter two families are much more divergent than species within the family *Herpesviridae* (Davison, 2002; Hanson et al., 2011; King et al., 2012b).

This section of the introduction is structured as follows: it begins with a general phylogenetic overview of the order *Herpesvirales* and a review of the main and specific properties of herpesviruses serving as a general introduction to herpesviruses, followed by a more detailed focus on the key characteristics of the family *Alloherpesviridae*, comprising of herpesviruses that infect fish and amphibians serving as a prelude to the a detailed introduction of *Cyprinid herpesvirus 2* in the third section.

2.1.1 Phylogeny of the order *Herpesvirales*

Historically, the classification of viruses has primarily relied on their distinct virion morphology and genome structure (described later). Before the order *Herpesvirales* was created, the family *Herpesviridae* consisted of all known herpesviruses and the classification of herpesviruses into subfamilies relied on these general biological criteria. In more recent times, with advancements in sequencing technology and bioinformatics, the classification of a virus as a herpesvirus now predominantly relies on sequence data.

The family *Herpesviridae* occupies the largest clade in the order *Herpesvirales* and comprises 115 species listed by ICTV. This family is further divided into three subfamilies: *Alphaherpesvirinae*, *Betaherpesvirinae*, and *Gammaherpesvirinae*, which encompass five, five, and seven genera, respectively with the establishment of this taxonomical structure supported by numerous phylogenetic analyses (ICTV, 2023; McGeoch et al., 2006, 2000; McGeoch and Gatherer, 2005). Fig. 5 presents a phylogenetic description of 65 viruses classified in this family, based on the complete sequences of the highly conserved viral DNA polymerase gene. The overall relatedness of this family is evident, with 43 genes are conserved among its members, referred to as core herpesvirus genes (Davison, 2007), strongly

supporting a monophyletic origin for these viruses from a common ancestor, which is estimated to have lived approximately 400 million years ago (McGeoch et al., 2006).

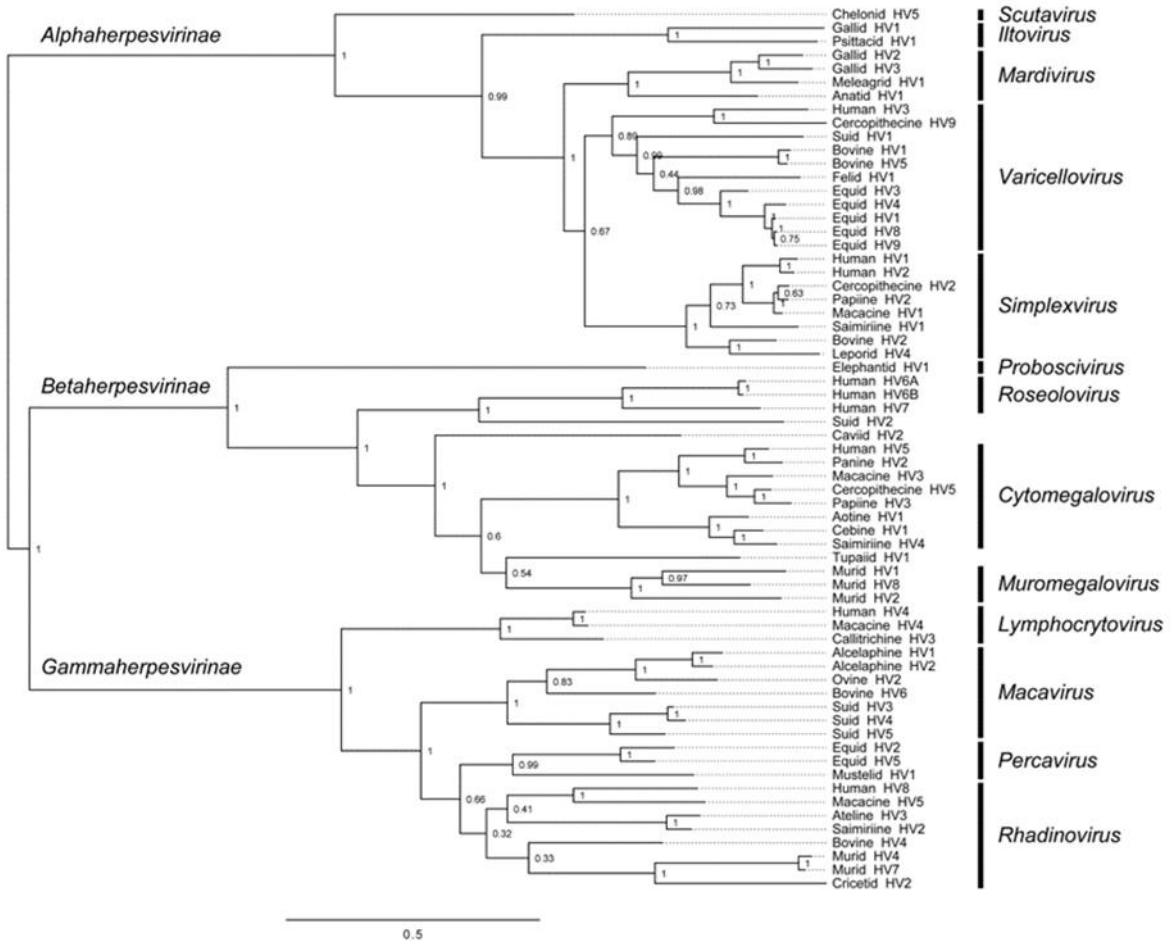

Figure 5 - Phylogenetic analysis of the family *Herpesviridae*. Unrooted phylogenetic tree based on the full-length DNA polymerase amino acid sequences of members of the family *Herpesviridae*. The sequences (996-1357 amino acid residues in length) were derived from relevant GenBank accessions. Virus names are aligned at the branch tips in the style that mirrors the species names (e.g. chelonid herpesvirus 5 (Chelonid HV5) is in the species *Chelonid herpesvirus 5*). The names of subfamilies and genera are marked on the left and right, respectively (McGeoch et al., 2006).

Malacoherpesviridae, the second family in the order *Herpesvirales*, consists of two genera: *Aurivirus*, which includes *Haliotid herpesvirus 1* (Abalone herpesvirus) (Corbeil, 2020; Savin et al., 2010), and *Ostreavirus*, which includes *Ostreid herpesvirus 1* (Oyster herpesvirus) (Davison et al., 2005; Steward et al., 2013). Finally, a third family, *Alloherpesviridae*, consists of viruses that infect fish and amphibians (Boutier et al., 2021; King et al., 2012b; Waltzek et al., 2009a), and a more comprehensive description of these viral species and their phylogeny will be provided later. Viral species in the families *Malacoherpesviridae* and *Alloherpesviridae* all exhibit common characteristics of herpesviruses, as evident from the morphological conservation of the virion, particularly the capsid. However, the genetic similarities between these viruses and those within the family *Herpesviridae* are minimal (Davison et al., 2005; Hanson et al., 2024; Savin et al., 2010). The most convincingly conserved protein between viral species within these families is that of the DNA packaging terminase subunit 1, a

component of the enzyme complex responsible for incorporating genome DNA into preformed capsids (Davison et al., 2005; Hanson et al., 2024; Savin et al., 2010; Waltzek et al., 2009a) Interestingly, the conservation of this gene among distantly related herpesviruses and tailed bacteriophages (Davison, 1992), along with conserved structural elements in other proteins (Rixon and Schmid, 2014), suggests that all herpesviruses originated from ancient precursors that existed in bacteria.

2.1.2 Genome structure

Despite their distant evolutionary relationships, herpesviruses still share common genome structures. The genomes of herpesviruses consist of a single long double-stranded DNA (dsDNA) molecule, ranging from 124 to 295 kilobase pairs (kbp) in length, with a GC content varying from 31% to 77% (Aoki et al., 2007). Most members of the family Herpesviridae have complex genomes composed of one long or sometimes two short unique regions flanked by internal and terminal repeats containing conserved signals essential for DNA packaging into capsids and cleavage of concatemeric genomes to unit length (Pellett et al., 2011). The number of internal and terminal repeat sequences can vary between species, and these sequences can be lost or duplicated during cell culture passage (Pellett and Bernard, 2013). These observations have led to the classification of six genome types, labelled A to F (Fig. 6) (Pellett et al., 2011). However, In recent years, sequencing of Testudinid herpesvirus 3 (TeHV 3) revealed a seventh class of genome consisting of a long unique region (U_L), extended at its right end by a short unique region (U_S) flanked by an inverted repeat (IR_S and TR_S) and at its left end by a third unique region (U_T) also flanked by an inverted repeat (TR_T and IR_T), yielding the overall configuration TR_T-U_T-IR_T-U_L-IR_S-U_S-TR_S (Fig. 6) (Gandar et al., 2015).

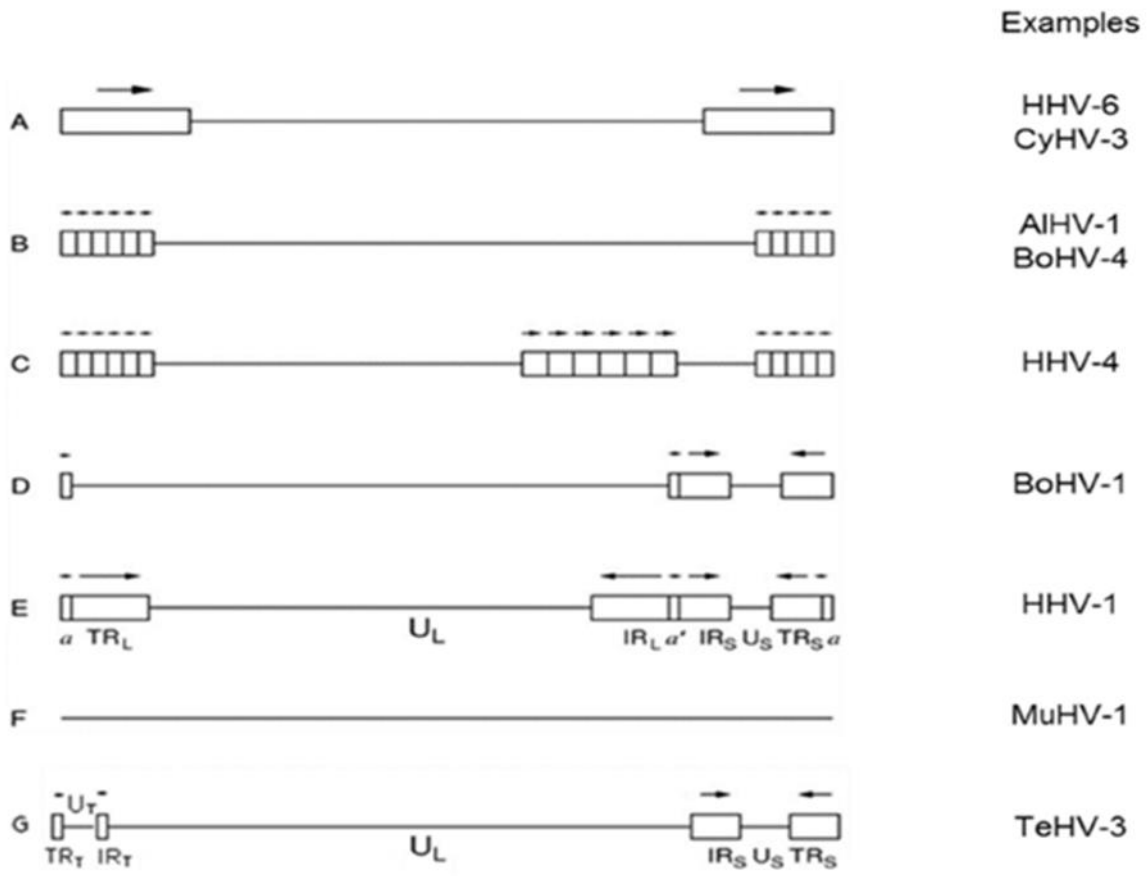

Figure 6 - Classes of herpesvirus genome structures. Classes of herpesvirus genome structures. Unique and repeat regions are shown as horizontal lines and rectangles, respectively. The orientations of repeats are shown by arrows. The nomenclature of unique and repeat regions are indicated for classes E and G. (A) The genome consists of a unique sequence flanked by a direct repeat. (B) The genome has direct repeats at the termini, themselves consisting of variable copy numbers of a tandemly repeated sequence of 0.8–2.3 kb. (C) This structure derives from the class B structure, in which an internal set of direct repeats is present but is unrelated to the terminal set. (D) The genome contains two unique regions (long and short unique regions U_L and U_S), each flanked by inverted repeats (TR_L/IR_L and TR_S/IR_S). U_S can be inverted compared to the U_L giving two different isomers. (E) This class is similar to class D, except that TRL/IRL is much larger and segment inversion gives rise to four equimolar genome isomers. Also, class E genomes are terminally redundant, containing a sequence of a few hundred bp that is repeated directly at the genome termini (a) and inversely at the IR_L-IR_S junction (a'). (F) Terminal repeats are not described for the F class. (G) New genome structure recently described for *Testudinid herpesvirus 3* (TeHV-3) with a third unique region (U_T) (Gandar et al., 2015). *Human herpesvirus 1* (HHV-1), *4* (HHV-4) and *6* (HHV-6), *Alcelaphine herpesvirus 1* (AlHV-1), *Bovine herpesvirus 1* (BoHV-1) and *4* (BoHV-4), *Murine herpesvirus 1* (MuHV-1), *Cyprinid herpesvirus 3* (CyHV-3) and *Testudinid herpesvirus 3* (TeHV-3) were chosen as examples, adapted from (Gandar et al., 2015; King et al., 2012a).

2.1.3 Virion structure

Viruses belonging to the order *Herpesvirales* have historically been defined based on virion structure. From the centre outwards, the structure is as follows: (a) a densely packed core consisting of a single copy of linear double-stranded DNA (dsDNA) genome, encapsulated in an icosahedral nucleocapsid (T=16) with a diameter of 100-130 nm; (b) an amorphous proteinaceous tegument layer; and

(c) a lipid bilayer envelope acquired from the host and bearing various viral glycoproteins (Fig. 7). This architecture is remarkably conserved throughout the order *Herpesvirales* (Davison et al., 2009). It was demonstrated, for example, that the nucleocapsid of *Ictalurid herpesvirus 1* (IcHV-1, family *Alloherpesviridae*) is strikingly similar to that of *Human herpesvirus 1* (HHV-1, also known as herpesvirus simplex 1, family *Herpesviridae*).

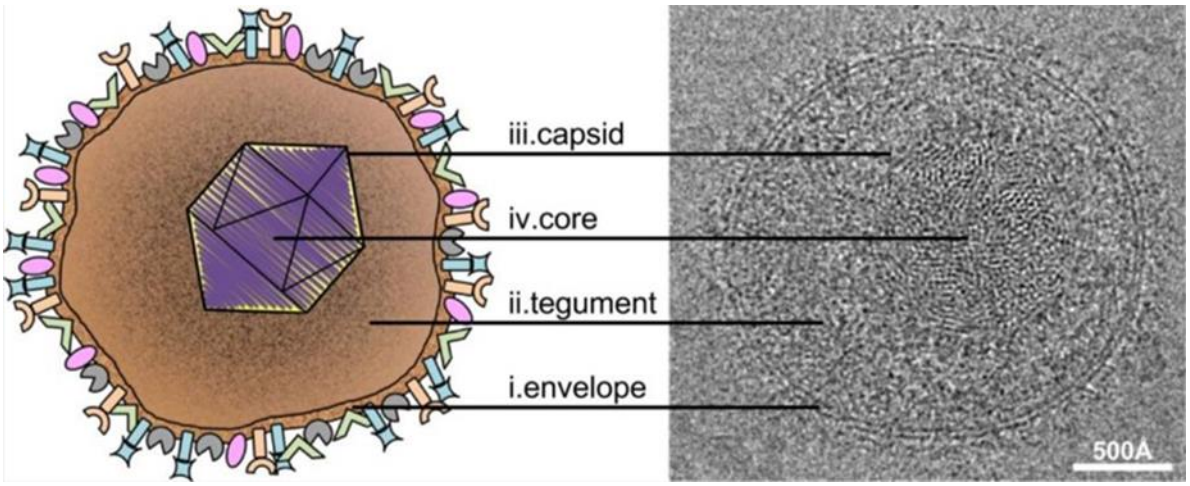

Figure 7 - Herpesvirus morphology. The diagram at left depicts the four major structural components of the Herpes simplex virus type I (HSV-1) virion: (i) the outer envelope studded with various glycoproteins, (ii) the proteinaceous tegument layer, and (iii) the icosahedral nucleocapsid that houses (iv) the dsDNA core. Corresponding features in a cryo-electron micrograph of a virion are indicated at right. Bar = 500 Å, adapted from (Heming et al., 2017).

2.1.4 Main biological properties and lifecycle

In addition to shared morphological traits, in all members of the order *Herpesvirales* exhibit several common biological properties (Ackermann, 2004; Pellett et al., 2011): (i) they encode their own DNA synthesis machinery, including a wide variety of genes involved in the metabolism and synthesis of nucleic acid, such as thymidine kinase, thymidylate synthase, dUTPase, ribonucleotide reductase, DNA polymerase, primase and helicase; (ii) viral DNA replication and nucleocapsid assembly takes place in the nucleus while additional processing to give rise to mature virions occurs in the cytoplasm; (iii) the production of new infective viral progeny usually results in lysis of the host cells; (iv) they can establish lifelong latent infection, which has been described as an absence of regular viral transcription and replication, and a lack of production of infectious virus particles, but presence of intact viral genomic DNA and transcription of latency-associated genes; (v) their ability to undergo long-term latency in immunocompetent hosts is the result of immune evasion mechanisms targeting major elements of the immune system; and (vi) the general herpesvirus replication cycle consists of seven main steps, attachment, penetration, DNA replication, capsid assembly, envelopment, and release (Pellett et al., 2011).

Herpesviruses initiate infection by attaching to host cellular surface receptors via viral surface glycoproteins (Fig. 8). Viruses enter the cell through fusion with the plasma membrane or by endocytosis (fusion of the viral envelope with the endosome membrane) and release the nucleocapsid, coated

by tegument proteins, into the cytoplasm (Lussignol and Esclatine, 2017; Madavaraju et al., 2021). Because of the macromolecular density and highly structured nature of cytoplasm, viral particles are unable to migrate from the cell surface to the nucleus by diffusion alone. For this reason, retrograde transport of the nucleocapsid surrounded by the tegument proceeds along microtubules to the nuclear pores, where the viral linear genome is delivered into the nucleus (Pellett and Bernard, 2013). After forming extrachromosomal episome, the viral genome circularizes and it undergoes methylation, histone modification and chromatinization. This is part of a process that determines whether the virus adopts enters lytic replication or remains in a dormant/inactive state to as part of a latent infection (Cheng et al., 2021) and relies mainly on the nature of chromatinization and the availability and state of particular viral and cellular transcription regulators (Nevels et al., 2011).

During lytic infection, the virus replicates in a host cell and leading to cell lysis and the release of new viral progeny. These new infectious virions go on to infect other cells and/or hosts (Brown, 2017). This lytic replication process exploits cellular transcription machinery for expression of viral genes as a cascade, starting with immediate early (IE), followed by early (E) and late (L) categories. The gene categories include immediate early (α), early (β), leaky-late (γ1), and true late (γ2) genes (Heath and Dembowski, 2022). IE gene expression starts in the absence of *de novo* viral protein synthesis. It is initiated by tegument proteins which interact with cellular transcriptional proteins, such as RNA polymerase II, to activate transcription. IE gene products mainly perform regulatory functions, including inhibition of IE gene expression and activation of E gene transcription (Pellett and Bernard, 2013).

As a result of E gene expression, replication of the viral genome is mediated by viral DNA polymerase, leading to the synthesis of long continuous DNA molecules containing multiple copies of the same DNA sequence linked in tandem (concatemers). Finally, late gene expression results in the generation of structural proteins for assembly of mature virions. Once capsids are assembled in the nucleus, viral genomes are loaded into them, with concatemers cleaved before entry to ensure that a single copy of the viral genome is packaged into each capsid.

Nuclear egress begins with primary envelopment whereby budding at the inner nuclear membrane occurs, with release into the perinuclear space. From there, nucleocapsids exit the nucleus by fusion of the primary envelope with the outer nuclear membrane (de-envelopment). The next assembly steps occur in the cytoplasm and consist of the addition of tegument proteins to the nucleocapsid. Capsids then bud into vesicles belonging to the trans-Golgi network, where tegument addition and secondary envelopment with acquisition of the glycoprotein-studded envelope arise. The progeny virion is finally released from the cell by exocytosis or cell lysis. In alternative models, viral capsids bud into endocytic organelles, that originate from endocytosis of cell membranes containing viral glycoprotein (Ahmad and Wilson, 2020)

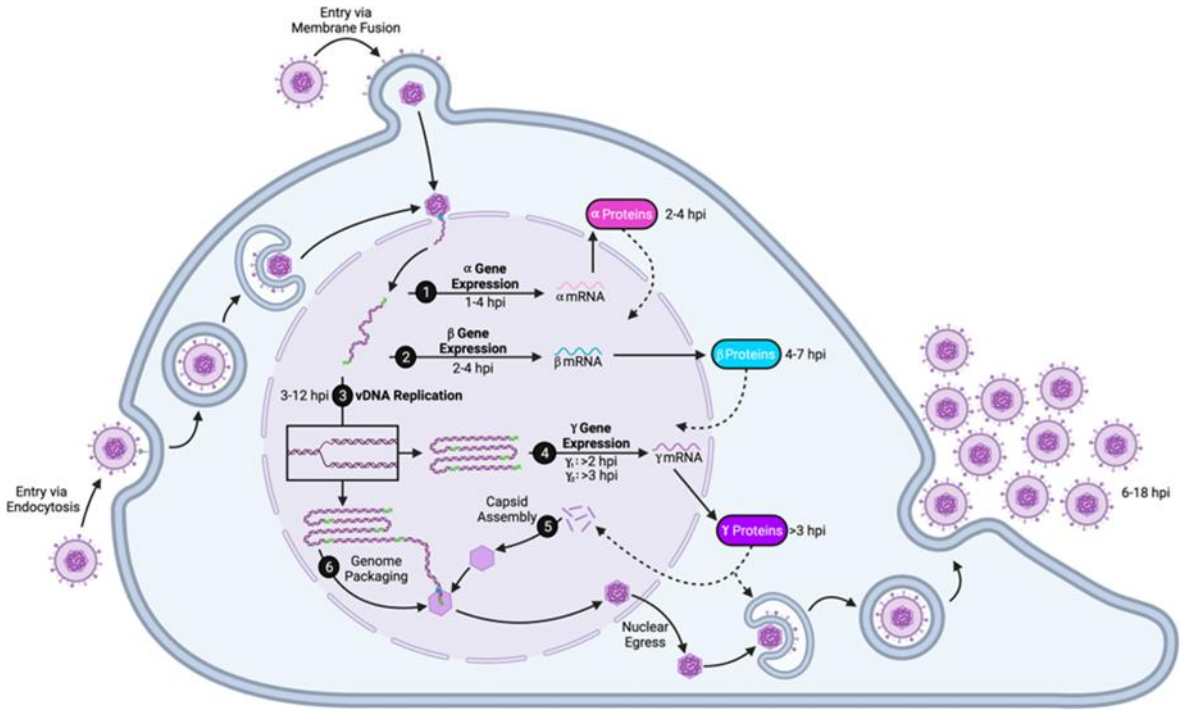

Figure 8 - The HSV-1 infectious cycle. Virions enter the cell via fusion with the host-cell membrane or endocytosis. The capsid docks at the nuclear pore and viral DNA enters the nucleus through the portal in the capsid (drawn in teal above). The HSV-1 genome is then expressed: (1) α genes are expressed upon entry; (2) α gene products drive β transcription; (3) after β protein expression, vDNA replication occurs; (4) γ1 gene expression is amplified, and γ2 gene expression is enabled by DNA replication; (5) capsid proteins, which are γ gene products, assemble; and then (6) replicated genomes are packaged into capsids through the portal. Packaged capsids leave the nucleus through nuclear egress and move through the secretory pathway, obtain an envelope with embedded viral glycoproteins, and nascent virions are released from the cell by exocytosis. Transcript and protein timing pictured above are approximated based on previous studies (Harkness et al., 2014; Honess and Roizman, 1974). Note that the viral genome forms concatemers during replication as indicated above, and unit length genomes (flanked by green) are packaged into capsids. Also note that some models indicate that the viral genome circularizes after entry into the nucleus. Tegument proteins were omitted for simplicity. Figure created using www.biorender.com. hpi, hours post infection; HSV-1, herpes simplex virus type-1, adapted from (Heath and Dembowski, 2022).

2.2 The family Alloherpesviridae

As previously noted, the family *Alloherpesviridae* includes herpesviruses of fish and amphibians. This group of herpesviruses is phylogenetically distant from the better-characterized herpesviruses that mammals, birds and reptiles (members of the family *Herpesviridae*). However, many biological and structural properties are conserved in the order *Herpesvirales*, including genome structure, virus structure, and latency. Furthermore, all known alloherpesviruses typically exhibit a high degree of host specificity which is a biological feature shared by nearly all herpesviruses. However, one big difference is that, unlike members of the family *Herpesviridae*, disease outbreaks associated with members of the family *Alloherpesviridae* are heavily temperature-dependent (Hanson et al., 2024). These, and other features of viruses in the family *Alloherpesviridae* will be described in more detail in the following subsections.

2.2.1 Phylogeny of the family *Alloherpesviridae*

Currently, the family *Alloherpesviridae* is represented by 13 virus species, distributed among four genera: *Cyprinivirus* (recently renamed *Cyvirus*), *Ictalurivirus* (recently renamed *Ictavirus*), *Salmonivirus* (recently renamed *Salmovirus*) which all comprise of viruses that infect fish, and *Batrachovirus* (recently renamed *Batravirus*), which comprises of viruses that infect amphibians. For consistency with nomenclature used in papers published as part of this Ph.D. thesis, (occurring before the name changes), we will apply the previous nomenclature in this introduction. Table 3 includes classified and unclassified fish and amphibian alloherpesviruses according to the ICTV (Lefkowitz et al., 2018).

Table 3 – A list of classified and unclassified fish and amphibian alloherpesviruses

Genus	Viral species (acronym)	Alternative viral name (s)	Susceptible host (s)
Batrachovirus	*Ranid herpesvirus* 1 (RaHV-1)	Lucké tumor herpesvirus	Northern leopard frog (*Lithobates pipiens*)
	Ranid herpesvirus 2 (RaHV-2)	Frog virus 4	Northern leopard frog (*Lithobates pipiens*)
	Ranid herpesvirus 3 (RaHV-3)	-	Common frog (*Rana temporaria*)
Cyprinivirus	*Anguillid herpesvirus* 1 (AngHV-1)	European eel herpesvirus (HVA)	Japanese and European eel (*Anguilla japonica* and *A. anguilla*)
	Cyprinid herpesvirus 1 (CyHV-1)	Carp pox herpesvirus	Common carp (*Cyprinus carpio*)
	Cyprinid herpesvirus 2 (CyHV-2)	goldfish haematopoietic necrosis virus	Goldfish (*Carassius auratus*), Gibel carp (*Carassius gibelio*) and various other *Carassius spp.*
	Cyprinid herpesvirus 3 (CyHV-3)	Koi herpesvirus	Common carp (*Cyprinus carpio*)
Ictalurivirus	*Acipenserid herpesvirus* 2 (AciHV-2)	White sturgeon herpesvirus 2	Sturgeon (*Acipenser spp.*)
	Ictalurid herpesvirus 1 (IcHV-1)	Channel catfish virus	Channel catfish (*Ictalurus punctatus*)
	Ictaluried herpesvirus 2 (IcHV-2)	Ictalurus melas herpesvirus	Black bullhead (*Ameiurus melas*)
Salmonivirus	*Salmonid herpesvirus* 1 (SaHV-1)	Herpesvirus salmonis	Rainbow trout (*Oncorhynchus mykiss*)
	Salmonid herpesvirus 2 (SaHV-2)	Oncorhynchus masou herpesvirus	Salmon and trout (*Oncorhynchus spp.*)
	Salmonid herpesvirus 3 (SaHV-3)	Epizootic epitheliotropic disease virus	Lake trout (*Salvelinus namaycush*)
Unclassified by ICTV	*Acipenserid herpesvirus* 1 (AciHV-1)	White sturgeon herpesvirus 1	white sturgeon (*Acipenser transmontanus*)
	Cyprinid herpesvirus 4 (CyHV-4)	Sichel herpesvirus	Sichel (*Pelecus cultratus*)
	Esocid herpesvirus 1 (EsHV-1)	Blue spot disease virus	Northern pike (*Esox lucius*)
	Gadid herpesvirus 1 (GaHV-1)	Atlantic cod herpesvirus	Atlantic cod (*Gadus morhua*)

Genus	Viral species (acronym)	Alternative viral name (s)	Susceptible host (s)
	Percid herpesvirus 2 (PeHV-2)	European perch herpesvirus	European perch (*Perca fluviatilis*)
	Salmonid herpesvirus 4 (SalHV-4)	Atlantic salmon papillomatosis virus	Atlantic salmon (*Salmo salar*)
	Salmonid herpesvirus 5 (SalHV-5)	Namaycush herpesvirus	Lake trout (*Salvelinus namaycush*)
	Silurid herpesvirus 1 (SiHV-1)	-	Glass catfish (*Kryptopterus bicirrhis*)
	Bufonid herpesvirus 1 (BfHV-1)	-	Common toad (*Bufo bufo*)

The genus *Cyprinivirus* comprises the alloherpesviruses of cyprinids (CyHV-1; 2 and 3) and that of eel (AngHV-1). The genus *Ictalurivirus* includes viruses isolated from catfish (*Ictalurid her pesvirus* 1 and 2 [IcHV]) and sturgeon species (*Acipenserid herpesvirus* 2 [AciHV]), while the genus *Salmonivirus* consists of herpesviruses of salmonids (*Salmonid herpesvirus* 1; 2 and 3 [SalHV]) (Fig. 9A) and Table 3. Official taxonomical classification of nine more viruses is still pending as only partial sequence data are available for these species. However, according to initial phylogenetic analyses based on partial genome sequence data, these viruses undoubtedly belong to the family *Alloherpesviridae*. Furthermore, some of these unclassified species clearly cluster into already existing genera e.g., SalHV-4 and SalHV-5 will likely be added to the genus *Salmonivirus*, and for the same reason, CyHV-4 will likely be added to the genus *Cyprinivirus* (Fig. 9B). On the other hand, other viruses (e.g., AciHV-1; EsHV-1) cannot be grouped with viruses in any of the existing genera within the family *Alloherpesviridae*.

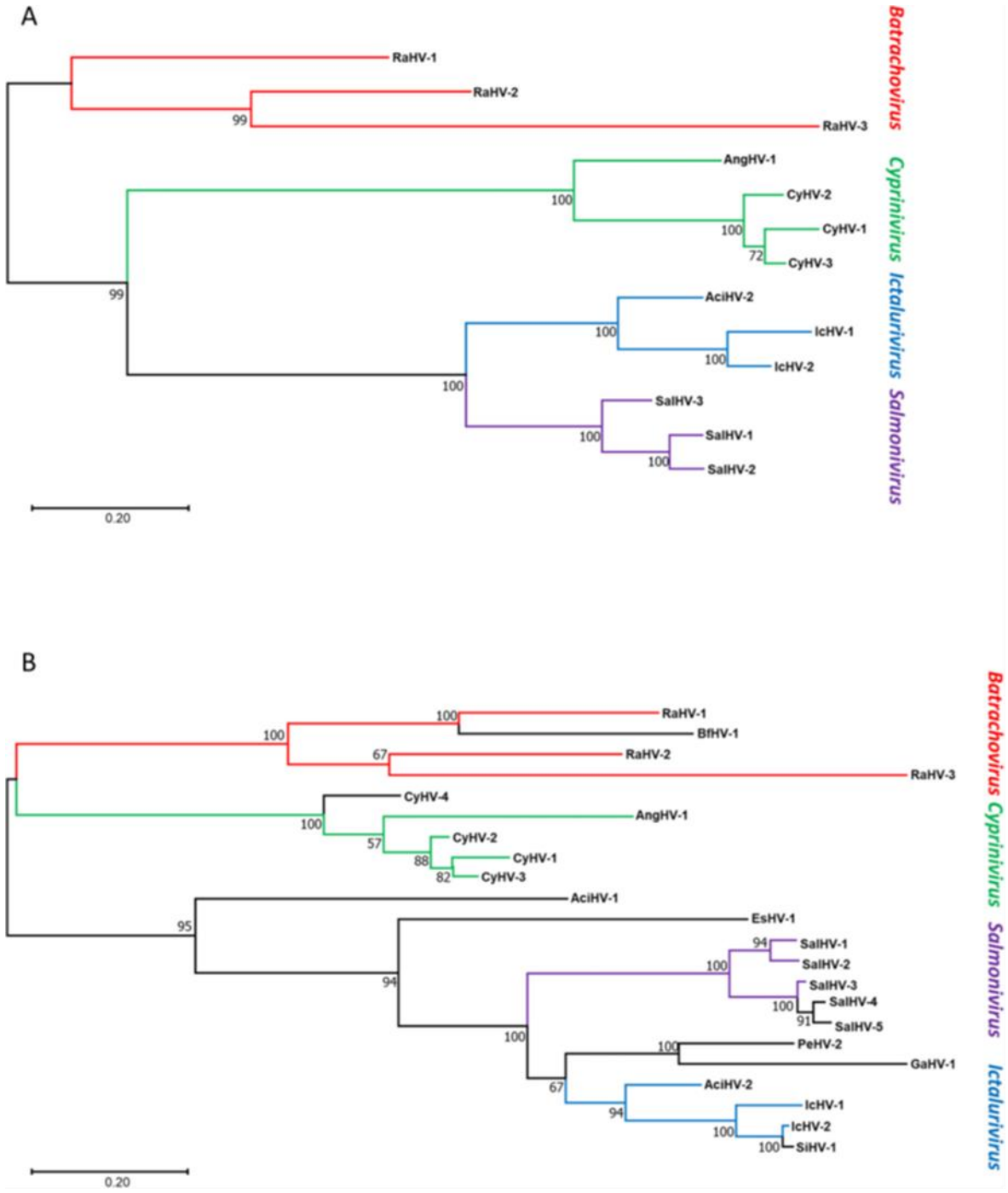

Figure 9 - Phylogenetic tree of the family *Alloherpesviridae*. The analyses were based on the Bayesian analysis (WAG amino acid model) of the deduced amino acid sequences of DNA polymerase genes (134 and 113 amino acid residues, respectively for panel A and B). High statistical values confirm the topology of the trees. The four main genera within the family *Alloherpesviridae* are designated by different colored lines on the trees. Panel A: phylogenetic tree of the classified viral species in the family *Alloherpesviridae*. Panel B: phylogenetic tree of the classified and unclassified potential members of the family *Alloherpesviridae*. AciHV: *Acipenserid herpesvirus*; AngHV: *Anguillid herpesvirus*; BfHV: *Bufonid herpesvirus*; CyHV: *Cyprinid herpesvirus*; EsHV: *Esocid herpesvirus*; GaHV: *Gadid herpesvirus*; IcHV: *Ictalurid herpesvirus*; PeHV: *Percid herpesvirus*; RaHV: *Ranid herpesvirus*; SalHV: *Salmonid herpesvirus*; SiHV: *Silurid herpesvirus*. GenBank and RefSeq accession numbers: AciHV-1: EF685903; AciHV-2: FJ815289; AngHV-1: NC_013668; BfHV-1: MF143550; CyHV-1: NC_019491; CyHV-2: NC_019495; CyHV-3: NC_009127; CyHV-4: KM357278; EsHV-1: KX198667;

GaHV-1: HQ857783; IcHV-1: NC_001493; IcHV-2: NC_036579; PeHV-2: MG570129; RaHV-1: NC_008211; RaHV-2: NC_008210; RaHV-3: NC_034618; SalHV-1: EU349273; SalHV-2: FJ641908; SalHV-3: EU349277; SalHV-4: JX886029; SalHV-5: KP686090; SiHV-1: MH048901. From (Boutier et al., 2021).

Interestingly, with the exception of one herpesvirus identified in shark species (Hanson et al., 2011), all currently known fish herpesviruses occur in bony fish. Further genomic data will be needed from this virus species in order to establish its relationship to other fish herpesviruses and ultimate taxonomic classification. Interestingly, in addition these viruses, it has become apparent that many fish species have experienced integration of alloherpesvirus sequences into their genomes through fusion with Piggyback-like transposons (Aswad and Katzourakis, 2017; Inoue et al., 2018, 2017). Interestingly, these may represent additional lineages within the family *Alloherpesviridae*, but it is unclear if they are derived from older, extinct species, or if they are closely related to novel extant species, that are yet to be described.

The common ancestry within the family is well supported by the identification of 12 core genes present in all members (Davison et al., 2013). This lower number of conserved genes, compared to the family *Herpesviridae* (43 core genes), suggests that the last common ancestor of alloherpesviruses is considerably older (van Beurden et al., 2010). Interestingly, species within the genera *Cyprinivirus* and *Ictalurivirus* are able to infect hosts from two different superorders (*Elopomorpha* and *Ostariophysi*) or subclasses (*Chondrostei* and *Neopterygii*), respectively. This observation supports a more recent viral species divergence within the family *Alloherpesviridae*, that is somewhat less connected to co-speciation with their hosts, compared to species within the family *Herpesviridae*. Furthermore, even within viral genera, the phylogenetic relationship between AngHV-1 and other cypriniviruses is much closer than the relationship between their hosts, again suggesting that one of these lineages emerged via a host jump rather than co-speciation with their hosts (Donohoe et al., 2021; Waltzek et al., 2009a).

2.2.2 Genomes of alloherpesviruses

The genome size of alloherpesviruses ranges from 134 to 295kb containing 90–186 Open Reading Frames (ORFs). Within the family *Alloherpesviridae* there are significant differences in the genome size of viruses belonging to different genera. Species within the genus *Ictaluriviruses* have the smallest genomes ranging from 134 to 149 kb, while the estimated genome size of *Salmoniviruses* is around 170 kb. The genomes of the genus *Batrachoviruses* range 200–232 kb, and the largest genomes are presented by *Cypriniviruses* ranging from 245 to 295 kb. Among the herpesviruses, the *Cyprinid herpesvirus 3* (CyHV-3) has the largest genome size of 295 kb. As described earlier, species within the family *Alloherpesviridae* have 12 core genes with notable levels of amino acid sequence conservation. These genes play roles in DNA replication, including the catalytic subunit of DNA polymerase, the helicase-primase helicase subunit, and the helicase-primase primase subunit. Additionally, they contribute to DNA packaging (DNA packaging terminase subunit 1) and are involved in capsid morphogenesis, encompassing

the major capsid protein, capsid triplex subunit 2, and capsid maturation protease (Davison et al., 2013; Donohoe et al., 2021; Walker et al., 2022).

The structure of alloherpesvirus genomes is less diverse than species within the family *Herpesviridae*. Most of the alloherpesvirus genomes contain only one unique region, which is flanked by direct terminal repeats (TR) (Boutier et al., 2021), consistent with herpesvirus structure A, in Fig. 6 . However, although not fully sequenced yet, hybridization experiments have revealed that the genome structure of SalHV-1 is slightly different, consisting of a short unique region (US) flanked by an inverted repeats (RS) and a longer unique region (UL) which is not flanked by a detectable repeat (Davison, 1998). Interestingly, this arrangement is similar to mammalian alphaherpesviruses in the *Varicellovirus* genus, such as pseudorabies virus, equine herpesvirus 1, bovine herpesvirus 1, and varicella-zoster virus (consistent with herpesvirus structure D, Fig. 6). Furthermore, within the family *Alloherpesviridae* the genomes of viral species that infect amphibian hosts appear to lack any repeat regions (consistent with herpesvirus structure F, Fig. 6). Full genome sequences are available for eleven viruses within the family *Alloherpesviridae* including some non-classified viruses (Table 4).

Table 4 - Data on complete genome sequences of fish and amphibian alloherpesviruses

Viral species	Genome size	Genome structure	Structures size	GC%	ORFs (No)	GenBank Genome Accession
Anguillid herpesvirus 1	248.53 kbp	TR-U-TR	U: 226 kbp TR: 11 kbp	53.0	134	NC_013668.3
Cyprinid herpesvirus 1	291.14 kbp	TR-U-TR	U: 224 kbp TR: 33 kbp	51.3	143	NC_019491.1
Cyprinid herpesvirus 2	290.3 kbp	TR-U-TR	U: 260 kbp TR: 15 kbp	51.7	154	NC_019495.1
Cyprinid herpesvirus 3	295.15 kbp	TR-U-TR	U: 250 kbp TR: 22 kbp	59.2	163	NC_009127.1
Ictalurid herpesvirus 1	134.23 kbp	TR-U-TR	U: 97 kbp TR: 18 kbp	56.2	90	NC_001493.2
Ictalurid herpesvirus 2	142.92 kbp	TR-U-TR	U: 101 kbp TR: 20 kbp	53.8	91	NC_036579.1
Silurid herpesvirus 1	149.34 kbp	TR-U-TR	U :100 kbp TR :24 kbp	53.7	94	MH048901.1
Ranid herpesvirus 1	220.86 kbp	TR-U-TR	U: 219 kbp TR: 0.6 kbp	54.6	132	NC_008211.1
Ranid herpesvirus 2	231.8 kbp	TR-U-TR	U: 230 kbp TR: 1 kbp	52.8	147	NC_008210.1
Ranid herpesvirus 3	207.91 kbp	U	U: 207 kbp	41.8	186	NC_034618.1
Bufonid herpesvirus 1	158.25 kbp	U	U: 158	40.6	152	MF143550.1

2.2.3 Biological features of alloherpesvirus

Members of the family *Alloherpesviridae* which infect animals that live in aquatic environments share several biological traits that distinguish them from members of the family *Herpesviridae* infecting mammals, birds, and reptiles which live in terrestrial environments (*Herpesviridae*).

Firstly, while members of the family *Herpesviridae* generally cause only mild pathogenicity in their natural immunocompetent hosts, members of the family *Alloherpesviridae* infecting fish generally cause highly contagious and pathogenic disease outbreaks among their main host populations with high mortality rates, even up to 100% mortality. This substantially higher virulence may be due to either a lower degree of adaptation to their hosts, or to factors linked to intensive fish farming practices, such as low genetic diversity and high-density rearing conditions. Furthermore, age-dependent sensitivity and permissivity have been reported for several alloherpesviruses that infect fish. For example, AciHV-1, AciHV-2, CyHV-1, CyHV-2, SalHV-2, SalHV-3 and IcHV-2 are especially pathogenic for hosts at earlier developmental stages (S. van Beurden et al., 2012; Hanson et al., 2011), with CyHV-3 being a notable exception to this pattern (Ronsmans et al., 2014).

Secondly, the tropism most members of the family *Herpesviridae* is known to be restricted to their natural host species or closely related species. In contrast, for members of the family *Alloherpesviridae* that infect fish, several fish species have been thought to play a role in their epidemiology. For example, AngHV-1 (Nguyen Thuc et al., 2016) and CyHV-3 (Kempter et al., 2012; Kielpinski et al., 2010) genomes can be detected in a large number of sympatric fish species (i.e. fish also present in their environment). However, given the absence of any clinical disease or pathogenies, the extent to which these viruses to replicate in these sympatric species, and hence whether they may serve as vectors in viral transmission, remains to be investigated.

Thirdly, as opposed to mammalian and avian hosts, the hosts of alloherpesviruses are poikilothermic, implying that their body temperature cannot be naturally maintained constant at constant temperatures, that are independent of environmental temperatures. Thus, the environmental temperature heavily influences the outcome of infection, both *in vitro* and *in vivo*. For example, the replication of AngHV-1 in eel kidney 1 (EK-1) cells occurs at temperatures between 15-30 °C, with an optimum around 20-25 °C (Beurden S. J. et al., 2012; Sano et al., 1990). In contrast, low temperatures facilitates RaHV-1 replication *in vivo*, whereas induction of tumor metastasis is promoted by high temperatures (McKinnell and Tarin, 1984). Furthermore, CyHV-3 outbreaks typically occur in warm environmental water temperature (18-28 °C) (Ilouze et al., 2012) while SalHV-3 outbreaks occur at much lower temperatures (6-15 °C) (S. van Beurden et al., 2012). If the ambient water temperature is suboptimal for these events to occur, infection caused by fish alloherpesviruses is generally less severe or even asymptomatic, providing an explanation for the seasonal occurrence of disease caused by some alloherpesviruses of fish (Gilad et al., 2003). In practice, these biological traits have been exploited successfully as a means of disease mitigation, by subjecting host species to water temperatures outside of the optimum ranges which these viruses can cause disease. Striking examples include the successful reduction of disease caused by CyHV-3 when hosts are subjected to increased water temperatures (Ronen et al., 2003), and similar outcome during AngHV-1 infections, when hosts are subjected to decreased water temperature (Haenen et al., 2002).

And lastly, mounting data suggests that alloherpesviruses can establish latent infections. Evidence supporting this hypothesis has been provided for CyHV-1, CyHV-2, CyHV-3, SalHV-2, IcHV-1 and AngHV-1 (Chai et al., 2020; Hanson et al., 2016, 2011). Given that a latent state may be interrupted by transient virus reactivation, the balance between productive lytic infection and latency is likely to be intricately associated to host biology with water temperature playing a critical role in the transition from productive to latent infections (Hanson et al., 2024).

2.2.4 Herpesviruses affecting economically important fish species

Members of the family *Alloherpesviridae* cause severe diseases in fish species that are important for aquaculture, including carp, salmon, catfish, sturgeon (Table 3). Even though these viruses can also infect sympatric species beyond their primary host, pathogenic disease caused by viruses is highly host-specific, with disease mainly occurring in specific fish species or closely related fish species within the same genus (Dharan et al., 2022).

The very first herpesvirus that was identified as a threat to the aquaculture industry was IcHV-1, which generated mass mortalities among catfish in the US, mainly impacting fish early developmental stages. Historically, this virus has been regarded as the prototypic fish herpesvirus However, IcHV-1 has predominantly only affected the catfish industry in the US, and the control of this disease was achieved through modification of aquaculture facility management practices (Hanson et al., 2011; Kucuktas and Brady, 1999). In the late 1990s, mass mortalities in cultured carp caused by CyHV-3 urged the scientific community to investigate this emerging disease (Bretzinger et al., 1999; Hedrick et al., 2000; Pearson, 2004; Waltzek et al., 2005). Due to its economic impact on carp culture and its rapid spread across the world, CyHV-3 was listed as a notifiable disease by the World Organization for Animal Health OIE (Michel et al., 2010). Since then, an increased interest in understanding CyHV-3 emerged with the aim of protecting common and koi carp from this devastating virus. Incidentally, the common carp (*Cyprinus carpio*) had been already selected for fundamental research on fish immunology, making it a perfect model for applied research to study host-virus interactions (Adamek et al., 2018; Rakus et al., 2013). Consequently, advancement in the understanding of CyHV-3 including genomics (Aoki et al., 2007; Gao et al., 2018), biological properties between strains (Gao et al., 2023), evolution (Donohoe et al., 2021; Gao et al., 2023) pathogenesis (Costes et al., 2009, 2008; Raj et al., 2011; Ronsmans et al., 2014), epidemiology (Gilad et al., 2004; St-Hilaire et al., 2005) host interaction (Diallo et al., 2022; Ouyang et al., 2013; Rakus et al., 2017; Sunarto et al., 2012) and disease mitigation (Boutier et al., 2015a; Ronen et al., 2003) knowledge on CyHV-3 now far exceeds that of any other of the alloherpesviruses leading to now be considered the archetypal fish herpesvirus (Boutier et al., 2015b).

Around the same time, *Cyprinid herpesvirus 2* (CyHV-2), closely related to the well-studied CyHV-3, began to attract the attention of researchers (Jung and Miyazaki, 1995; Groff et al., 1998). CyHV-2 primarily causes significant mortality in ornamental goldfish (Goodwin et al., 2006a) and

prussian carp (Luo et al., 2013), - both of which are from the genus *Carassius*, leading to substantial economic losses worldwide. Consequently, an urgent need to develop strategies to control the spread of CyHV-2 and mitigate these economic impacts emerged (Zhang et al., 2016). However, compared to CyHV-3, research on CyHV-2 is less comprehensive. Specifically, the host range and the stages of host susceptibility to infection remain unclear, the mode of transmission and pathogenic mechanisms require further investigation, and the development of vaccines and specific disease management strategies is still needed (Thangaraj et al., 2021). In short, despite various approaches being adopted, CyHV-2 continues to pose a significant epidemic threat, causing ongoing losses and impacts on the aquaculture industry. It is with this in mind, this Ph.D research project was developed, with the aim address some of these major knowledge gaps using the CyHV-3 experience as a useful template to propel CyHV-2 knowledge beyond the current state of the art. This virus, which is be the main focus of this Ph.D. thesis, will be introduced in more detail in the next section.

3. The *Cyprinid herpesvirus 2*

3.1 General description

3.1.1 Structure and morphogenesis

Like all members of the order *Herpesvirales*, CyHV-2 possesses an icosahedral capsid housing double-stranded DNA, enveloped by a lipid bilayer containing viral glycoproteins. The virus replicates most efficiently within the hematopoietic cells of the spleen and kidney, as well as within the gills of infected fish (Hedrick et al., 2000; Xu et al., 2013). CyHV-2 morphogenesis is a complex process similar to that described for mammalian herpesviruses. The morphology of CyHV-2 viral particles was initially delineated in the first Japanese reports (Jung and Miyazaki, 1995). Within infected cells, virions within the nucleus adopt a distinctive spherical or hexagonal shape, with the nucleocapsid exhibiting a diameter ranging from 115 to 117 nm. Concurrently, rounded enveloped virus particles, measuring 170 to 220 nm in diameter, accumulate within the cytoplasm. Similar descriptions have been echoed in the electron microscopy findings of several research teams (Jeffery et al., 2007; Luo et al., 2013; Stephens et al., 2004). Wu *et al*. employed high-magnification TEM to observe virus particles at various stages of assembly within kidney cells and further described the morphological characteristics of the virus particles (Wu et al., 2013). As observed previously, within the nucleus, naked herpetiform virus nucleocapsids with a diameter of approximately 95-110 nm were evident, while in the cytoplasm, enveloped virus particles measuring approximately 170-200 nm in diameter accumulated (Fig. 10). Notably, their results suggested that the Golgi apparatus plays an important role in the maturation of CyHV-2, with final maturation occurring by the budding immature CyHV-2 viral particles into trans-Golgi network vesicles containing viral glycoproteins. In 2014, Lovy *et al*. used electron microscopy to describe histological samples (preserved with 10% formalin) in detail (Lovy and Friend, 2014). Similarly, three types of virions can be observed in the nucleus of infected cells: capsids with a central dense core, empty capsids and capsids with a concentric linear density. In the cytoplasm, aggregates of capsids with

a dense core were apparent, and capsids within host membrane-bound vesicles or capsids within a membrane-derived envelope were observed. Similar findings were provided by Xu *et al* and Jiang *et al* (Jiang et al., 2015; Xu et al., 2013).

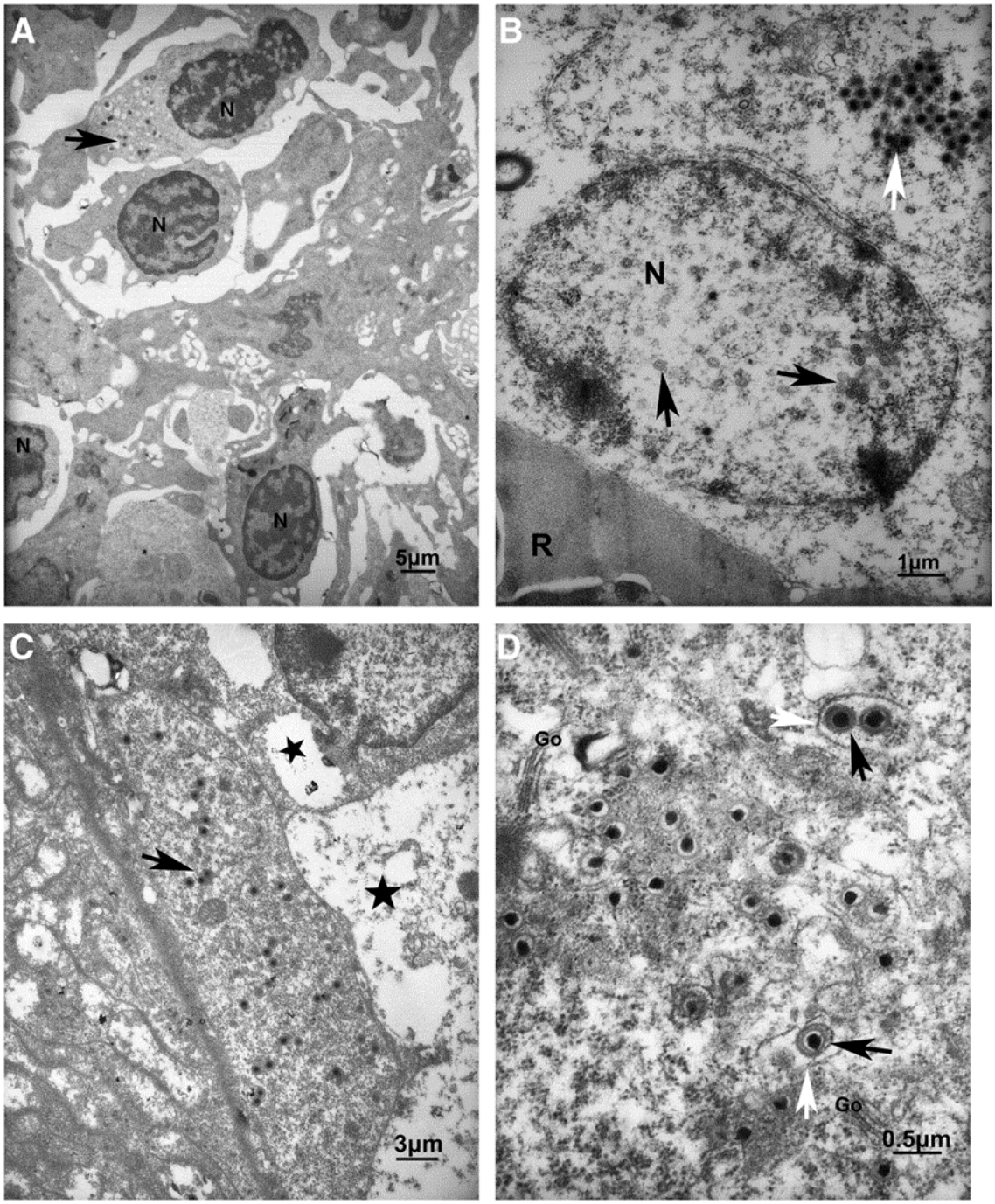

Figure 10 - Ultrathin sections of gill (A), kidney (B, D) and spleen (C) from diseased C. gibelio infected with CyHV-2 showing ultrastructural characters of infected cells and tissues. Many virus particles of CyHV-2 occur in infected leukocytes in gill (A) and hematopoietic cells in kidney (B, D) or spleen (C). (1) Karyopyknosis was observed in the infected leukocyte (black arrow) of gill tissue (A). Nucleus (N). (2) In kidney (B), hematopoietic cells evidenced marginal chromatin and karyorrhexis and many CyHV-2 particles being assembled in both nucleus (black arrows) and cytoplasm (white arrows). (3) In splenic pulps (C), many splenocytes were necrotized showing nuclear degeneration evidenced by pyknosis and karyorrhexis. Cytoplasmic vacuolation (★) was obvious in CyHV-2-infected cells of the spleen (C). (4)

Detailed images of viruses multiplying and assembling in hematopoietic cells of kidney (D) can be seen at higher magnification. There is some evidence of Golgi apparatus (Go) associated with virus assemblage, and occurrence of some mature virus, whose finished packaging (black arrows) were observed in an enveloped virion within a cellular vesicle (white arrow). Adapted from (Wu et al., 2013).

3.1.2 Genome

The first comprehensively characterized strain of CyHV-2 is ST-J1 (Sat-1), which was isolated in 1992 from an ornamental goldfish afflicted with herpesviral hematopoietic necrosis in Japan (Davison et al., 2013; Jung and Miyazaki, 1995). Since its isolation, ST-J1 has been regarded as the well-studied standard strain for subsequent genome comparisons (Liu et al., 2018; Yang et al., 2022). The ST-J1 strain was the first CyHV-2 strain to be sequenced, and consequently it has been designated as the CyHV-2 genome reference sequence on GeneBank (Accession: NC_019495.1). The sequencing of the ST-J1 strain genome revealed that the full length of the CyHV-2 genome is approximately 290 kb and contains approximately 150 protein-coding genes (including 12 core ORFs) (Davison et al., 2013). This also revealed that this virus has the same genome structure as CyHV-1 and CyHV-3, consisting of a unique region flanked at each terminus by a sizeable direct repeat. The CyHV-2 terminal repeats contain four protein coding genes (ORF5, ORF6, ORF7 and ORF8) (Fig. 11). In addition, it has 6 paralogous gene families, and the GC content of the genome is approximately 51.7%. Subsequent sequencing of additional strains revealed various mutations relative to the ST-J1 sequence, including single-nucleotide mutations, insertions, deletions, and rearrangements, but overall sequence identity remains high (>95%). For example. in 2015, a newly isolated CyHV-2 variant (SY-C1) was found to share a high sequence identity of 98.8% with the full-length genome of ST-J1 (L. Li et al., 2015), and similar identity with other strains such as SY (Liu et al., 2018) and SH-01 (Yang et al., 2022) (although the later has not been made publicly available on GeneBank). In total, in addition to the CyHV-2 reference strain, there are now five fully sequenced genomes classified as CyHV-2 strains on NCBI Viral Genome Browser (available here). Notably, these genomes, obtained from various geographical origins exhibit highly similar structures, with the majority of genes remaining unchanged. An additional virus isolated from Crucian Carp, which is referred to as *Crucian carp herpesvirus* (CaHV), is almost certainly another strain of CyHV-2, rather than another separate viral species. Although compared to other CyHV-2 strains, it does exhibit notable changes, including insertions and the apparent loss of terminal repeats, it still exhibits high sequence identity with the CyHV-2 (Zeng et al., 2016). Furthermore, comparing DNA polymerase, Terminase and Helicase, protein sequences between CaHV and other CyHV-2 strains revealed almost no difference in these highly conserved core genes. (Donohoe et al., 2021). However, as of the preparation of this thesis, the CaHV genome sequence is not currently listed among the fully sequenced CyHV-2 genome strains in the NCBI Viral Genome Browser.

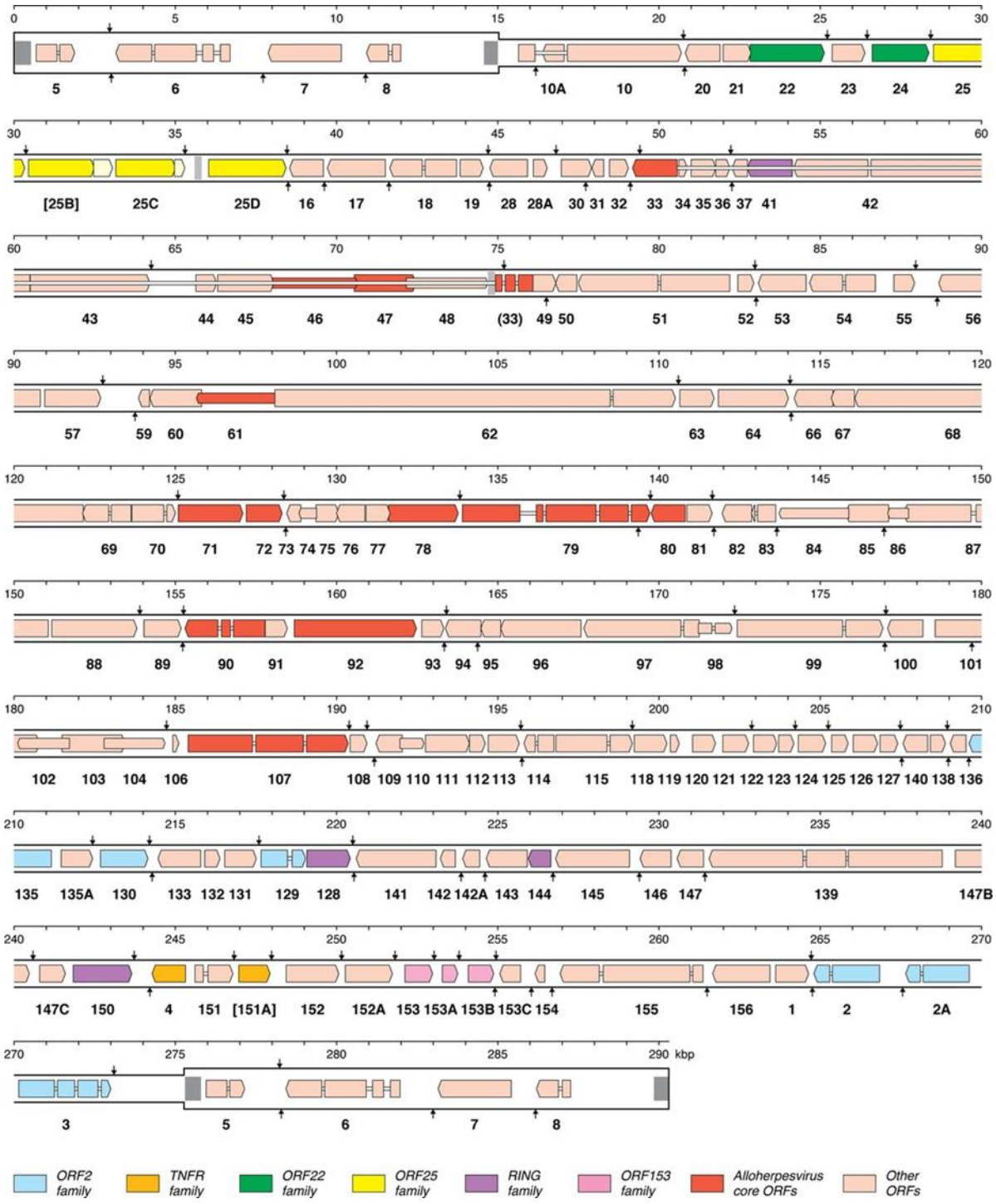

Figure 11 – CyHV-2 genome map. The terminal direct repeat (TR) is shown in a thicker format than the unique region (U). ORFs predicted to encode functional proteins are indicated by colored arrows (see the key at the foot), with nomenclature lacking the ORF prefix given below. Introns are shown as narrow white bars. Colors of protein-coding regions indicate core ORFs that are convincingly conserved among alloherpesviruses, families of related ORFs, and other ORFs. Telomere-like repeats at the ends of TR are shown by gray-shaded blocks. Predicted poly(A) sites are indicated by vertical arrows above and below the genome for rightward- and leftward-oriented ORFs, respectively. Inverted repeats at approximately 36 and 75 kbp are indicated by light-gray-shaded blocks. Names of fragmented ORFs are given in square brackets, with the ORFs depicted as intact. Pale yellow ORFs downstream from ORF25B and ORF25C represent remnants of additional ORFs in the ORF25 family. From (Davison et al., 2013).

3.1.3 Genotypes

To date, six complete genomes of CyHV-2 isolates have been sequenced, and listed on the NCBI Viral Genome Browser, these include ST-J1 (JQ815364.1 or NC_019495.1, which are identical), SY-C1 (KM200722.1), SY (KT387800.1), CNDF-TB2015 (MN201961.1), YZ-01 (MK260012.1), YC-01 (MN593216.1). Among these, ST-J1 originates from goldfish, while CNDF-TB2015 and YZ-01 are sourced from crucian carp, and SY-C1, SY, and YC-01 are derived from gibel carp. Based on genetic differences, Li *et al*. proposed the division of CyHV-2 into two distinct genotypes: the China genotype (C genotype) and the Japan genotype (J genotype), based on the locations where they were isolated [13]. However, these two genotypes exhibit a high sequence identity. Moreover, molecular epidemiological surveys have suggested that the predominant CyHV-2 genotypes circulating in mainland China resembles the C genotype more closely than the J genotype. Alternative CyHV-2 genotype groupings have also been proposed by *Ito et al.* based on a genomic region, referred to as marker A (mA) (Ito et al., 2017), which they used to categorize CyHV-2 isolates into four distinct genotypes. However, as additional strains of CyHV-2 are sequenced, based on the extent of genetic diversity among CyHV-2 strains, genotype classification systems may need to be modified further.

3.1.4 Transcriptome

As mentioned previously, Herpesvirus gene transcription and expression follow a coordinated temporal pattern upon infection of permissive cells. Immediate-early (IE) genes are first transcribed and regulate the subsequent expression of the following genes. Early (E) genes encode enzymes and proteins involved in the interaction with host cell metabolism and the viral DNA replication complex. Finally, the late (L) genes are mainly dependent (true L genes) on viral DNA synthesis, and primarily encode the viral structural proteins (Mettenleiter, 2004; Mettenleiter et al., 2009). In 2009, Tombacz *et al*. developed and applied a quantitative reverse transcriptase-based real-time PCR technique to profile transcription from the whole-genome of pseudorabies virus (PRV; a mammalian herpesvirus classified in subfamily *Alphaherpesvirinae*, family *Herpesviridae*) after lytic infection in porcine kidney cells (Tombácz et al., 2009). Firstly, gene transcription was studied by RT-PCR or RT-qPCR during the early hours post-infection (hpi). Secondly, protein synthesis inhibitor cycloheximide (CHX) and viral DNA polymerase inhibitor cytosine-β-arabinofuranoside (Ara-C) or phosphonoacetic acid (PAA) can be used to block de novo protein synthesis and viral DNA replication, respectively. In the presence of CHX, only IE genes are transcribed whereas in the presence of Ara-C or PAA, only IE and E genes are transcribed, but not the true L genes. Tang *et al*. utilized this approach to analyse the genome-wide gene transcription of CyHV-2 (Tang et al., 2020). By inhibiting protein synthesis or viral DNA replication during CyHV-2 infections, five CyHV-2 IE genes, thirty-four CyHV-2 E genes, and thirty-nine CyHV-2 L genes were identified. In general, all IE genes were transcribed at 0.5 hpi, most E genes between 1 and 2 hpi, and most L genes at 6 hpi. Additionally, among the five CyHV-2 IE genes, two (ORF54 and ORF155) are homologs of IE genes identified in CyHV-3, which is the closest known related virus to

CyHV-2 (Ilouze et al., 2012), indicating that these two viruses may employ similar processes in the early stages of infection.

3.1.5 Proteome

Comparisons of orthologous ORFs between alloherpesviruses, as well as bioinformatic predictions of protein properties, enable putative insight into the functions of some proteins (Davison et al., 2013; Liu et al., 2018). However, as of now, only a limited number of CyHV-2 proteins have been identified and characterized using specific polyclonal antibodies or monoclonal antibodies (mAbs). For instance, several proteins including pORF25 (Zhou et al., 2015), pORF146 (Cao et al., 2019), pORF72, pORF66, pORF81, and pORF82 (Li et al., 2019) have been identified as promising vaccine candidates against CyHV-2. Moreover, proteins such as pORF72 (Kong et al., 2017), pORF92 (Shen et al., 2018), pORF66 (Guo et al., 2022), and pORF121 (Gao et al., 2022) have been demonstrated to be useful in immunological detection of CyHV-2. In 2020, Gao *et al*. successfully identified the structural proteins of CyHV-2 by purifying virions using a sucrose density gradient in conjunction with ultracentrifugation (Gao et al., 2020). Subsequently, the viral proteins were separated via SDS-PAGE and characterized through mass spectrometry analysis. Their findings revealed that the mature CyHV-2 virion comprises a total of 74 proteins, encompassing 3 capsid proteins, 18 membrane proteins, and 53 additional proteins. Furthermore, eight immunogenic proteins were identified, namely pORF92, pORF115, pORF25, pORF57, pORF66, pORF72, pORF131 and pORF132. In addition to this, further investigations into the functions of several pivotal CyHV-2 proteins have been conducted. Du *et al*. discovered that CyHV-2 ORF104 is capable of activating the p38 signalling pathway, facilitating viral invasion into host cells (Du et al., 2015). Additionally, Zhu *et al*. revealed that CyHV-2 ORF98 encodes uracil DNA glycosylase (UDG), which generates circular RNAs and contributes to gene transcription and splicing regulation (Zhu et al., 2022). Moreover, it has also been revealed that Actin-binding Rho-activating protein (ABRA) interacts with the ORF55 protein, thereby modulating its biological function (Qian et al., 2023). Recent investigations have identified ORF23 and ORF141 as potential viral ribonucleotide reductase homologs in CyHV-2, involved in catalyzing the conversion of ribonucleotides into deoxyribonucleotides and thus playing an important role in virus replication (Cheng et al., 2023). Further understanding of the CyHV-2 proteome and the functions of individual proteins will be vital in terms of understanding the mechanisms that this virus uses to successfully infect and replicate in host cells, and may also facilitate the development of effective protein-based rapid diagnostic methods for CyHV-2.

3.2 Disease caused by CyHV-2

3.2.1 Epidemiological history

The initial descriptions of a fatal disease induced by CyHV-2 dates back to a paper by Jung *et al*. in 1995 (Jung and Miyazaki, 1995). In this, they reported that during the spring of 1992 and 1993, a novel disease leading to substantial mortality among cultivated goldfish emerged across various locations in Japan. Subsequent investigations led to the isolation of a herpes virus from moribund goldfish,

and transmission experiments confirmed that it was the causative agent of this disease among goldfish. Further scrutiny revealed that afflicted goldfish predominantly exhibited lesions concentrated in the hematopoietic organs, specifically the kidney and spleen. Consequently, the disease was designated as herpesviral haematopoietic necrosis (HVHN). A few years later, a comparable scenario unfolded on a fish farm in the United States, also during the spring season (Groff et al., 1998). The affected goldfish, which were in the juvenile stage (2 months old), experienced a remarkably high mortality rate ranging between 50-100%. Findings from autopsies revealed a similar pattern of internal lesions predominantly localized in the kidneys and spleen. Notably, it was observed that not all infected fish consistently displayed lesions in both the kidneys and gills. Using a transmission electron microscope, viruses with morphological characteristics similar to herpesviruses were again observed. The following year, histopathological and ultrastructural analysis of diseased fish in northeast Taiwan revealed the presence of a herpes-like virus associated with a similar disease in goldfish fry of a breeding facility (Chang et al., 1999). Further examination of import records indicated that goldfish from Japan were likely to be the origin of the virus. In the following years, outbreaks of CyHV-2 were also reported in Australia (Stephens et al., 2004), UK (Jeffery et al., 2007), China (Wang et al., 2012), Italy (Fichi et al., 2013), India (Sahoo et al., 2016), Switzerland (Giovannini et al., 2016), Germany (Adamek et al., 2018), France (Boitard et al., 2016), The Netherlands (Ito et al., 2017), Turkey (Kalayci et al., 2018),Poland (Panicz et al., 2019), Hungary (Doszpoly et al., 2011), Serbia (Radosavljevic et al., 2018), South Korea (Jung et al., 2022), and Thailand (Piewbang et al., 2024). In 2009, the ICTV officially designated the pathogen as *Cyprinid herpesvirus 2* (CyHV-2) and assigned it to the *Cyprinivirus* genus (ICTV, 2011).

In addition to goldfish, as more CyHV-2 outbreaks were reported, it became apparent that other related cyprinid fish species could also be impacted. The first reports of CyHV-2 infection in Gibel carp occurred in 2011 in Hungary (Doszpoly et al., 2011). Additional reports of the disease in this fish species demonstrated that the virus was able to efficiently spread in both cultured and wild fish (Daněk et al., 2012; Fichi et al., 2013; Wang et al., 2012). CyHV-2 was also found to infect other fish species such as Crucian carp and hybrids resulting for the crossing of gibel carp (female) and common carp (male) (Fichi et al., 2013; Wu et al., 2013). Collectively these observations indicate that CyHV-2 may have a host range broader than observed for related viruses of the genus *Cyprinivirus*.

In summary, this disease has been reported around the world in diverse environments including in Asia, North America, Oceania and Europe. This growing geographic distribution and transcontinental prevalence of CyHV-2, underscores the need the need for international collaboration in terms of monitoring and reporting order to understand and better mitigate against the continued spread of this virus.

3.2.2 Host range

Herpesviruses are host-specific pathogens widely distributed among vertebrates. Characterized by their expansive genomes and intricate mechanisms, these viruses employ sophisticated strategies to ensure prolonged persistence within their hosts. This intricate interplay results in a remarkable degree

of host specificity (Hanson et al., 2011; King et al., 2012c; Payne, 2017). Initially, the historical host range of CyHV-2 was confined to goldfish (Jung and Miyazaki, 1995; Groff et al., 1998). And, in addition to common goldfish, some varieties such as Wakin, Demekin, Ryukin, Edonishiki and Ranchu also display heightened susceptibility to the virus (Wei et al., 2019; Ito and Maeno, 2014a). As broader reports surfaced, additional species such as gibel carp, Crucian carp, gynogenetic gibel carp and golden crucian carp were included in the host range (Doszpoly et al., 2011; Fichi et al., 2013; Wu et al., 2013; Xiao et al., 2022). Intriguingly, three Japanese indigenous sub-species (*C. auratus langsdorfii*; ginbuna, *C. auratus buergeri*; nagabuna, *C. auratus grandoculis*; nigorobuna), belonging to the *Carassius* genus, demonstrated lower sensitivity than goldfish (Ito and Maeno, 2014a). Notably CyHV-2 was demonstrated not to be pathogenic towards other cyprinid and related host species such as koi carp (*Cyprinus rubrofuscus var. "koi"*) and common carp (*Cyprinus carpio*), Grass carp (*Ctenopharyngodon idella*), Silver carp (*Hypophthalmichthys molitrix*), Wuchang fish (*Megalobrama amblycephala*), Snakehead (*Channa argus*), Bighead carp (*Hypophthalmichthys nobilis*), and Tilapia (*Oreochromis mossambicus*) (Hedrick et al., 2006; Liang et al., 2015). In addition to direct inoculation of potential addional hosts, reports relating to CyHV-2 outbreaks noted that other fish species present in mixed-breeding waters did not exhibit the same clinical symptoms. For example, Wu *et al.* noted the lack of any symptoms in Silver carp (*Hypophthalmichthys molitrix*), big-head carp (*Aristichthys nobilis*), bluntnose black bream (*Carnis megalobramae*), and grass carp (*Ctenopharyngodon idella*) cultured alongside *C. gibelio* in the same pond (Wu et al., 2013). Another report from Jeffery *et al*. mentioned that the koi carp, orfe, tench and even some larger goldfish were unaffected within the same holding system (Jeffery et al., 2007). However, with advancements in detection technology, perspectives have evolved. In 2015, Zhu *et al.* documented diseased *Aristichthys nobilis*, *Erythroculter ilishaeformis*, *Culter alburnus*, *Hypophthalmichthys molitrix*, and *Mylopharyngodon piceus* in China's Jiangsu province, exhibiting clinical features akin to *C. auratus* with gill haemorrhagic disease. Subsequent diagnosis through LAMP assay and electron microscopy confirmed CyHV-2 positivity in these species, suggesting the virus's capacity for cross-infection among different fish species beyond its initial association with goldfish (Zhu et al., 2019).

In fact, crucian carp and gibel carp exhibit a broader geographical distribution and sustain larger wild populations than goldfish (Hänfling et al., 2005). Both species, as members of the same genus as goldfish, face a significant threat from CyHV-2. Despite their close relation, the introduction of crucian carp into aquaculture for food purposes occurred relatively late, with its status in the industry only rising in the 1980s. This shift was largely driven by the development and widespread application of polyploid, all-female allogynogenetic gibel carp, which utilize gynogenetic reproduction with heterologous sperm to initiate embryonic development. As a result, gibel carp was rapidly adopted across nearly all regions of China, leading to a marked increase in aquaculture production (Li et al., 2018). By leveraging various local strains and several high-yield varieties of allogynogenetic gibel carp, annual production surged from 48,000 tons in 1983 to 2,912,258 tons by 2015 (China Fishery Statistical Yearbook 2016).

Currently, most crucian carp cultivated in managed aquaculture systems are improved strains of allogynogenetic gibel carp, particularly the "CAS III" variety (Gui, 2024). The primary breeding centers are located in Jiangsu and Hubei provinces, with Jiangsu notably experiencing multiple disease outbreaks (Jiang et al., 2015; Wang et al., 2012; Xu et al., 2013). As goldfish serve primarily as a model organism in this study, they will not be discussed further.

3.2.3 Transmission

Horizontal transmission of CyHV-2 between infected fish has been confirmed through direct contact with infected fish including asymptomatic carriers (Goodwin et al., 2009; Wei et al., 2019). Histological analysis suggests that CyHV-2 may undergo replication in the gills, leading to mucosal detachment and necrosis. This process can result in the release of viral particles into the water, serving as a mechanism for effective transmission of the virus (Ding et al., 2014). While the possibility of CyHV-2 transmission through other vectors is possible, and indeed, a closely related virus, CyHV-3, can be transmitted through vectors such as faeces and birds (Dishon et al., 2005; Hanson et al., 2011), currently there is a lack of data on vector mediated transmission of CyHV-2.

Another effective mode of viral transmission is vertical transmission (from parent to offspring), and evidence would indicate that CyHV-2 can spread through this mechanism. In 2009, Goodwin *et al.* confirmed that seemingly healthy broodfish can harbor exceptionally high virus loads, while surviving for many years as carriers. Moreover, quantitative PCR revealed the presence of viral DNA in disinfected fish eggs, providing clear evidence of vertical transmission of CyHV-2 (Goodwin et al., 2009). Expanding on this, Zhu *et al.* successfully employed LAMP, PCR, and RT-PCR techniques to amplify viral DNA fragments from diseased fish eggs, and demonstrated the transcription of the CyHV-2 helicase gene within infected fish eggs. Furthermore, virus particles were also observed in fish eggs through electron microscopy (Zhu et al., 2015, 2019). Taken together, these findings provide strong evidence for CyHV-2 vertical transmission from parents to offspring. In summary, as a highly contagious virus, CyHV-2 exhibits the transmission capacity both horizontally, through direct contact, and vertically, through reproductive behaviour. This situation where past outbreaks can still impact successive generations, emphasizes the devastating impact that this virus can have in aquaculture facilities, underscores the need for effective disease mitigation and prophylactic approaches.

3.2.4 Clinical signs

While there are some slight differences, the clinical symptom descriptions in reports of CyHV-2 disease generally exhibit many similarities. In an initial report from Japan, researchers observed a listless state and a tendency for affected fish to remain at the bottom of ponds (Jung and Miyazaki, 1995). Subsequently, Groff *et al*. noted that infected juvenile goldfish displayed lethargy, anorexia, difficulty breathing, and gill pallor. Autopsies revealed varying degrees of paleness and swelling in the kidneys and spleen (Groff et al., 1998). Concerning goldfish fry, reports included anorexia, lethargy, and discoloration (Chang et al., 1999). Further descriptions from Australia highlighted the presence of

white lesions on the skin in diseased fish (Stephens et al., 2004). As far as appearance is concerned, affected goldfish have protruding scales (Giovannini et al., 2016; Piewbang et al., 2024). Comprehensive symptoms were documented in UK case reports, where mortality extended over several days, with smaller fish experiencing higher mortality rates (Jeffery et al., 2007). Affected fish exhibited pale skin, mucus-like blister-like pustules in fin tissue, severe gill necrosis, abdominal distension, and *bilateral exophthalmos*. Internally, kidneys and liver were pale, intestines lacked food, and splenomegaly was universal, with some fish showing large white nodules. Importantly, researchers attribute the clinical symptoms of diseased fish to the synergy of bacterial pathogens and CyHV-2 virus, a perspective also supported by Korean case reports (Jung et al., 2022). In summary, classical characteristic signs of CyHV-2-infected fish include lethargic behavior, dorsal fin folding, gasping difficulty with erratic swimming, lying down at the tank bottom before death, discoloration, pale gills, abdominal distension, *bilateral exophthalmos*, patches of necrosis on gills, and mortality across various fish sizes (Adamek et al., 2018; Sahoo et al., 2016). Diseased gibel carp exhibit clinical symptoms similar to those of goldfish, including anorexia, lethargy, and gill necrosis, etc. However, some differences exist, with gibel carp displaying a more acute onset, higher mortality rates, and skin by distinctive hemorrhage or stasis. Moreover, the bleeding points are distributed around the gills, mandible, abdomen, and fin base. In severe cases, the end of the tail fin may turn white, and spotting may occur in the swim bladder (Daněk et al., 2012; Ma et al., 2015; Wang et al., 2012; Wu et al., 2013; Xu et al., 2013; Zhu et al., 2019). The symptoms of affected Crucian carp are close to those of gibel carp (Fig. 12) (Fichi et al., 2013; Wen et al., 2021).

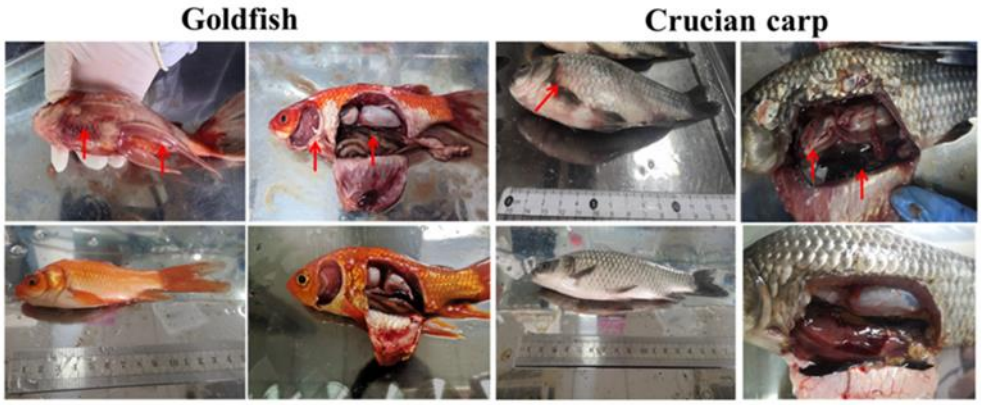

Figure 12 – Gross symptoms of CyHV-2 in infected goldfish and crucian carp. Goldfish infected by intraperitoneal injection: dorsal and caudal fins bleeding from the base, and liver and spleen enlargement. Crucian carp infected by intraperitoneal injection: gill bleeding, massive abdominal hemorrhage, abdominal swelling and congestion, eyeball protrusion. Red arrows show the representative symptoms of CyHV-2 infection in experimental fish. Adapted from (Wen et al., 2021).

3.2.5 Histopathology

During CyHV-2 infection, the organs displaying clinical symptoms, the gills, kidney, and spleen, undergo significant histopathological changes (Fig. 13). In the gills, particularly in the lamellae, researchers have observed infiltration of hemocytes, diffuse hypertrophy, and hyperplasia of the

branchial secondary lamellar epithelium leading to extensive fusion with severe necrosis. Additionally, sloughing of the epithelial cells is commonly observed (Ding et al., 2014; Fichi et al., 2013; Jeffery et al., 2007; Piewbang et al., 2024; Wen et al., 2021). In the kidney, a key target organ during CyHV-2 infection, pathological changes include diffuse necrosis, dilatation of glomerulus capillaries, infiltration of hemocytes and lymphoid cells, hypertrophied nuclei (or ring-like shaped nuclei) exhibiting pyknosis and karyorrhexis, and serious vacuolization (Adamek et al., 2018; Ding et al., 2014; Jiang et al., 2020, 2015; Wu et al., 2013). Researchers have focused on understanding these complex pathological changes as they unfold within the kidney, providing insights into the impact of CyHV-2 on this vital organ. The pathology of the spleen in infected individuals is associated with the severity of the disease, displaying distinctions between mild and severe cases (Adamek et al., 2018; Groff et al., 1998). Typically, spleen tissue shows necrosis, splenocytes exhibit serious vacuolization, marginal chromatin and karyorrhexis, and cytoplasmic hypertrophy. Additionally, hemosiderin deposits may be observed in some splenocytes, along with the deposition of a high number of melanomacrophages (Adamek et al., 2018; Ding et al., 2014; Jeffery et al., 2007; Jung and Miyazaki, 1995; Sahoo et al., 2016; Wu et al., 2013). In addition, histopathological examination of the liver, intestine, brain and heart is also commonly reported. Ding *et al.* observed in diseased gibel carp that hepatocytes exhibited enlarged nuclei with intranuclear inclusion bodies, hypertrophied nuclei with pyknosis, and significant vacuolization (Ding et al., 2014). Jiang *et al.* reported widespread necrosis in the liver, intestine, heart, and brain of CyHV-2-affected gibel carp. Comparing affected cells (hepatocytes, intestine submucosa cells, intestine mucosa cells, neurons, and cardiac muscle cells) with healthy cells in the same organs, they noted consistent margination or fragmentation of nuclei. Additionally, hepatic sinusoids and cardiac muscle cells displayed serious infiltrates of granulocytes (Jiang et al., 2015). In organs from CyHV-2-infected goldfish analyzed by *Jiang et al*., mild changes were observed in the heart, brain, and intestines. Histological alterations in the heart were inconsistent, showing mild to marked necrotizing myocarditis with associated mononuclear leukocyte infiltration. The intestinal epithelium remained intact, with leukocyte infiltration in the lamina propria and submucosa. The brain exhibited matrix disorganization and low-frequency perivascular gliosis (Jiang et al., 2020). In summary, regarding the significance and the degree of tissue changes during CyHV-2 infection, the most prominent and extensively affected organs are the kidney, spleen, and fish gills. On the other hand, the heart, liver, intestine, and brain may not exhibit obvious histopathological changes, suggesting a lower impact or fewer alterations in these organs during CyHV-2 infection (Groff et al., 1998; Jung and Miyazaki, 1995; Wu et al., 2013).

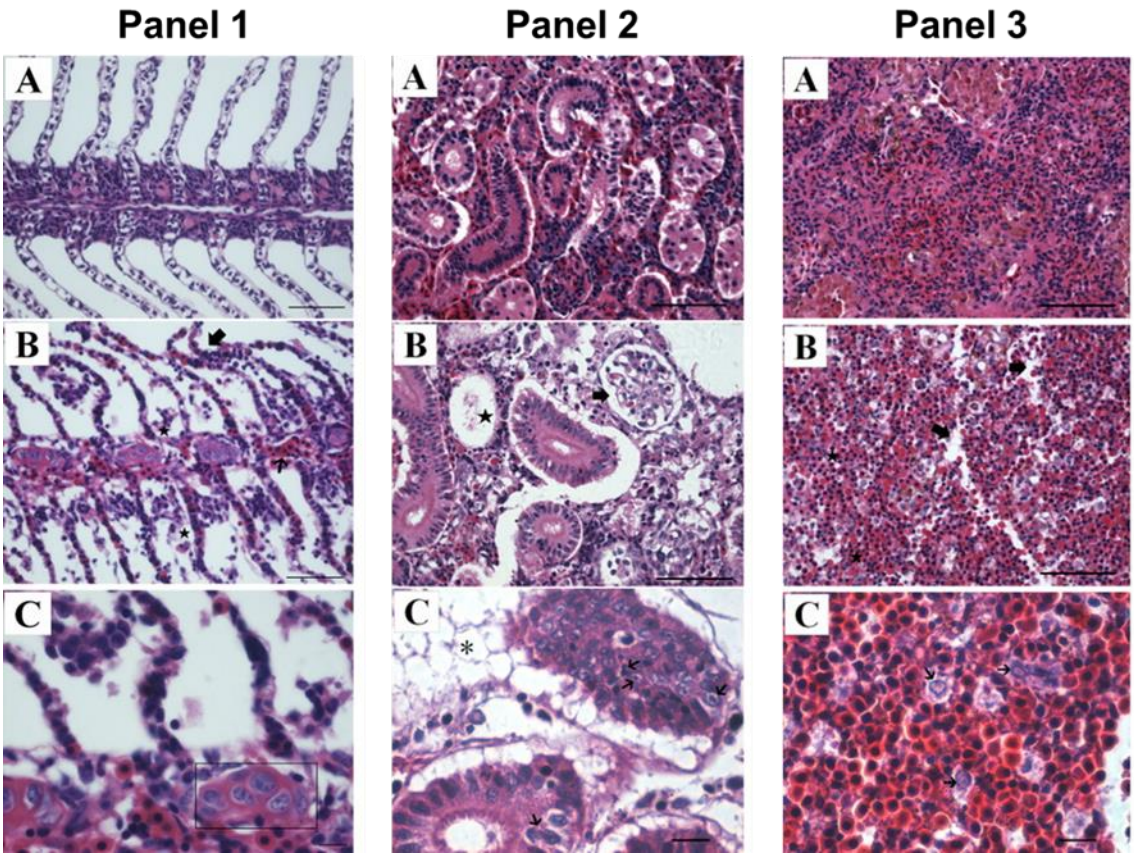

Figure 13 – CyHV-2 infection caused severe Histopathological changes in the gibel carp organs. CyHV-2 infection caused severe Histopathological changes in the gibel carp organs. Panel 1: Histopathological findings of the gill (H&E stain). (A) No pathological changes could be observed in gill from healthy gibel carp. (B) Infiltration of hemocytes (thin arrow), fusion of the secondary lamellae with necrosis (thick arrow) and sloughing of the epithelial cells (star). (C) Agglomerated phagocytic cells with cytoplasmic vacuoles of variable size appeared to be faintly basophilic (frame). Panel 2: Histopathological findings of the kidney (H&E stain). (A) No pathological changes could be observed in kidney from healthy gibel carp. (B) Infected kidney had focal necrotic lesions (star), dilatation of glomerulus capillaries (thick arrows). (C) Hypertrophied nuclei with pyknosis and karyorrhexis (thin arrows), and serious vacuolization (asterisk). Panel 3: Histopathological findings of the spleen (H&E stain). (A) No pathological changes could be observed in spleen from healthy gibel carp. (B) Infiltration of hemocytes and lymphoid cells (star) and serious vacuolization (thick arrow). (C) Many splenocytes had marginal chromatin and karyorrhexis (thin arrows). All scale bars A and B = 50 μm; C = 10 μm. Adapted from (Ding et al., 2014).

3.2.6 Pathogenesis

The pathogenesis of infections relates to how and why disease develops and progresses. Like most members of the family *Alloherpesviridae* infecting fish hosts, water temperature plays a huge role in the occurrence of high mortality CyHV-2 outbreaks. Such outbreaks predominantly occur in spring and autumn where water temperatures are more likely to range from 15–25°C. Outside of these temperatures, the occurrence of clinical disease is reduced (Goodwin et al., 2009). However, the exact reasons why outbreaks occur at this temperature is not fully understood, but it has been speculated that it may be due to changes in the host's innate immune defence with respect to temperature (Thangaraj et al.,

2021). However, the absence of disease at non-permissive temperature does not mean that the viral infection has been cleared, as it may persist as a latent infection, which will be discussed in more detail in the next section.

In addition to temperature, host developmental stage also appears to be a factor in the occurrence of highly pathogenic CyHV-2 outbreaks, with such outbreaks mainly occurring among host populations that are at earlier developmental stages. Indeed, CyHV-2 was initially identified as being mainly a cause of disease in juvenile goldfish (Chang et al., 1999; Groff et al., 1998; Jung and Miyazaki, 1995). While this may indicate that earlier goldfish developmental stages are more susceptible (Thangaraj et al., 2021), to date, there has been no in-depth and systematic comparisons between a range of different host developmental stages in this regard. Another important aspect of pathogenesis is the portal of entry into the host, as it can provide insights into the series of events that occur after infection, in terms of host response and how progression of clinical disease begins. In fish, mucosal surfaces, including the skin, gills and gastrointestinal mucosa are in constant contact with the surrounding environment, and can thus serve as the primary entry routes for pathogens. However, as with CyHV-2 susceptibility between developmental stages, there have been no systematic comparisons between different tissue groups at early time points post infection, thus the CyHV-2 portal of entry has not been definitively established. Of course, these knowledge gaps may be partially due to the lack of appropriate tools, that would facilitate such studies. Such tools include the development of recombinant CyHV-2 strains expressing reporter genes to facilitate *in vivo* imaging of viral infections, allowing viral load and disease progression to be monitored with much greater ease.

3.2.7 Latency

A key biological property of all herpesviruses is their ability to establish a lifelong latent infection, a biological trait considered a hallmark of all herpesviruses (King et al., 2012c). Numerous reports have demonstrated the ability of members of the family *Alloherpesviridae*, including CyHV-2, to establish long-term latent infections (Nieuwstadt et al., 2001; Reed et al., 2014; Thompson et al., 2005; Wei et al., 2019). According to Goodwin *et al.*, in some cases of latent infection, CyHV-2 viral load in apparently healthy juveniles/young adults fish reached the range of 10^6-10^7 copies of the viral genome per μg of DNA (/μg), and were kept at water temperatures of 18–23 °C when sampled. Furthermore a subset of broodfish were also found to have survived for several years despite exhibiting viral loads of 10^6/μg and were kept at water temperatures of 21–30 °C when sampled. (Goodwin et al., 2009). This indicated that CyHV-2 could be present at significant levels in hosts, in the absence of any apparent viral replication or clinical disease, in a similar manner to latent infections established by other herpesviruses.

Furthermore, in a goldfish challenge experiment conducted by Ito and Maeno, it was observed that goldfish infected with CyHV-2 in a lower water temperature (15°C), had better survival rates than those infected at higher temperatures (25°C), but later exhibited high mortality when introduced to

permissive temperatures (25°C). This suggested that lower water temperatures promoted the establishment of latent CyHV-2 infections, and that the re-activation could coincide with a return to the optimum temperature range for CyHV-2 lytic replication (Ito and Maeno, 2014b). This conclusion was further supported by the research of Chai *et al*., who observed that CyHV-2 remains latent for the entire lifespan of gibel carp, even those survive CyHV-2 infection at 23-25 °C, which is permissive for CyHV-2 clinical disease. The they demonstrated that in fish that were transferred to a low non-permissive temperature of 14 °C, CyHV-2 infection could be reactivated upon return to 25 °C (Chai et al., 2020). Additionally, they established a latently infected cell line (GCBLat1) derived from the brain of latently infected gibel carp, and were able to demonstrate greater reactivation of virus after treatment of cells with trichostatin A (TSA) or phorbol 12-myristate 13-acetate (TPA), which may serve as a useful *in vitro* model for studying the latency and reactivation mechanisms of CyHV-2. Similarly, another group demonstrated that CyHV-2 DNA could be detected in apparently healthy gibel carp maintained at 15 °C in several commercial aquaculture facilities across Jiangsu Province of China, despite the absence of any recorded CyHV-2 outbreaks on these sites. Notably, some fish also tested positive for CyHV-2 gene transcription in various organs indicating that an infection, of some kind, was still ongoing. Interestingly, viral DNA and RNA transcription levels increased after *in vivo* organ culture of tissue explants from these fish, and homogenates of the tissue explants could be used to infect naive fish with CyHV-2 (Wei et al., 2023). Other studies demonstrated that transferring CyHV-2 infected goldfish to higher non-permissive temperatures >25°C also results in increased host survival, and that viral DNA could still be detected in various tissues in survivors (predominantly spleen and kidney) after fish are returned to a permissive temperature of 25°C. It was also observed that in some survivors, viral DNA could not be detected in freshly dissected tissue explants, however, viral DNA could later be detected in media after *in vitro* organ culture (at 25°C) using the same explants, and that virus harvested from these *in vitro* cultures could be used to infect more hosts (Wei et al., 2019). Taken together, these studies reveal that *(i)* low or high non-permissive temperatures result in the establishment of persistent or latent infections and *(ii)* reactivation can often (but not always) be achieved by exposing fish or organ explants to optimum temperature ranges for CyHV-2 disease.

At lower non-permissive temperatures, it is highly unlikely that CyHV-2 infected fish survive better due to increased suppression of the virus. This is because there is lots of evidence to indicate that the immune response in teleosts may be less effective at these lower temperatures (Abram et al., 2017). Furthermore, from an evolutionary perspective, the establishment of latency during lower temperatures may represent a common advantageous adaptation of viruses to poikilothermic hosts, which are subject to declines in immune response when they encounter low environmental temperatures. In the case of CyHV-2, the establishment of a latent infection at low temperatures would act to prevent the virus from killing its immuno-suppressed hosts, allowing the host to survive the periods of lower water temperature, for example during winter. In this scenario, the host can act as reservoir for new infectious viral progeny in spring when water temperatures increase, and hosts start to interact in high numbers during

spawning. Confining CyHV-2 reactivation to these periods, may be much more advantageous in terms of viral transmission. Furthermore, as latently infected hosts often become resistant to disease caused by CyHV-2, and thus surviving CyHV-2 reactivation events, they can continue to act as long-term reservoirs of virus over successive spawning seasons.

Furthermore, in cyprinid fish species, increased immune response is much more likely to happen at higher temperatures (Le Morvan et al., 1998, 1996; Scharsack and Franke, 2022). Notably, during infections with CyHV-3, a virus closely related to CyHV-2, hosts seek out warmer water during infection in order to increase survival, exhibiting what is referred to as behavioural fever. It is unclear if this happens in goldfish during CyHV-2 infections also. However there is evidence that goldfish exhibit behavioural fever in response to challenge with bacterial pathogens (Torrealba et al., 2018), indicating that higher temperatures may help goldfish counteract infection, thus explaining why clinical disease caused by CyHV-2 decreases at higher temperatures. In this scenario, it would also be an evolutionary advantage for CyHV-2 to establish latent infections. Deactivating genes involved in lytic replication, would act as a way of evading detection by the host immune system while it is at its peak.

The exact mechanisms underlying the establishment of CyHV-2 latency and re-activation remain unclear. Notably, temporary immunosuppressive stress can also occur as a consequence of temperature shifts (Abram et al., 2017). This may provide some insight into the underlying reasons for reactivation of CyHV-2 after a shift to CyHV-2 permissive temperatures. Interestingly, in addition to temperature-based reactivation of CyHV-2, it has been demonstrated that reactivation can also be induced through the administration of immunosuppressive agents, specifically dexamethasone (Dex) and cyclosporine A (CsA) (C. Wei et al., 2020). Taken together, this indicates that immunosuppressive events may be an important prelude to CyHV-2 reactivation.

However, the underlying mechanisms may be more nuanced than this, especially when considering that potential temporary immune suppression resulting from a shift to low non-permissive temperatures, would appear to have the opposite effect, resulting in the inhibition of CyHV-2 replication. Furthermore, although the immune response may be greater at higher non-permissive temperatures, any initial immune suppression at early stages post temperature increases, would also still appear to result in the inhibition of lytic replication. In order to understand this, it may be important to consider that physiological changes occurring when fish are moved to or from CyHV-2 permissive temperatures may coincide with (or even be caused by) many epigenetic changes. Indeed, different epigenetic profiles may be initiated when hosts are moved to low or high non-permissive temperatures, compared when hosts are moved to permissive temperatures, and this may have an impact on CyHV-2 infection. Notably, treatment with TSA (which inhibits cellular factors that are important for epigenetic remodelling of host and viral genomes) can cause reactivation of CyHV-2 *in vitro* in latently infected cells (Chai et al., 2020). This key observation indicates that epigenetic changes in the host or viral genome may play a key role in establishment of CyHV-2 latency, and that the reversal or inhibition of these changes promotes reactivation. Epigenetic remodelling often occurs in cells due to Histone Deacetylases

(HDACs) and can be inhibited by anti-HDAC drugs such as TSA. Indeed, HDAC activity leading to epigenetic remodelling of viral genomes is a strategy that is exploited by other herpesviruses to prevent the expression of IE genes, inhibiting lytic replication cycles, thus resulting in the establishment and long-term maintenance of latent infections. For example, HHV-1 latency heavily relies on HDAC-mediated epigenetic repression of important HHV-1 IE gene promoters, which can also be counteracted by TSA (Nicoll et al., 2012).

Switching form latent to lytic infection, involves substantial changes to viral gene transcription, and evidence may indicate that CyHV-2 has evolved to exploit epigenetic remodelling that occurs in host cells in response to temperature change, to modulate its own transcriptome. Indeed, this would represent an elegant viral adaptation to seasonal changes in host behaviour and physiology that would reduce disruption of viral transmission chains. This this mechanistic hypothesis on CyHV-2 latency, may better explain why temperature shifts, outside of the CyHV-2 permissive temperature range, increase the survival of infected fish as latent carriers. It may also explain why viral reactivation may occur upon re-introduction to permissive temperatures, despite the fact that all temperature changes may, at least temporarily, negatively impact the immune response.

However, this hypothesis would require that CyHV-2 establishes latent infections in cells that are sufficiently responsive to these temperature changes. On this note, recent evidence indicates that CyHV-2 primarily establishes latent infections in monocytes/macrophages in long-term survivors of CyHV-2 infection (C. Wei et al., 2020). Interestingly, in carp (a cyprinid fish species related to goldfish) and other fish species, these types of cells exhibit major temperature dependent changes, in terms of respiratory burst response and phagocytic index (Abram et al., 2017). Taken together with the observation that TSA can stimulate reactivation of latent CyHV-2 (Chai et al., 2020), it raises an interesting hypothesis that CyHV-2 latent infections in monocytes/macrophages may occur due to epigenetic remodelling of the CyHV-2 genome or host genomes in response to temperature change. Therefore, it may be interesting to compare viral and host transcriptomes between monocytes/macrophages undergoing latent and lytic CyHV-2 infection, under different temperature and TSA treatment regimes, in order to gain a further understanding of the underlying mechanisms associated with this process.

3.2.8 Co-infections

Co-infections involving viruses and bacteria are frequently documented in cases related to CyHV-2, with certain bacteria identified as primary agents of fish disease. Case reports from Italy highlight mixed infections of *Aeromonas sobria* and CyHV-2 as the predominant cause of mass mortality observed among crucian carp in natural water habitats (Fichi et al., 2013). Subsequently, in a study focusing on gibel carp, She *et al*. elucidated alterations in the intestinal microbiota between healthy specimens and those infected with CyHV-2 (She et al., 2017). Notably, Plesiomonas exhibited elevated levels in infected samples, suggesting its potential utility as a microbial biomarker for CyHV-2 infection. In 2021, Ren *et al*. conducted a gibel carp study to investigate the pathogenicity and mechanisms

underlying co-infections involving CyHV-2 virus and bacteria (Ren et al., 2021). Their findings revealed that CyHV-2 infection disrupts the integrity of the intestinal mucosal barrier, leading to subsequent bacterial infections. Importantly, they noted that the temporal relationship between viral and bacterial interactions predominantly influenced the outcome, either synergistic or antagonistic, of co-infections. Furthermore, mortality resulting from co-infection with CyHV-2 and *A. hydrophila* was found to be contingent upon the pathogen load. Recently, Chen *et al*. corroborated these findings by utilizing high-throughput sequencing and gas chromatography/mass spectrometry (Chen et al., 2023). Once more, their study emphasized that manipulation of the gut microbiota presents therapeutic avenues for controlling CyHV-2 infection in gibel carp. The abundance of pathogens and the composition of bacterial communities in the external environment play crucial roles in CyHV-2 disease dynamics. Gao *et al*. conducted an analysis of spatiotemporal dynamic changes in environmental parameters and microbial communities within aquaculture settings during disease outbreaks (Gao et al., 2019). Indeed, this research direction warrants further exploration and investigation.

3.2.9 Diagnosis

Viral isolation. Monitoring and detection of CyHV-2 is important element of disease cintrol in the aquaculture industry and in the wild. The isolation of viruses in cell culture has always been considered a highly valued method for the diagnosis of viral diseases and is the basis for *in vitro* characterization of viruses (George et al., 2015). As early as 1995, Jung *et al*. carried out an attempt to culture the CyHV-2 *in vitro*. They used a range of cell lines to attempt to isolate CyHV-2, including fathead minnow (FHM), papule epithelioma carp (EPC), eel kidney (EK-1), Chinook salmon embryos (CHSE-214), Rainbow trout gonad (RTG-2) and tilapia ovary (TO-2). However, CPE (cytopathic effect) was consistently observed only in FHM, but this cell line did not support its continuous propagation beyond passage 4 (Jung and Miyazaki, 1995)., The subsequent development of sensitive cell lines also was also problematic, as it involved the use of some non-goldfish-derived cell lines, which like FHMs leading to unsatisfactory results (Groff et al., 1998; Jeffery et al., 2007; Fichi et al., 2013; Goodwin et al., 2006a; Lovy and Friend, 2014). This led to CyHV-2 being mainly isolated employing koi fin (KF-1) cells, but the virus was not able to be sustainably propagated (Jeffery et al., 2007; Xu et al., 2013). Afterward, two cell lines, GFF and RyuF-2, obtained from the fins of two goldfish species, were developed for the propagation of CyHV-2. GFF cells exhibited a very low virus yield, reaching a maximum titer of $10^{2.0}$ $TCID_{50}$/mL. The RyuF-2 demonstrated a significantly higher virus yield, reaching levels of $10^{5\text{-}6}$ $TCID_{50}$/mL when supplemented with kidney extract (Li and Fukuda, 2003; Ito et al., 2013; Shibata et al., 2015). Observing the capability of CyHV-2 to infect and damage neural tissues such as the brain and retina in susceptible fish, Ma *et al.* opted to use the brain tissue of gibel carp as the source to establish a new cell line, named GiCB. The results show that the virus cultured using GiCB demonstrated a high virus titer of $10^{7.5 \pm 0.37}$ $TCID_{50}$/mL and could be successfully passaged more than 50 times. In experimental infections (intraperitoneal injection), gibel carp subjected to CyHV-2 achieved a 100%

mortality rate within two weeks. This outcome is crucial for providing essential support for the establishment of both *in vitro* and *in vivo* models of CyHV-2 infection, facilitating further research into the virus's pathogenicity (Ma et al., 2015). Based on the natural ability of the caudal fin to regenerate, Lu *et al.* achieved the successful isolation of a new cell line, named GiCF, derived from the caudal fin of *Carassius auratus gibelio* (Akimenko et al., 2003; Lu et al., 2018). Additionally, their research demonstrated that CyHV-2 can induce apoptosis in GiCF cells. This finding establishes a foundation for subsequent investigations into the molecular mechanisms underlying the pathogenicity of CyHV-2 (Lu et al., 2019, 2018). Subsequently, two cell lines, CrCB (derived from the brain tissues of silver crucian carp) and GFB (derived from the brain tissues of goldfish), were established (Xu et al., 2019). These two cell lines have demonstrated susceptibility to infection with CyHV-2, manifesting CPE as early as 3 dpi. Chai *et al*. established a new cell line (GCBLat1) derived from the brain of gibel carp, which was proven to support CyHV-2 latent infection and act as an important tool for studying CyHV-2 latent infection and reactivation (Chai et al., 2020). In addition, another cell line, FtGF (fantail goldfish fin) was established and characterized. Derived from goldfish tail fin samples, these cells exhibited remarkable stability in passaging, reaching up to 56 passages. Significantly, the FtGF cell line was utilized to continuously propagate CyHV-2 for over 20 generations, resulting in a high virus titer of $10^{7.8 \pm 0.26}$ $TCID_{50}$/mL. The harvested virus demonstrated high lethality to high-quality goldfish, underscoring the general utility of the developed cell line for virus propagation and subsequent research on CyHV-2 (Dharmaratnam et al., 2020). Another cell line derived from the spinal cord of gibel carp referred to as CSC, was found to produce high virus titer of CyHV-2 (Y.-J. Wei et al., 2020). In addition, a new continuous fish cell line, CCG, from the gill tissues of *Crucian carp* has been established and passaged up to 90 times and exhibiting high transfection efficiency (Wu et al., 2022). However, the sensitivity of cell lines derived from goldfish organs to CyHV-2 can vary. As reported by Jing *et al*., not all cell lines isolated from goldfish organs exhibit sensitivity to CyHV-2. Specifically, two cell lines derived from the goldfish snout (GFSe) and kidney (GFKf) could not support CyHV-2 passagng beyond the 4 passages (Jing et al., 2016). In summary, various cell lines derived from different organs of goldfish have been successfully developed, and they exhibit high permissiveness for CyHV-2 replication. These cell lines prove valuable for tasks such as virus isolation, propagation, and further characterization. Like the previously developed goldfish cell lines, these newly developed cell lines will play a vital role in future research on CyHV-2, including studying the molecular pathogenesis of HVHN disease and developing prevention and control strategies for the disease (Rougée et al., 2007; Yan et al., 2011).

Polymerase chain reaction. To assist in the accurate taxonomy of *Cyprinid herpesvirus 3* (CyHV-3), Waltzek *et al*. designed amplification primers specific to three CyHV-2 core key genes: helicase, DNA polymerase, and intra capsomeric triplex protein. (Waltzek et al., 2005). Subsequently, in the report of CyHV-2 infection in goldfish in the UK, Jeffery *et al*. designed new PCR primers that targeted the conserved polymerase gene sequence shared among fish herpesviruses CyHV-1, CyHV-2, and CyHV-3. The developed PCR reaction reliably amplified a 362 bp product, providing a specific

molecular tool for detecting CyHV-2 (Jeffery et al., 2007). Afterward, Waltzek *et al*. developed another conventional PCR reaction based on the CyHV-2 helicase gene (Waltzek et al., 2009b). With its inherent high efficiency and universality, this solution was welcomed by subsequent researchers and widely adopted (Jeong et al., 2023; Saito et al., 2024a; Wei et al., 2023; Wu et al., 2022). Between 2009 and 2012, an outbreak of CyHV-2 disease occurred in all gibel carp breeding areas in Jiangsu Province, China, resulting in substantial economic losses. To facilitate rapid diagnosis during this period, Xu *et al*. designed new PCR primers based on the helicase gene of CyHV-2, and this design successfully amplified a 357 bp product (Xu et al., 2013). In the initial report of the CyHV-2 outbreak in France, Boitard *et al*. employed improved primers targeting DNA Polymerase, along with primers previously developed by Waltzek, for PCR detection (Boitard et al., 2016). Additionally, two pairs of primers were developed for genotyping: mA, located in the intergenic region between CDS2 and CDS3 within the terminal direct repeat, and mB, situated at the 3' end of ORF117. Notably, mB was found to be suitable for PCR diagnosis, while mA facilitated rapid genotyping.

Herpesvirus latency is characterized by the presence of low amounts of dormant viral genome and limited gene expression (Minarovits et al., 2007). Therefore, screening apparently healthy fish populations for latent infections, involves the use of quantitative polymerase chain reaction (qPCR) as it offers higher sensitivity and specificity, In 2006, Goodwin *et al*. developed a highly specific real-time 5'-nuclease PCR method (TaqMan) targeting the CyHV-2 DNA polymerase gene, demonstrating a linear response exceeding 8 logs of the target concentration (Goodwin et al., 2006b). The reported sensitivity of this method is 1 target molecule per reaction. Importantly, the test does not exhibit cross-reactivity with other similar fish herpesviruses, including CyHV-1 and CyHV-3. Indeed, several conventional and real-time polymerase chain reaction (RT-PCR) protocols have been developed for the molecular detection of CyHV-2 from various sources, including natural infections, experimental infections, and cell cultures (Table 5).

Table 5 - List of primer used for detection of CyHV-2 infection in natural disease outbreak and experimental challenge studies.

No.	Gene	Sequence	Product Size	References
1	Helicase	F: CTGATCATCGACGAGTACGG	867	(Waltzek et al.,
		R: CACACGCGTGCACACNACRTA		2005)
2	Intracapsomeric	F: CACTCTGGCGACGCNTTYATG	259	
	triplex protein	R: CATCACAGAGTTCTTGACNGC		
3	DNA Polymerase	F: CGGAATTCTAGAYTTYGCNWSNYTNTAYCC	497	
		R: CCCGAATTCAGATCTCNGTRTCNCCRTA		
4	DNA polymerase	F: TCGGTTGGACTCGGTTTGTG	170	(Goodwin et
		R: CTCGGTCTTGATGCGTTTCTTG		al., 2006a)
		P: FAM-CCGCTTCCAGTCTGGGCCACTACC-BHQ1		
5	DNA Polymerase	F: CCAGCAACATGTGCGACGG	362	(Jeffery et al.,
		R: CCGTARTGAGAGTTGGCGCA		2007)
		F: CGACGGVGGYATCAGCCC	339	
		R: GAGTTGGCGCAYACYTTCATC		
6	Helicase	F: GGACTTGCGAAGAGTTTGATTTCTAC	366	(Waltzek et al.,
		R: CCATAGTCACCATCGTCTCATC		2009b)
7	Helicase	F: GAACACCGCTGCTCATCATC	357	(Xu et al.,
		R: ACTCTTCGCAAGTCCTCACC		2013)
8	DNA Polymerase	F: CCCAGCAACATGTGCGACGS	362	(Boitard et al.,
		R: CCGTARTGMGAGTTGGCGCA		2016)
9	Marker A (mA)	F: CCACTTAGAGTAACCACTTAGAG	432	
		R: GCGTTGACTCATTTGCGGTTTG		
10	Marker B (mB)	F: ATCATGGAAGATGTTCTGGCCAG	475	
		R: CAGCAGCAACTGAGCGTCATG		

From Thangaraj (Thangaraj et al., 2021).

Loop-mediated isothermal amplification. To overcome the need for a thermal cycler and reduce the use of expensive consumables associated with traditional PCR methods, some laboratories have developed the loop-mediated isothermal amplification (LAMP) technique. This method involves amplifying DNA with high specificity and sensitivity under isothermal conditions. He *et al*. pioneered the use of LAMP for detecting CyHV-2 (He et al., 2013). Their comparative results demonstrated that the detection limit of LAMP was 1.09×10^{-4} μg/μL, surpassing conventional PCR and real-time PCR in terms of sensitivity. LAMP proved to be more suitable for rapid detection under field conditions. Similarly, Zhang *et al*. developed a LAMP detection method based on the DNA helicase gene, allowing visual detection through color changes induced by the addition of SYBR Green I stain (Zhang et al., 2014). In comparison to the approach employed by Zhang *et al*., Zhu *et al*. introduced an enhancement to the LAMP method for CyHV-2 detection, by incorporating a pair of loop primers, CyHV-LF and CyHV-LB, resulting in a reduced reaction time of 30 minutes (Zhu et al., 2015). Notably, in this experimental setup, template DNA preparation was simplified by boiling in a water bath for just 5 minutes,

significantly enhancing the convenience of the procedure. In another LAMP assay developed by Liang *et al*., the detection limit reached 10 copies/μl per reaction, while PCR was 100 times less sensitive, at 1000 copies/μl (Liang et al., 2014). Similarly, according to Yang *et al*.'s description, their design has a detection limit of about 15 copies of the cloned viral genome fragment, with good specificity (Yang et al., 2014). In contrast to these two cases, Xie *et al*. reported a lower sensitivity, achieving only 3.5×10^2 copies/μl (Xie et al., 2019). Overall, LAMP technology has demonstrated high convenience, rapidity, sensitivity, and specificity in detecting CyHV-2 at relatively low concentrations. It surpasses traditional PCR methods in sensitivity and is particularly suitable for detection scenarios outside the laboratory.

Immunoassays. Immunological methods have been used for viral diagnosis for more than 100 years. Identification of viral antigens in clinical samples can be accomplished quickly by using more traditional immunofluorescence and enzyme immunoassays in the virology laboratory (Atmar and Ramani, 2020; Cassedy et al., 2021). Ding *et al*. pioneered the development of highly specific and stable fluorescence in situ hybridization (FISH) probes labelled with 6-Carboxyfluorescein (6-FAM) (Ding et al., 2014). These probes were designed for the detection of CyHV-2 polymerase gene sequences in tissue samples. In practical applications, in situ hybridization (ISH) technology has been demonstrated to effectively detect the presence of CyHV-2 virus in both kidneys and peripheral blood cells of gibel carp, thus establishing its efficacy as a reliable detection method (Wang et al., 2016; Xu et al., 2014). Moreover, staining with mouse monoclonal antibody (MAb) 3D3 directed against CyHV-2 nucleocapsid protein and FITC-conjugated anti-mouse IgG goat antibody has been demonstrated to be useful in terms of visualizing viral proteins in tissue. In subsequent studies, monoclonal antibodies targeting various proteins encoded by CyHV-2, including ORF72 (Kong et al., 2017), ORF92 (Shen et al., 2018), ORF25 (Wu et al., 2020b), ORF121 (Gao et al., 2022), ORF66 (Guo et al., 2022), ORF88, ORF55R, ORF115, and ORF151R (Zhao et al., 2022), were sequentially developed. When coupled with techniques such as indirect immunofluorescent assay or immunohistochemistry (IHC), these monoclonal antibodies have emerged as crucial tools for the studying CyHV-2 infection *in vivo* or *in vitro*. Furthermore, Wu *et al*. developed and characterized a monoclonal antibody targeting gibel carp serum immunoglobulin, enabling the non-lethal serological diagnosis of CyHV-2 infection (Wu et al., 2020a). Based on this, they devised an immunochromatography test strip (ICS) employing two monoclonal antibodies targeting the ORF25 protein: MAb 2C3-1E6 as the capture antibody and 3H2-1G5 as the detection antibody (Wu et al., 2021). This rapid test can be conducted within 10 minutes and demonstrates a consistent sensitivity of 1 μg/mL.

3.2.10 Immune response

The mechanism of teleost response to external pathogens has not been fully explored, but like all vertebrates, it broadly operates through two interconnected mechanisms: innate (non-specific) immunity and adaptive (specific) immunity (Bo et al., 2012; Xu et al., 2014). However, detailed immunological analysis of goldfish, gibel car or crician carp immune responses during CyHV-2 infections is

limited by the lack of antibodies specific to goldfish cytokines and immune cell markers etc. However important elements of the innate immune response to CyHV-2 infection have been described. Xia *et al.* identified crucian carp IFNc (ccIFNc) from the analysis of differentially expressed genes of challenged with CyHV-2. This gene belongs to the type I interferon family, and as such plays an important role in protecting the host from CyHV-2 infection. This was demonstrated by intramuscular injection of a eukaryotic expression plasmid encoding ccIFNc (pEGFP-cIFNc), which resulted in significantly reduced mortality after challenge with CyHV-2 (Xia et al., 2018). The complement C3 gene in gibel carp (*CagC3*) was also identified as a major element of the innate immune response to CyHV-2, with expression differing between tissue groups, and highest expression in the liver. CagC3 transcription was significantly upregulated in liver, spleen and kidney with the peaks at 24 hr, 2 d, and 2 d, respectively. Further analysis, CagC3 expression in the Gibel carp brain cell line showed that both CyHV-2 and polyinosinic-polycytidylic acid (poly I:C) induced the same CagC3 expression *in vitro* experiments. The poly I:C stimulates the same cellular innate immune receptors that often detect viral nucleic acid, causing the cells to enter an antiviral state. It can often provide insights into what responses are important for antiviral defence *in vitro* and *in vivo*. Zhang *et al.* utilized this characteristic of poly I:C to perform transcriptome analysis on poly I:C-stimulated gibel carp. They found that in the spleen, 1006 genes were upregulated, and 280 genes were downregulated. These differentially expressed genes (DEGs) were primarily associated with immune pathways such as the "TNF signaling pathway," "p53 signaling pathway," and "JAK-STAT signaling pathway." Additionally, the expression of miRNAs in the head kidney also exhibited differences, with 7 miRNAs upregulated and 17 miRNAs downregulated. These differences were mainly enriched in the metabolism, endoplasmic reticulum protein processing, and oxidative phosphorylation signalling pathways (J. Zhang et al., 2020; Zhang et al., 2023). Das *et al.* analysed the expression of immune genes in peripheral blood leukocytes (PBL) of goldfish sensitized to CyHV-2 by co-culturing them with CyHV-2 infected FtGF cells. The results indicated significant increase CD8α, IFNγ, b2m, MHC I, LMP 7, IL-10, IL-12 and GATA3 expression and the authors concluded that goldfish showed both Th1- and Th2-mediated immune responses to CyHV-2 (Das et al., 2021). Immune responses *in vitro* are also of significant interest. These studies help to elucidate the mechanisms by which immune cells respond to CyHV-2 infection, providing valuable insights into potential therapeutic strategies and the development of effective vaccines. Elsewhere other teams have focused on microRNA (miRNA) expression in response to CyHV-2 infection. In early work in this field focused on miRNA expression in the kidney, which was selected because it acts as the main replication site for CyHV-2. In these studies, high-throughput sequencing was initially used to analyze host miRNA and mRNA expression profiles in gibel carp after CyHV-2 infection, but was also later used to identify 17 CyHV-2-encoded miRNAs (Lu et al., 2017). Analysis of miRNAs-mRNA pairs revealed the regulation of diverse signalling pathways, including the RIG-I-like receptor and JAK-STAT pathways in response to CyHV-2 infection. They also presented evidence that the virally encoded miRNA miR-C4 was involved in negatively regulating three genes involved in RIG-I-like pathways,

including IRF3, RBMX and PIN1, providing an insight into virus host interaction. Apoptosis is another important part of the innate immune response in cells, and can be a very effective antiviral response, thus many viruses have evolved to interfere with this process. Interestingly, it has been revealed that a CyHV-2-encoded miRNA miR-C12 inhibits virus-induced apoptosis and promotes viral replication by targeting caspase 8, which is a key component of the apoptosis pathway (Lu et al., 2019). Furthermore, on similar note, it was also shown that host cell miRNA miR-124 may also act to block apoptosis during CyHV-2 infection *in vitro*, however the mechanisms by CyHV-2 may induce this response is this is still unclear (Fu et al., 2023). By comparison there has not been as much investigation into the host adaptive immune response to CyHV-2 infections outside of vaccinology which will be discussed in more detail later. However, the limited work that has been done in this field includes a serological study on surviving goldfish, where it was demonstrated that neutralizing antibodies from survivors could promote acquired immunity in survivors (Nanjo et al., 2017b).

3.2.11 Prophylaxis and control

Presently, CyHV-2 has attained widespread prevalence in certain regions, precipitating substantial economic repercussions within the aquaculture sector (Goodwin et al., 2009; Jiang et al., 2020; Wang et al., 2012). Moreover, facilitated by global trade dynamics, instances of CyHV-2 outbreaks have emerged in additional countries (Ito et al., 2017; Jung et al., 2022; Piewbang et al., 2024; Zhao et al., 2019). Regrettably, the absence of efficacious countermeasures leads to lagging reactions in the majority of cases, underscoring the imperative for expeditious and comprehensive CyHV-2 prevention protocols.

Physical. Water temperature is crucial to fish survival, and different fish species have their preferred temperature ranges (Charnov and Gillooly, 2004). Generally, outbreaks of HVHN typically manifest between spring and summer, or during temperature declines in summer and autumn. Clearly, temperature stands out as one of the crucial factors influencing fish disease dynamics (Groff et al., 1998; Jung and Miyazaki, 1995; Piewbang et al., 2024; Sahoo et al., 2016). It has been proven in practice that regulating water temperature can control CyHV-2 outbreaks. In the United States, dealers quickly control the death of goldfish by raising the water temperature to above 27°C (Goodwin et al., 2009). According to the findings of Ito and Maeno, the optimal temperature range for CyHV-2 infection in goldfish falls between 20-25°C. And, if the water temperature ranges between 13-15°C at the time of infection, the infected individuals may develop resistance to the virus and subsequently become carriers (Ito and Maeno, 2014b). However, the effectiveness of this approach is host dependent. In contrast to goldfish, CyHV-2 replication in gibel carp necessitates lower water temperatures. Danek *et al*. reported that within gibel carp, the virus exhibits replication within the temperature range of 15 to 23°C (Daněk et al., 2012). This finding was also supported by Liang *et al* (Liang et al., 2015). Even water temperatures as low as 10°C can still cause illness (Ouyang et al., 2020). Notably this also indicates that there is nothing inherent with CyHV-2 that prevents it from replicating at low temperatures, and reinforces the

idea that it is changes in the host at low temperatures that prevent clinical disease, leading to the establishment of latent infection. Nanjo *et al*. further demonstrated that manipulating the rearing water temperature to either 32–35°C or 13–15°C effectively mitigated mortality associated with CyHV-2 infection (Nanjo et al., 2017a). Similarly, virus replication *in vitro* exhibited a consistent trend, with negligible growth observed at temperatures of 34°C or higher. Cultures maintained at 30°C and 32°C yielded lower virus titers compared to those cultured at 15°C, 20°C, and 25°C (Shibata et al., 2015). Interestingly, Panicz *et al*., have concluded that the stress effect of water temperature fluctuations leading to a significant reduction in fish immunity is more important than the absolute value of temperature (Panicz et al., 2019). In brief, altering the rearing water temperature has emerged as a promising strategy in combating CyHV-2 infection. However, the underlying mechanisms driving increased survival at non-permissive temperatures (briefly discussed earlier) necessitate further exploration.

Chemicals. In the initial report from Japan, the authors discovered that 5-iodo-2-deoxyuridine (IUdR, 10^{-4} M) and an acidic environment (pH=3) was able to diminish CyHV-2 virus infectivity. Conversely, exposure to Ether and an alkaline environment (pH=11) had less of an impact on reducing CyHV-2 infectivity (Jung and Miyazaki, 1995). In subsequent investigations into the pathogenicity and biological attributes of CyHV-2, Liang *et al*. observed that pH and salinity exerted only limited inhibitory effects on viral replication. Moreover, following treatment with ether or chloroform, the virus lost its pathogenicity, rendering inoculation into gibel carp nonlethal (Liang et al., 2015). In 2021, Su *et al*. documented the inhibitory effects of berberine hydrochloride (BBH) on CyHV-2 replication, along with its capacity to prevent CyHV-2 induced disease in gibel carp in a dosage-dependent manner (Su et al., 2021). Subsequently, in further investigations, epigallocatechin-3-gallate (EGCG), an antioxidant, exhibited similar inhibitory effects *in vitro*. From the perspective of mechanism, both compounds augmented the expression of genes pertinent to the Keap1-Nrf2 pathway and mitigated the induction of intracellular reactive oxygen species (ROS) within infected cells, thereby effectively suppressing CyHV-2 virus amplification (Lu et al., 2022; Su et al., 2021).

Vaccination. Disease prevention is an important research topic for the continued development of world aquaculture, among which vaccination has become a promising and sustainable means of aquatic disease management (Jose Priya and Kappalli, 2022). So far, a several CyHV-2 vaccination strategies have been tested in goldfish or gibel carp.

In 2013, Ito and Ototake developed an inactivated vaccine for CyHV-2 using formalin (0.1% v/v) (Ito and Ototake, 2013). Their study revealed promising results, indicating that goldfish inoculated with two doses of formalin-inactivated SaT-1-infected GFF cell supernatant inferred some protection against disease. The relative percentage survival (RPS) reached 57%. Notably, this was the first vaccine development for CyHV-2, and the immersion method was employed during the challenge process. Upon further investigation, it was revealed that the protective efficacy of this vaccine persisted for at least 8 weeks post-vaccination. Moreover, adjustments to the booster vaccination interval, extending it to 4 weeks, resulted in an enhanced protective effect (Ito and Maeno, 2014a). Subsequently, in a study

conducted by Zhang *et al*., the feasibility of developing an inactivated CyHV-2 vaccine using gibel carp was explored, utilizing β-propiolactone (BPL) as the inactivating agent (Zhang et al., 2016). Through comprehensive assessments including blood cell count, white blood cell differential count, phagocytic activity, serum biochemical indicators, neutralizing antibody titration, immune gene expression analysis, and challenge tests, it was demonstrated that BPL-inactivated CyHV-2 serves as an effective candidate vaccine.This vaccine was shown to elicit both non-specific and specific immune responses in gibel carp, ultimately providing significant protection against HVHN disease with an RPS of 71.4%. In subsequent study, Yan *et al*. found that β-glucan and anisodamine could improve the immunostimulatory (or adjuvant) effect of a β-propiolactone-inactivated vaccine on gibel carp. Pairing with administration by immersion, this had the effect of improving the survival rate compared to other immunostimulants or in the absence of immunostimulants (Yan et al., 2020). Recently, Dharmaratnam *et al*. from India characterized two inactivated vaccines targeting CyHV-2 (Dharmaratnam et al., 2023, 2022). They cultured viruses in FtGF cells ($10^{7.8}$ $TCID_{50}$/ml) and then inactivated them using either formalin (0.1%) or heat (80°C). Under identical vaccination conditions, both trials resulted in significant up-regulation of immune genes, while the protective efficiency of the heat-inactivated vaccine was slightly higher.

In addition to inactivated vaccines, researchers have explored the use of recombinant subunit CyHV-2 vaccines as an alternative approach. Zhou *et al*. took an approach by utilizing the yeast expression system (*Pichia pastoris*) to produce three recombinant truncated proteins of CyHV-2, namely tORF25, tORF25C, and tORF25D (Zhou et al., 2015). Following intramuscular vaccination with 20 μg of these proteins, specific antibodies were detectable in all three groups, accompanied by an increase in the expression of immune-related genes. Challenge studies demonstrated that the RPS of the three immunized groups was 75%, 63%, and 54%, respectively. These findings suggest that these recombinant truncated proteins hold promise as potential vaccine candidates against CyHV-2 infection in Gibel carp.

Oral vaccines for CyHV-2 have also been explored. Dong *et al*. devised an oral vaccine targeting CyHV-2 utilizing yeast cell surface display technology (Dong et al., 2022). Consistent with previous studies by Zhou *et al*., ORF25 was chosen as the antigen, with S. cerevisiae selected as the yeast strain to facilitate oral administration (Dong et al., 2022; Zhou et al., 2015). Experimental findings demonstrate that the vaccine effectively elicits innate and adaptive immune responses, bolstering mucosal and systemic immunity in gibel carp. In a separate investigation, the oral administration of egg yolk immunoglobulin (Anti-D4ORFs IgY), as part of a passive immunization approach, demonstrated an enhancement in the survival rates of CyHV-2-infected gibel carp (B.-Y. Sun et al., 2023).

Indeed, with the advantages of delivering a single immunogen and minimizing interference from impurities, DNA vaccines have started to make inroads into the aquatic industry (Corbeil et al., 2000). In 2020, Yuan *et al*. conducted epitope analysis on the membrane proteins of CyHV-2, identifying 8 antigen-rich peptide fragments (Yuan et al., 2020). Upon comparison, it was discovered that the titer of antibodies induced by the tORF25 protein was the highest. Leveraging this finding, the first

DNA vaccine candidate, pEGFP-N1-ORF25, for CyHV-2 disease was constructed, exhibiting an RPS of 70%. Similarly, Huo *et al*. employed a comparable approach (Huo et al., 2020). In essence, when the DNA vaccine (pcORF25) and adjuvant (pcCCL35.2) are administered concurrently, they synergistically stimulate the immune system in fish, resulting in increased protection than administering the vaccine alone. Another study conducted by the same research team revealed that inactivated vaccines, when combined with the adjuvants β-glucan or astragalus polysaccharide (APS), demonstrated efficacy against CyHV-2 infection (Huo et al., 2023). Moreover, a novel vaccine utilizing protein microcrystals (polyhedra) for antigen delivery was developed, based on the codon-optimized sequence D4ORF (Li et al., 2019; Zhang et al., 2021). While demonstrating impressive effectiveness and stability, this approach entails complex manufacturing, possibly making it less feasible or more expensive.

Reports on live attenuated CyHV-2 vaccines are limited, however, Saito *et al*. have made strides in this area (Saito et al., 2022). Their approach involves utilizing low-sensitivity CFS and KF-1 cells for continuous passages to develop an attenuated vaccine. Results indicate that the SaT-1 P7-P8 candidate strain, passaged 7 times in CFS and then 8 times in KF-1, exhibited the most promising outcomes, with an RPS as high as 90%. Importantly, virulence recovery experiments revealed no signs of virulence resurgence following the passage of the vaccine strain *in vivo* and *in vitro*. Sun *et al.* used a similar method to obtain the attenuated strain G-RP7 of CyHV-2 (Y. Sun et al., 2023). The results showed that G-RP7 has good safety and stability as a candidate vaccine. The protection rates of G-RP7 in gibel carp were 92% by immersion and 100% by intraperitoneal injection. In 2019, both Li *et al*. and Cao *et al*. published papers consecutively, demonstrating the possibility of developing CyHV-2 live vector vaccines using baculovirus surface display systems (Cao et al., 2019; Li et al., 2019). The distinction lies in the approach taken by each team: Li's team fused four partial ORF regions into a single antigen gene, whereas Cao's team directly expressed nine truncated CyHV-2 membrane glycoproteins. Gibel carp injected with the former achieved a RPS of up to 80.01%, while the latter reached as high as 87.5% with immersion vaccination. These two designs collectively illustrate that baculovirus serves as an efficient protein delivery tool and holds promise as a potential vaccine candidate for preventing CyHV-2 infection.

In summary, various vaccines have been developed and utilized to prevent and manage CyHV-2 infection, including inactivated vaccines, live vaccines, vector vaccines, DNA vaccines, subunit vaccines and oral vaccines. However, these strategies remain incomplete, and both the manufacturing process and application methods require optimization. Among the candidates described, the live attenuated vaccine developed by Saito *et al*. stands out as having the most potential for commercial development. This vaccine is potent, capable of eliciting a long-lasting immune response, and as it can be administered via immersion, it closely mimics the natural pathogen infection route, maximizing mucosal surface immunity and is potentially compatible with mass vaccination of subjects at earlier developmental stages. This last point also offers, advantages in terms of application in the field including reduced labour and lower cost (Saito et al., 2024a, 2022). Further, research focusing on the development of

effective vaccines and immunostimulants is urgently needed for the comprehensive containment of the disease. Details about the CyHV-2 vaccines are documented in Table 6.

3.2.12 Research status and future perspective

Currently, CyHV-2 is widely spread across different countries, causing significant reductions in the production of goldfish and crucian carp, profoundly impacting aquaculture (Jung et al., 2022; Kurobe et al., 2024; Ouyang et al., 2020; Wang et al., 2012). Reports of CyHV-2 emergence in markets of some emerging countries, like Thailand, suggest that the virus might already be prevalent in areas where has not been previously officially reported (Piewbang et al., 2024). Therefore, a comprehensive understanding of the virus's pathogenesis and the development of effective prevention measures are crucial research priorities. Given the many gaps in CyHV-2 research, we now list the major research gaps related to the present study.

The susceptibility and permissivity of the host at different developmental stages has not yet been fully characterized. Drawing from the available literature, it is evident that CyHV-2 can affect all life stages of the host, spanning from the egg and fry to the juvenile and adult phases (Groff et al., 1998; Chang et al., 1999; Liang et al., 2015; Zhu et al., 2019; Goodwin et al., 2009). Indeed, it is observed that distinct sensitivities to CyHV-2 exist among different developmental stages, with the juvenile stage displaying heightened susceptibility (Adamek et al., 2018; Chang et al., 1999; Goodwin et al., 2009; Groff et al., 1998; Panicz et al., 2019; Sahoo et al., 2016). Notably, within the same environments, adult fish exhibit a notable resistance compared to their younger counterparts (Jeffery et al., 2007). However, these observations are based on natural reports, where environmental conditions vary, the host lacks consistency and cannot be compared horizontally (using the same batch of fish from early to late developmental stages). Therefore, setting uniform infection conditions in the laboratory to study the susceptibility and permissivity of different developmental stages to CyHV-2 is of great significance. This approach helps establish a reliable infection model and aids in the reasonable development of vaccines. In summary, the ability of CyHV-2 to affect multiple developmental stages demonstrates its pervasive impact on the host species throughout their life cycle. However, the infection characteristics at different stages of development need further elucidation, and this information may be important for future decisions related to vaccination strategies.

The pathogenesis of CyHV-2 has not been fully characterized, and there are divergences in the mechanisms by which the virus invades hosts. From the above-detailed description of clinical symptoms in diseased fish, it becomes evident that the gills are prominently affected, which often exhibit a pale colour or severe necrosis. The universality and typical nature of these gill-related symptoms have led some researchers to name this epizootic as a haemorrhagic disease of the gill (Zhu et al., 2019). Accordingly, several researchers have postulated that the gills might be the portal of entry for CyHV-2 (Ding et al., 2014; Giovannini et al., 2016; Jiang et al., 2020). However, there have been reports of infected fish having no gill lesions, or the gills and kidneys of infected fish are not always impacted at

the same time (Groff et al., 1998). Not only that, because infection with CyHV-2 virus can lead to the destruction of the intestinal mucosal barrier, which in turn triggers bacterial translocation, the intestine is also suspected to be a key portal for viral invasion (Ren et al., 2021). However, there is a lack of evidence to support this speculation, and intestinal involvement does not appear in all reports (Groff et al., 1998; Stephens et al., 2004). In addition to the gills and intestines, the skin is also prime candidate as the CyHV-2 portal of entry. Previous research with CyHV-3, a closely related virus to CyHV-2, involving the use of bioluminescent imaging and an original system to perform percutaneous infection restricted to the posterior part of the fish, the skin covering the fin and body was shown to mediate the entry of CyHV-3 into carp (Costes et al., 2009). Given the similarities to CyHV-3, and host similarities, it is plausible that the skin is also the primary portal of entry for CyHV-2. Indeed, viral DNA detected in the skin and mucus may support this, (Chai et al., 2020; Piewbang et al., 2024) however, detection of DNA does not indicate the presence of ongoing active infection in the skin. In short, the mechanisms of host invasion by CyHV-2, especially remain a significant question we aim to address in this study, as it will have important implications for vaccine design.

Epidemiological research on CyHV-2 still needs more support. Multiple strains of CyHV-2 have been successfully isolated, often originating from different host species and primarily from Asian geographical areas, using various cell lines for isolation (Davison et al., 2013; L. Li et al., 2015; Liu et al., 2018; Yang et al., 2024, 2022). Despite the known widespread presence of CyHV-2 in European aquaculture farms and natural waters, the lack of permissive cell lines has restricted the isolation and comprehensive understanding of these strains (Thangaraj et al., 2021). Therefore, conducting a detailed survey in Europe will help analyse the current severity of CyHV-2 and provide essential guidance for subsequent control and prevention measures. Further, the connections and differences between these existing strains, as well as the unique characteristics of each strain, such as prevalence and virulence have yet to be thoroughly compared and understood. Thes may also be very important in terms of identifying the most relevant and virulent strains to use in vaccine challenge trials.

Aquatic animals are often experimentally challenged to study disease pathogenesis, pathogen-host interactions in different environments, and to compare the performance of various existing and novel diagnostic tests, treatments, and vaccine efficacy (Thangaraj et al., 2021). An effective laboratory challenge model is essential for these studies. Currently, CyHV-2 laboratory challenges are primarily performed by intraperitoneal (ip) injection of infected tissue homogenates or cell culture medium containing the virus, which can rapidly induce clinical signs and high mortality (Chai et al., 2020; Liang et al., 2015; Ouyang et al., 2020; Wen et al., 2021; Xiao et al., 2022). For example, Xu *et al.* experimentally infected healthy silver carp (*C. auratus gibelio*) by intraperitoneal injection of filtered tissue homogenates of diseased fish, resulting in fish mortality beginning at 6 dpi and reaching 100% by 12 dpi (Xu et al., 2013). However, to better understand the invasion process of CyHV-2, as well as the clinical symptoms and immune responses exhibited by the host after infection, the natural infection route (immersion) remains a necessary challenge method, especially with adult hosts with intact immune

systems. Presently, only the SY strain caused 100% mortality in juvenile silver crucian carp and fingerlings, while IP injection was required to achieve the same mortality rate in adult fish (Liang et al., 2015). Only Sat-1 (ST-J1) could stably induce high mortality in goldfish (Wakin) when immersed in low concentrations, but the subject species were very limited (Saito et al., 2024a, 2024b, 2022; Wei et al., 2019). Moreover, we have observed that with many other goldfish populations, the ST-J1 strain induces no mortality when administered by immersion. This may be because CyHV-2 strains commonly used in research are either too old and not representative of current circulating strains, and/or may exhibit some degree of *in vitro* adaptation, possibly leading to some degree of *in vivo* attenuation. This indicates that it will be very important to identify new robust and reproducible CyHV-2 *in vivo* infection models in order to facilitate highly relevant vaccine challenge trials in the future.

In summary, we have identified several critical knowledge gaps and scientific challenges that currently exist in the field of CyHV-2 research. The main purpose of this study, which will be elaborated on in the objectives section, is to address the identified knowledge gaps as a first steps towards vaccine development including the establishment of a more suitable *in vivo* infection model for use in future vaccine trials.

Table 6 - Current status of CyHV-2 vaccine development.

No.	Name	Type	Fish species	Vaccination strategy	Challenge strategy	Protective effect	References
1	Formalin-inactivated cell culture supernatant (SaT-1 strain)	Inactivated vaccine	Goldfish (Edonishiki)	Intraperitoneal injection (Each inoculation is 0.1 mL, and the interval between the first injection and the booster injection is 9 days)	Immersed for 1 h in 10TCID50 l^{-1} virus culture supernatant (SaT-1 strain)	RPS*=57%	(Ito and Ototake, 2013)
2	Truncated proteins (ORF25, ORF25C, and ORF25D) expressed by *Pichia pastoris*	Subunit vaccines	Gibel carp	Intramuscular injection (0.1 ml that contained 20 μg proteins)	400 μL of live CyHV-2 (1.0×10^7 $TCID_{50}$ mL^{-1}) was injected intraperitoneally	OFR25 RPS = 75%; ORF25C RPS = 63%; ORF 25D RPS = 54%	(Zhou et al., 2015)
3	β-propiolactone inactivated CyHV-2	Inactivated vaccine	Gibel carp	Intraperitoneal injection (0.5 ml of inactivated vaccine)	0.5 ml of CyHV-2 was injected intraperitoneally (1.0×10^7 $TCID_{50}$ mL^{-1} per fish)	RPS = 71.4%	(Zhang et al., 2016)
4	Recombinant baculovirus BacCarassius-D4ORFs	Live vector vaccine	Gibel carp	Injection immunization: intraperitoneal injection (100 μL of BacCarassius-D4ORFs (2.2×10^{11} Tu/ml) per fish) Oral immunization: fed with the fodder containing BacCarassius-D4ORFs	Injection with diseased fish kidney homogenate (100 μL per fish) at the base of the pectoral fin	Injection immunization RPS = 80.01%; Oral immunization RPS = 59.3%	(Li et al., 2019)
5	Recombinant baculoviruses displaying CyHV-2 membrane proteins	Live vector vaccine	Gibel carp	Immersion immunization: 30 mL of recombinant baculoviruses (at a dose of 6×10^5 $TCID_{50}$/mL) were diluted into 5 L freshwater, and gibel carp were immersed in the tanks for 2 h.	At 47 days post-immunization, 50 μL diseased fish kidney homogenate was intraperitoneally injected	rAcMNPV-ORF25 RPS = 83.3%; rAcMNPV-ORF25C RPS = 87.5%; rAcMNPV-ORF146 RPS = 70.8%	(Cao et al., 2019)

No.	Name	Type	Fish species	Vaccination strategy	Challenge strategy	Protective effect	References
6	pEGFP-N1-ORF25	DNA vaccine	Hybridized gibel carp	Intramuscular injection: 10 μg (100 μl) liposome-encapsulated eukaryotic recombinant plasmid	At the third week after immunization, intraperitoneally injected 0.1 ml tissue solution of CyHV-2 virus (10^5 copies/ml)	RPS = 70%	(Yuan et al., 2020)
7	pcORF25/pcCCL35.2	DNA vaccine	Gibel carp	The recombinant plasmid (10 μg pcORF25/10 μg pcCCL35.2) was solved in 100 μL PBS and injected in dorsal muscle.	14-day post injection, CyHV-2 (50 μL, 1×10^7 $TCID_{50}mL^{-1}$) was intraperitoneally injected	RPS = 70%	(Huo et al., 2020)
8	H1-D4ORF/D4ORF-VP3 (co-expressing BmCPV polyhedrin)	Subunit vaccines	Gibel carp	Intraperitoneal injection: 200 μL of BmNPV-H1-D4ORF-polh polyhedral/ BmNPV-D4ORF-VP3-polh polyhedra	Fish (31 days post-vaccination) were challenged by injection at the base of the pectoral fin with CyHV-2 stock (10^7 copies of virus per fish)	H1-D4ORF RPS = 64.7%; D4ORF-VP3 RPS = 58.82%	(Zhang et al., 2021)
9	P7-P8	Live attenuated vaccine	Goldfish (Wakin)	Immersion immunization: fish were kept in 1 L water and the vaccine candidate virus was added at a 1/1000 volume	At 29 days after vaccination, fish were challenged with virulent CyHV-2 SaT-1 at $10^{1.1}$ $TCID_{50}$/mL for 2 h by immersion.	RPS = 90%	(Saito et al., 2022)
10	G-RP7	Live attenuated vaccine	Gibel carp	Immersion immunization: immersion with G-RP7 ($10^{2.3}$ $TCID_{50}$/mL) for 2 h at 25 °C. Intraperitoneal injection: 100 μL of G-RP7 ($10^{3.3}$ $TCID_{50}$/mL).	After 21 days of immunization, the fish were challenged with 100 μL of YC-1 ($10^{7.5}$ copies viral DNA/ml).	Immersion RPS = 92%. IP injection RPS = 100%	(Y. Sun et al., 2023)
11	EBY100/pYD1-ORF25	Recombinant subunit vaccine	Gibel carp	The yeast vaccine (6×10^{-2} CFU g^{-1}) and feed were mixed at a mass ratio of 1:100. Feed 1.3mg/fish for three days. On the 18-day, booster feeding。	At 41 days post vaccination, injection with diseased fish organ homogenate (100 μL per fish) at the base of the pectoral fin	RPS = 66.7%	(Dong et al., 2022)

No.	Name	Type	Fish species	Vaccination strategy	Challenge strategy	Protective effect	References
12	Formalin-inactivated CyHV-2 vaccine	Inactivated vaccine	Goldfish	Intraperitoneal injection: 300 μL of Formalin-inactivated CyHV-2 vaccine (0.1%)	At 30 days post vaccination, 100μl of CyHV-2 was injected intraperitoneally ($10^{7.8}$ $TCID_{50}$ mL^{-1} per fish)	RPS = 74.03%	(Dharmaratnam et al., 2022)
13	Heat-inactivated CyHV-2 vaccine	Inactivated vaccine	Goldfish	Intraperitoneal injection: 300 μL of Heat-inactivated CyHV-2 vaccine (80°C)	At 30 days post vaccination, 100μl of CyHV-2 was injected intraperitoneally ($10^{7.8}$ $TCID_{50}$ mL^{-1} per fish)	RPS = 83.34%	(Dharmaratnam et al., 2023)

Objectives

Carassius spp. is one of the major finfish groups in global freshwater aquaculture, including Goldfish (*Carassius auratus*), gibel carp (*Carassius gibelio*), and Crucian carp (*Carassius carassius*), among others (Rylková et al., 2013). Goldfish hold significant value as the most important pet fish worldwide due to their high ornamental value (Chen et al., 2020). In contrast, gibel carp, and Crucian carp are produced in large quantities for consumption and represent an important source of protein in many regions. According to FAO statistics data, 2,748.6 thousand tons (live weight) of *Carassius spp.* were produced in 2020, accounting for 5.6% of total finfish production and ranking seventh globally (Li et al., 2018; FAO, 2022). However, in the spring of 1992 and 1993, a new disease occurred causing severe mortality among cultured goldfish in Japan, and a herpesvirus, *Cyprinid herpesvirus 2* (CyHV-2), was later isolated from these moribund fish (Jung and Miyazaki, 1995). Since its initial detection, CyHV-2 has been found in more geographical areas and has spread globally through the aquatic trade (Chang et al., 1999; Groff et al., 1998). In addition to goldfish, the host range of CyHV-2 has expanded to include gibel carp, Crucian carp, and some hybrid strains, causing significant economic losses (Doszpoly et al., 2011; Daněk et al., 2012; Wang et al., 2012; Xiao et al., 2022). Therefore, increasing fundamental knowledge on this virus has become crucial for ensuring the long-term sustainability of aquaculture involving *Carassius spp.*

During the past two decades, the huge economic impact of CyHV-2 on aquaculture has subsequently stimulated more and more basic and applied research. Substantial progress has been made in understanding the etiology, diagnosis, impact of infection on fish, prophylaxis, and control of CyHV-2 (Thangaraj et al., 2021). However, knowledge gaps persist regarding the host range, mode of transmission, pathogenesis, and host responses. Given these gaps and the expertise of the host lab, the broad objective of this thesis was to address these knowledge gaps related to pathogenesis and to establish a more optimum *in vivo* experimental infection model for future research. Accordingly, this Ph.D. project had the following three main objectives:

Objective 1: To investigate the Susceptibility and Permissivity of *Carassius auratus* to *Cyprinid herpesvirus 2* According to the Developmental Stage using multiple types of *in vivo* imaging technologies. Prior to this study, essential knowledge on CyHV-2 pathogenesis, such as the susceptibility and permissivity of CyHV-2 at different developmental stages of the host, has not been fully characterized. Additionally, the identification of its portal of entry into the host is still unclear. Consequently, we aimed to investigate the pathogenesis of CyHV-2 in its natural host, the goldfish, using a bioluminescent *in vivo* imaging system. To achieve this, we aimed *(i)* to produce a recombinant strain of CyHV-2 encoding a luciferase expression cassette, *(ii)* to compare various aspects of this recombinant strain to the parental wild-type strain to ensure its compatibility with our goal, *(iii)* to use the same immersion inoculation route to infect goldfish to explore the relative susceptibility (ability to support CyHV-2 entry) and permissivity (ability to support CyHV-2 replication) of different developmental stages, and *(iv)* to confirm the major route(s) of viral entry into the host.

Objective 2: To investigate the potential ability of zebrafish models to support cyprinivirus infection both *in vitro* and *in vivo* by testing the susceptibility and permissivity of the ZF4 cell line and zebrafish larvae to three cyprinivirus. Prior to this study it was known that CyHV-3, a closely related virus to CyHV-2, can infect zebrafish cell lines, and adult zebrafish. However, no studies have investigated the extent to which CyHV-2 can infect zebrafish cell lines or zebrafish larvae, or directly compared this to other viral species in the genus *Cyprinivirus.* The objective of this second study was to investigate these questions, utilizing several recombinant viral strains expressing green fluorescent proteins (GFP) and Firefly Luciferase (Luc) as reporters.

Objective 3: To characterize newly isolated CyHV-2 strains through *in vitro* and *in vivo* comparisons and identify a sufficiently virulent strain to use in adult goldfish infection models. The Shubunkin goldfish is highly relevant as an economically important goldfish model. It is also relatively easy to breed, which is extremely useful in terms of sustaining a supply of hosts for experimental infection trials. However, the lack of a broadly virulent CyHV-2 strain that can be used with this model and others (for example those commonly traded globally, or intensively cultured breeds), limits the study of CyHV-2 pathogenesis in the most useful biological contexts most relevant to disease mitigation and control. More specifically, despite several CyHV-2 strains being isolated and fully sequenced, there is a lack of detailed characterization and consistent information on strains that exhibit high virulence in adult goldfish though viral challenge by immersion. These kinds of strains are much more compatible with experimental designs that are representative of natural infection, but such strains have not been formally described in any great detail. Consequently, we sought to identify novel CyHV-2 strains that 1) could be efficiently and stably passaged *in vitro* and 2) exhibit sufficient virulence in Shubunkin goldfish via challenge by immersion. To achieve this, we aimed to isolate new CyHV-2 strains originating from high mortality CyHV-2 outbreaks in various goldfish breeds including Shbunkin goldfish, and characterize them further in terms of genome sequence, *in vitro* growth kinetics and virulence in adult goldfish via challenge by immersion.

Experimental Section

Experimental Section

1st study

In Vivo Imaging Sheds Light on the Susceptibility and Permissivity of *Carassius auratus* to *Cyprinid Herpesvirus 2* According to Developmental Stage

Preamble

Cyprinid herpesvirus 2 (CyHV-2), belonging to the family *Alloherpesviridae*, is causative agent of herpesviral hematopoietic necrosis (HVHN) in various freshwater fish species including goldfish (*Carassius auratus*), crucian carp (*Carassius carassius*), and gibel carp (*Carassius gibelio*), which are economically important cultivated fish species. The highly transmissible and lethal nature of CyHV-2 has led to significant economic losses in the aquaculture industry, and high mortality outbreaks in wild habitats, such as lakes and rivers. Despite an expanding scientific literature on CyHV-2 focusing on etiology, diagnosis, transmission, and prevention, critical aspects of its pathogenesis remain poorly understood. These include the portal of viral entry into the host and differences in susceptibility and permissiveness across various developmental stages of goldfish. In order to resolve these knowledge gaps, this first study associated with this Ph.D. thesis aimed to utilize a recombinant version of CyHV-2 to *(i)* compare the susceptibility and permissivity of goldfish to CyHV-2 at different developmental stages, and *(ii)* confirm of the major portal of entry for CyHV-2, thereby offering a more comprehensive mechanistic insight into CyHV-2 infection.

Experimental Section 1

In Vivo Imaging Sheds Light on the Susceptibility and Permissivity of *Carassius auratus* to *Cyprinid Herpesvirus 2* According to Developmental Stage

Viruses 2023, 15(8), 1746

He, B.; Sridhar, A.; Streiff, C.; Deketelaere, C.; Zhang, H.; Gao, Y.; Hu, Y.; Pirotte, S.; Delrez, N.; Davison, A.J.; Donohoe, O.; Vanderplasschen, A.

My contribution to this study consisted of the recruitment of experimental materials, viral recombinant production, verification of recombinant representativeness, goldfish reproduction, infection at all developmental stages, imaging at all developmental stages, and data collection and analysis. The paper was published in the Journal *Viruses* in August of 2023.

viruses

MDPI

Article

In Vivo Imaging Sheds Light on the Susceptibility and Permissivity of *Carassius auratus* to Cyprinid Herpesvirus 2 According to Developmental Stage

Bo He [1], Arun Sridhar [1], Cindy Streiff [1], Caroline Deketelaere [1], Haiyan Zhang [1], Yuan Gao [1], Yunlong Hu [1], Sebastien Pirotte [1], Natacha Delrez [1], Andrew J. Davison [2], Owen Donohoe [1,3] and Alain F. C. Vanderplasschen [1,*]

[1] Immunology-Vaccinology, Department of Infectious and Parasitic Diseases, Fundamental and Applied Research for Animals & Health (FARAH), Faculty of Veterinary Medicine, University of Liège, B-4000 Liège, Belgium
[2] MRC-University of Glasgow Centre for Virus Research, Glasgow G61 1QH, UK
[3] Bioscience Research Institute, Technological University of the Shannon, Athlone N37 HD68, Co. Westmeath, Ireland
* Correspondence: a.vdplasschen@uliege.be; Tel.: +32-4-366-43-79

Abstract: Cyprinid herpesvirus 2 (CyHV-2) is a virus that causes mass mortality in economically important *Carassius* spp. However, there have been no comprehensive studies into host susceptibility or permissivity with respect to developmental stage, and the major portal of viral entry into the host is still unclear. To help bridge these knowledge gaps, we developed the first ever recombinant strain of CyHV-2 expressing bioluminescent and fluorescent reporter genes. Infection of *Carassius auratus* hosts with this recombinant by immersion facilitated the exploitation of various in vivo imaging techniques to establish the spatiotemporal aspects of CyHV-2 replication at larval, juvenile, and adult developmental stages. While less susceptible than later developmental stages, larvae were most permissive to CyHV-2 replication, leading to rapid systemic infection and high mortality. Permissivity to CyHV-2 decreased with advancing development, with adults being the least permissive and, thus, also exhibiting the least mortality. Across all developmental stages, the skin was the most susceptible and permissive organ to infection at the earliest sampling points post-infection, indicating that it represents the major portal of entry into these hosts. Collectively these findings provide important fundamental insights into CyHV-2 pathogenesis and epidemiology in *Carassius auratus* with high relevance to other related economically important virus-host models.

Keywords: virology; Cyprinid Herpesvirus 2; *Alloherpesviridae*; Cyprinivirus; *Carassius auratus*; aquaculture; pathogenesis; portal of entry; recombinant viruses; in vivo imaging

Citation: He, B.; Sridhar, A.; Streiff, C.; Deketelaere, C.; Zhang, H.; Gao, Y.; Hu, Y.; Pirotte, S.; Delrez, N.; Davison, A.J.; et al. In Vivo Imaging Sheds Light on the Susceptibility and Permissivity of *Carassius auratus* to Cyprinid Herpesvirus 2 According to Developmental Stage. *Viruses* **2023**, *15*, 1746. https://doi.org/10.3390/v15081746

Academic Editor: Neal A. DeLuca

Received: 24 July 2023
Revised: 10 August 2023
Accepted: 11 August 2023
Published: 15 August 2023
Corrected: 1 November 2023

1. Introduction

The goldfish (*Carassius auratus*) is a freshwater teleost species belonging to the Carassius genus within the *Cyprinidae* family. It has a rich history of domestication in China, spanning approximately 1000 years, and has emerged as a highly popular ornamental fish species. Goldfish were introduced to Japan and Europe during the early 17th century and subsequently reached North America around 1850 CE, where they gained significant popularity. Breeders and enthusiasts worldwide have successfully produced over 180 variants of goldfish, which continue to be highly sought after due to their remarkable morphological diversity and colour variations [1,2]. Beyond their ornamental value, the varied morphologies of goldfish strains have captured the interest of biologists and has been utilized as an experimental organism in the study of developmental biology and even as models for diseases including cardiac and retinal conditions [1,3,4].

In addition, goldfish have also been utilized as models to study infectious diseases, in particular prokaryotic pathogens [5–7]. Like other cultured fish species, goldfish have

highly distinct, well studied developmental stages, which may make them ideal models for assessing the impact of the developmental stage on susceptibility to infectious disease. Briefly, after egg fertilization, goldfish embryo development typically lasts three days, after which larvae hatch and exhibit vigorous swimming and feeding behaviors [6,7]. By 45 to 49 days post-fertilization (dpf), larvae acquire an adult shape, lose their fin fold, and transition into the juvenile stage. Finally, possibly up to one-year post-fertilization, goldfish reach a body length exceeding 5 cm and begin to develop external reproductive characteristics, coinciding with the commencement of the adult stage [8,9]. Studying the impact of developmental stage on susceptibility and permissivity to infectious disease may be of particular importance to the goldfish aquaculture industry, in terms of better understanding and assessment of risk at various stages of the rearing process. Findings gained from goldfish models may be of relevance to other closely related economically important *Carassius* spp., which may be susceptible to many of the same pathogens, and account for much larger portions of global aquaculture output [10].

In addition to bacterial, fungal, and parasitic pathogens, diseases caused by viral infection represent a major cause of economic loss within the aquaculture industry [11–13]. Indeed, viral disease is also a serious problem in the goldfish aquaculture sector. The most problematic and frequently isolated virus of goldfish is cyprinid herpesvirus 2 (CyHV-2), which causes mass mortality among goldfish populations. CyHV-2 is a member of the genus *Cyprinivirus*, in the family *Alloherpesviridae*. Two closely related viruses within the *Cyprinivirus* genus, cyprinid herpesvirus 1 (CyHV-1) and cyprinid herpesvirus 3 (CyHV-3) also infect cyprinid fish species, such as common carp (*Cyprinus carpio*).

The first known CyHV-2 outbreaks occurred in goldfish in Japan in 1992 and 1993 and were described in 1995 [14]. Further major outbreaks in goldfish were reported in 1998 in the western United states [15] and a year later in Taiwan [16]. In the following years, disease caused by CyHV-2 also reported among goldfish in many other regions including Australia [17], UK [18], India [19], Switzerland [20], Germany [21], France [22], Netherlands [23], Turkey [24] and Poland [25]. While initial reports were restricted to goldfish, outbreaks were also observed among populations of closely related fish species, Crucian carp (*Carassius carassius*) and Gibel carp (*Carassius gibelio*) [26–30], which both represent much larger aquaculture production sectors relative to goldfish [10,31].

However, like many related fish viruses, systemic replication of CyHV-2 in hosts is dependent on water temperature. Indeed, outbreaks of CyHV-2 that cause mass mortality are largely restricted to periods when water temperatures are within a 15–25 °C range [18,30,32]. During infections, the main external clinical signs associated with CyHV-2 infection are lethargy, anorexia, pale skin accompanied by hemorrhaging and blisters on the fins, pale gills, and elevated respiratory efforts. Infected fish also exhibit internal lesions and pale and swollen kidney and spleen (extensively reviewed elsewhere [30]). CyHV-2 may also establish persistent infections [33], which may re-emerge in response to stress, for example changes in water temperature or transportation processes [30], and during periods of immunosuppression [34]. While horizontal transmission may be the dominant mode of CyHV-2 between fish, evidence indicates that vertical transmission (from parents to offspring) may also occur [35,36].

There is a large and growing body of scientific literature describing investigations into the aetiology, diagnosis, transmission, and prevention of CyHV-2 [14,15,30]. However, to date, there is only limited knowledge of key aspects of CyHV-2 pathogenesis (such as the portal of entry of the virus into its host), and no systematic comparison of the differences in susceptibility and permissivity between goldfish developmental stages. On the later point, given that CyHV-2 was initially identified as being mainly a cause of disease in juvenile goldfish [14–16], this may indicate that earlier goldfish developmental stages are more susceptible [30].

In the present study, we generated and characterized the first ever recombinant strain of CyHV-2 expressing both luciferase 2 (Luc) and copepod GFP (copGFP) reporter genes, which we refer to in this study as the LucGFP strain. Using this recombinant strain, we

focused on elucidating two key fundamental aspects of CyHV-2 pathogenesis in goldfish: (1) the relative susceptibility (the ability to support CyHV-2 entry) and permissivity (the ability to support CyHV-2 replication) across different developmental stages and (2) the route of viral entry into the host. Closing these knowledge gaps provides important insights into CyHV-2 pathogenesis.

2. Materials and Methods

2.1. Cells and Viruses

The RyuF-2 cell line, derived from the caudal fin of Ryukin goldfish, was used to propagate the virus in this study [37]. Cells were cultured at 25 °C using Medium 199 (HEPES buffered; Sigma, Kawasaki, Japan) supplemented with 10% fetal bovine serum (FBS; Gibco, Life Technologies, Carlsbad, CA, USA), penicillin (100 U/mL), and streptomycin (100 µg/mL). The CyHV-2 YC-01 strain (GenBank: MN593216.1) was isolated from diseased gibel carp [38] and kindly provided by Prof. Lu (Shanghai Ocean University, Pudong, Shanghai, China). CyHV-2 was cultured in RyuF-2 cells at 25 °C using the same cell culture media described above. After the widespread CPE was observed, viral culture media were collected and centrifuged at 2000× *g* for 20 min (min) (Allegra X-15R Centrifuge, Beckman, Brea, CA, USA) to remove cell debris. The resulting viral supernatant was stored at −80 °C. Titers of infectious CyHV-2 particles were determined by triplicate plaque assays conducted in 6-well plates. Briefly, a series of 10-fold dilutions were made from viral supernatant, using serum free cell culture medium as diluent. A total of 1 mL of each dilution was applied to each well containing fresh RyuF-2 cells, 18–24 h (hour) post-seeding (80–100% confluent), and incubated for 2 h at 25 °C. Subsequently, the initial inoculum was removed from each well and replaced with 3 mL complete cell culture media with carboxymethylcellulose (CMC) (final concentration 2% *w*/*v*) and incubated for 4 days at 25 °C. Plaques were visualized using an epifluorescence microscope (Leica DM2000), either indirectly using fluorescent immunostaining or directly using a virally expressed fluorescent reporter. Dilutions exhibiting 20–200 plaques were used to estimate titers.

2.2. Production of the LucGFP Recombinant Strain of CyHV-2 by Recombination in Eukaryotic Cells

The CyHV-2 LucGFP strain was produced by homologous recombination in RyuF-2 cells (Figure 1). The LucGFP cassette consisted of an EF1α promoter driving the transcription of a bicistronic mRNA encoding Luc and copGFP proteins linked by a T2A peptide. The LucGFP cassette was inserted in the intergenic region between ORF64 and ORF66 of CyHV-2 genome to produce the LucGFP recombinant strain. This targeted insertion was achieved by initially ligating the LucGFP cassette into a pGEMT vector, flanked by 500-bp sequences corresponding to the end and the beginning of CyHV-2 ORF64 and ORF66, respectively, to create the pGEMT LucGFP vector. To create the pGEMT LucGFP vector, target fragments were first amplified using the Phusion High-Fidelity PCR Kit (New England Biolabs, Ipswich, MA, USA), with overlaps for assembly incorporated into the primers. All corresponding templates and primers are listed in Table 1. The amplified fragments and an empty pGEMT vector were assembled together using the NEBuilder HiFi DNA Assembly Kit (New England Biolabs), with the ligation product transformed into competent bacterial strains. The pGEMT LucGFP vector was purified using the NucleoSpin Plasmid Mini Kit (Macherey Nage, Düren, Germany). One day after transfection with the pGEMT LucGFP vector, RyuF-2 cells were infected with the CyHV-2 YC-01 strain (WT parental strain) at the multiplicity of infection (MOI) of 0.1 plaque forming units (pfu)/cell. After 4 days, the supernatant was collected and used to make a series of 10-fold dilutions in serum free cell culture media, which were then used to infect fresh RyuF-2 cells. Cells were infected in the same way as described for viral titration above. Isolated viral plaques expressing copGFP were picked and subcultured until 100% of plaques in subsequent sub-cultures were observed to express the reporter gene. Plaques were viewed using an epifluorescence microscope (Leica DM2000).

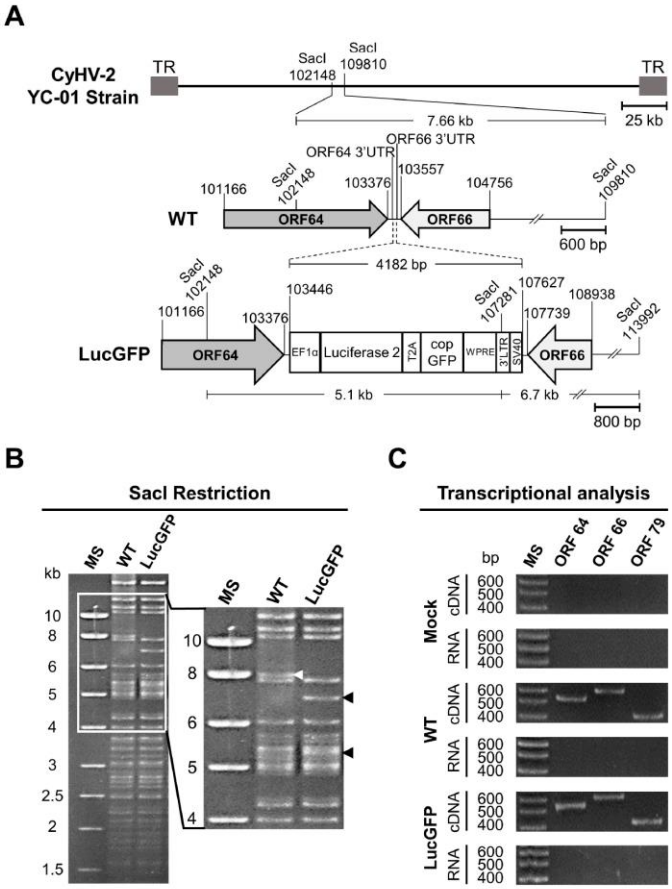

Figure 1. Production of the CyHV-2 LucGFP recombinant strain. (**A**) Schematic representation of the genome structure of the recombinant produced. The genome of the CyHV-2 YC-01 strain, flanked by two terminal repeats (LTR and RTR), is shown at the top. A bicistronic reporter expression cassette was inserted into the non-coding ORF64-ORF66 intergenic region. SacI restriction sites and genome coordinates are marked. (**B**) Genomic analysis of CyHV-2 strains. The genomes of the WT and LucGFP strains were analyzed by SacI RFLP analysis. The white arrowhead indicates the fragment (7.66 kb) of the WT strain genome containing the insertion site. The black arrowheads indicate two new fragments (5.1 and 6.7 kb) that were generated due to the insertion of the LucGFP cassette. The ladder indicates the approximate sizes of each fragment. (**C**) Transcriptional analysis of genes flanking the insertion site of the transgene. Using reverse transcriptase polymerase chain reaction (RT-PCR), transcription of ORF64 and ORF66 was compared between the LucGFP strain and WT strain during viral replication in vitro. Both ORF64 (546 bp) and ORF66 (610 bp) transcripts were detected in RNA from WT and LucGFP infected cells, indicating that flanking genes were not impacted by the reporter gene insertion. Importantly, the absence of a detectable product in the RT-negative controls (RNA, bottom row) indicated that results were not the result of residual genomic DNA contaminants. Marker sizes (MS) are indicated on the left. ORF79 (CyHV-2, DNA polymerase gene) was used as a loading control, as it is located in a distant part of the CyHV-2 genome and, thus, should not be impacted by the reporter gene insertion between ORF64 and ORF66.

Table 1. Primers and templates used in this study.

Description	Primer Name	Sequence (5′-3′)	Coordinates on Target Template [1]
For synthesis of LucGFP recombination cassette [2]			
Left homologous region	ORF64 HR Fw	*GGCGGCCGCGGGAATTCGAT*TCACT ATGTATTTTCCCGC	102946-102964
	ORF64 HR Rev	GCAGATCCTTATTACATCGTGTGTC ATTTATTAAG	103421-103445
LucGFP cassette	LucGFP Fw	ACGATGTAATAAGGATCTGCGATC GCTC	N/A: Template generated via ligation of several synthetic dsDNA fragments
	LucGFP Rev	TAATATGAACCCAGACATGATAAG ATACATTGATG	
Right homologous region	ORF66 HR Fw	TCATGTCTGGGTTCATATTATATAT ATTTTATTGACGACAATAAAACC	103446-103483
	ORF66 HR Rev	*GCCGCGAATTCACTAGTGAT*ACGCA GACATCAACCTCATC	103926-103945
For transcriptional analysis			
ORF64	ORF64 Fw	CTGCATTGACAACAAGAAACGC	102098-102119
	ORF64 Rev	AAGAAGGGTTGGAGTCTCGAGC	102622-102643
ORF66	ORF66 Fw	CGTACTCTACCATGGGATGC	103739-103758
	ORF66 Rev	GTGGACATCATCACACAGGC	104329-104348
ORF79	ORF79 Fw	TTTGTGCTCTCTGAATCGGAGC	123777-123798
	ORF79 Rev	GCTGGTGACTTCTTTGTAGC	124177-124196

[1] Coordinates relate to CyHV-2 YC-01 strain, GenBank accession number: MN593216.1. [2] Underlined, bases corresponding to CyHV-2 genome sequence; italic, bases corresponding to the pGEMT vector sequence; non-italic and no underlining, bases corresponding to the LucGFP expression cassette sequence.

2.3. Genetic Characterization of the CyHV-2 LucGFP Recombinant

The genotype of the recombinant strain was confirmed by SacI restriction fragment length polymorphism (RFLP) analysis. Briefly, 3 µg of genomic DNA was digested using SacI (New England Biolabs). Digested DNA was run in 0.8% agarose gel at 60 V for 18 h. Full-length genome sequencing was performed as described previously [39].

2.4. Transcription Analysis

RyuF-2 cells were mock-infected with cell culture media or infected with CyHV-2 at an MOI of 0.1 pfu/cell. RNA was isolated 24 h post-infection (hpi) using the NucleoSpin RNA Mini Kit (Macherey-Nagel), and residual DNA was removed using the TURBO DNA-free Kit (Invitrogen, Waltham, MA, USA). Reverse transcription reactions were performed on 5 µg of RNA using Superscript III Reverse Transcriptase with oligo (dT) primers (Invitrogen). Finally, ORF64, ORF66 and ORF79 (CyHV-2 DNA polymerase) were amplified using the Phusion High-Fidelity DNA polymerase kit (New England Biolabs) with the pairs of primers described in Table 1.

2.5. Polyclonal Antibody Production

CyHV-2-specific rabbit polyclonal antibodies (pAbs) were produced following a 70-day rabbit immunization protocol. Viral supernatant was prepared from infected RyuF-2 cells as described above. Virions were then pelleted by centrifugation of 100,000× *g* for 2 h using an ultracentrifuge (Optima LE-80K Ultracentrifuge, Beckman). The supernatant was removed, and the virion pellet was resuspended in 1 mL PBS to create a CyHV-2 antigen suspension. The total protein concentration of the CyHV-2 antigen suspension was measured using a Pierce BCA assay kit (Thermo Fisher, Waltham, MA, USA), after which it was diluted accordingly in PBS. Diluted CyHV-2 antigen was mixed thoroughly with

adjuvant (50:50 v/v) using a TissueLyser (QIAGEN) in order to obtain an antigen-adjuvant emulsion solution. This emulsion was administered to specific pathogen-free rabbits via a series of subcutaneous injections (100 ng of total protein per injection). The primary immunization consisted of 500 µL of antigen and 500 µL of Freund's complete adjuvant administered at 5 different injection sites. All boosters consisted of 500 µL antigen and 500 µL incomplete Freund's adjuvant emulsion and were also administered at 5 different injection sites. Boosters were administered at two, four, and six weeks after the primary immunization. Blood was collected two weeks after the final booster and incubated at 37 °C for 1–2 h before being transferred to 4 °C overnight. The samples were subsequently centrifuged at 900× g for 20 min, and serum was collected and stored at −80 °C.

2.6. Indirect Immunofluorescence Staining

RyuF-2 cells in 6-well plates (mock-infected with cell culture media or infected with CyHV-2) were fixed with PBS containing 4% (w/v) paraformaldehyde at 4 °C for 15 min and then 20 °C for 15 min. After washing with PBS, samples were permeabilized in PBS containing 0.1% (v/v) NP-40 at 37 °C for 15 min. Immunofluorescent staining (incubation and washes) was performed in PBS containing 10% FCS (v/v). The primary antibody, consisting of rabbit anti-CyHV-2 pAbs, was diluted 1:2000 in FCS-PBS and incubated on fixed and permeabilized cells at 37 °C for 2 h. The secondary antibody, Alexa Fluor 568 goat anti-rabbit immunoglobulin G (H + L) (2 µg/mL; Molecular Probes, Invitrogen), was diluted 1:1000 in 10% (v/v) FCS-PBS and incubated at 37 °C for 30 min. After washing, stained cells were treated using Prolong Gold Antifade Reagent (Invitrogen). Cells were viewed using an epifluorescence (Leica DM2000) or confocal (Nikon A1R) microscope.

2.7. Viral Growth Assay

CyHV-2 was diluted in serum-free media to give a MOI of 0.01 pfu/cell in each well. Triplicate cultures of RyuF-2 cells grown in 6-well plates were infected with 1 mL viral supernatant. After an incubation period of 2 h, the cells were washed with PBS and overlaid with complete cell culture medium. At 2-, 4-, and 6-days post-infection (dpi), both viral supernatant and infected cells were collected from each well, combined, and stored at −80 °C for one week. These samples were thawed and analyzed by viral titration using triplicate plaque assays in RyuF-2 cells, as described above.

2.8. Viral Plaque Assay

RyuF-2 cells were cultured in six-well plates and inoculated with 100 pfu/well of CyHV-2 for 2 h, and then overlaid with culture medium supplemented with CMC (2% w/v). At 3, 4, 5, and 6 dpi, viral plaques were visualized by indirect immunofluorescent staining. After the final wash with PBS, 20 randomly selected individual plaques were then imaged using a Nikon A1R confocal microscope, and areas were measured using ImageJ software (Version 1.53) [40].

2.9. Fish

Three different development stages of Shubunkin goldfish (*Carassius auratus*) were used in the present study. (i) Mature shubunkin goldfish were obtained from an accredited commercial company (Ruinemans Aquarium, Montfoort, The Netherlands). Microbiological, parasitic, and clinical examinations were conducted immediately after arrival in the animal facility and then monthly to monitor fish health. Adult goldfish from the colony were determined to be free of CyHV-2 based on polymerase chain reaction (PCR) analysis of kidney homogenate. Fish were maintained in 60 L freshwater recirculation tanks at 25 °C until used for breeding or transferred to L2 facilities for infection experiments. (ii) Shubunkin goldfish larvae (4 dpf) were produced using standard artificial reproduction methods applied previously [41]. The larvae were hatched in Zoug bottles, then transferred to 60 L freshwater recirculation tanks maintained at 25 °C after hatching until being transferred to a L2 laboratory setting for infection experiments at 4 dpf. (iii) Juvenile shubunkin

goldfish (75 dpf) were generated through rearing of the larvae mentioned above, and were maintained in 60 L freshwater recirculation tanks at 25 °C.

2.10. Inoculation of Fish with CyHV-2

Different modes of inoculation were used depending on the developmental stage. In all cases, viral inoculum was thawed and used immediately. (i) Inoculation of adult goldfish by intraperitoneal (IP) injection: Shubunkin adult goldfish (average weight 3.5 ± 0.4 g, 8 months old) were first anesthetized by immersion in water containing benzocaine (25 mg/L) and weighed. The virus was diluted in serum free cell culture medium (final concentration = 5×10^5 pfu/mL) and injected intraperitoneally using a 300 µL insulin syringe (BD Micro-Fine), with each fish receiving a dose of 10^4 pfu/g (total body weight). After injection, the fish were placed in an aerated recovery bath for 10 min and returned to the tank. (ii) Inoculation of larvae by immersion in infectious water: Goldfish larvae (4 dpf, average length = 5.2 ± 0.1 mm) were infected by immersion in E3 medium containing virus. Briefly, larvae were transferred to a single petri dish (1 larvae per mL of E3 media) and CyHV-2 was added (final concentration = 1×10^5 pfu/mL) followed by gentle mixing. The larvae were incubated at 25 °C for 2 h, and subsequently transferred to new petri dishes containing 50 mL of E3 medium. (iii) Inoculation of juvenile fish by immersion in infectious water: Juvenile shubunkin goldfish (75 dpf, average length = 2.3 ± 0.3 cm) were immersed in water containing CyHV-2 (final concentration = 1×10^5 pfu/mL) for 2 h under constant aeration (20 fish/L), and then moved to a separate virus free tank. (iv) Inoculation of adult fish by immersion in infectious water: Adult shubunkin goldfish (1.5 years old, average weight = 12 ± 3.7 g) were immersed in water containing CyHV-2 (final concentration = 1×10^5 pfu/mL) for 2 h under constant aeration (10 fish/L), and then moved to a 60 L tank. In all experiments, mock-infected fish were also prepared by the substitution of viral inoculum with serum-free cell culture medium.

2.11. Scoring of Morbidity and Mortality

The percentage of fish expressing clinical signs was determined by daily examination of each tank. The percentage of morbid fish was defined as the proportion of fish in each tank expressing one or several of the following clinical signs: hyperemia of cephalic skin, hyperemia of the gills, hyperemia of the skin covering the body or the fins, multifocal skin lesions, or abnormal swimming. Mortality was recorded daily, and the survival rate was calculated at the end of the experiment.

2.12. Bioluminescent Imaging

Luminescent emission from firefly (*Photinus pyralis*) luciferase was imaged using an in vivo imaging system (IVIS) (Spectrum, Perkin Elmer, Rowville, Australia) as described previously [42]. For in vivo analysis, adult and juvenile fish were anesthetized with benzocaine (25 mg/L), in aerated water. Once anesthetized, D-luciferin (Caliper LifeSciences) was administered by IP injection (150 mg/kg of body weight). Fish were kept for 15 min in aerated water before bioluminescence was measured. Larvae were anesthetized by transferring to a new petri dish with 0.2 mg/mL tricaine (MS222, Sigma-Aldrich, St. Louis, MI, USA) in E3 medium (1 fish/mL). This E3 also contained methylcellulose (2%) in order to reduce drifting of the larvae during subsequent procedures. D-luciferin (150 µg/mL) was administered to larvae by pericardial microinjection (3 nL/fish). After 5 min incubation, larvae were imaged by IVIS. For all developmental stages, the bioluminescent signal originating from the skin was imaged first. Each fish was analyzed lying on its left and right side, except larvae, which were acquired for a single position. After euthanasia of fish with benzocaine (250 mg/L), organs (adult: gill, gut, heart, spleen, and kidney; juvenile: gill and gut; larvae: not applicable) were dissected and bioluminescence signals were measured by IVIS separately from the body. Adult images presented in this study were acquired using a field view of C while juvenile and larvae were acquired using the field view B. Other settings, including binning factor = 8, f/stop = 1, and maximum auto-exposure time of

1 min, were constant for all developmental stages. Data were analyzed using the Living Image software (v3.2) (Perkin Elmer). Each region of interest (ROI) was drawn manually by tracing the organs or body outlines, and the average radiance (p/sec/cm^2/sr) was taken as the final measure of the bioluminescence emitted over the ROI. Images were annotated to show the average radiance signal according to location in the subject, using a colour scale ranging from violet (lowest signal) to red (highest signal). For the skin, the average radiance (individual values, mean + standard deviation or SD) was measured on both sides of the body (except for larvae), and the results for individual fish were expressed as the mean of both sides. For each fish, corresponding average radiance values from gills (mean of left and right gills) and internal organs (gut, heart, spleen, and kidney), were measured and presented separately. The cut-off for positivity (dotted line in all related figures) consisted of the mean +3 SD of the values obtained for mock-infected fish (negative control). For measurement of bioluminescence in vitro, cell culture media was replaced with a fresh serum-free media containing D-luciferin (150 µg/mL). After a 10 min incubation at room temperature, bioluminescence signals were acquired using the same IVIS settings as used for adult fish, and the entire well was used as the ROI when establishing the average radiance.

2.13. In Vivo Epifluorescence Microscopy

For epifluorescence microscopy analysis of adults (skin and caudal fin), juveniles (eye, gill, skin, and caudal fin), and larvae (whole body), fish were anesthetized as described for IVIS analysis above. Images were captured with a Leica DM2000 epifluorescence microscope using the GFP filter set at 5× or 10× magnification.

2.14. Light Sheet Microscopy Imaging

This experimental procedure was adapted from previous methodology used with zebrafish larvae [43–45]. Briefly, larvae were infected or mock-infected with the CyHV-2 LucGFP strain by immersion as described previously. After 24 h of incubation, infection was confirmed using epifluorescence microscopy to identify the GFP signal. To stain the nuclei of living cells of skin epidermis, infected larvae were incubated in E3 media containing DRAQ5 (1:1000 dilution) for 30 min. In parallel, immobilizing agarose was prepared by dissolving low-melting agarose (Bio-Rad, Hercules, CA, USA) (final concentration 0.1% w/v). Once the agarose was dissolved, tricaine was added to the immobilizing agarose solution (0.1% w/v final concentration). An additional agarose solution consisting of standard high melting point agarose (final concentration 1% w/v) in E3 was also prepared for sealing the sample chambers. After the DRAQ5 staining was complete, larvae were anesthetized as described above, and transferred to the immobilizing agarose solution containing 0.1% (w/v) tricaine. Fluorinated ethylene–propylene (FEP) tubing (Bola, S1815-07, refractive index 1.338, inner diameter 2 mm, outer diameter 3 mm) was used as the sample chamber and attached to the end of a capillary. By placing a plunger in the capillary, a single larvae suspended in immobilizing agarose solution was drawn up into FEP tubing (headfirst). The end of the FEP tubing was sealed by drawing up standard high melting point agarose (1% w/v) which solidified quickly after entry to the FEP tubing. A three-dimensional image was acquired using a Zeiss Light-sheet Z1 10× objective along the y axis, pairing 488 nm and 638 nm laser to excite GFP and DRAQ5, respectively. The subsequent data was used to generate a maximum-intensity projection video with ImageJ.

2.15. Confocal Microscopy Imaging

DRAQ5-stained larvae were prepared as described for light-sheet microscopy. They were anesthetized in E3 medium containing 0.2 mg/mL of tricaine and transferred to a glass slide with a small droplet of E3 medium. A cover slip with spacers was placed over larvae, providing enough space to accommodate the subject under the coverslip. The slides were analyzed by confocal microscopy (Nikon A1R) using 488 nm and 633 nm lasers to excite GFP and DRAQ5, respectively. A series of Z-stack confocal images were acquired to

generate a 3D representation of the area of interest. The acquired images were rendered using Imaris viewer software (v10.0) (Oxford Instruments, Oxfordshire, UK).

2.16. Immunohistochemistry

For immunohistochemistry (IHC), tissues were fixed in 4% PAF for 18 h at 4 °C then dipped in 70% (*v*/*v*) ethanol and embedded in paraffin. Immunoperoxidase staining was performed on tissue sections (5 µm) after dewaxing and epitope unmasking in citrate buffer (0.01 M, pH 6.0). Endogenous peroxidases were blocked by incubation in 3% H_2O_2 for 15 min at room temperature (RT). After blocking of non-specific binding sites, tissues were incubated for 1 h at 22 °C in the primary antibody (mouse monoclonal turboGFP antibody, OriGene Technologies) diluted 1:500. Sections were then incubated for 1 h at room temperature (RT) with the secondary antibody (Envision anti-mouse + System-HRP, Agilent). Peroxidase was detected with Liquid DAB + Substrate Chromogen System (Agilent). After rinsing with demineralized water, sections were counterstained with Carazzi's hematoxylin (EMD Millipore, Burlington, MA, USA). Sections of mock-infected fish served as negative controls. Specimens were scanned using a Nanozoomer Digital Pathology 2.0 HT scanner (Hamamatsu Photonics, Shizuoka, Japan) and were analyzed using NDP.view2 Viewer software (Hamamatsu Photonics).

2.17. Statistical Analysis

Residuals for each dataset were first tested for normality using the Shapiro–Wilk test (GraphPad Prism v8.0.1) to determine if parametric and non-parametric tests were required. Two-way omnibus tests on data from the viral growth curve and plaque size experiments were conducted using two-way analysis of variance (ANOVA) with multiple comparisons between groups of interest made using the Benjamini–Hochberg (BH) post hoc test. One-way tests on data generated from the in vivo experiments were conducted using the one-way ANOVA test with BH post hoc test for data sets exhibiting normal distribution, or the Kruskal–Wallis Test with Dunn's post hoc test for data not exhibiting normal distribution. Survival curves were compared using the log-rank test. All tests were implemented in GraphPad prism 8.0. Only significant *p*-values (<0.05) are reported in the results section. Similarly, for the purposes of visual clarity, only significant results from post hoc multiple comparisons are indicated in each corresponding figure, and are represented using the following symbols: * = $p < 0.05$; ** = $p < 0.01$; *** = $p < 0.001$.

2.18. Ethics Statement

The experiments, maintenance, and care of fish complied with the guidelines of the European Convention for the Protection of Vertebrate Animals used for Experimental and other Scientific Purposes (CETS No. 123). The animal studies were approved by the local ethics committee of the University of Liège, Belgium (Laboratory accreditation No. 1610008). All efforts were made to minimize suffering.

3. Results

The primary aim of this study was to conduct a systematic investigation into the spatiotemporal aspects of CyHV-2 replication using in vivo imaging in goldfish across larvae, juvenile, and adult developmental stages. To maximize the consistency and homogeneity between experimental subject populations at different developmental stages, all the fish used in this study were derived from a single batch, thus maximizing the overall scientific validity of our findings. Specifically, goldfish were selectively bred and raised to reach adulthood, attaining an age of 1.5 years, before being segregated into two distinct schools. One group of fish was subjected to direct infection with CyHV-2, serving as the experimental host population. Simultaneously, another group of fish was utilized solely for breeding purposes, facilitating the generation of offspring. The resulting progeny were further divided into two subgroups: a portion was utilized in experimental infections at the

larvae stage, while the remaining individuals were allowed to grow to the juvenile stage for subsequent experimentation.

3.1. Generation of the CyHV-2 LucGFP Recombinant Strain

We have previously demonstrated that in vivo imaging is a highly effective methodology for the comprehensive investigation into pathogenesis associated with CyHV-3 [39,41,42,46–49] which is closely related to CyHV-2 [50,51]. To facilitate in vivo imaging during CyHV-2 experiments, the YC-01 CyHV-2 strain (WT) was selected as the parental strain for generation of a recombinant expressing Luc and copGFP as reporter proteins, which we refer to as the LucGFP strain. The reporter cassette was inserted between ORF64 and ORF66 of the WT CyHV-2 genome, as depicted in Figure 1A. This insertion of the construct resulted in the introduction of a new SacI restriction site at position 107281 of the LucGFP genome, resulting in the expected loss of the 7.66 kb SacI restriction fragment in the parental WT strain and an appearance of two smaller 5.1 KB and 6.7 kb SacI restriction fragments in the LucGFP strain (Figure 1A). The expected pattern was observed in subsequent SacI RFLP analysis (Figure 1B), thus, confirming the correct integration of the reporter cassette, which was also confirmed by whole genome sequencing (data not shown). Furthermore, transcriptomic analysis of ORF64 and ORF66 genes during LucGFP replication in vitro confirmed that the reporter cassette did not prevent the expression of genes adjacent to the insert in the LucGFP strain (Figure 1C).

3.2. Comparison of LucGFP Recombinant and WT Strains In Vitro and In Vivo

The ability of the LucGFP recombinant to express Luc and copGFP was confirmed in vitro. Briefly, RyuF-2 cells were infected with a 10^{-5} dilution of the original LucGFP and WT stock, and then cultured under the conditions described for plaque assays. At 4 dpi, bioluminescence imaging was performed by IVIS, confirming the expression of Luc in the LucGFP-infected monolayer, with no signal observed in WT and mock-infected cells (Figure 2A, left panel). Replicate plates were examined through indirect immunofluorescent staining and epifluorescence microscopy, confirming both the expression and colocalization of copGFP and viral plaque signals (Figure 2A, right panel). Taken together, these results confirmed the correct expression of both reporter genes by the LucGFP recombinant.

To verify that the insertion of the construct in the LucGFP strain did not have any impact on viral growth in vitro relative to the WT, the two strains were compared using a multistep growth curve. This revealed that both strains exhibited remarkably similar growth kinetics in vitro (Figure 2B, top panel). Multiple comparisons tests conducted at each individual time point revealed no statistically significant differences between the WT and LucGFP strains, with similar observations made in a comparison of viral plaque areas (Figure 2B, lower panel). Collectively these findings indicate that the presence and expression of the reporter genes in the LucGFP recombinant had no discernible impact on replication kinetics, with the LucGFP recombinant strain maintaining comparable fitness to its parental strain in cell culture.

Next, the pathogenicity exhibited by the LucGFP recombinant in vivo was compared to that of its parental WT strain. WT and LucGFP recombinant strains inoculated by IP injection to adult fish showed comparable virulence as revealed by quantification of morbidity and mortality (Figure 2C). The clinical signs associated with CyHV-2 disease were inducted by both strains, and the intensities of the clinical signs were comparable in the two infection groups. Specifically, at 4 dpi, fish populations began to show recognizable clinical symptoms, including apathy, redness on the cephalic part, congestion, and hyperemia on the gills. One-week post-infection, the incidence rate reached 100%. In both groups, morbidity lasted for approximately one week, after which the survivors recovered and returned to a healthy state. The onset of mortality coincided closely with the onset of morbidity. This began at 5 dpi, with the number of deaths subsequently increasing rapidly. Mortality rate ceased approximately two weeks after infection. No significant difference in survival curves was detected between the WT and LucGFP groups. PCR assays targeting

the LucGFP insert (Table 1) were performed on dead fish from the LucGFP group in order to exclude the possibility of contamination with the WT strain, and these confirmed the absence of contamination. These results indicated that the LucGFP recombinant exhibits comparable pathogenicity to that of its parental WT strain in vivo upon challenge by IP injection. Consequently, the LucGFP recombinant was deemed suitable to use in subsequent experiments to systematically investigate the spatiotemporal aspects of CyHV-2 replication in goldfish across larvae, juvenile, and adult developmental stages, using various in vivo imaging techniques.

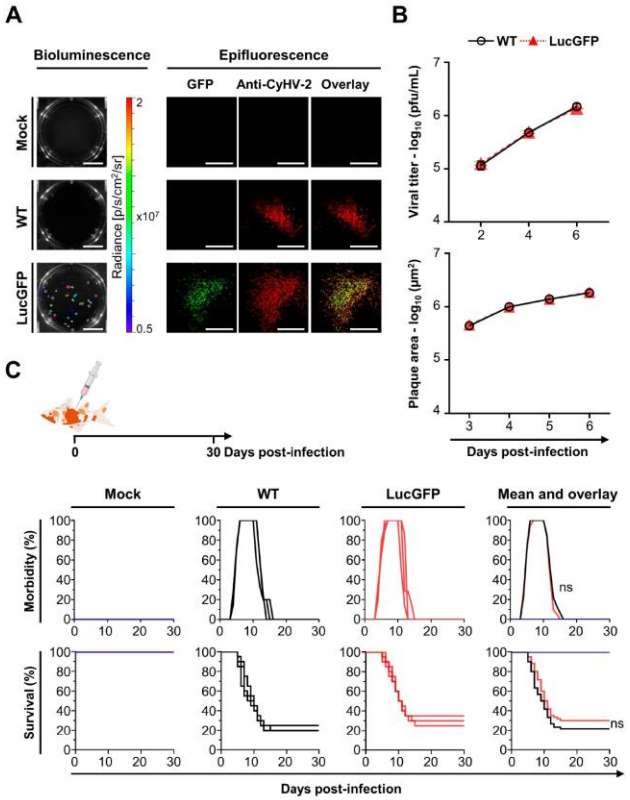

Figure 2. Phenotypic characterization of CyHV-2 strains. (**A**) Expression of reporter genes. RyuF-2 cells grown in 6-well plates were infected with the indicated strains and then overlaid with medium containing CMC. At 4 dpi, infected cells were analyzed for bioluminescent and fluorescent signal from reporter genes. The Luc signal was detected using an IVIS system (**left** column, scale bar = 1 cm). The copGFP signal was detected by epifluorescence microscopy (**right** panels, scale bar = 500 µm). Viral plaques were revealed by indirect immunofluorescent staining. (**B**) Comparisons of viral growth in vitro. Viral growth assay (**top** panel). RyuF-2 cells were infected with the indicated strains and the $\log_{10}$ value of the titer (pfu/mL) in the supernatant was determined at the indicated dpi. Data represent the mean ± SEM of triplicate measurements. Viral plaque assay (**lower** panel). RyuF-2 cells were infected with the indicated strains, and plaque areas were measured over time. Data represent the mean ± SEM of 20 individual plaques. No significant differences were detected between WT and LucGFP strains. (**C**) Comparison of virulence in vivo. The virulence of the indicated strains was tested in adult Shubunkin goldfish (triplicate groups each consisting of 20 subjects, average weight 3.5 ± 0.4 g, 8 months old). Fish were mock-infected or infected by IP injection with the indicated strains (10^4 pfu/g). The fish were examined daily for clinical signs of CyHV-2 disease, and fish reaching the endpoints were euthanized. No significant differences were detected between WT and LucGFP strains in the experiments described in (**B**,**C**).

3.3. Goldfish Larvae Are Susceptible and Highly Permissive to CyHV-2 Infection after Inoculation by Immersion in Infectious Water with the Skin of the Larvae Acting as the Portal of Entry of the Virus

The LucGFP strain was used to establish the susceptibility and permissivity of goldfish larvae to CyHV-2. Larvae were challenged by immersion in infectious water, with survival and spatiotemporal aspects of infection subsequently examined using various methods. The experiment and designs are illustrated in Figure 3A. CyHV-2 challenge of larvae (4 dpf) by immersion resulted in 100% mortality in both WT and LucGFP infected groups by 5 dpi (Figure 3B). Most mortality occurred between 3–5 dpi and, consistent with Figure 2C (adult subjects, challenged by IP injection), there was no significant difference between WT and LucGFP survival curves (Figure 3B). In contrast, there was much less mortality in mock-infected groups, with 80% of subjects surviving up to 7 dpi.

Notably, the exceptionally high mortality observed (Figure 3B) suggested that goldfish larvae are highly susceptible to CyHV-2 infection, and possibly highly permissive to CyHV-2 replication once infections are established. The replication in larvae over time was subsequently investigated by using an IVIS to detect Luc expression after infection with the LucGFP strain, thus, facilitating relative quantitative analysis of viral load. This experiment also permitted the estimation of susceptibility, revealing that 60% of the population were positive for CyHV-2 (i.e., Luc expression) at 1 dpi, the earliest sampling point, with prevalence increasing to 100% by 3 dpi. The evolution of Luc expression over time (representing viral load) revealed that time post-infection had a significant impact on viral load ($p < 0.0001$). Viral load increased dramatically from 1–4 dpi, particularly after 3 dpi, with a significant increase in viral load observed between 2–3 dpi (Figure 3C, top panel), and was consistent with earlier observations indicating the onset of mortality peak at 3 dpi (Figure 3B). This indicated that goldfish larvae are highly permissive to CyHV-2 replication. This pattern was also reflected in a series of representative images from this analysis, showing that localized Luc signals, representing viral replication foci, were initially small and dispersed on larvae (1–3 dpi), but subsequently grew and coalesced into larger patches of infected tissue after 3 dpi (Figure 3C, lower panel).

Identical infection experiments were conducted in parallel where CyHV-2 replication was monitored by epifluorescence microscopy, exploiting copGFP expression by the LucGFP strain. Consistent with the IVIS analysis (Figure 3C, top panel), this revealed an increase in copGFP signal with respect to time post-infection, in particular, after 3 dpi (Figure 4). Interestingly, careful microscopic examination of some subjects in different orientations suggested that the GFP signal may be entirely localized in the skin at 1 dpi (Figure 4, left panel), meaning that the skin may be the primary portal of entry of the virus into its host.

To investigate this further, in a more conclusive manner, we sought to selectively stain the epidermal skin cells in infected larvae and test for co-localization of epidermal and viral signal in 3D renderings of infected tissue. To achieve this, we first identified infected larvae via epifluorescence microscopy (Figure 5, first row), and exposed them to the DRAQ5 nuclear stain via addition to E3 media. The short DRAQ5 exposure and limited penetration during this period resulted in the selective staining of living epidermal skin cells in larval outer body. After this, fish were anesthetized and subjected to confocal microscopy to acquire Z-stacks from infected regions, which were subsequently used to generate 3D renderings (Figure 5, second row). In order to determine if the viral signals were localized in the skin only, and not originating from deeper tissue within the infected larvae, three optical sections intersecting with infected zones were generated from the 3D renderings (Figure 5, third row), which were examined further individually. These optical sections revealed co-localization of the copGFP and DRAQ5 signals in infected larvae (Figure 5, last three rows, optical sections d, e, and f,), thus, confirming that virally infected cells were restricted to the skin at 1 dpi. No viral signals were detected in a corresponding analysis of mock-infected fish (Figure 5, left panel).

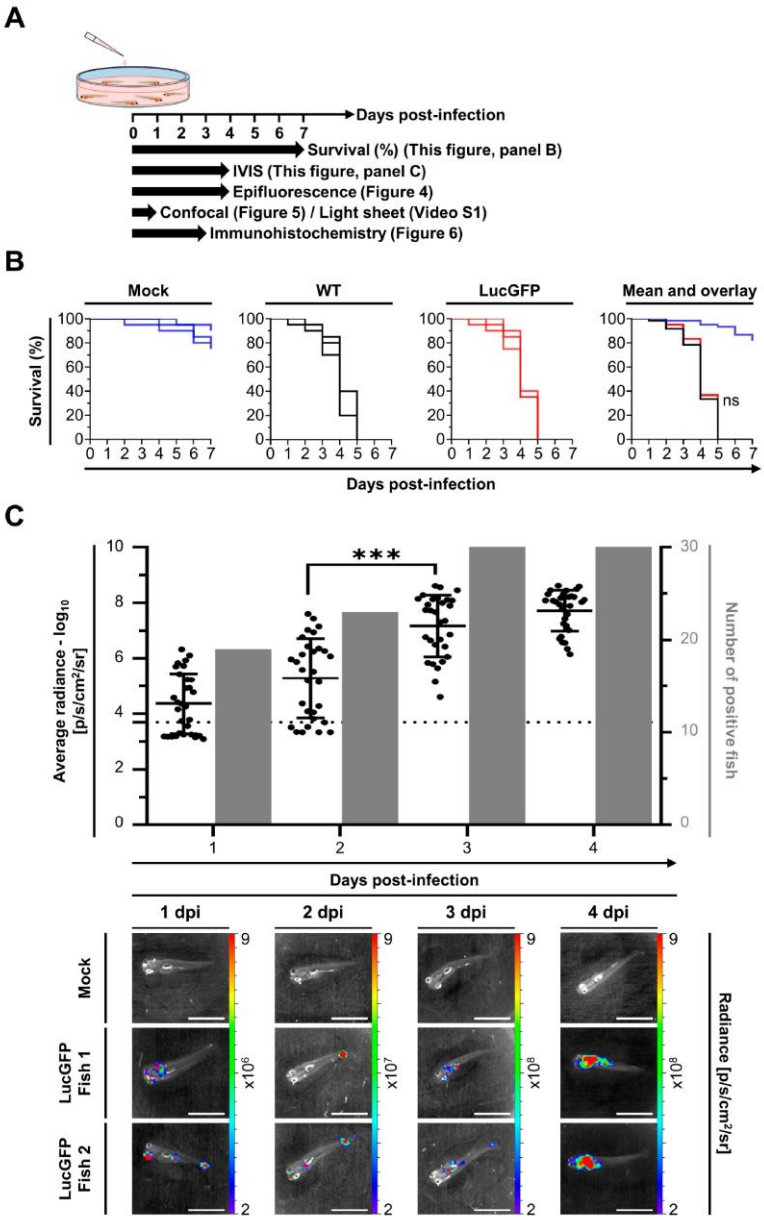

Figure 3. Susceptibility and permissivity of goldfish larvae to CyHV-2. (**A**) Flowchart of the experiments performed to investigate the susceptibility and permissivity of goldfish larvae (4 dpf or 1 d post-hatching, average length = 5.2 ± 0.1 mm) to CyHV-2 after infection by immersion in water containing the virus. (**B**) Survival curves of larvae following infection with the indicated strain. On day zero, 3 independent replicates of larvae, each group consisting of 60 subjects, were infected by immersion in E3 media containing the virus. Fish were examined daily, and those reaching the endpoints were euthanized. The percentage survival is expressed according to dpi. The three left panels show the survival curves observed for replicates. The right panel shows the mean survival curves based on the three replicates. (**C**) **Top** panel: Quantitative measurements of CyHV-2 replication in goldfish larvae obtained by IVIS. On day zero, three independent replicates of larvae, each group

consisting of 50 subjects, were infected by immersion in E3 media containing the virus (5×10^5 pfu/mL). At the indicated dpi, larvae (n = 30, i.e., 10 per replicate) were analyzed by IVIS. The average radiance (p/sec/cm^2/sr) emitted by individual infected larvae corrected for the background of each image is represented by dots. For each time point, a group of mock-infected larvae was analyzed to define the threshold of positivity (dotted line), defined as the mean +3 SD. The number of positive larvae among 30 analyzed infected larvae is presented by grey bars. **Lower** panel: Representative images of analyzed larvae are presented in the lower part of the figure. Images are presented with a relative photon flux scale manually adapted to use the full dynamic range of the pseudo-color scale. Scale bar = 3 mm.

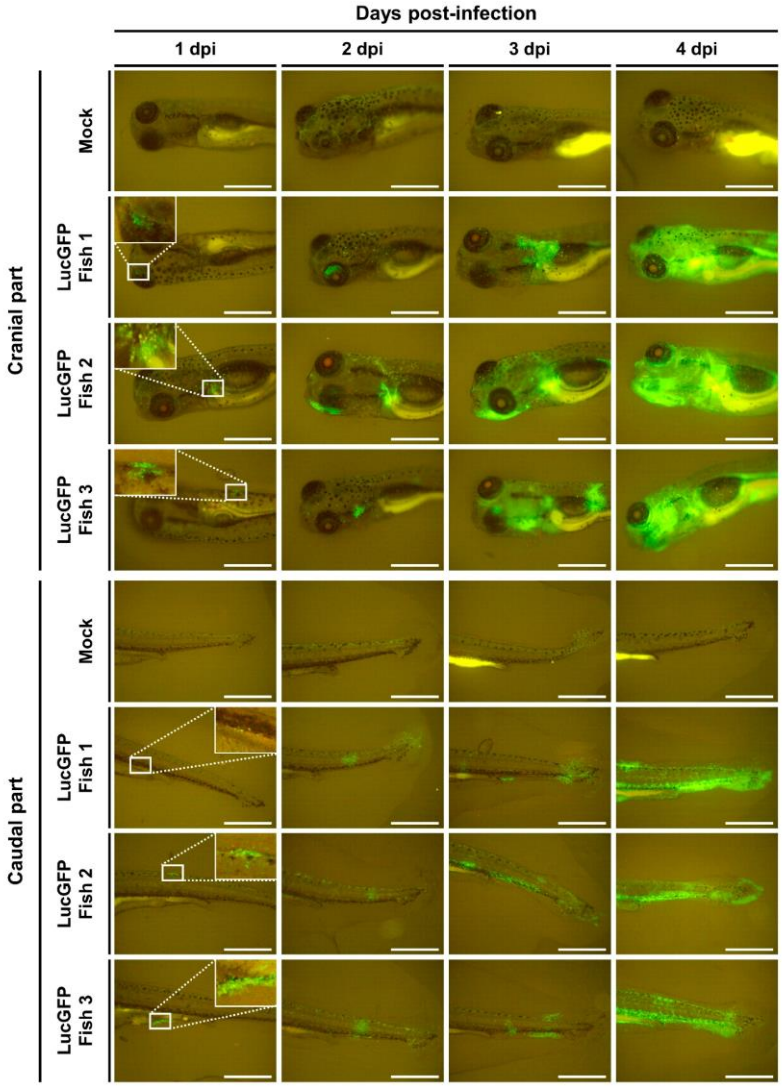

Figure 4. Visualization of CyHV-2 infection in goldfish larvae using epifluorescence microscopy. The timeline of this experiment has been described in Figure 3A. Epifluorescence microscopy images representative of larvae mock-infected and infected with the LucGFP strain according to time post-infection. Scale bar = 1 mm.

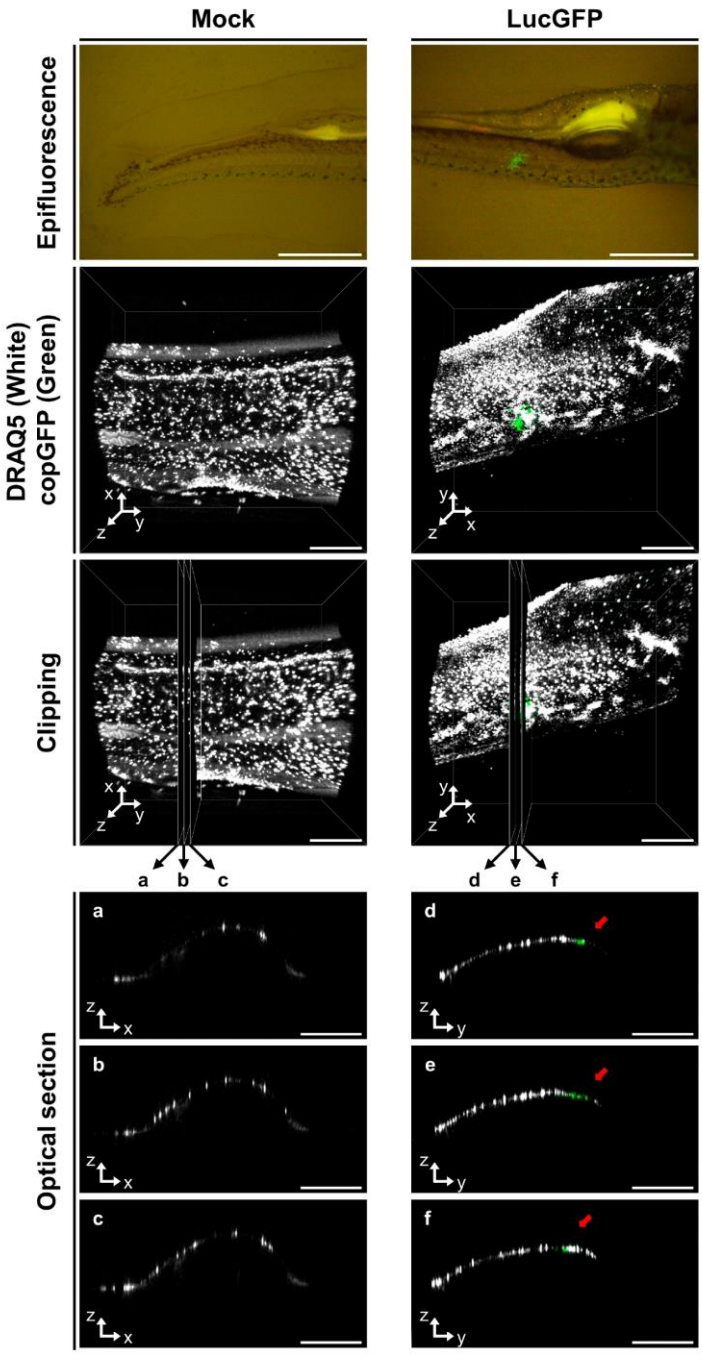

Figure 5. Visualization of CyHV-2 infection in goldfish larvae using confocal microscopy. The timeline of this experiment has been described in Figure 3A. The larvae were infected (LucGFP strain) or mock-infected by immersion in water containing the virus. At 1 dpi, fish were first observed by epifluorescence microscopy, and infected fish were identified based on the copGFP reporter signal (first row of panels, scale bar = 1 mm). Living skin epidermal cells on the outer body were then stained

with DRAQ5. A series of Z-stacks were acquired using a confocal microscope in order to generate a 3D representation of the region of interest, with skin cells (DRAQ5-stained) in white and virally infected cells (copGFP expression) in green (second row of panel, scale bar = 300 μm). These data were used to generate three 2D optical sections in each sample (third row on panel), separated by a distance of 30 μm. These sections were denoted as a, b, and c for the mock-infected group, and d, e, and f for the LucGFP-infected group (each 0.662 μm in thickness). These optical sections are also displayed individually (three last rows, scale bar = 300 μm). Within the optical sections d, e, and f, it can be seen that the virally infected cells (copGFP green) only co-localize with skin epidermal cells (DRAQ5, white) and are indicated by red arrows. Conversely, no viral signal is detected in the mock-infected samples.

In order to provide further support for these observations, rather than just focusing on specific regions of interest using confocal microscopy, 3D rendering was extended to entire larvae using light-sheet microscopy. In a similar experimental set-up, skin and virally infected cells in larvae (1 dpi) were again visualized using DRAQ5 live cell staining and copGFP expression, respectively. The findings from this experiment were consistent with the confocal analysis, indicating colocalization of viral signal in the skin only. A representative larval subject from this analysis is presented in Video S1, in which viral signal detected in the dorsal region is seen to be entirely localized in the skin.

In parallel to these experiments, epifluorescence was used to select additional infected and mock-infected larvae (1 dpi), which were processed for analysis by IHC. This indicated that at 1 dpi, virus-infected cells were located primarily in the superficial layer of the skin at both cranial and caudal sites (Figure 6, left panel). Conversely, at the same time-point, the pericardial region exhibited a staining pattern that was comparable to the control group, with both being devoid of any viral staining, indicating the absence of systemic infection at this initial time point. Earlier IVIS analysis indicated that in infected larvae, a dramatic increase in viral load typically occurs after 3 dpi (Figure 3C). Consistent with this, IHC analysis of larvae sampled at 3 dpi revealed dramatic changes in viral distribution relative to observations at 1 dpi. By this timepoint, we observed that infection had breached the skin barrier and infiltrated other areas of the subject body, leading to the detection of CyHV-2 infected cells within the subcutaneous myotome and cardiac regions (Figure 6, right panel). These observations are likely to represent the onset of systemic infection and coincide with the expected onset of mortality peak at 3–5 dpi (Figure 3B).

Collectively, these findings provide compelling evidence that the portal of entry of CyHV-2 in goldfish larvae is the skin, and, from here, CyHV-2 spreads to other regions in larvae, leading to a systemic infection and ultimately to mortality.

3.4. Juvenile Goldfish Are Susceptible but Less Permissive than Goldfish Larvae to CyHV-2 Infection, with Initial Infection Predominantly Occurring in the Skin

The same LucGFP strain was also used to investigate the spatiotemporal aspects of CyHV-2 replication in juvenile goldfish. The experiment and designs are illustrated in Figure 7A. When subjected to challenge by immersion at the same dose used earlier with larvae, juvenile goldfish exhibited a survival rate of ~40% which was much higher than observed with larvae. Furthermore, mortality commenced at 5 dpi, which is later than in larvae, and continued until approximately 12 dpi, representing a much more gradual rate of mortality compared to larvae (Figure 7B). As per larvae, mortality rates were comparable between the WT and LucGFP infected groups, with no statistically significant difference observed.

Despite the lower mortality, in contrast to the larvae, the IVIS analysis in juvenile subjects revealed that all subjects were positive at 1 dpi and the viral load in the skin was much higher than in larvae at 1–2 dpi (Figure 7C, top panel). However, unlike in larvae, the viral load in the skin did not increase, with time post-infection having no significant impact on Luc signal. This developmental stage also facilitated ex vivo analysis of the gastrointestinal tract (gut) and gills. However, viral loads were extremely low in the gut,

with no virus detected at 1 dpi, and virus detected in a single fish at 2 and 3 dpi. Notably, viral levels in the gut increased at 4 dpi (Figure 7C, top panel), which was immediately prior to the onset of mortality at 5 dpi (Figure 7B), but overall time post-infection had no impact on viral load in the gut. The prevalence and evolution of viral load in the gills was similar to the skin, with time having no significant impact on Luc signal; however, viral load in the gills was approximately 10-fold lower than in the skin (Figure 7C, top panel).

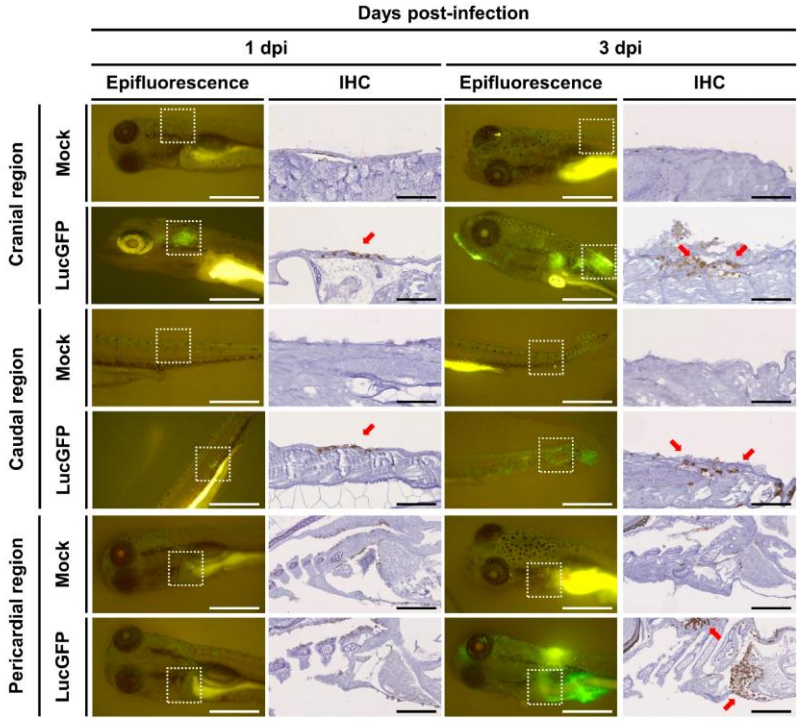

Figure 6. Viral tropism of CyHV-2 in goldfish larvae. The timeline of this experiment has been described in Figure 3A. Mock-infected and infected larvae (LucGFP strain) were first observed by epifluorescence microscopy (Epifluorescence, scale bar = 1 mm) at the indicated dpi, then processed for IHC detection of copGFP. The white boxes with dotted outlines in epifluorescence images indicate the regions analyzed by IHC. The virus was detected by staining for copGFP, with positive staining indicated by brown coloration filling entire cells (red arrows). Scale bars in IHC images represent 100 μm for anterior and caudal regions, and 200 μm for the pericardial region.

These patterns are also reflected in a series of representative images from IVIS analysis (Figure 7C, bottom panel). Notably the Luc signals from the skin are broadly distributed over a wide area. This pattern may have formed through coalescence of many initial infection foci. However, for this to be the case at 1 dpi, such coalescence would either have had to have occurred very rapidly, or there would need to have been a remarkably high initial number of infection foci. Both of these scenarios are consistent with the skin being more susceptible and permissive to CyHV-2 replication in juveniles, relative to other potential portals of entry. Conversely, signals from the gills tended to be more localized, originating from a singular source, with a similar distribution of viral signals in the gut, suggesting lower susceptibility or permissivity to CyHV-2 infection in these organs relative to the skin.

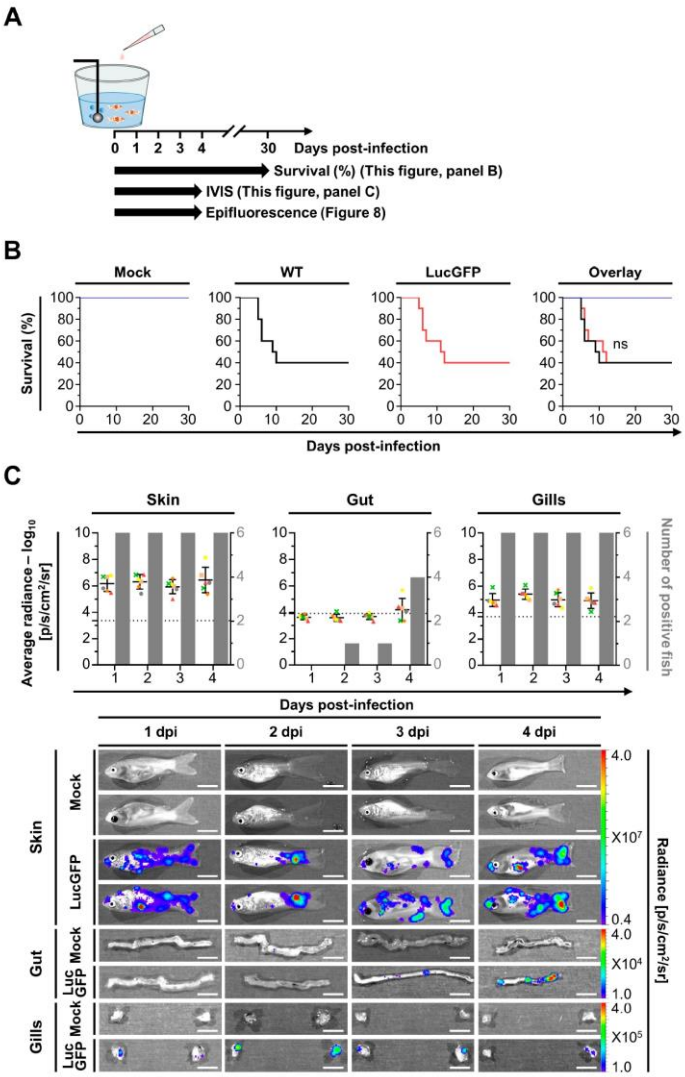

Figure 7. Susceptibility and permissivity of juvenile goldfish to CyHV-2 infection. (**A**) Flowchart of the experiments performed to investigate the susceptibility and permissivity of juvenile goldfish (75 days post fertilization, average length = 2.3 ± 0.3 cm) to CyHV-2 after infection by immersion in water containing the virus. (**B**) Survival rates of juveniles following infection with the indicated strain. On day zero, 10 subjects were infected by immersion in water containing the virus. Fish were examined daily and fish reaching the endpoints were euthanized. The percentage of survival is expressed according to dpi. The three left panels show the survival curves observed, respectively, for Mock, WT, and LucGFP groups. The right panel shows the overlay of the three groups. No statistically significant difference was observed between the WT and LucGFP strains. (**C**) **Top** panel: Quantitative measurements of CyHV-2 replication in juvenile goldfish by IVIS. Juveniles (n = 30) were infected (LucGFP strain) or mock-infected by immersion in infectious water. At the indicated dpi, juveniles (n = 6 per group) were analyzed by IVIS in vivo (skin) and ex vivo (gut and gills). The average radiance (p/sec/cm^2/sr) emitted by individual infected juvenile corrected for the background of each image is represented by dots. For each time point, a group of mock-infected juvenile fish was analyzed to define the threshold of positivity (dotted line), defined as the mean +3 SD. The number

of positive subjects among six analyzed infected juveniles is presented by grey bars. **Lower** panel: Representative images of analyzed juveniles are presented in the lower part of the figure. Images are presented with a relative photon flux scale manually adapted to use the full dynamic range of the pseudo-color scale. Scale bar = 5 mm.

As per earlier larvae experiments, the expression of copGFP by the LucGFP strain facilitated further analysis of infected juveniles by epifluorescence microscopy (Figure 8). Four distinct areas exhibiting overt signs of infection were selected for further analysis, namely the eye, gill, skin, and caudal fin, with representative images displayed in Figure 8. Curiously, the edge of the cornea seemed to be particularly susceptible to infection. As indicated by the distribution of the Luc signal (Figure 7C, lower panel) viral infection foci on the skin and particularly in the caudal fin tended to be larger and proliferated slightly better over time, relative to other infection foci in the gills (Figure 8).

The three organs that were investigated in juveniles, namely skin, gills, and gut, represent the main mucosal surfaces in contact with the external environment, and, thus, should have equal contact with CyHV-2 during challenge by immersion. However, these results indicate that relative to other mucosal surfaces, the skin, being more susceptible and permissive, may play a much greater role in the entry of the virus into the host. Thus, the skin may represent the major portal of entry at this developmental stage, which is consistent with earlier observations in larvae.

The results from the juvenile stage provide an insight into changes in susceptibility and permissivity at an intermediate point in goldfish development after the larval stage but prior to the adult stage. On this note, given that CyHV-2 was detected in more juvenile subjects and at higher levels at 1 dpi, relative to what was observed in larvae, this may indicate that juveniles are in fact more susceptible than larvae. However, the lack of increase in viral load over time, coupled with the lower mortality, indicates that, overall, relative to larvae, the goldfish juvenile developmental stage may ultimately be less permissive to CyHV-2 replication.

3.5. Adult Goldfish Are Susceptible to CyHV-2 Infection, but Exhibit Lower Permissivity than Earlier Developmental Stages, with Initial Infection also Predominantly Occurring in the Skin

The spatiotemporal aspects of CyHV-2 infection in adults were also investigated, with experiments and designs illustrated in Figure 9A. In contrast to earlier developmental stages, adult goldfish demonstrated remarkably low mortality following challenge with CyHV-2 LucGFP and WT strains by immersion, with an almost 100% survival rate at 30 dpi (Figure 9B). This indicated that this goldfish developmental stage exhibits reduced permissivity to CyHV-2 replication, relative to earlier developmental stages. However, like the juvenile stage, all subjects were found to be infected at 1 dpi (Figure 9C). Viral load was also highest in the skin at 1 dpi compared to other organs, which was also consistent with the observations in juvenile goldfish. While the viral load was lower than the levels observed in the skin of juveniles at 1 dpi, it was higher than the levels observed in larvae at the same time point, indicating that adult goldfish are still relatively susceptible to CyHV-2 infection.

Being at a more advanced developmental stage, adult subjects also facilitated the ex vivo analysis of more internal organs, with heart, spleen, and kidney being added to the panel for this experiment. However, there was little viral signal detected in any internal organs across all timepoints (Figure 9C), indicating the absence of a low level of systemic infection. While skin and, to a lesser extent, gills, were more susceptible to infection than internal organs, a general decrease in viral load occurred in both of these organs after 1 dpi, with time post-infection having a significant negative impact on viral load (skin: $p = 0.0002$, gills: $p = 0.0025$), leading to virus replication being undetectable in most subjects by 4 dpi. This indicates that, while susceptible, adult goldfish were much less permissive to CyHV-2 infections relative to earlier developmental stages, and this is consistent with the extremely low mortality rate that was observed.

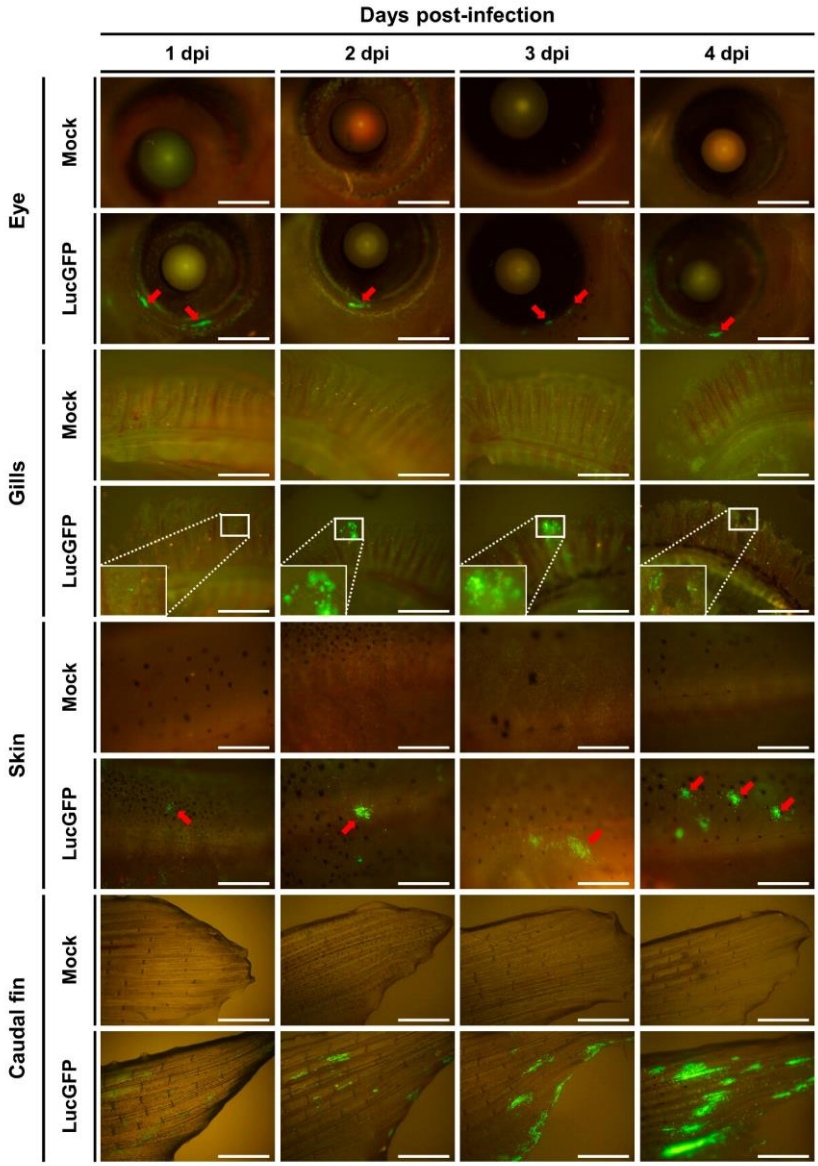

Figure 8. Visualization of CyHV-2 infection in juvenile goldfish using epifluorescence microscopy. The timeline of this experiment has been described in Figure 7A. Epifluorescence microscopy images representative of juvenile fish mock-infected and infected with the LucGFP strain according to time post-infection. Typical infection foci observed in the eye and skin regions are indicated with red arrows. Scale bars related to pictures of eye, skin, and caudal fin represent 1 mm. Scale bars related to pictures of gills represent 400 µm.

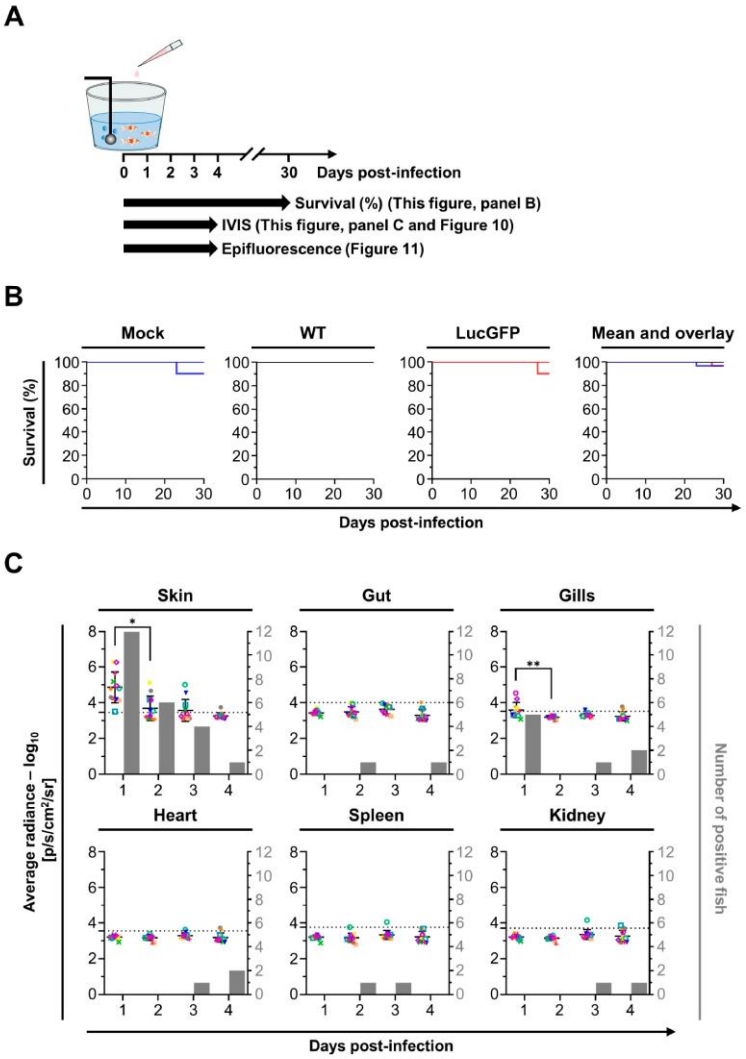

Figure 9. Susceptibility and permissivity of adult goldfish to CyHV-2 infection. (**A**) Flowchart of the experiments performed to investigate the susceptibility and permissivity of adult goldfish (1.5 years old, average weight = 12 ± 3.7 g) to CyHV-2 after infection by immersion in water containing the virus. (**B**) Survival rates of adults following infection with the indicated strain. On day zero, three independent replicates of adult fish (n = 30) were infected by immersion in water containing the virus. Fish were observed for 30 days and fish reaching the endpoints were euthanized. The percentage of survival is expressed according to dpi. The three left panels show the survival curves observed for replicates. The right panel shows the mean survival curves based on three replicates. (**C**) Quantitative measurements of CyHV-2 replication in adult goldfish by IVIS. Fish were infected or mock-infected with the LucGFP strain by immersion in infectious water. At the indicated dpi, fish (n = 12 per group) were analyzed by IVIS in vivo (skin) and ex vivo (gut, gills, heart, spleen, and kidney). The average radiance (p/sec/cm^2/sr) emitted by individual infected fish corrected for the background of each image is represented by dots. For each time point, a group of mock-infected fish was analyzed to define the threshold of positivity (dotted line), defined as the mean +3 SD. The number of positive fish among 12 analyzed infected fish is presented by grey bars.

Interestingly, examination of the Luc signal distribution in skin and gills revealed that the caudal fin was particularly susceptible or possibly more permissive to infection at 1 dpi (Figure 10). A similar pattern was observed in further analysis by epifluorescence microscopy, with more signals again observed in the caudal fin relative to elsewhere on the skin (Figure 11). This is consistent with observations in juvenile subjects, where the caudal fin also exhibited a higher viral load (Figure 7C, lower panel and Figure 8). Taken together these results indicate that adult goldfish are much less permissive to CyHV-2 replication, compared to earlier developmental stages. However, consistent with other developmental stages, relative to other organs tested, the skin exhibited higher viral loads at earlier timepoints, indicating that it may naturally act as the major portal for CyHV-2 entry in populations of goldfish adults.

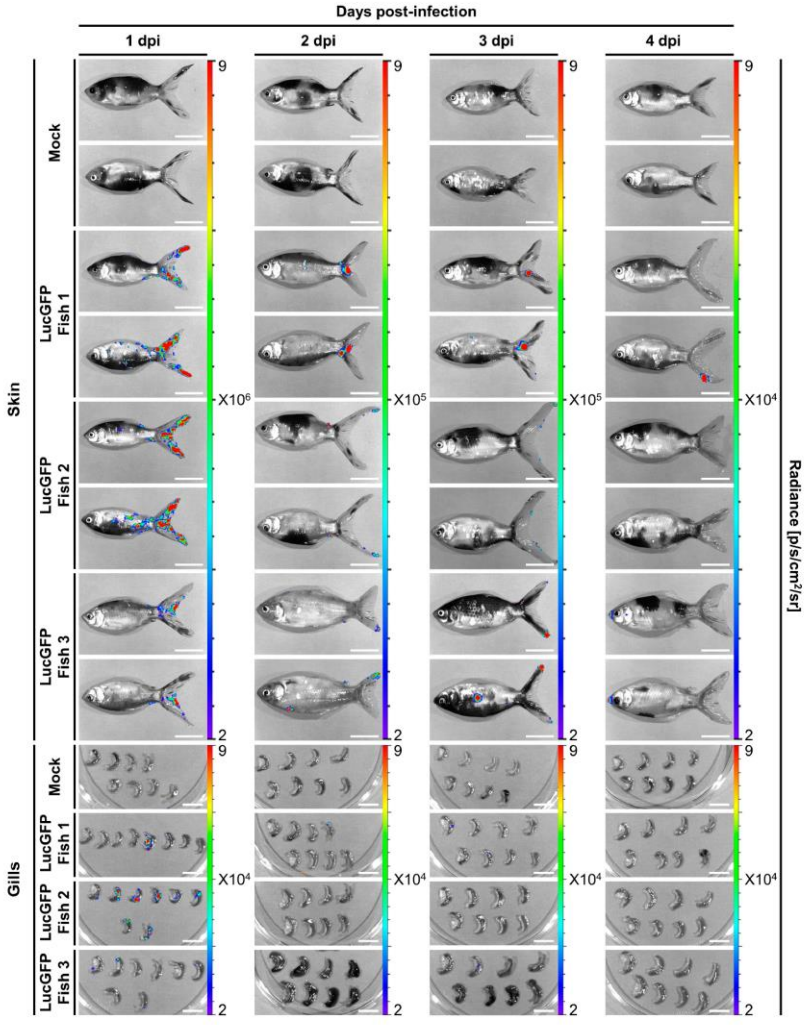

Figure 10. Illustration of CyHV-2 tropism detected by IVIS in adult fish. This figure is related to the experiment described in Figure 9C. Representative images of IVIS analysis are presented for skin and gills. Images are presented with a relative photon flux scale manually adapted in order to use the full dynamic range of the pseudo-color scale. Scale bars in panels related to skin and gills represent 2 and 1 cm, respectively.

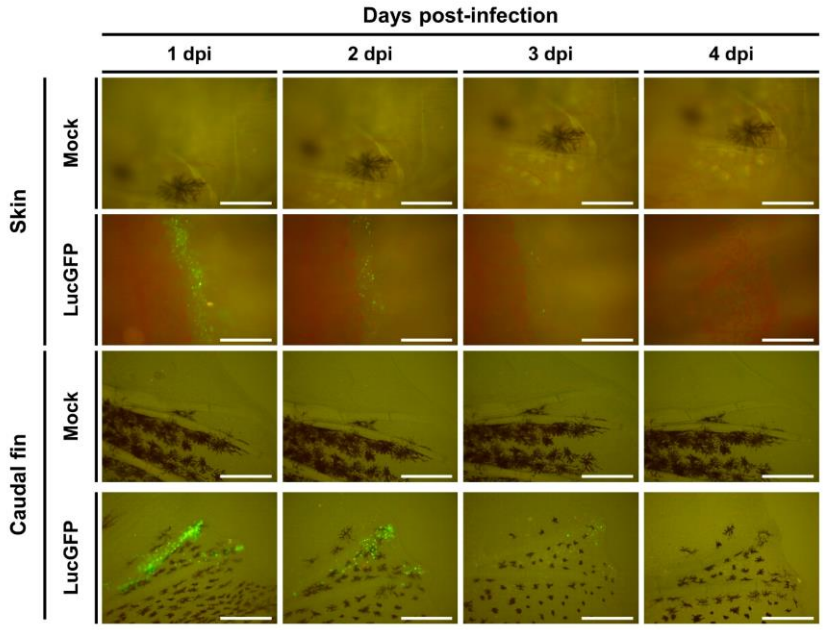

Figure 11. Visualization of CyHV-2 infection in adult goldfish using epifluorescence microscopy. This figure is related to the experiment described in Figure 9C. Epifluorescence microscopy images representative of adult fish mock-infected and infected with LucGFP strain according to time post-infection. Scale bar = 1 mm.

4. Discussion

In the present study, we developed a novel CyHV-2 recombinant strain expressing luciferase and GFP reporters. We subsequently successfully exploited this recombinant in the first investigation of the spatiotemporal aspects of CyHV-2 replication in goldfish across three key developmental stages. This facilitated the comparison of susceptibility and permissivity between different developmental stages and the identification of the CyHV-2 portal of entry in its natural host.

A crucial starting point for this study was the development of the CyHV-2 recombinant strain. Our initial systematic comparison of this new recombinant strain to the parental YC-01 strain revealed no difference in terms of expected genome structure (Figure 1B), expression of genes flanking the insertion site (Figure 1C), replication in cell culture (Figure 2B), and virulence by IP challenge (Figure 2C). Taken together, these results indicate that the LucGFP recombinant produced exhibits adequate properties for the study of CyHV-2 pathogenesis. This new recombinant is the first of its kind in the field of CyHV-2 research. We have previously developed a comparable recombinant to utilize in the study of CyHV-3, which is closely related to CyHV-2 and infects common carp, a species related to goldfish. The use of these earlier CyHV-3 recombinants had a profound impact on our ability to gain an increased fundamental understanding of this related virus and the development of adequate mitigation strategies [39,41,42,46–49]. In a similar manner, this novel CyHV-2 recombinant also represents a potentially valuable research tool for our future investigations with CyHV-2 and may also be of interest to the wider research community. Furthermore, in parallel to this present study, this novel CyHV-2 recombinant was also successfully utilized in zebrafish infectivity studies [45], demonstrating its immediate utility in other CyHV-2 related research.

One of the primary aims of this present study was to compare the susceptibility and permissivity of goldfish to CyHV-2 across the three distinct developmental stages: larvae, juvenile, and adults. This revealed that all stages were susceptible to infection

(Figures 3C, 7C and 9C). Notably, infection was not as prevalent among larval subjects at the early time points post-infection by immersion and they also exhibited lower average radiance (representing viral load) at these time points, indicating reduced susceptibility. Despite this, larvae were still much more permissive to CyHV-2 replication, exhibiting the greatest increase in viral load over time, ultimately exceeding that of other developmental stages by 4 dpi, leading to much greater mortality (Figure 3B,C). In contrast, while the virus was detected in all juvenile hosts (indicating greater susceptibility) and the viral load was initially higher than in larvae, these levels remained stable over time (Figure 7C), resulting in reduced mortality in juveniles relative to the larval stage (Figure 7B). Finally, despite similarly high susceptibility, the adult stage was observed to be the least permissive to CyHV-2 replication with a decrease in viral load with respect to time (Figure 9C), and lower mortality relative to other developmental stages (Figure 9B).

The low mortality observed in this population of adult Shubunkin goldfish after CyHV-2 challenge by immersion (Figure 9B) relative to higher mortality by IP challenge (Figure 2C), is similar to previous findings involving comparisons between other breeds of goldfish [52]. However, given that Shubunkin goldfish are known to exhibit high mortality via natural infection routes [23], our observations may be specific to the population of Shubunkin goldfish that we used. It is highly likely that these contrasting phenotypes between different populations of Shubunkin goldfish may be due to genetic or epigenetic factors, which can have a significant impact on disease resistance in teleost fish hosts [53–55], including impacts on innate immune response to viral infection in cyprinid hosts [56]. Despite the lower mortality, challenge by immersion is much more representative of natural infection and had no impact on susceptibility to CyHV-2 among adults or juveniles in this study, which remained at 100%.

Interestingly, while viral prevalence was initially lower among larvae, it also increased with respect to time (Figure 3C). However, it is unclear if this was due to active viral transmission or simply due to the general increase in viral load, which may have been below the threshold for detection at earlier time points, leading to underestimation of initial infection prevalence. Notably, both of these scenarios are consistent with lower susceptibility to CyHV-2 at the larval stage in goldfish. Furthermore, this is consistent with our previous findings regarding susceptibility with CyHV-3 infection in carp [41], which represents the most closely related virus–host model to the CyHV-2-goldfish model [50,51]. The CyHV-3-carp model revealed that earlier carp developmental stages were less susceptible to CyHV-3 replication [41]. This reduced susceptibility was primarily due to the epidermal mucus being more inhibitory to CyHV-3 entry into hosts during earlier developmental stages. In addition to acting as a physical barrier, teleost epidermal mucus contains a multitude of antimicrobial proteins including proteases, immunoglobulins, complement components and innate immune cells that collectively inhibit viral infection at all developmental stages [57–59]. However, it is possible that the profiles of antimicrobial agents or physical uniformity of this protective barrier may change during development, as we discussed previously [41]. As observed in carp, it is possible that the epidermal mucus barrier in goldfish also plays a much greater inhibitory role at earlier developmental stages, resulting in lower CyHV-2 viral loads in larvae at earlier time points post CyHV-2 challenge by immersion. Currently, it is unclear which CyHV-2 factors may be responsible for providing some kind of resistance to this innate barrier in goldfish, leading to greater susceptibility at later developmental stages. However, we have recently demonstrated that in CyHV-3, mutations in ORF131 (which we previously determined to be a viral transmembrane protein [60]) have a significant impact on CyHV-3 resistance to innate immune components of carp epidermal mucus [48], although the implications at different developmental stages have yet to be determined. Notably, CyHV-2 and CyHV-3 share 19 homologous transmembrane proteins, including ORF131 [61]. It is plausible that this ORF131 homolog in CyHV-2 also plays a role in helping the virus overcome goldfish mucosal defenses, with potentially more efficacy at later developmental stages, thus, contributing to an initial greater viral load and prevalence among subjects at these later developmental stages. A combined

investigation into the contribution of both the goldfish mucosal barrier and specific CyHV-2 membrane proteins at different developmental stages represents an interesting avenue for further investigation in the future, and may reveal factors impacting susceptibility, that are, evidently, independent from permissivity.

Despite potential differences in susceptibility, our observations indicate that the main factors dictating CyHV-2 related mortality at each developmental stage are differences in permissivity to CyHV-2 replication. Earlier goldfish developmental stages were much more permissive, leading to more mortality, despite being less susceptible to infection. This is in stark contrast to what we observed previously using the related CyHV-3-carp model, where in addition to being less susceptible, earlier carp developmental stages were also less permissive to CyHV-3 replication relative to later stages, which was accompanied by reduced mortality at earlier developmental stages [41]. This difference between CyHV-2 and CyHV-3 is surprising given how closely related they are [51,52]; however, this may be a consequence of differing adaptation to their respective hosts, or host-habitat. For example, unlike CyHV-3, CyHV-2 exhibits vertical transmission (i.e., from parent to offspring), and we hypothesize that this may be directly connected to differences between these two models in terms of permissivity at early developmental stages. Initial evidence for vertical transmission of CyHV-2 emerged in 2009 with the detection of CyHV-2 in disinfected eggs from infected goldfish [35]. Further investigation into this elsewhere led to the observation of viral particles in eggs of infected fish via electron microscopy and even the detection of active CyHV-2 gene transcription in eggs via RT-PCR [62]. Increased social contact between individuals during spawning potentially represents major mechanism for viral transmission among some fish species [50]. Given that (i) spawning is replaced by artificial reproduction practices in aquaculture settings and (ii) larger brood-stock may be subject to much lower stocking densities, and separated from the rest of the population, this may create selective pressure favoring viral strains capable of vertical transmission. However, it remains unclear if vertical transmission by CyHV-2 represents an adaptation to goldfish rearing practices, or if it emerged independently. Moreover, faced with potentially similar selective pressure associated with carp domestication, it is unclear why CyHV-3 does not also exhibit vertical transmission. However, recent phylogenetic dating studies that we conducted using different node calibration hypotheses consistently indicated that the CyHV-2 species clade emerged much more recently than CyHV-3, and also cast doubt on the plausibility that CyHV-3 emerged after the commencement of human aquaculture activities [50], which may explain these differences. However, such dating estimates need be supported by further investigation including collaborative efforts towards generating short-term evolutionary rate estimates for these viral species.

Regardless of the reasons why CyHV-2 evolved to exhibit vertical transmission, at a fundamental level, for it to occur, it is essential that extremely early developmental stages (−1 to 3 dpf) are permissive to CyHV-2 replication. More specifically, CyHV-2 must be capable of replicating in the populations of omnipotent, pluripotent, and rapidly dividing cells and undifferentiated tissue, which are in abundance at these stages. Such conditions may largely persist through the larval and, to some extent, during the juvenile stages investigated in this study (4 dpf and 75 dpf, respectively), and ultimately to a lesser extent as development continues, accompanied by further development of innate immune responses. While no other members of the genus *Cyprinivirus* are known to exhibit vertical transmission [50], in other more distantly related members of the family *Alloherpesviridae* that do, similar patterns can be observed across developmental stages. For example, Ictalurid herpesvirus 1 (IcHV-1, or Channel catfish virus) can also spread via vertical transmission, and, similarly to CyHV-2, disease caused by IcHV-1 is also primarily associated with earlier developmental stages [12,63,64]. Thus, it stands to reason that the ability of these alloherpesviruses to undergo vertical transmission may, as a natural consequence, also result in greater host permissivity at earlier developmental stages. However, this hypothesis needs to be further explored through more in-depth comparative virology across a wider range of relevant teleost virus–host models.

Another important aspect of the present study was to identify the portal of entry of the virus into the host. Previously it has been hypothesized that either the skin or gill could represent the portal of CyHV-2 entry in goldfish [20]. Others have speculated that in gibel carp, the gut represents a CyHV-2 portal of entry, supporting potential future oral vaccination strategies. Here, we compared the CyHV-2 viral loads during infection in different tissues in larval, juvenile, and adult developmental stages at 1, 2, and 3 dpi (and 4 dpi for the latter two). Unlike previous investigations, the experimental approach in this present study involved using a recombinant CyHV-2 strain expressing a reporter. The levels of this recombinant could be measured by IVIS and compared between different organs. As viral load can vary greatly between different regions of the skin, conducting such comparisons using other viral quantification approaches (e.g., PCR, ELISA, etc.) was not practical due to the inherent difficulty in identifying exactly which areas of the skin should be sampled prior to measurement. The use of the novel recombinant in this study was a key factor in facilitating non-biased measurements of viral load across the entire skin surface, thus, allowing valid comparisons to other organs.

In all developmental stages, we observed higher viral load in the skin at 1 dpi, the earliest sampling point post-infection, indicating that the skin represents a highly susceptible and the most permissive organ at early stages of infection after challenge by immersion. For example, in juvenile and adult subjects, viral load was higher in the skin than other organs, remaining so throughout the monitoring period (Figures 7C and 9C). Furthermore, in adults and juveniles, the main source of signal in the skin was on the caudal fin, indicating that this region may be more susceptible to infection, and, hence, may act as the main portal of entry at these developmental stages. However, further comparison will be required to establish if this may in fact be related to the specific physiology of the Shubunkin goldfish caudal fin, rather than being the case for all goldfish breeds. While IVIS analysis was suitable for monitoring viral load over time at the larval stage allowing us to establish susceptibility and permissivity, given the constraints due to subject size, unlike the juvenile and adult stages, comparison between the skin and other organs in larvae, was not possible using this method. However, by selectively staining epidermal cells in the skin of larval subjects, we were able to confirm exclusive viral localization in this tissue at the earliest time point post-infection using 3D renderings generated from confocal (Figure 5) and light-sheet microscopy (Video S1). Furthermore, we established through histopathology that, in larvae, this initial infection on the skin was followed by spread to internal organs (Figure 6). Taken together, this indicates unequivocally that the skin represents the major portal of entry for the establishment of CyHV-2 infection in goldfish hosts. Furthermore, these findings across earlier and later developmental stages in CyHV-2-goldfish are entirely consistent with our previous findings in the CyHV-3-carp model [41,42], indicating a common host entry strategy in these two closely related models.

5. Conclusions

The present work represents the first systematic study of CyHV-2 pathogenesis and comparison between three major host developmental stages. It revealed that in goldfish (i) earlier developmental stages are less susceptible but more permissive to CyHV-2 infection relative to later developmental stages, ultimately leading to higher mortality in the former, and (ii) the skin represents the major portal of viral entry into the host. Collectively these findings provide important fundamental insights in CyHV-2 pathogenesis in goldfish, with high relevance to CyHV-2 infection in closely related economically important fish species and other related virus-host models. Furthermore, this work has resulted in the generation of the first recombinant CyHV-2 strain, and we have demonstrated that it represents a powerful new research tool that may be of interest to the wider CyHV-2 research community.

Supplementary Materials: The following supporting information can be downloaded at: https://www.mdpi.com/article/10.3390/v15081746/s1, Video S1: Visualization of CyHV-2 virus infection in larvae using light-sheet fluorescence microscopy. Shubunkin goldfish larvae were infected by immersion with CyHV-2 LucGFP-contaminated water as described in Section 2. At 24 h pi, infected larvae were examined using light-sheet fluorescence microscopy. Nuclei of live skin epidermal cells in the larvae were stained with DRAQ5 (white contour around the body) while cells infected with LucGFP strain express GFP (green). In this 3D representation, virally infected cells were detected in the dorsal region of the larvae, and were entirely localized in the skin, with no virus detected in the internal tissue, thus, consistent with the observations in Figure 5.

Author Contributions: Conceptualization, A.F.C.V.; data curation, B.H., A.J.D. and O.D.; formal analysis, B.H., A.J.D. and O.D.; funding acquisition, A.J.D., O.D. and A.F.C.V.; investigation, B.H., A.S., H.Z., Y.G., O.D. and A.F.C.V.; methodology, B.H., C.S., Y.G., C.D., H.Z., S.P., N.D., Y.H., O.D. and A.F.C.V.; project administration, A.F.C.V.; supervision, O.D. and A.F.C.V.; validation, B.H., O.D. and A.F.C.V.; visualization, B.H., A.S., O.D. and A.F.C.V.; writing—original draft, B.H., O.D. and A.F.C.V.; Writing—review and editing, all co-authors. All authors have read and agreed to the published version of the manuscript.

Funding: Haiyan Zhang, Yuan Gao, Yunlong Hu, and Bo He are research fellows of the Chinese Scholarship Council. Cindy Streiff is a research fellow of the University of Liège and the University of Reims Champagne-Ardenne. Sébastien Pirotte and Natacha Delrez are research fellows of the Fonds de la Recherche Scientifique de Belgique (F.R.S.-FNRS). This work was supported by the University of Liège (FSR-SS-2022/64, FSR-SS-2023/49), the FNRS (PDR T.0241.19), the European Maritime and Fisheries Fund (Eel4ever project), the Welbio (WELBIO-CR-2022 A-14 12), the Walloon Region (ERANets NucNanoFish 2010052) and the Medical Research Council (MC_UU_12014/3). Computational resources have been provided by the Consortium des Équipements de Calcul Intensif (CÉCI), funded by the F.R.S.-FNRS under Grant No. 2.5020.11 and by the Walloon Region.

Institutional Review Board Statement: Not applicable.

Informed Consent Statement: Not applicable.

Data Availability Statement: All data were include in this manuscripts.

Acknowledgments: The authors are grateful to Lorène Dams (Faculty of Veterinary Medicine, ULiège), Alexandre Hego (GIGA Imaging Platform, ULiège), Lefevre Gaëtan (GIGA Imaging Platform, ULiège), David Colignon (CECI, ULiège), and Tiffany Di Salvo (GIGA Immunohistology Platform, ULiège) for their excellent technical assistance.

Conflicts of Interest: The authors declare no conflict of interest.

References

1. Omori, Y.; Kon, T. Goldfish: An Old and New Model System to Study Vertebrate Development, Evolution and Human Disease. *J. Biochem.* **2019**, *165*, 209–218. [CrossRef]
2. Chen, D.; Zhang, Q.; Tang, W.; Huang, Z.; Wang, G.; Wang, Y.; Shi, J.; Xu, H.; Lin, L.; Li, Z.; et al. The Evolutionary Origin and Domestication History of Goldfish (*Carassius auratus*). *Proc. Natl. Acad. Sci. USA* **2020**, *117*, 29775–29785. [CrossRef]
3. Country, M.W.; Jonz, M.G. Goldfish and Crucian Carp Are Natural Models of Anoxia Tolerance in the Retina. *Comp. Biochem. Physiol. Part A Mol. Integr. Physiol.* **2022**, *270*, 111244. [CrossRef]
4. Filice, M.; Cerra, M.C.; Imbrogno, S. The Goldfish Carassius Auratus: An Emerging Animal Model for Comparative Cardiac Research. *J. Comp. Physiol. B* **2022**, *192*, 27–48. [CrossRef]
5. Choe, Y.; Yu, J.E.; Park, J.; Park, D.; Oh, J.-I.; Kim, S.; Moon, K.H.; Kang, H.Y. Goldfish, Carassius Auratus, as an Infection Model for Studying the Pathogenesis of Edwardsiella Piscicida. *Vet. Res. Commun.* **2017**, *41*, 289–297. [CrossRef]
6. Ruley, K.M.; Reimschuessel, R.; Trucksis, M. Goldfish as an Animal Model System for Mycobacterial Infection. *Methods Enzymol.* **2002**, *358*, 29–39. [CrossRef]
7. Talaat, A.M.; Reimschuessel, R.; Wasserman, S.S.; Trucksis, M. Goldfish, Carassius Auratus, a Novel Animal Model for the Study of Mycobacterium Marinum Pathogenesis. *Infect. Immun.* **1998**, *66*, 2938–2942. [CrossRef]
8. Li, I.-J.; Chang, C.-J.; Liu, S.-C.; Abe, G.; Ota, K.G. Postembryonic Staging of Wild-Type Goldfish, with Brief Reference to Skeletal Systems. *Dev. Dyn.* **2015**, *244*, 1485–1518. [CrossRef] [PubMed]
9. Li, I.-J.; Lee, S.-H.; Abe, G.; Ota, K.G. Embryonic and Postembryonic Development of the Ornamental Twin-Tail Goldfish. *Dev. Dyn.* **2019**, *248*, 251–283. [CrossRef] [PubMed]
10. FAO. FAO Fisheries Division—Yearbook of Fishery and Aquaculture Statistics. 2019. Available online: https://www.fao.org/fishery/static/Yearbook/YB2019_USBcard/navigation/index_intro_e.htm (accessed on 1 July 2023).

11. Kennedy, D.A.; Kurath, G.; Brito, I.L.; Purcell, M.K.; Read, A.F.; Winton, J.R.; Wargo, A.R. Potential Drivers of Virulence Evolution in Aquaculture. *Evol. Appl.* **2016**, *9*, 344–354. [CrossRef] [PubMed]
12. Hanson, L.; Dishon, A.; Kotler, M. Herpesviruses That Infect Fish. *Viruses* **2011**, *3*, 2160–2191. [CrossRef] [PubMed]
13. World Bank Reducing Disease Risk in Aquaculture. Available online: https://documents.worldbank.org/en/publication/documents-reports/documentdetail (accessed on 1 July 2023). (In English).
14. Jung, S.J.; Miyazaki, T. Herpesviral Haematopoietic Necrosis of Goldfish, *Carassius auratus* (L.). *J. Fish Dis.* **1995**, *18*, 211–220. [CrossRef]
15. Groff, J.M.; LaPatra, S.E.; Munn, R.J.; Zinkl, J.G. A Viral Epizootic in Cultured Populations of Juvenile Goldfish Due to a Putative Herpesvirus Etiology. *J. Vet. Diagn. Investig.* **1998**, *10*, 375–378. [CrossRef] [PubMed]
16. Chang, P.H.; Lee, S.H.; Chiang, H.C.; Jong, M.H. Epizootic of Herpes-like Virus Infection in Goldfish, *Carassius Auratus* in Taiwan. *Fish Pathol.* **1999**, *34*, 209–210. [CrossRef]
17. Stephens, F.; Raidal, S.; Jones, B. Haematopoietic Necrosis in a Goldfish (*Carassius auratus*) Associated with an Agent Morphologically Similar to Herpesvirus. *Aust. Vet. J.* **2004**, *82*, 167–169. [CrossRef]
18. Jeffery, K.R.; Bateman, K.; Bayley, A.; Feist, S.W.; Hulland, J.; Longshaw, C.; Stone, D.; Woolford, G.; Way, K. Isolation of a Cyprinid Herpesvirus 2 from Goldfish, *Carassius auratus* (L.), in the UK. *J. Fish Dis.* **2007**, *30*, 649–656. [CrossRef]
19. Sahoo, P.K.; Swaminathan, T.R.; Abraham, T.J.; Kumar, R.; Pattanayak, S.; Mohapatra, A.; Rath, S.S.; Patra, A.; Adikesavalu, H.; Sood, N.; et al. Detection of Goldfish Haematopoietic Necrosis Herpes Virus (*Cyprinid herpesvirus-2*) with Multi-Drug Resistant Aeromonas Hydrophila Infection in Goldfish: First Evidence of Any Viral Disease Outbreak in Ornamental Freshwater Aquaculture Farms in India. *Acta Trop.* **2016**, *161*, 8–17. [CrossRef]
20. Giovannini, S.; Bergmann, S.M.; Keeling, C.; Lany, C.; Schütze, H.; Schmidt-Posthaus, H. Herpesviral Hematopoietic Necrosis in Goldfish in Switzerland: Early Lesions in Clinically Normal Goldfish (*Carassius auratus*). *Vet. Pathol.* **2016**, *53*, 847–852. [CrossRef]
21. Adamek, M.; Hellmann, J.; Jung-Schroers, V.; Teitge, F.; Steinhagen, D. CyHV-2 Transmission in Traded Goldfish Stocks in Germany—A Case Study. *J. Fish Dis.* **2018**, *41*, 401–404. [CrossRef]
22. Boitard, P.-M.; Baud, M.; Labrut, S.; de Boisséson, C.; Jamin, M.; Bigarré, L. First Detection of Cyprinid Herpesvirus 2 (CyHV-2) in Goldfish (*Carassius auratus*) in France. *J. Fish Dis.* **2016**, *39*, 673–680. [CrossRef]
23. Ito, T.; Kurita, J.; Haenen, O.L.M. Importation of CyHV-2-Infected Goldfish into The Netherlands. *Dis. Aquat. Organ.* **2017**, *126*, 51–62. [CrossRef]
24. Kalayci, G.; Ozkan, B.; Pekmez, K.; Kaplan, M.; Mefut, A.; Cagirgan, A. First Detection of Cyprinid Herpesvirus-2 (CyHV-2) Followed by Screening and Monitoring Studies in Goldfish (*Carassius auratus*) in Turkey. *Bull. Eur. Assoc. Fish Pathol.* **2018**, *38*, 94–103.
25. Panicz, R.; Sadowski, J.; Eljasik, P. Detection of Cyprinid Herpesvirus 2 (CyHV-2) in Symptomatic Ornamental Types of Goldfish (*Carassius auratus*) and Asymptomatic Common Carp (*Cyprinus carpio*) Reared in Warm-Water Cage Culture. *Aquaculture* **2019**, *504*, 131–138. [CrossRef]
26. Doszpoly, A.; Benko, M.; Csaba, G.; Dán, Á.; Lang, M.; Harrach, B. Introduction of the Family Alloherpesviridae: The First Molecular Detection of Herpesviruses of Cyprinid Fish in Hungary. *Magy. Allatorvosok Lapja* **2011**, *133*, 174–181.
27. Wang, L.; He, J.; Liang, L.; Zheng, X.; Jia, P.; Shi, X.; Lan, X.; Xie, J.; Liu, H.; Xu, P. Mass Mortality Caused by Cyprinid Herpesvirus 2 (CyHV-2) in Prussian Carp (*Carassius gibelio*) in China. *Bull. Eur. Assoc. Fish Pathol.* **2012**, *32*, 164–173.
28. Daněk, T.; Kalous, L.; Veselý, T.; Krásová, E.; Reschová, S.; Rylková, K.; Kulich, P.; Petrtýl, M.; Pokorová, D.; Knytl, M. Massive Mortality of Prussian Carp Carassius Gibelio in the Upper Elbe Basin Associated with Herpesviral Hematopoietic Necrosis (CyHV-2). *Dis. Aquat. Organ.* **2012**, *102*, 87–95. [CrossRef]
29. Fichi, G.; Cardeti, G.; Cocumelli, C.; Vendramin, N.; Toffan, A.; Eleni, C.; Siemoni, N.; Fischetti, R.; Susini, F. Detection of Cyprinid Herpesvirus 2 in Association with an Aeromonas Sobria Infection of *Carassius carassius* (L.), in Italy. *J. Fish Dis.* **2013**, *36*, 823–830. [CrossRef]
30. Thangaraj, R.S.; Nithianantham, S.R.; Dharmaratnam, A.; Kumar, R.; Pradhan, P.K.; Thangalazhy Gopakumar, S.; Sood, N. Cyprinid Herpesvirus-2 (CyHV-2): A Comprehensive Review. *Rev. Aquac.* **2021**, *13*, 796–821. [CrossRef]
31. Zhou, L.; Gui, J. Natural and Artificial Polyploids in Aquaculture. *Aquac. Fish.* **2017**, *2*, 103–111. [CrossRef]
32. Liang, L.-G.; Xie, J.; Chen, K.; Bing, X.-W. Pathogenicity and Biological Characteristics of CyHV-2. *Bull. Eur. Assoc. Fish Pathol.* **2015**, *35*, 85–93.
33. Wei, C.; Iida, H.; Chuah, Q.; Tanaka, M.; Kato, G.; Sano, M. Persistence of Cyprinid Herpesvirus 2 in Asymptomatic Goldfish *Carassius Auratus* (L.). That Survived an Experimental Infection. *J. Fish Dis.* **2019**, *42*, 913–921. [CrossRef] [PubMed]
34. Wei, C.; Kakazu, T.; Chuah, Q.Y.; Tanaka, M.; Kato, G.; Sano, M. Reactivation of Cyprinid Herpesvirus 2 (CyHV-2) in Asymptomatic Surviving Goldfish *Carassius auratus* (L.) under Immunosuppression. *Fish Shellfish Immunol.* **2020**, *103*, 302–309. [CrossRef]
35. Goodwin, A.E.; Sadler, J.; Merry, G.E.; Marecaux, E.N. Herpesviral Haematopoietic Necrosis Virus (CyHV-2) Infection: Case Studies from Commercial Goldfish Farms. *J. Fish Dis.* **2009**, *32*, 271–278. [CrossRef] [PubMed]
36. Dharmaratnam, A.; Sudhagar, A.; Swaminathan, T.R. Evaluation of Protective Effects of Heat-Inactivated Cyprinid Herpesvirus-2 (CyHV-2) Vaccine against Herpesviral Hematopoietic Necrosis Disease (HVHND) in Goldfish (*Carassius auratus*). *Fish Shellfish Immunol.* **2023**, *132*, 108460. [CrossRef] [PubMed]
37. Shibata, T.; Nanjo, A.; Saito, M.; Yoshii, K.; Ito, T.; Nakanishi, T.; Sakamoto, T.; Sano, M. In Vitro Characteristics of Cyprinid Herpesvirus 2: Effect of Kidney Extract Supplementation on Growth. *Dis. Aquat. Organ.* **2015**, *115*, 223–232. [CrossRef]

38. Fei, Y.; Han, M.; Chu, X.; Feng, Z.; Yu, L.; Luo, Y.; Lu, L.; Xu, D. Transcriptomic and Proteomic Analyses Reveal New Insights into the Regulation of Immune Pathways during Cyprinid Herpesvirus 2 Infection in Vitro. *Fish Shellfish Immunol.* **2020**, *106*, 167–180. [CrossRef]
39. Boutier, M.; Ronsmans, M.; Ouyang, P.; Fournier, G.; Reschner, A.; Rakus, K.; Wilkie, G.S.; Farnir, F.; Bayrou, C.; Lieffrig, F.; et al. Rational Development of an Attenuated Recombinant Cyprinid Herpesvirus 3 Vaccine Using Prokaryotic Mutagenesis and In Vivo Bioluminescent Imaging. *PLOS Pathog.* **2015**, *11*, e1004690. [CrossRef]
40. Broeke, J.; Perez, J.M.M.; Pascau, J. *Image Processing with ImageJ—Second Edition*, 2nd ed.; Packt Publishing: Birmingham, Mumbai, 2015; ISBN 978-1-78588-983-7.
41. Ronsmans, M.; Boutier, M.; Rakus, K.; Farnir, F.; Desmecht, D.; Ectors, F.; Vandecan, M.; Lieffrig, F.; Mélard, C.; Vanderplasschen, A. Sensitivity and Permissivity of Cyprinus Carpio to Cyprinid Herpesvirus 3 during the Early Stages of Its Development: Importance of the Epidermal Mucus as an Innate Immune Barrier. *Vet. Res.* **2014**, *45*, 100. [CrossRef]
42. Costes, B.; Raj, V.S.; Michel, B.; Fournier, G.; Thirion, M.; Gillet, L.; Mast, J.; Lieffrig, F.; Bremont, M.; Vanderplasschen, A. The Major Portal of Entry of Koi Herpesvirus in Cyprinus Carpio Is the Skin. *J. Virol.* **2009**, *83*, 2819–2830. [CrossRef]
43. Huisken, J.; Swoger, J.; Del Bene, F.; Wittbrodt, J.; Stelzer, E.H.K. Optical Sectioning Deep Inside Live Embryos by Selective Plane Illumination Microscopy. *Science* **2004**, *305*, 1007–1009. [CrossRef]
44. Kaufmann, A.; Mickoleit, M.; Weber, M.; Huisken, J. Multilayer Mounting Enables Long-Term Imaging of Zebrafish Development in a Light Sheet Microscope. *Development* **2012**, *139*, 3242–3247. [CrossRef] [PubMed]
45. Streiff, C.; He, B.; Morvan, L.; Zhang, H.; Delrez, N.; Fourrier, M.; Manfroid, I.; Suárez, N.M.; Betoulle, S.; Davison, A.J.; et al. Susceptibility and Permissivity of Zebrafish (*Danio rerio*) Larvae to Cypriniviruses. *Viruses* **2023**, *15*, 768. [CrossRef]
46. Bercovier, H.; Fishman, Y.; Nahary, R.; Sinai, S.; Zlotkin, A.; Eyngor, M.; Gilad, O.; Eldar, A.; Hedrick, R.P. Cloning of the Koi Herpesvirus (KHV) Gene Encoding Thymidine Kinase and Its Use for a Highly Sensitive PCR Based Diagnosis. *BMC Microbiol.* **2005**, *5*, 13. [CrossRef] [PubMed]
47. Rakus, K.; Ronsmans, M.; Forlenza, M.; Boutier, M.; Piazzon, M.C.; Jazowiecka-Rakus, J.; Gatherer, D.; Athanasiadis, A.; Farnir, F.; Davison, A.J.; et al. Conserved Fever Pathways across Vertebrates: A Herpesvirus Expressed Decoy TNF-α Receptor Delays Behavioral Fever in Fish. *Cell Host Microbe* **2017**, *21*, 244–253. [CrossRef] [PubMed]
48. Gao, Y.; Sridhar, A.; Bernard, N.; He, B.; Zhang, H.; Pirotte, S.; Desmecht, S.; Vancsok, C.; Boutier, M.; Suárez, N.M.; et al. Virus-Induced Interference as a Means for Accelerating Fitness-Based Selection of Cyprinid Herpesvirus 3 Single Nucleotide Variants In Vitro and In Vivo. *Virus Evol.* **2023**, *9*, vead003. [CrossRef]
49. Diallo, M.A.; Pirotte, S.; Hu, Y.; Morvan, L.; Rakus, K.; Suárez, N.M.; PoTsang, L.; Saneyoshi, H.; Xu, Y.; Davison, A.J.; et al. A Fish Herpesvirus Highlights Functional Diversities among Zα Domains Related to Phase Separation Induction and A-to-Z Conversion. *Nucleic Acids Res.* **2022**, *51*, 806–830. [CrossRef]
50. Donohoe, O.; Zhang, H.; Delrez, N.; Gao, Y.; Suárez, N.M.; Davison, A.J.; Vanderplasschen, A. Genomes of Anguillid Herpesvirus 1 Strains Reveal Evolutionary Disparities and Low Genetic Diversity in the Genus Cyprinivirus. *Microorganisms* **2021**, *9*, 998. [CrossRef]
51. Waltzek, T.B.; Kelley, G.O.; Alfaro, M.E.; Kurobe, T.; Davison, A.J.; Hedrick, R.P. Phylogenetic Relationships in the Family Alloherpesviridae. *Dis. Aquat. Organ.* **2009**, *84*, 179–194. [CrossRef]
52. Ito, T.; Kurita, J.; Ozaki, A.; Sano, M.; Fukuda, H.; Ototake, M. Growth of Cyprinid Herpesvirus 2 (CyHV-2) in Cell Culture and Experimental Infection of Goldfish Carassius Auratus. *Dis. Aquat. Organ.* **2013**, *105*, 193–202. [CrossRef]
53. Liu, Z.; Zhou, T.; Gao, D. Genetic and Epigenetic Regulation of Growth, Reproduction, Disease Resistance and Stress Responses in Aquaculture. *Front. Genet.* **2022**, *13*, 994471. [CrossRef]
54. Roy, S.; Kumar, V.; Behera, B.K.; Das, B.K. Epigenetics: Perspectives and Potential in Aquaculture. In *Advances in Fisheries Biotechnology*; Pandey, P.K., Parhi, J., Eds.; Springer Nature: Singapore, 2021; pp. 133–150. ISBN 9789811632150.
55. Xiu, Y.; Shao, C.; Zhu, Y.; Li, Y.; Gan, T.; Xu, W.; Piferrer, F.; Chen, S. Differences in DNA Methylation Between Disease-Resistant and Disease-Susceptible Chinese Tongue Sole (*Cynoglossus semilaevis*) Families. *Front. Genet.* **2019**, *10*, 847. [CrossRef] [PubMed]
56. Shang, X.; Wan, Q.; Su, J.; Su, J. DNA Methylation of CiRIG-I Gene Notably Relates to the Resistance against GCRV and Negatively-Regulates MRNA Expression in Grass Carp, Ctenopharyngodon Idella. *Immunobiology* **2016**, *221*, 23–30. [CrossRef] [PubMed]
57. Fontenot, D.K.; Neiffer, D.L. Wound Management in Teleost Fish: Biology of the Healing Process, Evaluation, and Treatment. *Vet. Clin. N. Am. Exot. Anim. Pract.* **2004**, *7*, 57–86. [CrossRef] [PubMed]
58. Reverter, M.; Tapissier-Bontemps, N.; Lecchini, D.; Banaigs, B.; Sasal, P. Biological and Ecological Roles of External Fish Mucus: A Review. *Fishes* **2018**, *3*, 41. [CrossRef]
59. Dash, S.; Das, S.K.; Samal, J.; Thatoi, H.N. Epidermal Mucus, a Major Determinant in Fish Health: A Review. *Iran. J. Vet. Res.* **2018**, *19*, 72–81. [PubMed]
60. Vancsok, C.; Peñaranda, M.M.D.; Raj, V.S.; Leroy, B.; Jazowiecka-Rakus, J.; Boutier, M.; Gao, Y.; Wilkie, G.S.; Suárez, N.M.; Wattiez, R.; et al. Proteomic and Functional Analyses of the Virion Transmembrane Proteome of Cyprinid Herpesvirus 3. *J. Virol.* **2017**, *91*, e01209-17. [CrossRef]
61. Davison, A.J.; Kurobe, T.; Gatherer, D.; Cunningham, C.; Korf, I.; Fukuda, H.; Hedrick, R.P.; Waltzek, T.B. Comparative Genomics of Carp Herpesviruses. *J. Virol.* **2013**, *87*, 2908–2922. [CrossRef]

62. Zhu, M.; Li, K.; Xuan, Y.; Sun, Z.; Liu, B.; Kumar, D.; Jiang, M.; Pan, Y.; Zhang, Y.; Gong, Y.; et al. Host Range and Vertical Transmission of Cyprinid Herpesvirus 2. *Turk. J. Fish. Aquat. Sci.* **2019**, *19*, 645–652. [CrossRef]
63. Thompson, D.J.; Khoo, L.H.; Wise, D.J.; Hanson, L.A. Evaluation of Channel Catfish Virus Latency on Fingerling Production Farms in Mississippi. *J. Aquat. Anim. Health* **2005**, *17*, 211–215. [CrossRef]
64. Hanson, L.; Doszpoly, A.; van Beurden, S.J.; de Oliveira Viadanna, P.H.; Waltzek, T. Alloherpesviruses of Fish. In *Aquaculture Virology*; Kibenge, F.S.B., Godoy, M.G., Eds.; Academic Press: San Diego, CA, USA, 2016; pp. 153–172, ISBN 978-0-12-801573-5. [CrossRef]

Experimental Section

2nd study

Susceptibility and Permissivity of Zebrafish (*Danio rerio*) Larvae to Cypriniviruses

Preamble

The zebrafish (*Danio rerio*) represents an increasingly important model organism in virology. For instance, it has acted as a useful model to study a diverse range of viruses, including mammalian viruses such as *Human Herpesvirus* 1 (HHV-1), and viruses infecting reared fish such as the *Spring Viraemia of Carp virus* (SVCV). The ease at which zebrafish can be genetically manipulated is a key factor in its value as a vertebrate model organism, and unlike the natural host species of many viruses, this may greatly facilitate studies into viral host interaction. As a means of exploring the possibility of using this model to study economically important viruses from the genus *Cyprinivirus*, we investigated the susceptibility and permissivity of zebrafish cell lines and larvae to *Cyprinid herpesvirus 2* (CyHV-2, affecting goldfish, gibel carp and crucian carp), CyHV-3 (affecting common and koi carp) and *Anguillid herpesvirus 1* (AngHV-1, affecting eel species). Notably, in the context of this Ph.D. project, this was conducted on the basis that it may have led to the establishment of an interesting CyHV-2 *in vivo* model, which could complement the existing infection models utilizing natural CyHV-2 hosts. However, this revealed that zebrafish larvae were not susceptible to these viruses after immersion in virally contaminated water, but that infections with CyHV-2 and CyHV-3 could be established using artificial infection models *in vitro* (zebrafish cell lines) and *in vivo* (microinjection of larvae). Ultimately, these infections were transient, with rapid viral clearance associated with apoptosis-like death of infected cells, leading to the conclusion that the utility of this model with these viruses was limited. However, it may serve as a useful model to study viral clearance.

Experimental Section

2nd study

Susceptibility and Permissivity of Zebrafish (*Danio rerio*) Larvae to Cypriniviruses

Viruses 2023, 15(3), 768

Streiff, C.; He, B.; Morvan, L.; Zhang, H.; Delrez, N.; Fourrier, M.; Manfroid, I.; Suárez, N.M.; Betoulle, S.; Davison, A.J.; Donohoe, O.; Vanderplasschen, A.

This study was led by my colleague Cindy Streiff. My contribution to this study consisted of the CyHV-2 YC-01 viral recombinant production and the exploration of the susceptibility and permissivity of the zebrafish ZF4 cell line and zebrafish larvae to CyHV-2. As such, I was the primary person responsible for CyHV-2 infections in these two artificial models. The paper was published in the Journal *Viruses* in March of 2023.

viruses

MDPI

Article

Susceptibility and Permissivity of Zebrafish (*Danio rerio*) Larvae to Cypriniviruses

Cindy Streiff [1], Bo He [1], Léa Morvan [1], Haiyan Zhang [1], Natacha Delrez [1], Mickael Fourrier [1], Isabelle Manfroid [2], Nicolás M. Suárez [3], Stéphane Betoulle [4], Andrew J. Davison [3], Owen Donohoe [1,5,*,†] and Alain Vanderplasschen [1,*,†]

[1] Immunology–Vaccinology, Department of Infectious and Parasitic Diseases, Fundamental and Applied Research for Animals & Health (FARAH), Faculty of Veterinary Medicine, University of Liège, B-4000 Liège, Belgium
[2] Zebrafish Development and Disease Models Laboratory, GIGA-Molecular Biology of Diseases, University of Liège, B-4000 Liège, Belgium
[3] MRC-University of Glasgow Centre for Virus Research, Glasgow G61 1QH, UK
[4] UMR-I 02 Stress Environnementaux et BIOsurveillance des Milieux Aquatiques (SEBIO), UFR Sciences Exactes et Naturelles, Université de Reims Champagne-Ardenne, CEDEX 2, 51687 Reims, France
[5] Bioscience Research Institute, Technological University of the Shannon, N37 HD68 Athlone, Co. Westmeath, Ireland
* Correspondence: owen.donohoe@uliege.be (O.D.); a.vdplasschen@uliege.be (A.V.); Tel.: +32-4-366-43-79 (O.D.); +32-486-45-13-53 (A.V.)
† These authors contributed equally to this work.

Abstract: The zebrafish (*Danio rerio*) represents an increasingly important model organism in virology. We evaluated its utility in the study of economically important viruses from the genus *Cyprinivirus* (anguillid herpesvirus 1, cyprinid herpesvirus 2 and cyprinid herpesvirus 3 (CyHV-3)). This revealed that zebrafish larvae were not susceptible to these viruses after immersion in contaminated water, but that infections could be established using artificial infection models in vitro (zebrafish cell lines) and in vivo (microinjection of larvae). However, infections were transient, with rapid viral clearance associated with apoptosis-like death of infected cells. Transcriptomic analysis of CyHV-3-infected larvae revealed upregulation of interferon-stimulated genes, in particular those encoding nucleic acid sensors, mediators of programmed cell death and related genes. It was notable that uncharacterized non-coding RNA genes and retrotransposons were also among those most upregulated. CRISPR/Cas9 knockout of the zebrafish gene encoding protein kinase R (PKR) and a related gene encoding a protein kinase containing Z-DNA binding domains (PKZ) had no impact on CyHV-3 clearance in larvae. Our study strongly supports the importance of innate immunity-virus interactions in the adaptation of cypriniviruses to their natural hosts. It also highlights the potential of the CyHV-3-zebrafish model, versus the CyHV-3-carp model, for study of these interactions.

Keywords: anguillid herpesvirus 1; cyprinid herpesvirus 2; cyprinid herpesvirus 3; alloherpesvirus; cyprinivirus; zebrafish; PKR; PKZ; CRISPR/Cas9; innate immunity

Citation: Streiff, C.; He, B.; Morvan, L.; Zhang, H.; Delrez, N.; Fourrier, M.; Manfroid, I.; Suárez, N.M.; Betoulle, S.; Davison, A.J.; et al. Susceptibility and Permissivity of Zebrafish (*Danio rerio*) Larvae to Cypriniviruses. *Viruses* **2023**, *15*, 768. https://doi.org/10.3390/v15030768

Academic Editors: Isabel Bandín, Carlos P. Dopazo and Sandra Souto

Received: 16 February 2023
Revised: 8 March 2023
Accepted: 10 March 2023
Published: 17 March 2023

1. Introduction

The zebrafish (*Danio rerio*) is a member of the family *Cyprinidae*. It is an extremely useful experimental subject due to its high fecundity and short generation time and is currently one of the most widely used laboratory animal model organisms. Also, its transparent larval stage is highly suited to in vivo imaging, making it particularly well suited to studying host-pathogen interaction, including during viral infection [1]. Furthermore, the availability of a well-annotated zebrafish reference genome [2] and large range of recombinant and mutant zebrafish lines [3] greatly facilitates investigations into gene function in various biological contexts. The zebrafish is known to possess a well-developed immune system, composed of both innate and adaptive immune responses [4,5]. Despite some notable

differences and although sites of maturation differ [6], many mammalian immune system cell types have zebrafish counterparts [7,8]. Also, zebrafish orthologs of many (but not all) mammalian pathogen recognition receptors (PRRs), cytokines, adaptor proteins for signal transduction and other important components have been identified [6,9,10], indicating that zebrafish represent a relatively useful model for studying the mechanisms that vertebrates use to detect and respond to pathogen-associated molecular patterns (PAMPs).

Although juvenile and adult zebrafish utilize both the innate and the adaptive branches of the immune system, the embryonic and larval stages rely solely on innate immunity, which is detectable and active on the first day of zebrafish embryogenesis, whereas the adaptive system is fully matured by 4–6 weeks post-fertilization [11,12]. During these early life stages, cellular immunity is mediated by myeloid cells only, with macrophages and neutrophils acting as the main effector cells [13,14]. As in mammals, the zebrafish antiviral response is orchestrated by type I pathogen induced interferons (IFNs). These are named IFNϕ1, IFNϕ2, IFNϕ3, and IFNϕ4 [15] (referred to hereafter by the respective gene symbols *ifnphi1*, *ifnphi2*, *ifnphi3*, and *ifnphi4*) and are structurally similar to mammalian type I (α and β) and type III (λ) IFNs. As in all vertebrates, type I IFNs in zebrafish induce the expression of antiviral genes broadly referred to as interferon stimulated genes (ISGs). However, the IFN response in zebrafish larvae is mediated solely by *ifnphi1* and *ifnphi3*, with *ifnphi2* being expressed only in adults and with *ifnphi4* having little activity [16,17]. The zebrafish type II IFN family consists of two members, IFNγ1 and IFNγ2 which are also responsible for the induction of ISGs induced by type I IFNs [18].

Taken together, this indicates that the zebrafish represents a relevant and useful model for studying viral pathogenicity, vertebrate host immune response, and viral host-interactions. Strikingly, very few viruses are known to infect zebrafish naturally [19–22]. Moreover, despite the lower host temperature, several mammalian viruses can infect zebrafish under experimental conditions, with these hosts exhibiting varying degrees of susceptibility and permissivity to infection. This property has also been exploited to study human viruses such as influenza A virus, Chikungunya virus (CHIKV), herpes simplex virus type 1 (HSV-1) and human norovirus [23–26]. Moreover, infection of zebrafish has been explored in studying severe acute respiratory syndrome coronavirus 2 (SARS-CoV-2) [27,28].

Zebrafish can also be infected with several important fish viruses [29–35]. One of these, the spring viraemia of carp virus (SVCV), which is a rhabdovirus responsible for a highly contagious disease of the common carp (*Cyprinus carpio carpio*), has become one of the viruses most frequently used in infection models for studying the antiviral immune response in zebrafish larvae and adults [16,17,35–37]. Recent work by Rakus et al. [38] demonstrated that cyprinid herpesvirus 3 (CyHV-3) induces an abortive infection after intraperitoneal inoculation of adult zebrafish. CyHV-3 causes mass mortality in common carp and koi carp (*Cyprinus carpio koi*), resulting in massive economic losses [39]. CyHV-3 is a member of the genus *Cyprinivirus* in the family *Alloherpesviridae*, which consists of herpesviruses that infect fish and amphibians.

In addition to CyHV-3, the genus *Cyprinivirus* contains two other economically important viruses: anguillid herpesvirus 1 (AngHV-1) and cyprinid herpesvirus 2 (CyHV-2) [40]. AngHV-1 infects the European eel (*Anguilla anguilla*), Japanese eel (*Anguilla japonica*), and American eel (*Anguilla rostrata*) [41]; CyHV-2 also infects goldfish (*Carassius auratus*) and the closely related Prussian carp (*Carassius gibelio*) and crucian carp (*Carassius carassius*) [42]. Like zebrafish, the natural hosts of CyHV-2 and CyHV-3 are also members of the family *Cyprinidae*. Cypriniviruses cause diseases only in their natural host species, which suggests the existence of restrictions related to host cell susceptibility (i.e., the ability to support virus entry) and host cell permissivity (i.e., the ability to support viral replication and the transmission of viable viral progeny to new cells, although the former may occur without the latter). Notably, experiments relying on infection of cell lines have demonstrated the ability of cypriniviruses to infect, even if inefficiently, cells originating from non-natural host species. Indeed, both CyHV-2 and CyHV-3 are capable of infecting cell lines derived from species within the family *Cyprinidae* that are not their natural hosts [39,42], with CyHV-3

already known to infect zebrafish cell lines [38]. Similarly, despite not naturally infecting species outside of the family *Anguillidae*, it has been demonstrated that AngHV-1 can infect at least one cell line derived from a member of the family *Cyprinidae* [43]. These data suggest that the ability of cypriniviruses to induce diseases only in their natural host species may be related to complex host-virus interactions downstream of host cell susceptibility.

In the present study, we conducted an in-depth evaluation and comparison of AngHV-1, CyHV-2, and CyHV-3 in terms of their ability to infect zebrafish models both in vitro and in vivo. These experiments involved the exploitation of recombinant viruses expressing reporters, timelapse epifluorescence microscopy in vitro, live imaging and transcriptomics in vivo; and finally, the generation of CRISPR/Cas9 mutant hosts to investigate the potential modulation of zebrafish permissivity to infection. Our study strongly supports the importance of the innate immune response alone in clearing viral infection and emphasizes the high degree of adaptation that cypriniviruses have undergone to facilitate successful circulation within their respective natural hosts. It also highlights the potential value of the CyHV-3-zebrafish model versus CyHV-3-carp models to study the fundamental features of virus-host interactions.

2. Materials and Methods

2.1. Cells and Viruses

The zebrafish embryonic fibroblast cells line (ZF4) [44] was kindly provided by Dr K. Rakus (Department of Evolutionary Immunology, Jagiellonian University, Poland) and cultured in advanced Dulbecco's modified Eagle's Medium/Ham's F-12 (Gibco, New York, NY, USA), supplemented with 10% foetal calf serum (FCS), 2% penicillin–streptomycin (Sigma-Aldrich, St. Louis, MO, USA) and 1% L-glutamine (Lonza, Basel, Switzerland). Cells were cultured at 25 °C in a humid atmosphere containing 5% CO_2. Eel kidney (EK-1) [45], Ryukin goldfish fin (RyuF-2) [46], and common carp brain (CCB) [47] cell lines were used to produce stocks of AngHV-1, CyHV-2, and CyHV-3, respectively. These cells were cultured as described previously [46,48,49].

Three previously described recombinant viral strains were utilized. The CyHV-3 FL BAC revertant ORF136 Luc strain (referred to as CyHV-3 Luc; GenBank accession KP343683.1) was derived from the CyHV-3 FL BAC plasmid and encodes a firefly (*Photinus pyralis*) luciferase (Luc2) reporter cassette driven by a human cytomegalovirus (CMV) promoter inserted between ORF136 and ORF137 [50]. The AngHV-1 Luc-copGFP and the CyHV-2 Luc-copGFP recombinant strains both encode the same reporter genes consisting of the Luc2 cassette and a copepod (*Pontellina plumata*) GFP (copGFP) cassette linked by a T2A sequence, driven by a eukaryotic translation elongation factor 1 alpha (EF-1α) promoter. To generate these recombinants, the dual Luc2/copGFP cassette was inserted in the region between ORF32 and ORF33 in the AngHV-1 UK parental strain genome (GenBank accession MW580855.1) [40] (Delrez et al., unpublished data) and in the intergenic region between ORF64 and ORF66 in CyHV-2 YC-01 parental strain genome (GenBank accession no. MN593216.1) (He et al., unpublished data) using homologous recombination in eucaryotic cells, as described previously [50].

In addition to the three recombinant strains described above, a fourth strain, expressing enhanced (EGFP), referred to as the CyHV-3 EGFP strain, was derived from the CyHV-3 Luc strain and constructed specifically for this study. Details relating to the generation and verification of this strain are provided in Methods S1.

2.2. In Vitro Experiments

2.2.1. Virus Infections

ZF4 cells cultured in 24-well plates were mock-infected or infected at 24 hours (h) after seeding. Virus was diluted in 0.5 mL serum-free cell culture medium to provide a multiplicity of infection (MOI) of 3 plaque forming units (PFU)/cell. After incubating for 2 h, 1 mL fresh cell culture medium was added without removing the inoculum, and the cells were incubated at 25 °C with 5% CO_2.

2.2.2. Timelapse Imaging of Infected Cells

At 24 h post infection (hpi), virus-infected ZF4 cells in 24-well plates were placed in an IncuCyte Zoom HD/2CLR microscopy system (Sartorius), which was maintained at 25 °C with 5% CO_2. Each well was imaged at 9 different fields of view every 2 h from 1–11 days post infection (dpi). Images were collected in phase contrast and in the green (GFP) channels. Each infection was done in triplicate wells.

2.2.3. Image Analysis

Data from timelapse imaging of infected cells was analysed using the Fiji plugin TrackMate (v7.7.2) [51] to track fluorescent reporter expression from individual ZF4 cells infected with CyHV-2 or CyHV-3, and by extension, to identify cell infection and cell death events with respect to time. Image sequences containing 123 frames/field of view/well were generated using a series of images acquired from 1 to 11 dpi. Analysis was performed using the default settings with LoG Detector and Simple LAP Tracker. Additional parameters were adjusted empirically in order adequately to detect and monitor fluorescence from infected cells within frames (estimated object diameter: 28.6 pixels; quality threshold: 1). Data were exported in .csv format and imported into GraphPad Prism (v8.0.1) for further analysis and visualization.

2.3. Experiments Using Zebrafish

2.3.1. Zebrafish Larvae Maintenance

Wild-type (WT, +/+) AB strain adult zebrafish (*Danio rerio*) were obtained by natural spawning and maintained at 27 °C, on a 14/10 h light/dark cycle. They were housed in the GIGA Zebrafish facility in Liège (Belgium) according to animal research guidelines and with the approval of the local ethical commission for animal care and use. Larvae were obtained by pairwise mating of adults in mating cages and maintained in petri dishes with standard embryo medium (E3) and incubated at 25 °C prior to use in experiments.

2.3.2. Inoculation of Larvae by Immersion

Zebrafish larvae (3 days post-fertilization (dpf)) were placed in 24-well plates containing 1 mL E3 medium and either mock-infected or infected by immersion. For infection, virus suspensions were added to each well and mixed gently (final concentration: 4000 PFU/mL), and plates were incubated at 25 °C.

2.3.3. Inoculation of Larvae by Microinjection

Borosilicate glass capillaries were loaded with 10 µL of medium containing virus suspensions (1.2×10^6 PFU/mL) and then connected to a FemtoJet microinjector (Eppendorf, Framingham, MA, USA) as described elsewhere [52]. After breaking the capillary tip, the pressure was adjusted to obtain droplets with a diameter of ~0.13 mm. Larvae (3 dpf) were anesthetized in a bath containing tricaine (0.2 mg/mL). The fish were positioned on a petri dish, and the surface of the dish was dried entirely in order to avoid drifting of the larvae during viral injections. In order to visualize the hearts of the larvae, the petri dish was placed under a binocular magnifier (LEICA MZ6) at 4x magnification and illuminated by an external light source (LEICA CLS 50X). The capillary was then manually inserted into the pericardial cavity and three pulses were performed to inject approximately 3 nL of virus suspension (infected fish) or 3 nL of PBS (mock-infected fish). After microinjection,

the larvae were transferred into individual wells in a 24-well plate containing 1 mL E3 medium and incubated at 25 °C.

2.3.4. Epifluorescence Microscopy

The progression of infection with recombinant viruses expressing fluorescent reporters was monitored using epifluorescence microscopy. This facilitated longitudinal observation of the same larvae at multiple timepoints. Prior to observation, larvae were anesthetized in a bath of E3 medium containing tricaine (0.2 mg/mL) and methylcellulose (2% *w*/*v*) in order to avoid drifting of larvae. Imaging of larvae was performed using a Leica DM2000 epifluorescence microscope at 5× and 10× magnification. After imaging, larvae were immediately transferred back to their individual wells and returned to the incubator. After the final observation timepoint, larvae were euthanized using an overdose of tricaine in E3 media (400 mg/L).

2.3.5. In Vivo Bioluminescent Imaging

An in vivo imaging (IVIS) system (IVIS Spectrum, PerkinElmer) was used to detect bioluminescence in larvae infected with Luc2-expressing recombinant viruses, thus facilitating the monitoring and quantification of viral levels in vivo. At the time of imaging, larvae were anesthetized (as described for epifluorescence microscopy analysis), injected with ~3 nL of D-luciferin (15 mg/mL), and imaged 5 minutes (min) after injection. Images were acquired using the following settings: field of view A, small binning, automatic exposure time with a maximum of 1 min and a subject height of 0.30 cm. Unlike epifluorescence analysis, longitudinal monitoring of individual larvae was not possible due to the harmful effects of repeated D-luciferin injections in the same larvae. Relative bioluminescence intensities were analysed using Living Image software (v4.7.3). Regions of interest (ROIs) were drawn by manually outlining the larval body, and bioluminescence within the ROI was recorded in terms of mean radiance (photons/s/cm^2/sr).

2.3.6. In Vivo Timelapse Imaging

For time-lapse imaging, live larvae infected with CyHV-3 EGFP were imaged using a Zeiss Z1 light sheet microscope according to the protocol described elsewhere [53]. Briefly, larvae were embedded inside FEP tubes containing 0.1% low melting point agarose and tricaine (55 µg/mL) and maintained at 27 °C. Z-stacks encompassing the entire head and heart regions were acquired every 10 min from 2 to 3 dpi and were used to generate a maximum-intensity projection video with ImageJ.

2.3.7. Ethics Statement

The experiments performed in the present study did not require a bioethical permit as they involved the use of larvae before implementation of feeding. However, all experiments were designed and conducted in accord with the 3R rules and other bioethics standards.

2.4. RNA-Seq Analysis

2.4.1. Zebrafish Larvae Infection, Sampling and Lysis

WT AB zebrafish larvae were inoculated with CyHV-3 EGFP (1.2×10^6 PFU/mL) or mock-infected with PBS via pericardial microinjection. The larvae were placed in 24-well plates with 1 mL E3 medium per well and incubated at 25 °C. Infected and mock-infected larvae were sampled at 1, 2 and 4 dpi (triplicates at each timepoint with 5 larvae pooled per replicate). Prior to sampling, larvae were euthanized using an overdose of buffered tricaine in E3 media (400 mg/L). Each replicate group of euthanized larvae was transferred immediately to 1.5 mL tubes, excess E3 medium was removed, and 700 µL QIAzol lysis reagent (Qiagen, Hilden, Germany) was added. Whole larvae were then completely homogenized in lysis reagent by passing the lysate through a 21 G needle 20 times using a 2 mL syringe. After homogenization, lysates were stored at −80 °C until RNA isolation.

2.4.2. RNA Isolation, Library Construction and RNA Sequencing

Larvae lysates were thawed and incubated at room temperature for at least 5 min and 140 µL chloroform was added to each sample. Lysates were then vortexed for 15 s, incubated at room temperature for 3 min and centrifuged for 15 min at 12,000× *g* at 4 °C. After centrifugation, 240 µL of the aqueous layer was removed and 360 µL of 100% ethanol was added with immediate mixing by pipetting. Samples were then added to RNeasy spin columns, and RNA was isolated using an RNeasy Mini Kit (Qiagen, Hilden, Germany) with on-column DNase treatment. RNA was eluted in 100 µL RNase-free water using two 50 µL elution steps, and split into smaller aliquots for storage at −80 °C. For each sample, a single aliquot was used to check the quality of RNA using an Agilent Bioanalyzer, ensuring that RNA integrity (RIN) values were at least 9.5 before proceeding. Samples were used as input for barcoded RNA-Seq library preparation using the TruSeq Stranded mRNA kit (Illumina), and libraries were sequenced using the Illumina NextSeq 500 System.

2.4.3. Bioinformatics Analysis

Sequence reads were aligned to the zebrafish reference genome GRCz11 (Ref Seq: GCF_000002035.6) in order to generate gene expression data. The data were used to identify differentially expressed genes (DEGs) in infected samples relative to non-infected samples (defined as those with false discovery rate (FDR) adjusted *p*-values < 0.05). DEGs were analysed further to identify functional relationships, and expression data were analysed to identify gene-sets that were significantly enriched in infected samples relative to non-infected samples. A non-abbreviated summary of the bioinformatic analysis conducted in this study is provided in Methods S2.

2.5. Mutant Zebrafish Experiments

2.5.1. Generation of Mutant Zebrafish Strains Using CRISPR/Cas9

The *mut eif2ak2* (*pkr*)^{ulg025}, *mut pkz*^{ulg027}, and *mut eif2ak2* (*pkr*) *L15-1* knockout (KO) zebrafish lines, hereafter referred to as the PKR-KO, PKZ-KO and PKR-PKZ-KO mutant strains, were generated by CRISPR/Cas9 technology as described previously [54–56]. The nls-zCas9-nls mRNA was synthesized by transcription of the plasmid pT3TS-nCas9n (Addgene #46757). First, WT strain AB zebrafish were used to generate the mutant strains PKR-KO and PKZ-KO (Figure 1a). To generate the PKR-KO and the PKR-PKZ-KO mutant strains, CHOPCHOP [57] software was used to design two single-guide RNAs (sgRNA) GAGCACTCACAGTGATGAACCGG and CCACCGTGAACAGGCATCT (PAM motifs are underlined) to target exon 2 of the WT *eif2ak2* (or *pkr*) gene (NCBI/Entrez/GenBank Gene ID: 100001092) and exon 1 of the WT *pkz* gene (NCBI/Entrez/GenBank Gene ID: 503703), respectively (Figure 1a). sgRNAs were generated by in vitro transcription from oligonucleotide templates using the MEGAscript T7 transcription kit (Ambion) as described previously [58]. The DNA templates were prepared by annealing and filling two oligonucleotides containing the T7 promoter sequence and the target sequences as previously described [56]. One-cell stage zebrafish embryos were injected with approximately 1 nL of a solution containing 50 ng sgRNA and 300 ng nls-zCas9-nls mRNA. The efficiency of mutagenesis was checked by genotyping using heteroduplex migration assays after amplification of targeted genomic sequences. Founder embryos (F0 generation) carrying a germline mutation in *eif2ak2* or *pkz* were raised to adulthood and outcrossed with WT fish to generate heterozygous F1 fish. Fish harbouring frameshift mutations were kept and used to raise F2 homozygous stable knockout lines. Subsequently, PKZ-KO mutant strain zebrafish were then used to generate the double KO PKR-PKZ-KO mutant strain by repeating the process used to generate the PKR-KO mutant strain (Figure 1a). These mutations all resulted in genes producing truncated proteins and were verified by PCR (Figure 1b).

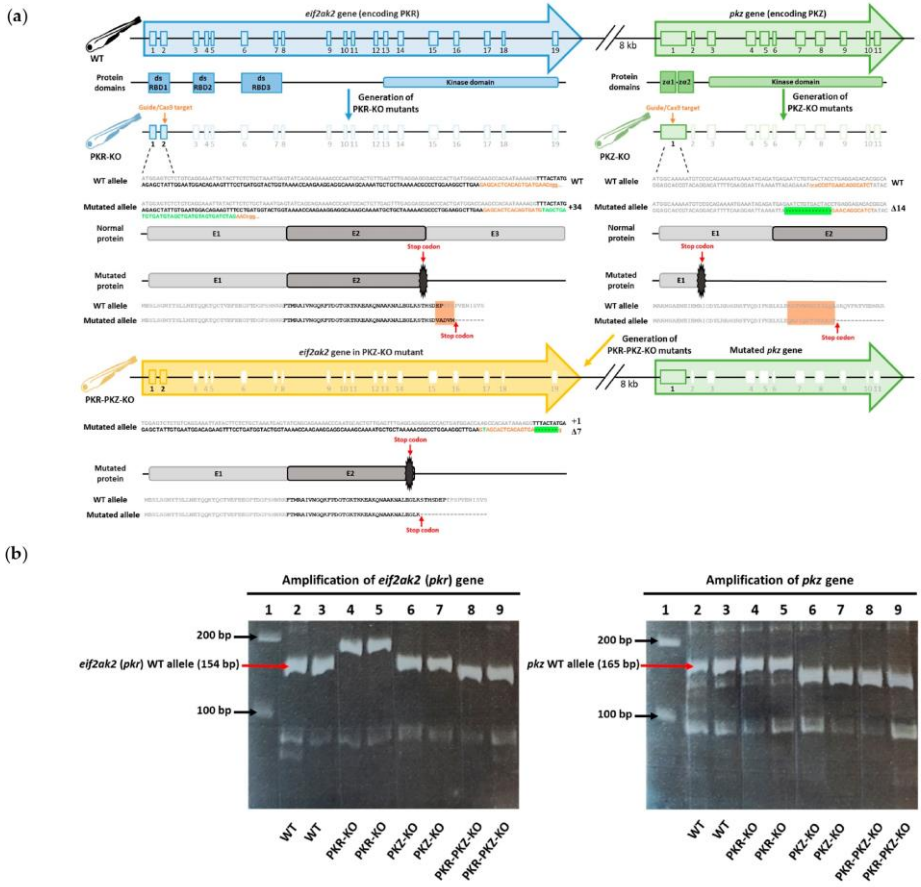

Figure 1. Generation and verification of CRISPR-Cas9 *eif2ak2* (*pkr*) and *pkz* mutations in zebrafish (**a**) Structure of zebrafish *eif2ak2* (*pkr*) and *pkz* genes and proteins. The protein domains including double stranded RNA-binding domains (dsRB), Z-DNA/RNA binding domains (zα) and kinase domains are aligned to the corresponding exons. The CRISPR/Cas9 gene editing targets were exon 2 in zebrafish *eif2ak2* gene and exon 1 in zebrafish *pkz* gene; sgRNA target sequences are also displayed (orange, PAM lower case). The CRISPR/Cas9-induced changes in the WT *eif2ak2* gene (34-base insertion) to generate PKR-KO, and WT *pkz* gene (14-base deletion) to generate the PKZ-KO mutant strains are displayed. After the generation of the PKZ-KO mutant strain, the WT *eif2ak2* gene in this strain was also mutated, resulting in the PKR-PKZ-KO mutant strain (displayed below). The mutated *eif2ak2* gene in the PKR-PKZ-KO strain exhibits a different mutation (7-base deletion with 1-base insertion) relative to the mutated *eif2ak2* gene in PKR-KO mutant. Inserted and deleted sequences are highlighted in green (deleted sequences are represented by "-"). (**b**) Results from genotyping of homozygous WT, PKR-KO, PKZ-KO and PKR-PKZ-KO zebrafish groups. This involved PCR amplification of *eif2ak2* (*pkr*) and *pkz* genes, in each mutant group (left and right gel images, respectively, with expected sizes of WT alleles indicated). Each gel consists of the same layout: Lane 1: 1kb Molecular Marker, Lanes 2–9 each represent a DNA extracted from single whole larva, Lanes 2–3: WT Larvae, Lanes 4–5: PKR-KO mutants, Lanes 6–7 PKZ-KO mutants, Lanes 8–9 PKR-PKZ-KO mutants. Mutant *eif2ak2* (*pkr*) alleles were detected in PKR-KO and PKR-PKZ-KO larvae exhibiting 188-bp and 148-bp amplicons, respectively (left gel). The mutant *pkz* allele was detected in in PKZ-KO and PKR-PKZ-KO larvae, both exhibiting 151-bp amplicons (right gel). Higher quality figures for the whole manuscript are available in the PDF version.

2.5.2. Genotyping of Zebrafish Mutant Lines

The genotyping of WT, PKR-KO, PKZ-KO, and PKR-PKZ-KO zebrafish was performed by polymerase chain reaction (PCR). In order to extract the DNA, two randomly selected zebrafish larvae (4 dpf) were euthanized per mutant line. Each larva was transferred to an Eppendorf tube containing 25 µL 50 mM NaOH, heated at 95 °C for 25 min, and cooled on ice for 10 min. Finally, 2.5 µL 1M Tris-HCl pH8.0 was added, and cellular debris was pelleted by brief centrifugation for 15 sec. DNA concentration was determined by measuring A260 (NanoDrop 2000, Thermo Scientific, Waltham, NJ, USA), and ~2.5 µL of the resulting lysate was used per standard PCR reaction with gene-specific primers (Table S1). PCR reactions consisted of 1× Thermopol buffer (New England Biolabs, Ipswich, MA, USA), 0.025 U/µL Taq Polymerase (New England Biolabs), 300 nM forward and reverse primers, and 60 nM dNTPs (total volume 25 µL). The cycling conditions were as follows: 95 °C for 2 min, 40 cycles of 45 s at 95 °C, 45 s at 60 °C, 20 s at 72 °C, and ending with 72 °C for 10 min.

2.5.3. Quantification of Viral Genome by TaqMan PCR

Larvae were euthanized using an overdose of tricaine, transferred into RNAlater (Thermo Fisher, Waltham, NJ, USA) and stored at −20 °C. DNA was extracted from whole larvae with a DNeasy Tissue Kit (Qiagen, Hilden, Germany), and approximately 1 ng genomic DNA was used for each TaqMan PCR reaction. TaqMan qPCR reactions consisted of 1× IQ Supermix (Bio-Rad, Hercules, CA, USA), 200 nM forward and reverse primers, and 400 nM TaqMan probe (total volume of 25 µL). The primers and probes used are provided in Table S1. The PCRs were performed using a CFX96 Touch real-time PCR detection system (Bio-Rad, Hercules, CA, USA) with detection in the FAM channel. The cycling conditions were as follows: 95 °C for 15 min, 40 cycles of 15 s at 94 °C, and 60 s at 60 °C. Each sample was analysed in triplicate. Viral genome copies were normalized to zebrafish genome copies (internal control) by also amplifying zebrafish genomic DNA as described previously [59]. Viral and zebrafish (internal control) PCRs were performed in separate wells, but always on the same plates. Negative template controls and positive controls were included on each plate. Data were exported to Excel using CFX Manager v3.0 software (Bio-Rad, Hercules, CA, USA). Relative levels of viral genome copies were calculated using the $2^{-\triangle\triangle CT}$ method as described previously [60].

2.6. Statistical Analysis

Each dataset was first tested for normality using the Shapiro–Wilk test, which was conducted as a stand-alone test or as part of a two-way ANOVA analysis of residuals implemented in GraphPad Prism (v8.0.1). The omnibus tests used were dependent on the outcome of the Shapiro-Wilk tests. For datasets exhibiting normal distribution, One-way ANOVA, Two-way ANOVA, or Two-way repeated measures (RM) ANOVA were used and implemented in GraphPad Prism. For datasets not exhibiting normal distribution, the Durbin test was used (PMCMR package v4.4 [61]), implemented in R (v4.2.0) [62]. The variables of interest relating to each of these tests and their significance are described in the text. Survival curves were compared using Logrank tests implemented in GraphPad Prism

Post-hoc multiple comparisons between groups of interest were made using either the Sidak test (two groups) or the Tukey test (more than two groups) implemented in Graphpad Prism (in conjunction with ANOVA tests), for data exhibiting normal distribution. Multiple comparisons were made using Dunn's pairwise test (FSA package v0.9.3 [63]) with Benjamini-Hochberg *p*-value adjustment done using the p.adjust function in R (in conjunction with the Durbin Test), for datasets not exhibiting normal distribution. For the purposes of visual clarity, only significant results from post-hoc multiple comparisons are indicated in each corresponding figure. The results of multiple comparisons tests are represented using the following symbols, * $p < 0.05$; ** $p < 0.01$; *** $p < 0.001$; **** $p < 0.0001$.

3. Results and Discussion

3.1. ZF4 Cells Express Low Susceptibility and Reduced or Even No Permissivity to Cyprinivirus Infection Leading to Abortive Infection of Cell Monolayers

In this experiment we tested the susceptibility and permissivity of the ZF4 cell line to infection with AngHV-1, CyHV-2 and CyHV-3, using recombinant strains expressing green fluorescent proteins as reporters. Cells were monitored from 1 dpi onwards using epifluorescence microscopy. At 1 dpi, infected cells were observed, with much less AngHV-1 infected cells relative to CyHV-2 and CyHV-3. The amount of CyHV-2 and CyHV-3-infected cells increased from 1–4 dpi, while the amount of AngHV-1-infected cells decreased after 2 dpi (Figure 2).

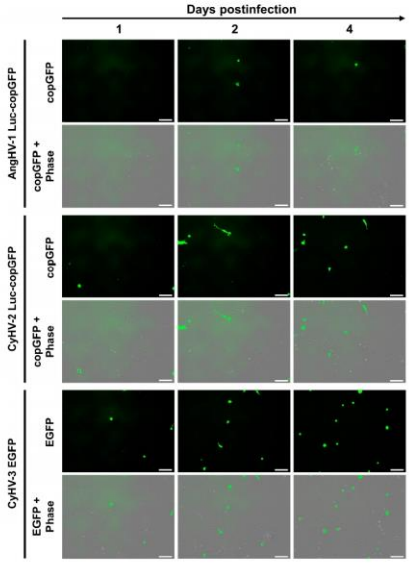

Figure 2. Infection of ZF4 cells by cyprinivirus. ZF4 cells were infected with the AngHV-1 Luc-copGFP, CyHV-2 Luc-copGFP and CyHV-3 EGFP recombinant strains. Infection progression was imaged by epifluorescence microscopy. Infected cells were identified based on green fluorescence expression at the indicated timepoints of infection. Scale bars = 100 µm.

Syncytia formation, lysis plaques, or other cytopathic effects (CPE), were not observed in monolayers infected with CyHV-2 or CyHV-3. Together, these data revealed that ZF4 cells expressed some level of susceptibility to the cyprinivirus tested, no permissivity to AngHV-1 infection, and greatly reduced permissivity to CyHV-2 and CyHV-3 infection relative to typical observations in cells derived from their respective natural hosts that are routinely used for culture of these viruses.

To further characterise the infection of ZF4 cells by the three cyprinivirus in a more quantitative manner, we utilized timelapse microscopy (Figure 3). ZF4 cells were infected, and the numbers of infected cells present with respect to time were tracked from 1–11 dpi as illustrated in Figure S2. Again, the number of AngHV-1 infected cells were low relative to CyHV-2 and CyHV-3 infections and did not increase over time. Consequently, AngHV-1 was excluded from further quantification analysis in vitro. None of the infections led to the formation of detectible CPE. We observed a steady increase in CyHV-2- and CyHV-3-infected cells from ~24–144 hpi, followed by a rapid clearance of both viruses from ZF4 monolayers (Figure 3). As evident in Figure 2, during the most rapid period of virus propagation within the monolayer (from ~24–144 hpi) the rate of CyHV-2 and CyHV-3 spread was not exponential (Figure 3), indicating poor replication efficiency within infected cells and/or reduced transmission of progeny virus to additional cells.

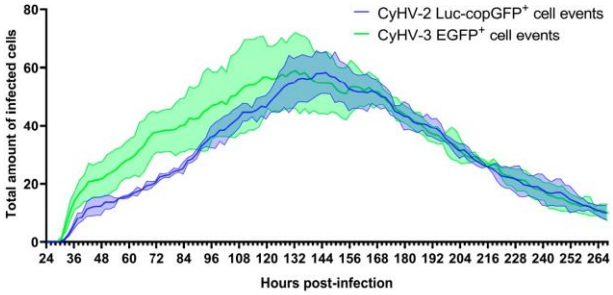

Figure 3. Quantification of CyHV-2 and CyHV-3-infected cells in ZF4 monolayer over time. This data was acquired via time-lapse fluorescent microscopy (IncuCyte). Cells were cultured in a 24-well plate and infected with CyHV-2 Luc-copGFP or CyHV-3 EGFP recombinants (1.2×10^6 PFU/mL for each recombinant). At 24 hpi, cells were imaged every 2 h for 11 days. Data represent the mean ± standard errors from three replicates/wells. Data from each replicate at each timepoint represent the sum of fluorescent cells observed in nine separate locations of each well.

In the CyHV-2-infected monolayers, the peak of infected cells occurred at 146 ± 4 hpi with a mean of 58 ± 7 infected cells observed per well (sum of nine different fields of view in each well, sums from three replicate wells used to derive mean). This peak occurred earlier in CyHV-3-infected monolayers at 124 ± 11 hpi with a mean of 59 ± 13 infected cells at this point. Overall, time postinfection was shown to have a significant effect on the number of CyHV-2 and CyHV-3-infected cells observed (Two-way RM ANOVA, p value < 0.0001), but there was no significant difference between the two viruses in this respect (Two-way RM ANOVA, p value = 0.3164) (Figure 3).

However, from ~24–144 hpi, the mean number of infected cells tended to be higher in the CyHV-3-infected monolayer. For example, at 48 hpi there was a mean of 21 ± 6 CyHV-3-infected cells observed per well compared to a mean of 12 ± 3 CyHV-2-infected cells. From ~144–264 hpi, the number of infected cells evolved similarly for both viruses, with infected cell numbers decreasing steadily until the end of the experiment, representing the gradual clearance of infected cells from the monolayer (Figure 3). Notably this clearance was largely characterized by apoptosis-like morphological changes.

These two time-ranges, i.e., ~24–144 hpi and ~144–264 hpi, corresponded to periods approximately before and after the peak of infected cells, respectively. Thus, we further scrutinized these two distinct periods separately in order to determine the extent of any differences between CyHV-2 and CyHV-3. After defining the timepoints corresponding to the latest infection peak in each replicate, we examined the two distinct periods of infection, comprised of viral propagation (pre-peak) and clearance (post-peak), by quantifying the appearance (beginning of infection) and disappearance (cell death) of infected cells (Figure 4). This revealed that infected cells appeared at a mean rate of 0.64 ± 0.05 cells per hour for CyHV-2 and 0.78 ± 0.13 cells per hour for CyHV-3 before the peak, with no significant differences between the two viruses in this respect (Two-way ANOVA, p value = 0.1704). It also revealed that a mean of 75 ± 4.16% and 72 ± 8.89% of newly infected CyHV-2 and CyHV-3 cells appeared before the peak of infection, respectively, in what appears to have been several waves of infection (Figure 4). For both viruses, in all replicates, an initial peak of infected cell appearance occurred at ~36 hpi, followed by a period of particularly low appearance of newly infected cells until after ~48 hpi. This may represent the transmission of the first generation of viral progeny to the second generation of infected cells (from ~24–36 hpi), and subsequent progeny to the next generation of infected cells (occurring after ~48 hpi). However, the low numbers of newly infected cells yielded from this transmission provides more evidence to support the possible inefficient replication and/or transmission of CyHV-2 and CyHV-3 between ZF4 cells (as observed in Figure 2).

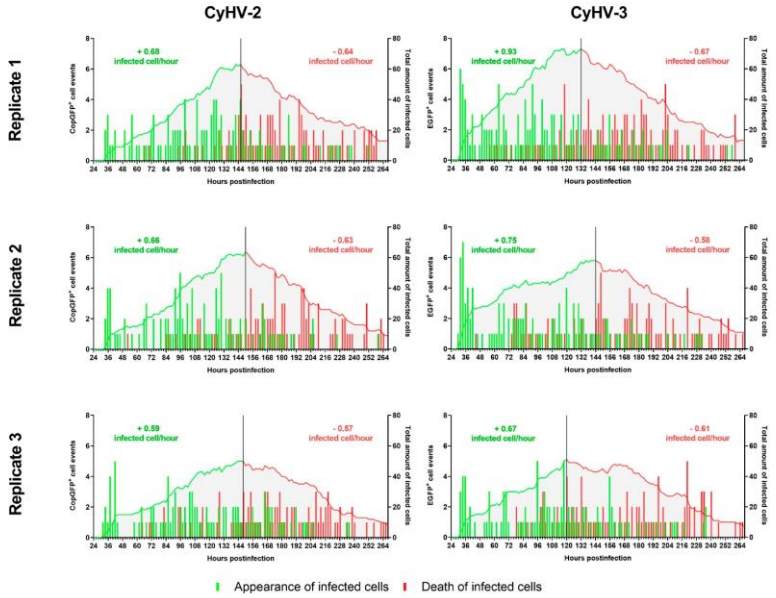

Figure 4. Kinetics of appearance and death of CyHV-2 and CyHV-3-infected cells before and after infection peak. The bars relate to the temporal pattern of appearance and disappearance of CyHV-2-infected or CyHV-3-infected cells (based on fluorescent reporter expression). The quantities are based on the total amount of observations made in 9 different locations in each well/replicate. The green and red curves show the total amount of infected cells up until the peak of infection (represented by the black vertical line) and after the peak, respectively. The values on top of the curves represent the average rate of appearance of infected cells per hour (green) and the average rate of death per hour (red). Analysing the rate of appearance/hour before the peak for CyHV-2 and CyHV-3 revealed no differences between the viruses.

For both CyHV-2 and CyHV-3, a substantial amount of newly infected cells (25–30%) appeared after the peak, even beyond 10 dpi, indicating that transmission of viral progeny was sustained into the later stages of the experiment. We have recently demonstrated that CyHV-3 virions lose infectivity rapidly in cell culture media (>95% by 24 h) [64], thus excluding the possibility that newly infected cells, particularly beyond 10 dpi, could have originated from the initial inoculum due to delayed viral entry into cells. It is also unlikely that we are observing delayed expression of viral genes, as all fluorescent reporters used in this experiment were driven by highly active constitutive promoters (CMV and EF-1α). Also, we reasoned that because cells expressing fluorescent reporters are actively cleared at increased rates and appear at decreased rates as the experiment continued, the outcome is distinct from that of spurious reporter expression (i.e., without expression of other viral genes, owing to integration of the expression cassette into the host cell genome), which should persist for longer without triggering cell death. Together, these observations indicated the occurrence of at least some viral progeny transmission to non-infected cells after an initial round of viral replication. However, as increase in the numbers of newly infected cells was not exponential, but linear, it indicated that efficient replication and/or transmission of CyHV-2 and CyHV-3 was very rare in ZF4 cells. Nonetheless, it provided evidence that ZF4 cells are transiently permissive to CyHV-2 and CyHV-3 infection. The observation of isolated infected cells without plaque formation indicated the absence of transmission via cell-cell contact. This may indicate a high degree of heterogeneity within ZF4 monolayers regarding susceptibility to these viruses, or very strong or fast innate responses in neighbouring cells. Within at least one permissive cell line, CyHV-3 cell-cell

transmission may be greatly enhanced by syncytia formation (in particular with CyHV-3 FL strain derived recombinants, which we recently described [64]). However, we observed a notable lack of syncytia formation among CyHV-3-infected ZF4s, which may also contribute to reduced transmission via cell-cell contact.

It is important to note that for all viruses used in this study, the use of a high MOI of 3 (although calculated in the context of permissive cell lines used for viral production), did not result in many initial infected ZF4 cells, indicating a general lack of cyprinivirus susceptibility among ZF4 populations. This may happen for many reasons, for example, a lack of optimum cell surface receptors, resulting in inefficient viral entry. Conversely, entry may occur, but the viral replication may not commence due to a lack of crucial cellular factors. The exact reasons for this remain speculative and are beyond the scope of this present study, but it provides an opportunity for further investigation via single cell sequencing analysis in the future.

Notably, cell death before the infection peak was low with 74 ± 0.03% and 74 ± 0.07% of CyHV-2 and CyHV-3-infected cells dying after the peak, respectively. Therefore, the higher transmission, prior to the peak, was not reliant on the release of virions via infected cell lysis/death but rather on the normal mechanism of herpesvirus egress [65,66]. Programmed cell death prior to completion of the viral replication cycle in particular acts as an innate defence mechanism which infected cells can employ to reduce virus replication [67]. Indeed, this is what was observed post infection peak, with an increase in cell death correlating with a reduction in newly infected cells (Figure 4). We propose that relative to cells at the earlier stages of the experiment, both infected and uninfected cells present at later stages would have been subject to cytokine stimulation as part of the innate immune response. Even if such stimulation was transient, these cells (many of which may exhibit limited susceptibility to begin with) may have adopted a stronger antiviral-state at later stages of the experiment.

In order to compare the virulence of CyHV-2 and CyHV-3 in ZF4 cells, we returned to the data Figure 3 and monitored all positive cells present at 120 hpi until their death, using this information to generate survival curves (Figure 5). This 120 hpi timepoint was selected, as it represented the earliest peak of infection out of the six that were defined in Figure 4, thus maximizing infected cell sample size while using a common timepoint for all groups. The median survival time for infected cells was 61 ± 3 h and 53 ± 12 for CyHV-2 and CyHV-3-infected groups, respectively. Although CyHV-2-infected cells tended to survive longer, there was no significant difference survival between the two groups (Log-rank Mantel-Cox test, p value = 0.0822).

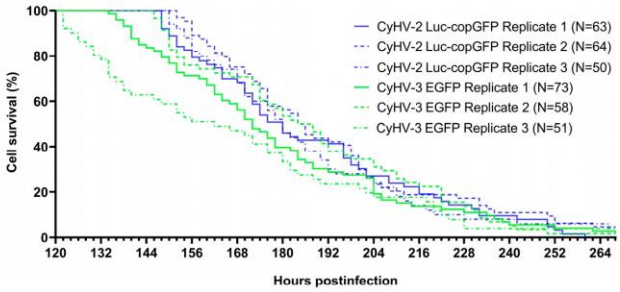

Figure 5. Survival kinetics for CyHV-2 and CyHV-3-infected cells displayed as Kaplan-Meier plots. CyHV-2 and CyHV-3-infected cells observed at 120 hpi were monitored until the end of the experiment. Cell death events and times were identified based on the disappearance of fluorescent signals (Figure S2). N = Number of cells followed.

In the majority of cases, death events were morphologically consistent with apoptosis, i.e., cell shrinkage, membrane blebbing leading to the appearance of cell debris resembling apoptotic bodies [68–70]) (Figure 6a, top panel). However, the occurrence of apoptosis

was not definitively confirmed by staining. We also observed another distinct type of cell death that was not morphologically consistent with apoptosis. In these cases, morphological features mostly included initial cell swelling, followed by cell shrinkage and an absence of cell debris resembling apoptotic bodies prior to disappearance of fluorescent signal (Figure 6a, bottom panel). This is somewhat morphologically consistent with necrosis, where cell-death is associated with membrane rupture and leaking of cytoplasmic contents [68–70].

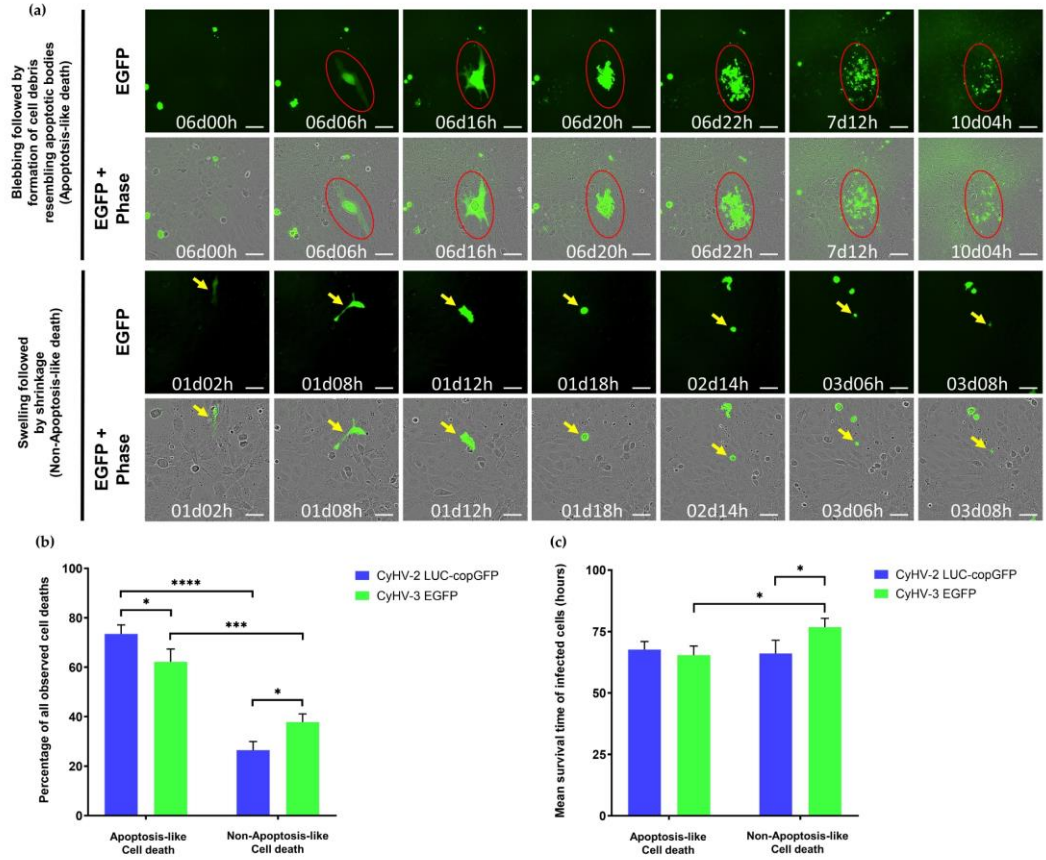

Figure 6. Cell death characteristics observed in CyHV-2 and CyHV-3 infections (**a**) Representative morphological observations among populations of infected cells (those exhibiting fluorescence) in the periods leading up to cell death (disappearance of fluorescence). Top panel: Morphological features consistent with apoptosis (cell shrinkage, membrane blebbing followed by the appearance of cell debris resembling apoptotic bodies, and progressive decrease of fluorescent signal). Bottom panel: Morphological features not consistent with apoptosis (cell swelling, followed by cell shrinkage, and absence of cell debris resembling apoptotic bodies prior to disappearance of fluorescent signal). Key examples of individual cells undergoing apoptosis-like and non-apoptosis-like death in each panel are highlighted by red circle and yellow arrows, respectively, which track the progression of morphology in a single cell with respect to time. Time postinfection (in days and hours) is indicated in images. Scale bars = 100 µm. (**b**) Percentage of infected cells exhibiting features of apoptosis-like or non-apoptosis-like cell death among those that died during the observation period (**c**) Mean survival time of infected cells undergoing cell death during the observation period according to the type of death observed. Data represents mean ± standard error from 3 replicates. **** $p < 0.0001$; *** $p < 0.001$; * $p < 0.05$.

Notably, necrosis can also be initiated in a highly regulated manner known as necroptosis, which acts as a back-up for apoptosis [71,72]. However, it was not possible to differentiate between necrosis and necroptosis based on our morphological observations alone, and as with apoptosis, neither were definitively confirmed via staining. In any case, the apoptosis-like form of cell death was observed to be the dominant form of death among infected cells (Figure 6b). However, there were differences between the two viruses in this respect (Two-way ANOVA, *p*-value = <0.0001), with the proportion of CyHV-3-infected cells undergoing apoptosis-like cell death being significantly lower (Figure 6b), possibly indicating that CyHV-3 may be more efficient at blocking this apoptosis-like death in ZF4 cells. There was no significant difference between the two viruses in terms of survival times (Two-way ANOVA, *p*-value = 0.1112). However, among CyHV-3-infected cells, those undergoing non-apoptosis-like death exhibited significantly longer survival times than those undergoing apoptosis-like death (Figure 6c).

Previously, a separate study demonstrated that CyHV-3 could indeed infect ZF4 cells, with increasing viral RNA levels observed from 1–4 dpi, and an absence of CPE was also noted [38]. However, the viral dosages used were not directly comparable with this present study, and the possibility of viral clearance after 4 dpi was not investigated. In this present study, we monitored the progression of CyHV-3 infections for much longer (up to 11 dpi). Crucially, through the exploitation of reporter genes, in addition to demonstrating viral gene expression, we were also able to identify and quantify new cell infection events. This revealed continuous CyHV-3 transmission right up until the clearance of infection, albeit with increasingly reduced rates of newly infected cells. While we demonstrated that ZF4s are certainly susceptible to CyHV-3 infection, any initial productive infections leading to transmission of viable progeny were not sustained. Thus, ZF4 cells are transiently permissive to CyHV-3 with inefficient viral replication/transmission unable to overcome the innate immune response among infected and non-infected cells. This may be similar to previous observations with snakehead fish vesiculovirus (SHVV) infections in ZF4 cells where initial increases in virus levels were followed by a decrease, corresponding to ISG upregulation [73].

Unlike CyHV-3, prior to this study, the susceptibility ZF4 cells to AngHV-1 and CyHV-2 had not been investigated. Our results indicate that while ZF4 cells are also susceptible to both AngHV-1 and CyHV-2 infection, they are only permissive to the latter. However, as with CyHV-3, permissiveness to CyHV-2 infection was moderate and transient. These similarities between CyHV-2 and CyHV-3, and their differences to AngHV-1 in this context may reflect the fact that CyHV-2 and CyHV-3 are phylogenetically closer to each other, than each are to AngHV-1 [40,74–76]. Furthermore, given their natural host species, it stands to reason that CyHV-2 and CyHV-3 may also be inherently better adapted to growing in ZF4 cells relative to AngHV-1. Despite the lack of sustained permissivity to cyprinivirus, these in vitro experiments with ZF4 cells did provide some indication that the same recombinant viruses may be used to study transient cyprinivirus infection and clearance in zebrafish larvae, which, for many reasons (outlined earlier), may represent a valuable virus-host model.

3.2. Zebrafish Larvae Are Susceptible to CyHV-2 and CyHV-3 but Not to AngHV-1 Infection. Inoculation by the Two Cyprinid Herpesviruses Leads to an Abortive Infection

We next investigated the susceptibility and permissivity of zebrafish larvae to the same three cyprinivirus. To investigate this, we used WT AB zebrafish larvae at 3 dpf. In the first experiment, larvae were infected with the same recombinants previously used (Figures 2–6). Larvae were inoculated by pericardial microinjection with 1.2×10^6 PFU/mL of each recombinant or PBS. In parallel, larvae were also infected by immersion with a final concentration of 4000 PFU/mL of each recombinant or PBS. The susceptibility of larvae to these viruses was assessed using epifluorescence microscopy to detect reporter expression from each recombinant. Independently of the mode of inoculation used or the virus, no morbidity or mortality was observed among larvae. Epifluorescence microscopy indicated

no infection in larvae inoculated by immersion. Conversely, viral infection was detected from 1 dpi in larvae inoculated with CyHV-2 and CyHV-3 by microinjection (Figure 7a) with no fluorescence detected in the AngHV-1 inoculated group. Fluorescence intensity in CyHV-2 and CyHV-3-infected larvae increased from 1–2 dpi. However, as per earlier in vitro observations, these infections were transient, with fluorescence intensity (Figure 7a) and the numbers of infected larvae (Figure 7b) decreasing by 4 dpi. While the pattern was similar for both viruses, the CyHV-3 group exhibited greater fluorescence intensity and significantly higher rates of infected larvae (Two-way RM ANOVA p-value = 0.0214). Infection clearance was most pronounced in the CyHV-2-infected group, with a significantly higher proportion of larvae infected at earlier timepoints exhibiting viral clearance by 4 dpi relative to CyHV-3 (Figure 7b). The differences between these three cypriniviruses were investigated further by measuring Luc2 expression from recombinants, representing a more quantitative comparison of viral levels in vivo. This involved the same AngHV-1 and CyHV-2 recombinants used in Figure 7a, with CyHV-3 EGFP replaced with CyHV-3 Luc. Larvae were inoculated or mock-inoculated as per Figure 7a. Again, no mortality was observed in any groups and no infection was detected in the AngHV-1 group. The CyHV-3-infected group exhibited significantly higher viral levels relative to CyHV-2 (Durbin Test, p-value = 0.0008), indicating that CyHV-3 replicates better in this model. Also, for both CyHV-2 and CyVH-3, a reduction in virus levels occurred at 3 dpi, coinciding with a reduction in the numbers of infected fish, indicating the initiation of viral clearance. However, as per Figure 7b, clearance was significantly greater within the CyHV-2-infected group by 4 dpi (Figure 7c).

These experiments revealed that zebrafish larvae are not susceptible to any of these viruses via immersion, which may be considered a more natural route. This is similar to previous findings with CyHV-3 in Tübingen zebrafish larvae [38]. Conversely, larvae were susceptible to CyHV-2 and CyHV-3 when inoculated via pericardial microinjection, but not to AngHV-1 via the same route. In line with earlier observations in vitro, CyHV-2 and CyHV-3, which naturally infect members of the family *Cyprinidae*, are much more fit in this zebrafish model relative to AngHV-1. For CyHV-2 and CyHV-3, a peak of infection was reached at 2 dpi, with viral clearance initiating from 2–3 dpi. Notably, this is the first report of cyprinivirus infection in zebrafish larvae. Our observations are largely consistent with previous description of CyHV-3 infections in adult zebrafish (inoculation by intraperitoneal injection) [38]. There was also a notable lack of mortality in previous studies involving the challenge of zebrafish with other viruses of cyprinid fish [38]. One explanation is that zebrafish may naturally possess robust defences against other viruses that are closely related to CyHV-2 and CyHV-3 which may have circulated in their natural habitat during their evolution. However, few viruses are known to naturally infect zebrafish [1,19], thus it would be useful to determine if any extant uncharacterized members of the family *Alloherpesviridae* naturally infect zebrafish as a primary host, as it would open up new avenues of investigation with a valuable homologous herpesvirus-host model in zebrafish. It is also possible that this lack of mortality is related to the viral dose or even inoculation site, both of which can impact the severity of viral infections in zebrafish larvae, as exemplified elsewhere [77,78].

Our observations indicated that CyHV-3 exhibits greater fitness in these zebrafish models relative to CyHV-2. Thus, in addition to CyHV-3 being the most studied and the archetype fish alloherpesvirus [39], it also represented a more valuable model to utilize in the further study of alloherpesvirus infections in zebrafish larvae. Thus, CyHV-3 was selected for all further in vivo investigations in this study.

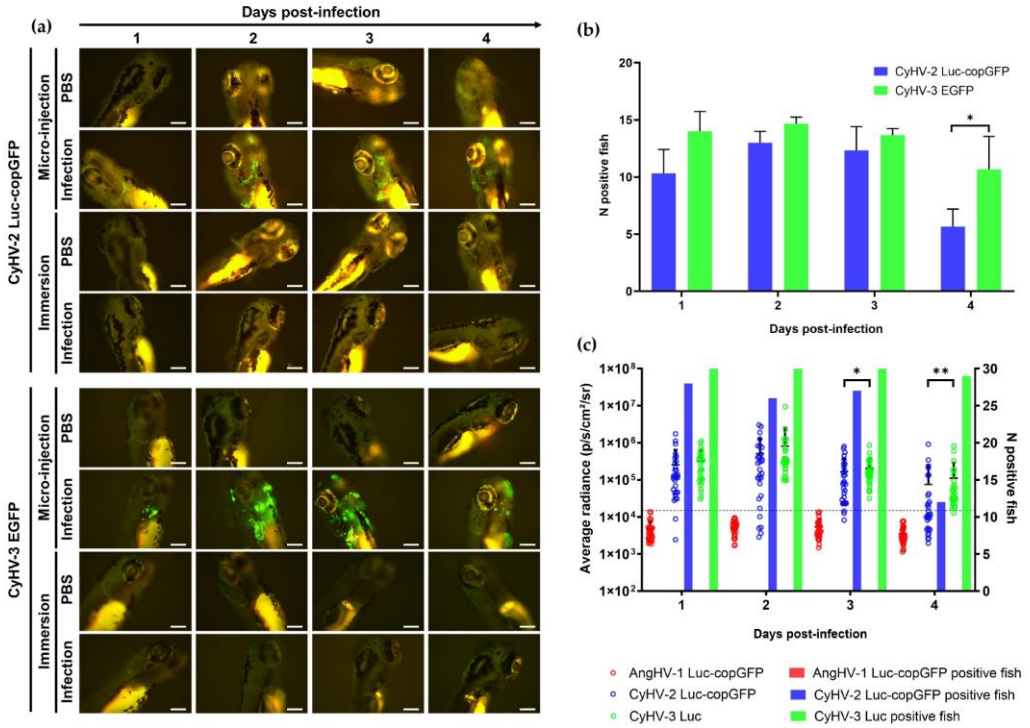

Figure 7. Susceptibility and permissivity of zebrafish larvae to infection with cypriniviruses after inoculation by microinjection (**a**) Epifluorescence microscopy images representative of larvae inoculated with CyHV-2 and CyHV-3 according to time postinfection (longitudinal observation of the same larvae over all timepoints) Scale bars = 200 µm. (**b**) Numbers of CyHV-2 and CyHV-3-infected larvae among groups inoculated by microinjection (n = 15). Data represents mean ± standard errors from 3 independent experiments (longitudinal observation of the same larvae over all timepoints). (**c**) Levels of AngHV-1, CyHV-2 and CyHV-3 detected in infected larvae according to time postinfection based on Luc2 signal expressed by viral recombinants. The data points represent the mean radiance per larvae according to time postinfection with mean ± standard error represented for each group at each timepoint (n = 30). The discontinuous line represents the cut-off for positivity and represents the mean + 3 × SD of the values obtained for mock-infected larvae. The number of positive larvae at each timepoint is represented by bars. * $p < 0.05$; ** $p < 0.01$.

3.3. Pericardial Inoculation of Zebrafish Larvae with CyHV-3 Leads to Infection of Resident and Motile Cells around the Inoculation Site Followed by Their Apoptosis-like Death and Viral Clearance

Earlier experiments revealed that the levels of CyHV-3 signal increased from 1–2 dpi with clearance commencing from 2–3 dpi (Figure 7a,c). However, it remained unclear if increases in viral signal were merely due to increasing levels of viral gene expression or the numbers of infected cells. We chose to investigate this using light sheet microscopy to capture epifluorescence and brightfield images at regular intervals in live CyHV-3-infected larvae from 2–3 dpi and subsequently generated a timelapse video with this data (Video S1). This timepoint was selected as it overlapped with the highest viral signals and the beginning of the viral clearance process (Figure 7), and because no viable virus from the original inoculum should have persisted to this timepoint [64].

As per Figure 7a, the infection was mainly localized around the heart area, reflecting the inoculation route. In line with earlier observations, a reduction in viral levels commenced between 2.5–3 dpi (Figure 8a and Video S1). Notably, the data revealed

a substantial upsurge in apoptosis-like cell death immediately prior to clearance, indicating that programmed cell death may also play a major role in this process in vivo (Figure 8b and Video S1). Although the occurrence of apoptosis in response to CyHV-3 infection in vivo was not confirmed by staining in this present study, our observations are similar to previous studies involving timelapse analysis of CHIKV-infected zebrafish larvae [23]. Throughout the monitoring period, highly motile cells, possibly macrophages or neutrophils, were also observed to be infected. These did not remain localized around the inoculation site. However, they were not observed to establish secondary infection sites elsewhere (Figure 8c and Video S1). Furthermore, some of these motile cells appeared also to undergo apoptosis-like and non-apoptosis-like cell death consistent with necroptosis (Video S1). Unlike earlier in vitro observations, this data did not provide unambiguous evidence of newly infected cells appearing before clearance commenced. Indeed, the induction of a programmed cell death response among infected cells in vivo, thus interrupting the CyHV-3 replication cycle, would lead to a reduction in successful CyHV-3 transmission to new cells. Consequently, CyHV-3 propagation in vivo may be sufficiently restricted to facilitate its clearance via the innate immune response alone. This hypothesis still implies that zebrafish cells are inherently permissive to CyHV-3 replication. However, this would, at the very least, require expression of all essential CyHV-3 protein coding genes in vivo. Thus, we subsequently investigated this and the nature of the innate immune response via transcriptomic analysis of infected larvae.

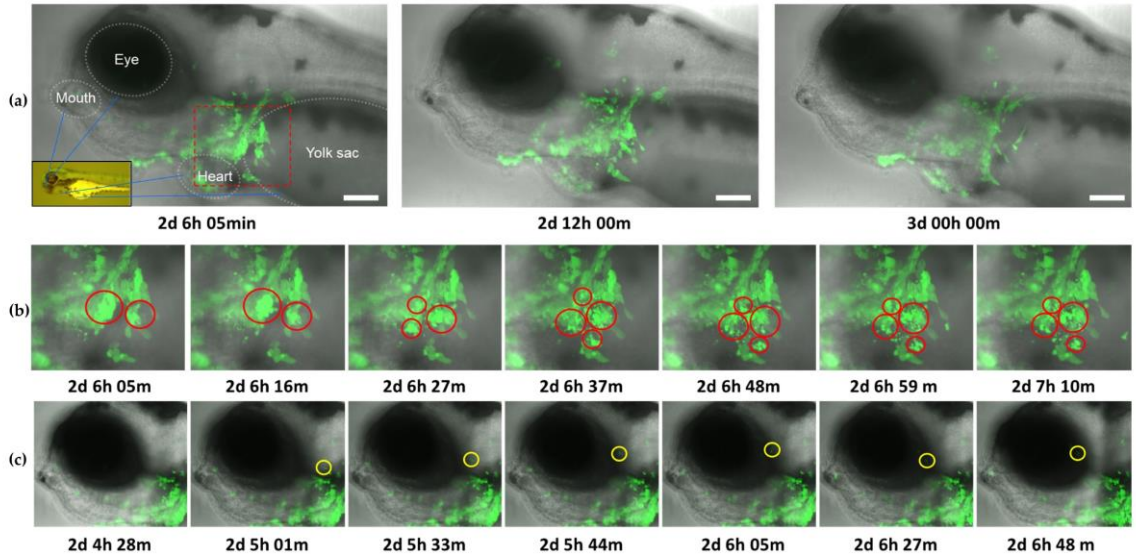

Figure 8. Frames from timelapse video of CyHV-3 EGFP infection in zebrafish larvae from 2–3 dpi (Video S1). The video represents overlay of brightfield/transmission and EGFP fluorescence (green). Time postinfection (in days, hours, and minutes) is indicated under each frame. (**a**) Entire field of view from light-sheet microscopy. For the purposes of visual orientation, identifiable anatomical features and corresponding locations within larvae body (inset image) are indicated in the first panel. Images show that the infection is primarily localized around the inoculation site (red square), and a decrease in viral levels from 2.5–3 dpi. Scale bars = 100 µm. (**b**) Enlarged images of the area within red square in (**a**), representing key examples of apoptosis-like death occurring among large numbers of infected cells (red circles) around the inoculation site, with such events primarily characterized by blebbing followed by the appearance of cell debris resembling apoptotic bodies (**c**) Key example of highly motile infected cell (highlighted with yellow circle), migrating away from the site of inoculation.

3.4. Transcriptomic Analysis of Infected Zebrafish Indicate Upregulation of ISGs, in Particular Those Involved in Programmed Cell Death, Innate Immune Response and PRR Signalling Pathways

In order to further characterise the response to CyHV-3 infection in this zebrafish larvae model in terms of the ISG upregulation, the potential involvement of programmed cell death (as indicated in Figure 8 and Video S1), and to establish the extent of CyHV-3 gene transcription in this model, we conducted transcriptomic analysis of infected zebrafish larvae. CyHV-3-infected and mock-infected larvae were sampled at 1, 2, and 4 dpi for RNA extraction and sequencing. RNA-Seq, yielded ~15–20 million reads per sample with data publicly available under BioProject Accession number PRJNA929940. Gene expression was compared between infected and mock-infected samples at each timepoint to identify DEGs. In line with viral levels observed in earlier experiments, viral RNA levels reached a peak at 2 dpi (0.34% of total transcriptome), falling considerably by 4 dpi (Table S2). Notably, transcription from all 155 CyHV-3 ORFs was detected by 2 dpi (Figure S3 and Table S3), indicating that indeed, in this model, cells may be permissive to CyHV-3 replication. Host differential gene expression in response to infection also peaked at 2 dpi, with 7.4% of expressed genes classified as DEGs (Table S2 and Figure S4).

Prior to this study, it was unknown how zebrafish larvae respond to CyHV-3 challenge in terms of type I IFN gene expression. Consistent with other reports [16], we found that *ifnphi2* was not expressed at this developmental stage. The IFN response in zebrafish larvae relies on expression of *ifnphi1* and/or *ifnphi3* genes [16]. However, we did not observe convincing expression from either gene at any timepoint. Our sampling points range from at 1–4 dpi, which equate to 96–168 hpf, with previous studies indicating that WT AB zebrafish larvae are capable of expressing *infphi1* and *infphi3* by this developmental stage [16,23]. Notably, these previous studies, involving SVCV and CHIKV challenge, utilized RT-qPCR to detect IFN gene transcription, which may be more sensitive than RNA-Seq in some situations.

While CyHV-3 is known to inhibit the IFN-response in vitro [79,80], our observations do not necessarily indicate inhibition of the IFN-response in zebrafish. It is possible that the upregulation of IFN genes occurs very early after infection, returning to basal levels rapidly, prior to the first sampling point. The effects of this rapid and short-lived IFN response should be still observed in the form of subsequent ISG induction. Indeed, in this present study, the list of the 250 most significant DEGs at 2 dpi is dominated by typical ISGs (Table S4). This ISG induction in the absence of IFN detection is similar to previous studies with WT zebrafish larvae infected with nervous necrosis virus (NNV) [78]. In both studies, it is likely that IFN upregulation occurred prior to the earliest sampling point. However, the kinetics of Type I IFN induction in WT AB zebrafish may depend on the nature of the viral challenge (virus, dosage and inoculation site/route). For example, in previous studies in which WT AB larvae were inoculated with HSV-I and CHIKV (72 hpf), *ifnphi1* upregulation peaked at 36 hpi [77] and 24hpi [23], respectively, with further differences in sustained upregulation after these timepoints. Furthermore, the expression of *infphi1* and *ifnphi3* may be model-specific. For example, Tübingen strain zebrafish larvae inoculated with Tilapia Lake Virus (TiLV) (48–60 hpf) were only observed to exhibit significant *ifnphi1* upregulation but not insignificant *infphi3* upregulation by 48 hpi [81]. It remains unclear if only one or both IFN genes are responsible for this ISG induction (Table S4) in our infection model, and this will be the subject of future studies, involving sampling at earlier timepoints.

We also conducted further characterisation of the main types of genes that were differentially expressed in response to CyHV-3 infection in zebrafish larvae. Using STRING, we generated a network (Figure 9) representing the functional relationships between the top 250 most significant DEGs at 2 dpi (Table S4). As expected, functional enrichment analysis of this network revealed that these DEGs were mainly associated with the immune and stress responses (Table S6). Three main clusters formed within this network. The largest cluster (Figure 9a) mainly represented genes involved in viral infection and cytokine responses. These include genes encoding the antiviral GTPase proteins such as *mxa*, *mxb*, *mxc*, and

mxe, as well as *rsad2* (or *vig-1*, *viperin*). This is consistent with previous observations in zebrafish larvae infected with NNV [78], Zebrafish Picornavirus (Zfpv) [19], and CyHV-3-infected adult zebrafish [38]. In terms of the cytokine response, genes encoding IFN regulatory factors *irf7* and *irf9* were also part of this main cluster. Notably, zebrafish *irf3* was also among the top 250 most significant DEGs (Table S4), however as STRING returned no results for this gene, it was not included in the network in Figure 9. In addition, genes encoding other important elements of the IFN response, *stat1a*, *stat1b*, *stat2*, and augmentation and regulation of this response such as *isg15* [30] were also featured in this cluster, consistent with zebrafish larvae responses to HHV-1 [77] and NNV [78].

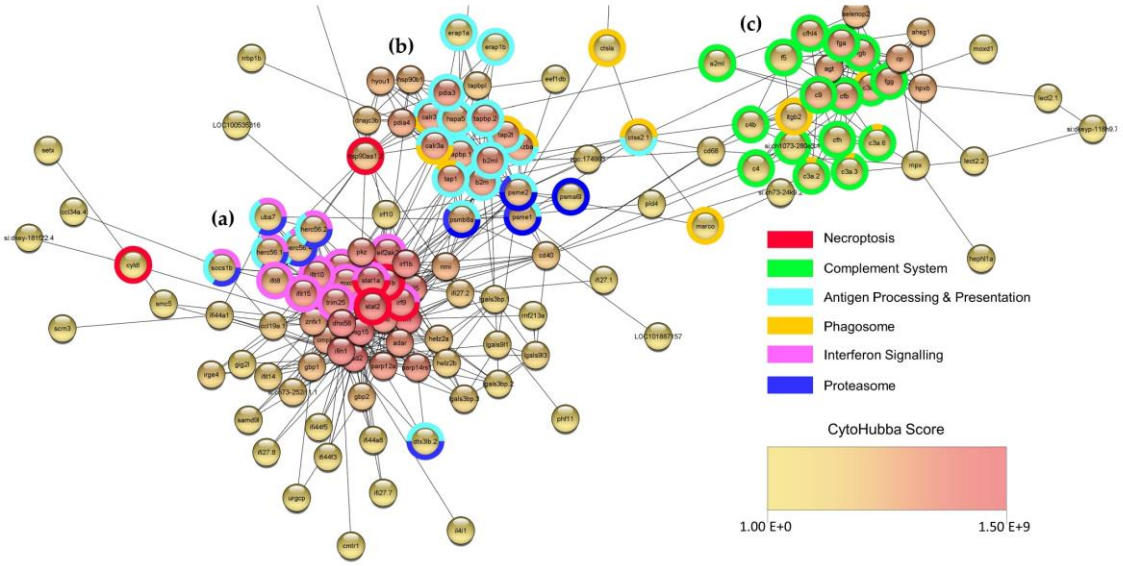

Figure 9. Network representing the functional associations between some of the top 250 most significant DEGs at 2 dpi. Using STRING protein query function in Cytoscape, 208 of the top 250 most significant DEGs were identified and scored based on functional association with each other. These data were used to generate a network in Cytoscape, which was then arranged based on GeneMania force directed layout. Each DEG is represented by a node, with edges (connecting lines) representing functional association. The largest contiguous network resulting from this analysis (136 nodes and 696 edges) is displayed. For visualization purposes, nodes in the peripheral regions of the network (representing DEGs *LOC100006895*, *rnasel3*, *ndrg1b*, *pde6ha*, and *serpinb1l1*) were omitted. This resulted in one large cluster (**a**), and two smaller clusters (**b**) and (**c**). STRING functional enrichment analysis indicated that most DEGs in this network were related to the immune response to infection (Table S6), and genes were labelled based on the main types of gene-set categories enriched in each of their respective clusters. This revealed distinct functions associated with each gene cluster, for example (**a**) interferon and PRR signalling, (**b**) antigen processing and presentation, and (**c**) complement response. The network was also analysed by CytoHubba, which was used to identify the potentially most important hub nodes within the network, with each node scored and coloured based on maximal clique centrality within the network, according to the CytoHubba score colour scale provided; however, this is better represented in Figure S5, with corresponding CytoHubba scores in Table S7.

The detection of "non-self" material in cells via PRRs is an important part of the innate immune response. Viral nucleic acids represent major PAMPs during infections, and genes encoding PRRs to detect these PAMPs were among the most significant DEGs in our experimental model. For example, genes encoding important zebrafish RIG-I-like receptor (RLR) orthologs, such as *ifih1* (encoding *MDA-5* ortholog) [82], and *dhx58* (encoding *LGP2*

ortholog) [83] were centrally located within this large cluster (Figure 9a). An additional gene, *rigi*, encoding the zebrafish ortholog of RIG-I, the most-studied RLR [84], was also significantly upregulated in response to infection, but not among the top 250 most significant DEGs used to generate this network (274th most significant DEG, Table S5). Genes encoding other important components of the RLR viral RNA sensing apparatus such as *trim25* [85,86] were also centrally located in this large cluster (Figure 9a). In addition to RLRs, other genes encoding RNA binding proteins are important actors in the innate immune response such as *adar* [87], *eif2ak2* (encoding PKR ortholog) [88], *pkz* [88–91], and *ifit10* (human *IFIT5* ortholog) [92–94] also co-locate within the same large cluster. Interestingly, we noted that two additional genes, *helz2*a and *helz2*b, encoding proteins that may act as evolutionarily conserved RNA sensors [95], can be observed at the peripheral regions of this main cluster. Many known vertebrate dsDNA sensing PRRs are absent in teleost fish [95,96]. Of the few known genes encoding dsDNA sensing PRRs in zebrafish, which include *ddx41* [77,97], *cgasa* [98], *dhx9* [77], and *dhx36* (the latter of which, may act as a conserved RNA and DNA PRR [99]), only *cgasa* was significantly upregulated, but not featured in the top 250 DEGs (623rd most significant DEG, Table S5). This may indicate that RNA sensing as opposed to DNA sensing PRRs represent an important part of the response to CyHV-3 infection in zebrafish larvae, even though it is a dsDNA virus. This is consistent with growing evidence for the role of RLRs in the detection of dsDNA viruses, such as members of the family *Herpesviridae* or *Adenoviridae* [100–104].

Within the largest cluster, in addition to genes being generally involved in antiviral responses, functional enrichment analysis identified a subset of clusters representing genes belonging to IFN signalling and necroptosis gene-sets (Figure 9a). The same functional enrichment analysis indicated that genes in the smaller central cluster were mainly involved in antigen processing and phagosome responses (Figure 9b), with genes in the smaller cluster on the right mainly related to the complement system (Figure 9c). Furthermore, the identification of the potentially most important hub nodes within the network in Figure 9 (based on maximal clique centrality) revealed that nodes representing RNA PRRs *ifih1* (MDA5 ortholog) and *dhx58* (LGP2 ortholog) were ranked highest, along with *rsad2* (or *vig-1*, *viperin* ortholog), *stat1a*, *irf7*, *isg15* and *stat1b* (Figure S5 and Table S7). Notably, all the top ten ranked hub nodes (twenty in total) represent genes located in the largest cluster (Figure 9a), most of which are described above.

Interestingly, in addition to many commonly studied ISGs, we also observed upregulation of genes encoding NACHT-domain and leucine-rich-repeat-containing (NLR) proteins, for example, *loc100535428* (Table S4). These represent a protein-class that is now increasingly recognised as representing important elements of the innate immune response in teleost fish [19,105]. We also note the upregulation of many genes encoding uncharacterized products in response to CyHV-3 infection, some of which were >1000–5000-fold upregulated (Table S4). Focusing on those within the top 250 significant DEGs that were >100 fold upregulated, we noted that four of these were not previously described as being upregulated in response to infection or immune stimulation (Table S4). We also noted the upregulation of five non-coding RNA genes in response to CyHV-3 infection, one of which was >3000 fold upregulated (Table S4), representing the 6th most upregulated gene in the dataset. All other uncharacterized genes occurring within the group of top 250 most significant DEGs were further cross-referenced with existing GenBank entry information on predicted protein domains (Table S4). This revealed that three of these genes potentially encode additional NLR proteins, three encode RNA binding domains, and three encode proteins containing retrotransposon derived reverse transcriptase-like (RT-like) domains (Table S4). In the case of the latter, the three genes encoding RT-like domains are all paralogs of each other (KEGG Database) and similarly upregulated (>29–35-fold, Table S4). Further inspection of corresponding entries for these gene products in UniProt and InterPro revealed predicted retrotransposon gag, aspartic proteinase, RT, RNase H, and integrase domains, indicating they may indeed encode retrotransposon polyproteins. The domain organization and motifs are consistent with retrotransposons within the family

Belpaoviridae [106] (also referred to as Bel/Pao, Class I retrotransposons based on previous classification systems [107]). It should be noted that the upregulation of retrotransposons and other transposable elements in response to infection has been observed in other organisms [108–110], and to the best of our knowledge this is the first description of this in a zebrafish model. Interestingly, upregulation of class I retrotransposons in zebrafish has also been observed in response to genome demethylation, leading to the induction of antiviral responses [111].

In further analysis, we expanded our investigation to all genes included in differential expression analysis at 2 dpi (Table S5), exploring the response to infection at a "gene-set level". Using GSEA, we identified GO and KEGG pathway gene-sets that were to a significant extent positively or negatively enriched in CyHV-3-infected larvae at 2 dpi (Tables S8 and S9, Figure S6). Cytoscape was used to generate a network of these significantly enriched gene-sets based on the functional relationships between them (Figure 10), providing a greater insight into what biological processes are implicated in the response to CyHV-3 infection in zebrafish larvae, and how they are related. Notably, only one gene-set, "Ribosome" (DRE03010), was found to be significantly negatively enriched, with all other significant gene-set responses involving positive enrichment. During the process of generating the network presented in Figure 10, nodes (i.e., gene-sets) were clustered together based on their similarity coefficient (related to gene-set/functional overlap). This process resulted in the formation of several large clusters, which we numbered. Cluster-1 is the largest of these and exhibits the highest quantity of functional connections with surrounding clusters, and as such, it represents a major aspect of the response to CyHV-3 infection. Within Cluster-1, there are two main sub-clusters. One of these is dominated by gene-sets related to programmed cell death, the other is dominated by PRR signalling, pathogen and inflammatory response gene-sets. Notably, enrichment of the RIG-I-like signalling pathway, the Toll-like receptor signalling pathway, and the Herpes simplex virus 1 gene-sets are consistent with zebrafish larvae response to NNV infection [78]. In Cluster-1, the KEGG Necroptosis pathway (DRE04217) is the most significant positively enriched gene-set, and joint most significantly enriched gene-set overall (Tables S8 and S9). Notably, this pathway gene-set is functionally related to other gene-sets in the apoptosis and PRR/inflammatory/pathogen response sub-clusters (manually isolated from these two sub-clusters in Cluster-1, Figure 10), exhibiting gene overlap with 15/19 of these gene-sets, with eight of these resulting in similarity coefficients >0.02 and thus displayed in Figure 10. This reflects the substantial crosstalk that exists between programmed cell death and PRR signalling in response to infection [67,112].

The prominence of positively enriched necroptosis and apoptosis related gene-sets in Cluster-1 supports the hypotheses derived from earlier observations in vitro and in vivo (Figures 6 and 8 and Video S1), that apoptosis-like and non-apoptosis-like programmed cell death feature heavily in the zebrafish response to CyHV-3 infection. One of the important genes in the necroptosis pathway is *eif2ak2* (or *pkr*). It was identified as one of the main genes contributing to the enrichment signal for the necroptosis gene-set (Figure S7). It represents an important link between the innate immune response and the initiation of necroptosis [113]. This gene encodes a protein referred to as "interferon-induced, double-stranded RNA-activated protein kinase", or more commonly, "Protein Kinase R" (referred to as PKR hereafter). PKR functions as both a general cellular stress sensor and PRR. Thus, it plays a diverse role in the innate immune response to viral infections and many fundamental cellular processes including programmed cell death [114].

PKR-mediated programmed cell death is important for the clearance of viral infections [113,115,116]; however, the antiviral roles of PKR are diverse. It also contributes to the antiviral actions of other enriched gene-sets within Cluster-1 (Figure 10). For example, in the "Herpes simplex virus 1" response gene-set (DRE05168), PKR is activated by dsRNA formed during infection, and subsequently phosphorylates eIF2α (its main substrate), resulting in the stalling of mRNA translation [114,115,117] (Figure 11a). However, some mRNA species are less affected by this [118–120]. This translational stalling also leads

to the formation of stress granules (SGs) [121–123], which in some cases are important for detection of viral RNA via PRRs as in the "RIG-I-like receptor signalling pathway" (DRE04622) [124,125]. Furthermore, PKR also facilitates/promotes the NF-κB pathway, indirectly [114,118]. While this induces a pro-inflammatory response which may be useful in terms of counteracting infection, the accompanying pro-survival response (although helpful to some aspects of immune-response [126]), is counter to the pro-apoptotic function of PKR, but may act to only temporarily delay cell death [127]. Notably, expression from the zebrafish *nfkb1* gene, which encodes the zebrafish NF-κB ortholog, was not significantly upregulated at 2 dpi in our model (Table S5 and Figure 11b).

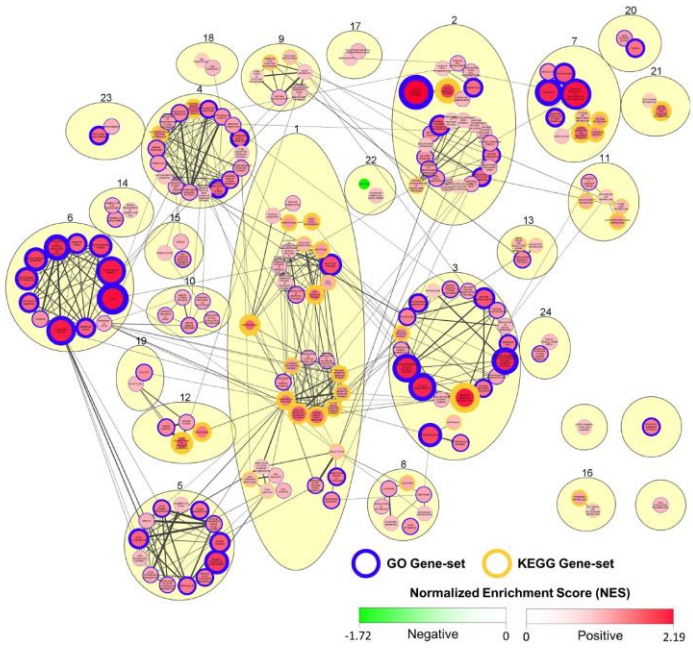

Figure 10. Summary of GSEA output indicating gene-set enrichment based on gene expression in CyHV-3-infected relative to mock-infected zebrafish larvae at 2 dpi. Cytoscape Network representing functional relationships between all significantly enriched gene-sets (positive or negative) identified in GSEA output (FDR adjusted *p*-value < 0.25). Nodes in the network represent GO (blue border) and KEGG Pathway (gold border) gene-sets. Edges (connecting lines) between nodes represent the similarity coefficient (measuring the functional/gene overlap between pairs of gene-sets). Edge thickness corresponds to magnitude of similarity coefficient (only edges with coefficient ≥2 are displayed). Each gene set exhibits either a positive or negative normalized enrichment score (NES), indicating predominant upregulation or downregulation of constituent genes, respectively. Accordingly, node colour and size both represent NES magnitude (exponentially transformed scale), with positive and negative enrichment represented by red and green, respectively, according to the colour scale provided. The node border thickness indicates the significance of enrichment (inverse of FDR adjusted *p*-values, thus the lower the FDR adjusted *p*-value, the greater the thickness). Using the MCL cluster algorithm, GO and KEGG gene-sets were clustered together based on their functional similarity as indicated by similarity coefficients (beige ovals), and numbers were assigned to each cluster. For the purposes of visual clarity, clusters were manually repositioned, and within some clusters, sub-clusters were manually grouped based on functional similarity. Clusters that are overlapping or touching in the absence of any visible edges between their respective nodes have shared edges below the 0.2 coefficient cut-off for display. Clusters that do not exhibit edges between their respective nodes and are also not touching or overlapping either have no common edges or have common edges with similarity coefficient >0.1. Higher quality figures for the whole manuscript are available in the PDF version.

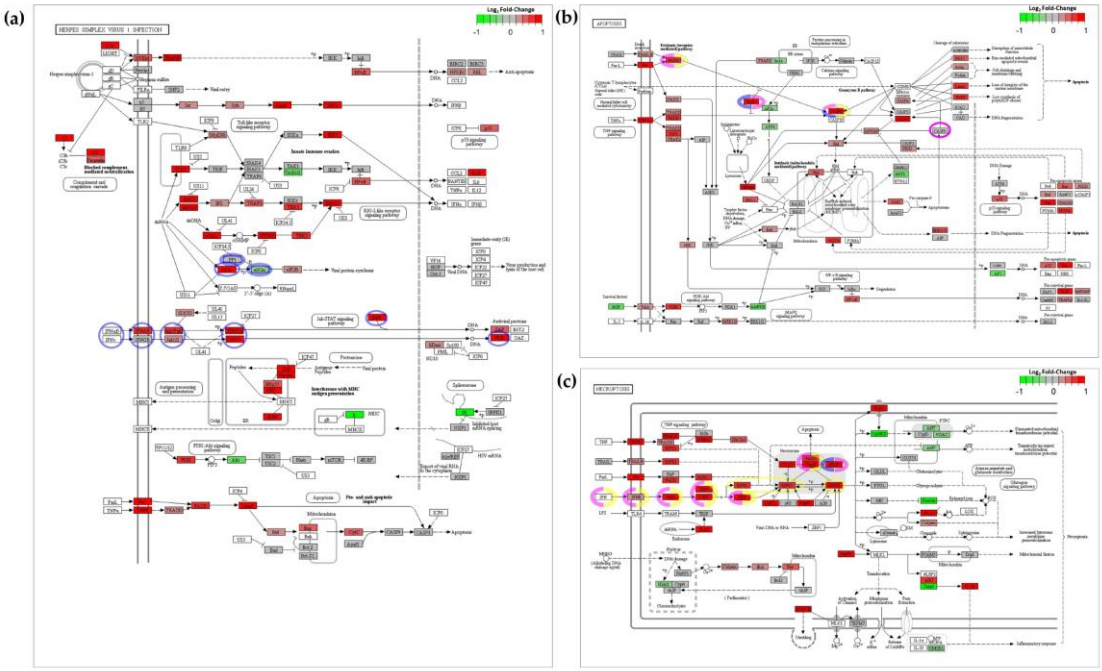

Figure 11. Visualization of differential gene expression in CyHV-3-infected zebrafish larvae (2 dpi) within KEGG pathway maps. Using the R package Pathview, gene expression data from our experiment was mapped to corresponding nodes in KEGG pathways (**a**) Herpes simplex virus 1 infection (**b**) Apoptosis and (**c**) Necroptosis pathways. Nodes represent zebrafish homologs of genes known to be involved in each pathway, with colour representing the $\log_2$-fold-change in gene expression in CyHV-3-infected relative to mock infected zebrafish larvae. Upregulated and downregulated genes are represented by red and green shades respectively, according to scale in the top right of each pathway. For visual clarity (due to large differences in fold change between genes) the maximum and minimum values in the colour scale is set at –1 and 1 $\log_2$-fold-change (corresponding to a two-fold change). It should be noted that many nodes represent combined differential expression from several zebrafish paralogs, thus the generic KEGG gene symbols are used as node names, which relate to the common names used to refer to protein products at each node. Not all the paralogs represented by each node are significantly differentially regulated. The list of zebrafish orthologs/paralogs corresponding to each node in these pathways can be accessed in the KEGG database using the corresponding gene-set references (Herpes simplex virus 1 infection (DRE05168), Apoptosis (DRE04210) and Necroptosis (DRE04217)), which can then be cross-referenced with data in Table S5 (using NCBI/Entrez/GenBank Gene IDs or Gene Symbols). Key genes involved in IFN-stimulated PKR-mediated programmed cell death, i.e., translational inhibition [114,116,128] leading to apoptosis [112] (blue), IFN-stimulated PKR-mediated apoptosis [129,130] (pink), and IFN-stimulated PKR-mediated necroptosis [113] (yellow) are highlighted. Genes with dashed line borders indicate instances where downregulation, translational inhibition or post-translational inactivation of protein products promote the processes in question (see main text and references provided within this caption for details). White nodes represent instances where zebrafish homologs have not been assigned thus far, or where gene expression from zebrafish homologs have not been detected. Higher quality figures for the whole manuscript are available in the PDF version.

PKR-mediated apoptosis can occur via the "extrinsic" FADD-caspase-8 mediated pathway [131]. The circumstances under which this occurs are quite diverse. For example, PKR-mediated translational inhibition leads to apoptosis [115,116] via depletion of cFLIP

protein [112] which acts as an important inhibitor of caspase-8 (Figure 11b) [132,133]. PKR phosphorylation by PACT (in response to stress) can also lead to translational inhibition leading to caspase-8 dependent apoptosis [134], as can overexpression of PKR [135–137]. In addition to IFN stimulation leading to upregulation of PKR, IFN-stimulated PKR-mediated apoptosis can also occur via JAK/TYK-mediated phosphorylation of PKR [129]. Notably, along with *eif2ak2* (encoding PKR), many other zebrafish genes encoding orthologs of ISGs involved in IFN-stimulated PKR-dependent apoptosis are also upregulated at 2 dpi in our model (Figure 11b,c). In parallel, PKR may also promote caspase-9 mediated apoptosis via the "intrinsic" apoptosis pathway. However, unlike caspase-8, caspase-9 was not upregulated at 2 dpi in our experiment (Figure 11b), indicating, as with other viral-host models [118,130,131], that caspase-8 mediated apoptosis also plays a more dominant role in response to infection in the CyHV-3-zebrafish larvae model.

Many viruses have evolved ways to interfere with apoptosis by disrupting elements of the FADD-caspase-8 pathway [72,114,138,139]. To counteract this, necroptosis may have evolved as a back-up mechanism of programmed cell death [72], which can occur via compromising of the cell membrane though action of MLKL [140] and/or production of reactive oxygen species [141]. This relies on the interaction of RIPK1 and RIPK3 for necrosome formation, a process that is inhibited by the FADD-caspase-8 complex [72,141,142]. Like apoptosis, PKR-mediated necroptosis can occur in response to IFNs, possibly requiring PKR interaction with RIPK1 [113]. While other groups have also observed a physical association between PKR and RIPK1 [143], the exact role that PKR plays in initiating necroptosis in response to IFN stimulation remains unclear [144]. Notably it has been proposed that IFN-stimulated PKR-mediated necroptosis is restricted to the G2M stage of the cell cycle, when FADD is disabled, preventing capase-8 inhibition of necrosome formation [113]. Given that in zebrafish larvae, and to lesser extent, in ZF4 monolayers, we expect widespread, frequent occurrence of mitosis, our models may be particularly predisposed to this type of PKR-mediated necroptosis. Notably, in addition to PKR itself, genes encoding zebrafish orthologs of ISGs involved in PKR-mediated necroptosis are also upregulated at 2 dpi (Figure 11c).

The *eif2ak2* gene encoding PKR was also among the top 250 most significant DEGs in this study (Table S4) and identified as an important hub gene in functional network in Figure 9, being ranked 3rd overall (Table S7). Given the importance of this ISG in terms of antiviral defence [112,115,145], particularly regarding programmed cell death, we hypothesized that the knock-out (KO) of the *eif2ak2* gene may impact CyHV-3 clearance in zebrafish larvae.

Unlike other vertebrates, members of the teleost fish families *Salmonidae* and *Cyprinidae* also encode an additional PKR-like protein referred to as "protein kinase containing Z-DNA binding domains" (or PKZ) [88,89,91]. PKZ genes may have evolved through duplication of the PKR encoding genes in these teleost fish families, after divergence from tetrapods [88]. Consequently, PKZ exhibits a high degree of sequence similarity to PKR proteins encoded in the same genomes, predominantly to the C-terminal kinase domain, which is responsible for eIF2α phosphorylation by PKR [89,146].

However, unlike PKR, PKZ contains Zalpha (Zα) domains instead of dsRNA binding domains in the N-terminal [146] (Figure 1). These domains are capable of binding to Z-DNA/RNA, which exist in the left-handed double helix conformation as opposed to the more common right-handed conformation of dsDNA/RNA (referred to as A and B-DNA/RNA) [90].These two features indicate that: (1) Like PKR, PKZ acts as an eIF2α kinase and mediates translational stalling, and induction of apoptosis via eIF2α phosphorylation [88,89,147,148], and (2) Like PKR, PKZ acts as a cytosolic PRR, but is activated by a greater diversity of nucleic acids than PKR. PKZ nucleic acid binding, B-to-Z conversion, and PKZ-mediated translational stalling have been best demonstrated using B and Z-DNA [89,149–152], indicating co-operative antiviral roles for PKZ and PKR. However, given that the Zα domains of PKZ do bind to RNA analogues [153] and that some Zα domains exhibit A-to-Z RNA conversion (as we recently demonstrated [90]), like PKR, PKZ may also detect and be activated by dsRNA. Thus, PKZ may provide at least some

degree of back-up for PKR, leading to some redundancy among zebrafish IFN induced eIF2α kinases.

Notably, the *pkz* gene (encoding PKZ) was the 23rd most significantly upregulated gene at 2 dpi in our model, upregulated more than the *eif2ak2* gene (encoding PKR, ranked 250th, Table S4), and the *pkz* expression levels were >3 fold higher. In addition, *pkz* was ranked 9th in hub gene analysis in Figure 9 (see also Table S7). Given their potentially overlapping functions, in addition to the PKR-KO mutant (lacking *eif2ak2*), we generated a separate mutant, PKZ-KO (lacking *pkz*, Figure 1), to investigate the importance of both these multifunctional eIF2α kinases in the clearance of CyHV-3 in zebrafish larvae.

3.5. The Absence of PKR and/or PKZ Does Not Impair the Clearance of CyHV-3 Infections in Zebrafish Larvae

In vitro and in vivo experiments performed in this study indicated that CyHV-3 infection was rapidly cleared in zebrafish models via programmed cell death. This was supported by the transcriptomic analysis from infected larvae, which also supported a potentially important role for the eIF2α kinases PKR and PKZ in this process. Based on this evidence, we tested the impact of these eIF2α kinases on CyHV-3 clearance using CRISPR/Cas9 generated PKR-KO and PKZ-KO zebrafish mutants (Figure 1). Mutant and WT zebrafish larvae were first infected with CyHV-3 EGFP by microinjection as per earlier experiments. As we hypothesized that the onset of infection clearance may take longer to occur in eIF2α kinase KO mutants, we also extended the monitoring period from 4 dpi (in earlier experiments) to 5 dpi. Epifluorescence microscopy suggested that PKR-KO and PKZ-KO mutants cleared viral infection as efficiently as WT larvae (Figure 12a). There was also no difference between the zebrafish strains in terms of the numbers of infected larvae at each timepoint (Two-way RM ANOVA, p-value = 0.6440), with all groups exhibiting a dramatic decrease in the number of positive fish at 5 dpi (Figure 12b).

Next, WT, PKR-KO, and PKZ-KO zebrafish strains were infected with CyHV-3 Luc as before, allowing viral replication to be compared between strains (Figure 12c). This revealed no significant difference in viral signal between the three zebrafish strains (Durbin Test, p-value = 0.6500). Relative differences in signals between the WT and PKR-KO strains were inconsistent over the monitoring period, with no clear trends to indicate a difference between the two strains. In contrast, virus levels in the PKZ-KO strain were consistently higher than both WT and PKR-KO strains from 1–4 dpi, with significant differences at 3 dpi. However, viral levels in PKZ-KO larvae were significantly lower than other strains by 5 dpi (Figure 12c), indicating greater clearance, despite higher viral levels from 1–4 dpi.

Cognisant of the possible redundancy in eIF2α kinase function (described earlier), which may have allowed PKZ to compensate for the absence of PKR in the PKR-KO mutant, and vice versa, we generated a third mutant, PKR-PKZ-KO, lacking both *pkz* and *eif2ak2* genes (Figure 1). This strain was included in an additional experiment, like the one presented in Figure 12. (Figure S8). However, surprisingly, the viral loads observed in the PKR-PKZ-KO mutants were not significantly different from the WT strain. Taken together, the results from these two experiments indicate that (1) PKR and PKZ are not essential for clearance of CyHV-3 infection in zebrafish larvae, and (2) even at this early developmental stage, the zebrafish immune system exhibits sufficient redundancy to enable clearance of CyHV-3 infection in the absence of PKZ and/or PKR.

If programmed cell death also features heavily in the response to CyHV-3 infection in these mutant zebrafish strains, as earlier observations in the WT strain suggested (Figures 8, 11 and Video S1), these processes would need to be mediated via other mechanisms. Notably, in addition to IFN-stimulated PKR/PKZ-mediated programmed cell death [112,113,129], these processes can be stimulated by other cytokines such as FAS, TNFα, and TRAIL [154–157] (the zebrafish orthologs for these proteins are encoded by the *faslg*, *tnfa*, and *tnfsf10* genes, respectively). Like IFN, these cytokines also operate by binding to their respective cell membrane receptors and downstream interactions between these and various other proteins are required to initiate apoptosis and/or necroptosis. Notably,

genes encoding zebrafish orthologs of most of the proteins involved in these processes are also upregulated in response to infection at 2 dpi (Figure 11), indicating some potential redundancy in terms of the programmed cell death response. However, no expression from the *faslg* and *tnfa* genes was observed in our model. While we did observe expression for *tnfsf10*, it was not upregulated in response to infection. Therefore, similar to what we have hypothesized regarding IFN expression kinetics, it is possible that with this model, the upregulation of these three cytokines is also extremely brief, occurring very early after infection with a rapid return to basal levels after. As with IFN, further investigation will be needed to establish the expression kinetics of these cytokines in response to CyHV-3 infection in this host model, and to what extent, if any, they contribute to programmed cell death and clearance of CyHV-3 infection.

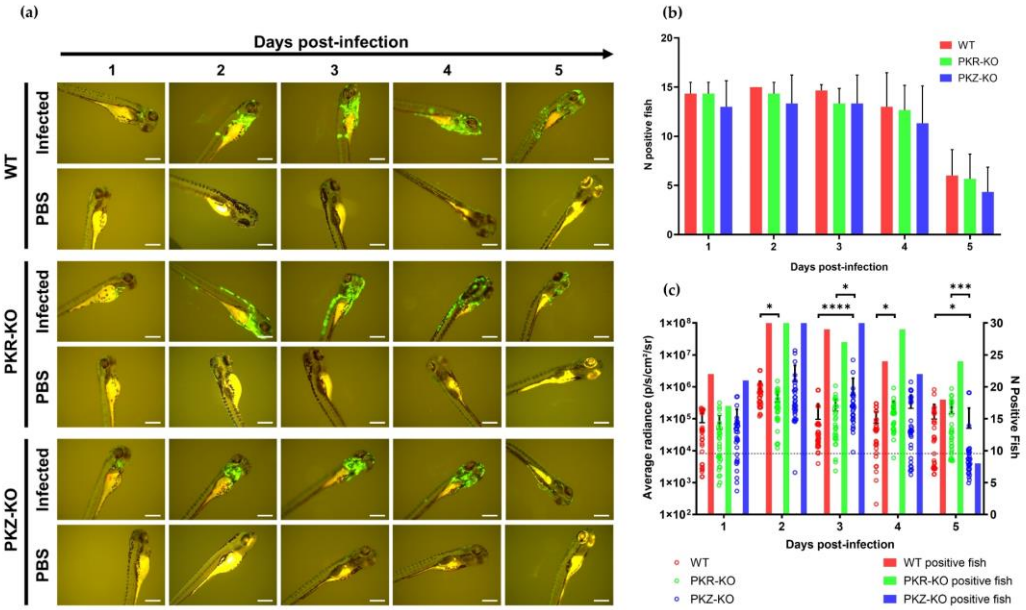

Figure 12. Replication of CyHV-3 in different zebrafish strains. (**a**) Epifluorescence microscopy images representative of larvae inoculated by microinjection with either CyHV-3 EGFP or mock-inoculated with PBS according to time postinfection (longitudinal observation of the same larvae over all timepoints). For all strains infection clearance commenced from 4–5 dpi. Scale bars = 500 µm. (**b**) Numbers of infected larvae among zebrafish strains inoculated with CyHV-3 EGFP (n = 15). Data represents mean ± standard errors from 3 independent experiments (longitudinal observation of the same larvae over all timepoints). (**c**) IVIS analysis measuring Luc2 expression in different zebrafish strains microinjected with CyHV-3 Luc (n = 30). The data points represent the mean radiance per larvae according to time postinfection with mean ± standard error represented for each group at each timepoint. The discontinuous line represents the cut-off for positivity and the mean + 3 × SD of the values obtained for mock-infected larvae. The number of positive larvae at each timepoint is represented by bars. * $p < 0.05$; *** $p < 0.001$; **** $p < 0.0001$.

In both experiments (Figures 12 and S8), the PKZ-KO mutant exhibited a higher viral load than other strains at the earlier stages of infection. The higher levels of CyHV-3 in the absence of PKZ may indicate the importance of host Zα domain-containing PRRs such as PKZ, in restricting CyHV-3 in the early stages of infection. This is consistent with our recent study where we provide strong evidence that the CyHV-3 ORF112 protein, which also contains a Zα domain, acts as an essential antagonist of RNA PRRs during CyHV-3 infection [90]. However, the absence of PKZ still leads to more dramatic viral clearance at 5 dpi relative to PKZ-competent strains (Figure 12c). We hypothesize that higher viral

replication, from 1–4 dpi, may have ultimately led to an increased innate immune response, priming a more dramatic clearance at 5 dpi. Even if the absence of PKZ does not prevent viral clearance, the higher levels of viral replication in earlier stages, may lead to increased tissue damage via potential inflammatory response, which may ultimately be harmful to the host. Therefore, having the complete repertoire of PRRs necessary for effective restriction of CyHV-3 replication prior to clearance may still be important. Surprisingly, we do not observe higher viral loads at earlier stages of infection in the PKR-PKZ-KO mutant (also lacking PKZ), which instead exhibited a similar phenotype to WT and PKR-KO strains in response to CyHV-3 (Figure S8). These observations open up several interesting avenues for further investigation, in particular the characterization of the innate immune response in zebrafish mutants lacking these important PRRs and the possible impact of reduced eIF2α phosphorylation on programmed cell death, if any, in response to CyHV-3 infection in this model.

4. Conclusions

The aim of this present study was to investigate the potential of the zebrafish model to study AngHV-1, CyHV-2, and CyHV-3, which are three economically important viruses in the family *Alloherpesviridae*. We conclude that while the zebrafish ZF4 cell line is moderately susceptible to these three viruses, it is less susceptible and not permissive to AngHV-1 (Figure 2). ZF4 cells do exhibit transient permissiveness to CyHV-2 and CyHV-3 infection. These cells are more permissive to CyHV-3, but both viruses exhibit inefficient cell to cell viral transmission in this in vitro model (Figures 3 and 4). These viruses are ultimately cleared from ZF4 monolayers, in a process which is preceded by what resembles widespread programmed cell death among infected cell populations (Figures 3, 4 and 6). As zebrafish larvae were not susceptible to these viruses via inoculation by immersion, we conclude that these viruses may not be capable of entering zebrafish larvae through natural routes in vivo (Figure 7). However, zebrafish larvae are susceptible to infections with CyHV-2 and CyHV-3 via microinjection, an artificial inoculation route (Figure 7). Conversely, we conclude that zebrafish larvae are not susceptible to AngHV-1 via both inoculation methods used in this study (Figure 7). This lower susceptibility to AngHV-1 in vitro and in vivo, may reflect the fact that, unlike CyHV-2 and CyHV-3, AngHV-1 does not naturally infect host species from the family *Cyprinidae*. Even though larvae exhibit greater susceptibility to CyHV-2 and CyHV-3, we conclude that these infections are rapidly cleared (Figures 7 and 12). We also conclude that zebrafish larvae exhibit more susceptibility (and possibly more permissivity) to CyHV-3, given higher viral levels and slower clearance, indicating the superior utility of this virus-host model in future studies. Interestingly, given that strains within each cyprinivirus species clad exhibit natural heterogeneity regarding replication in vitro and/or in vivo (at least with AngHV-1 and CyHV-3 [40,74]), it remains possible that the use of alternative cyprinivirus strains with the same zebrafish models may result in different outcomes, and is something which remains to be explored in the future.

As we observed transcription of all 155 known CyHV-3 protein coding genes in infected zebrafish larvae (Figure S3, Table S3), we conclude that zebrafish cells may be permissive to CyHV-3 replication in vivo. However, unlike infections in vitro, we observed no clear evidence of CyHV-3 transmission to new cells prior to clearance in vivo (Figure 8, Video S1). Thus, the extent to which this permissiveness leads to successful CyHV-3 transmission between cells in vivo remains unclear.

As per observations in vitro, CyHV-3 clearance in zebrafish larvae is also preceded by apoptosis-like death among infected cells (Figure 8, Video S1). These infections stimulate the upregulation of many ISGs (Figure 9, Tables S4 and S5). The upregulation of genes involved in programmed cell death and nucleic acid sensing PRR pathways represent a core part of this response (Figures 10 and 11). PKR and PKZ are also upregulated in response to infection (Figure 9, Table S4) and may contribute to both programmed cell death and nucleic acid sensing PRR pathways (Figures 10 and 11). However, their absence in mutant zebrafish strains does not impact CyHV-3 clearance (Figure 12). This may be due

to sufficient levels of redundancy within the zebrafish innate immune response processes, even at this early developmental stage (Figure 11). Interestingly, CyHV-3 may represent an ideal model to utilize in the study of viral clearance by the innate immune system in this important and widely studied host. This opens many interesting avenues for future investigation to determine what elements of the immune response are essential for this process. As part of this, the generation of new KO mutants, guided by the transcriptomic data generated in this study, may lead to the development of zebrafish strains that are more permissive to these economically important viruses, which may themselves be utilized as valuable research tools in the future.

This is the first report of the generation and use of PKR and/or PKZ KO zebrafish mutants (Figures 1 and 12), and they will represent useful subjects for further characterization and the study of other viruses in zebrafish models. Given the importance of PKR, and potentially PKZ, in the innate immune responses and in many more cellular processes, and the widespread use of zebrafish as a model organism, the KO mutants generated in this study will be of interest to many more researchers in the wider field. Thus, sperm corresponding to these mutants will be deposited in the European Zebrafish Resource Centre (EZRC) for ease of distribution elsewhere.

Furthermore, we note that many of the most significantly upregulated genes in response to CyHV-3 infection in zebrafish larvae were uncharacterized, and some were previously unreported as being involved in the immune response (Table S4). These include five non-coding transcripts (one of which was >3000-fold upregulated and the 6th most upregulated gene at 2 dpi). We propose to provisionally refer to these five transcripts as "Zebrafish Non-coding Infection Response Element" 1–5 (or ZNIRE 1–5, complete details in Table S4). This observation was particularly intriguing, and we propose that further research into their importance during the immune response will be necessary. We also observed the upregulation of three retrotransposons (all ~30-fold upregulated, Table S4). It is possible that this retrotransposon re-activation/upregulation in response to infection may be beneficial. Their cytoplasmic RNA and/or DNA genome intermediates may potentially act as ligands for PRRs [111], thus enhancing the innate immune response to viral infection and presenting an interesting hypothesis for further study with our model.

Supplementary Materials: The following supporting information can be downloaded at: https://www.mdpi.com/article/10.3390/v15030768/s1, Figure S1. Production and characterization of the CyHV-3 EGFP recombinant strain as described in Methods S1; Figure S2. Evolution of fluorescence intensity in infected ZF4 cells; Figure S3. Box Plots of read counts mapping to each known CyHV-3 open reading frame (ORF) at 2 dpi; Figure S4. Volcano plots of summarizing DEGs at each timepoint; Figure S5. CytoHubba Analysis of STRING protein query network; Figure S6. Summary of the top 40 positively enriched GO gene-sets; Figure S7. Leading edge analysis of the necroptosis pathway; Figure S8. Comparison of CyHV-3 replication and clearance between PKR-PKZ-KO and other zebrafish strains; Table S1. Primers used in this study; Table S2. Summary of DEGs from each timepoint; Table S3. Read Counts mapping to each known CyHV-3 Open Reading frame (ORF) at 2 dpi; Table S4. Top 250 significant DEGs in zebrafish larvae infected with CyHV-3 at 2 dpi; Table S5. Raw output of DESeq2 in zebrafish larvae infected with CyHV-3 at 2 dpi; Table S6. Summary of STRING enrichment analysis; Table S7. STRING CytoHubba Ranking; Table S8. Summary of Gene Ontology (GO) enrichment analysis; Table S9. Summary of Kyoto Encyclopaedia of Genes and Genomes (KEGG) pathway gene set enrichment analysis; Video S1; Methods S1. Production of CyHV-3 ORF136 EGFP recombinant strain [158–164], and Methods S2. Bioinformatic analysis [165–185].

Author Contributions: Conceptualization, I.M. and A.V.; Data curation, C.S., N.M.S., A.J.D. and O.D.; Formal analysis, L.M., A.J.D. and O.D.; Funding acquisition, I.M., S.B., A.J.D., O.D. and A.V.; Investigation, C.S., L.M., O.D. and A.V.; Methodology, C.S., B.H., L.M., H.Z., N.D., M.F., I.M., N.M.S., O.D. and A.V.; Project administration, S.B. and A.V.; Supervision, I.M., S.B., O.D. and A.V.; Validation, C.S., O.D. and A.V.; Visualization, C.S., O.D. and A.V.; Writing—original draft, C.S., O.D. and A.V.; Writing—review & editing, C.S., O.D. and A.V. All authors have read and agreed to the published version of the manuscript.

Funding: O.D. is a Marie Curie research fellow of the European Union, H.Z. and B.H. are research fellows of the Chinese Scholarship Council. This work was supported by the University of Liège (ARC15/19−12), the FNRS (CDR J.0094.15 and PDR T.0241.19), the European Maritime and Fisheries Fund, (Eel4ever project), the Welbio (WELBIO-CR-2022 A-14 12), Walloon Region (ERANets NucNanoFish 2010052) and The Medical Research Council (MC_UU_12014/3).

Institutional Review Board Statement: Not applicable.

Informed Consent Statement: Not applicable.

Data Availability Statement: All RNA-Seq data generated in this study is publicly available on https://www.ncbi.nlm.nih.gov/under BioProject Accession number PRJNA929940 (accessed on 13 March 2023).

Acknowledgments: The authors are grateful to Lorène Dams of the Faculty of Veterinary Medicine, David Colignon of the Consortium des Équipements de Calcul Intensif (CECI), and Jordane Bourdouxhe and Marie Dupont of the GIGA Zebrafish Facility, University of Liège, for their excellent technical assistance.

Conflicts of Interest: The authors declare no conflict of interest.

References

1. Levraud, J.-P.; Palha, N.; Langevin, C.; Boudinot, P. Through the Looking Glass: Witnessing Host-Virus Interplay in Zebrafish. *Trends Microbiol.* **2014**, *22*, 490–497. [CrossRef] [PubMed]
2. Howe, K.; Clark, M.D.; Torroja, C.F.; Torrance, J.; Berthelot, C.; Muffato, M.; Collins, J.E.; Humphray, S.; McLaren, K.; Matthews, L.; et al. The Zebrafish Reference Genome Sequence and Its Relationship to the Human Genome. *Nature* **2013**, *496*, 498–503. [CrossRef]
3. Kettleborough, R.N.W.; Busch-Nentwich, E.M.; Harvey, S.A.; Dooley, C.M.; de Bruijn, E.; van Eeden, F.; Sealy, I.; White, R.J.; Herd, C.; Nijman, I.J.; et al. A Systematic Genome-Wide Analysis of Zebrafish Protein-Coding Gene Function. *Nature* **2013**, *496*, 494–497. [CrossRef] [PubMed]
4. Traver, D.; Herbomel, P.; Patton, E.E.; Murphey, R.D.; Yoder, J.A.; Litman, G.W.; Catic, A.; Amemiya, C.T.; Zon, L.I.; Trede, N.S. The Zebrafish as a Model Organism to Study Development of the Immune System. *Adv. Immunol.* **2003**, *81*, 253–330. [PubMed]
5. Trede, N.S.; Langenau, D.M.; Traver, D.; Look, A.T.; Zon, L.I. The Use of Zebrafish to Understand Immunity. *Immunity* **2004**, *20*, 367–379. [CrossRef]
6. Meeker, N.D.; Trede, N.S. Immunology and Zebrafish: Spawning New Models of Human Disease. *Dev. Comp. Immunol.* **2008**, *32*, 745–757. [CrossRef]
7. Balla, K.M.; Lugo-Villarino, G.; Spitsbergen, J.M.; Stachura, D.L.; Hu, Y.; Bañuelos, K.; Romo-Fewell, O.; Aroian, R.V.; Traver, D. Eosinophils in the Zebrafish: Prospective Isolation, Characterization, and Eosinophilia Induction by Helminth Determinants. *Blood* **2010**, *116*, 3944–3954. [CrossRef]
8. Lugo-Villarino, G.; Balla, K.M.; Stachura, D.L.; Bañuelos, K.; Werneck, M.B.F.; Traver, D. Identification of Dendritic Antigen-Presenting Cells in the Zebrafish. *Proc. Natl. Acad. Sci. USA* **2010**, *107*, 15850–15855. [CrossRef]
9. Li, Y.; Li, Y.; Cao, X.; Jin, X.; Jin, T. Pattern Recognition Receptors in Zebrafish Provide Functional and Evolutionary Insight into Innate Immune Signaling Pathways. *Cell. Mol. Immunol.* **2017**, *14*, 80–89. [CrossRef]
10. van der Vaart, M.; Spaink, H.P.; Meijer, A.H. Pathogen Recognition and Activation of the Innate Immune Response in Zebrafish. *Adv. Hematol.* **2012**, *2012*, 159807. [CrossRef]
11. Herbomel, P.; Thisse, B.; Thisse, C. Ontogeny and Behaviour of Early Macrophages in the Zebrafish Embryo. *Development* **1999**, *126*, 3735–3745. [CrossRef]
12. Lam, S.H.; Chua, H.L.; Gong, Z.; Lam, T.J.; Sin, Y.M. Development and Maturation of the Immune System in Zebrafish, Danio Rerio: A Gene Expression Profiling, in Situ Hybridization and Immunological Study. *Dev. Comp. Immunol.* **2004**, *28*, 9–28. [CrossRef] [PubMed]
13. Lieschke, G.J.; Oates, A.C.; Crowhurst, M.O.; Ward, A.C.; Layton, J.E. Morphologic and Functional Characterization of Granulocytes and Macrophages in Embryonic and Adult Zebrafish. *Blood* **2001**, *98*, 3087–3096. [CrossRef] [PubMed]
14. Le Guyader, D.; Redd, M.J.; Colucci-Guyon, E.; Murayama, E.; Kissa, K.; Briolat, V.; Mordelet, E.; Zapata, A.; Shinomiya, H.; Herbomel, P. Origins and Unconventional Behavior of Neutrophils in Developing Zebrafish. *Blood* **2008**, *111*, 132–141. [CrossRef] [PubMed]
15. Stein, C.; Caccamo, M.; Laird, G.; Leptin, M. Conservation and Divergence of Gene Families Encoding Components of Innate Immune Response Systems in Zebrafish. *Genome Biol.* **2007**, *8*, R251. [CrossRef]
16. Aggad, D.; Mazel, M.; Boudinot, P.; Mogensen, K.E.; Hamming, O.J.; Hartmann, R.; Kotenko, S.; Herbomel, P.; Lutfalla, G.; Levraud, J.-P. The Two Groups of Zebrafish Virus-Induced Interferons Signal via Distinct Receptors with Specific and Shared Chains. *J. Immunol.* **2009**, *183*, 3924–3931. [CrossRef]

17. Levraud, J.-P.; Boudinot, P.; Colin, I.; Benmansour, A.; Peyrieras, N.; Herbomel, P.; Lutfalla, G. Identification of the Zebrafish IFN Receptor: Implications for the Origin of the Vertebrate IFN System. *J. Immunol.* **2007**, *178*, 4385–4394. [CrossRef]
18. Aggad, D.; Stein, C.; Sieger, D.; Mazel, M.; Boudinot, P.; Herbomel, P.; Levraud, J.-P.; Lutfalla, G.; Leptin, M. In Vivo Analysis of Ifn-Γ1 and Ifn-Γ2 Signaling in Zebrafish. *J. Immunol.* **2010**, *185*, 6774–6782. [CrossRef]
19. Balla, K.M.; Rice, M.C.; Gagnon, J.A.; Elde, N.C. Linking Virus Discovery to Immune Responses Visualized during Zebrafish Infections. *Curr. Biol.* **2020**, *30*, 2092–2103.e5. [CrossRef]
20. Binesh, C. Mortality Due to Viral Nervous Necrosis in Zebrafish Danio Rerio and Goldfish Carassius Auratus. *Dis. Aquat. Organ.* **2013**, *104*, 257–260. [CrossRef]
21. Bermúdez, R.; Losada, A.P.; de Azevedo, A.M.; Guerra-Varela, J.; Pérez-Fernández, D.; Sánchez, L.; Padrós, F.; Nowak, B.; Quiroga, M.I. First Description of a Natural Infection with Spleen and Kidney Necrosis Virus in Zebrafish. *J. Fish. Dis.* **2018**, *41*, 1283–1294. [CrossRef]
22. Shen, C.-H.; Steiner, L.A. Genome Structure and Thymic Expression of an Endogenous Retrovirus in Zebrafish. *J. Virol.* **2004**, *78*, 899–911. [CrossRef] [PubMed]
23. Palha, N.; Guivel-Benhassine, F.; Briolat, V.; Lutfalla, G.; Sourisseau, M.; Ellett, F.; Wang, C.-H.; Lieschke, G.J.; Herbomel, P.; Schwartz, O.; et al. Real-Time Whole-Body Visualization of Chikungunya Virus Infection and Host Interferon Response in Zebrafish. *PLoS Pathog.* **2013**, *9*, e1003619. [CrossRef] [PubMed]
24. Burgos, J.S.; Ripoll-Gomez, J.; Alfaro, J.M.; Sastre, I.; Valdivieso, F. Zebrafish as a New Model for Herpes Simplex Virus Type 1 Infection. *Zebrafish* **2008**, *5*, 323–333. [CrossRef]
25. Gabor, K.A.; Goody, M.F.; Mowel, W.K.; Breitbach, M.E.; Gratacap, R.L.; Witten, P.E.; Kim, C.H. Influenza A Virus Infection in Zebrafish Recapitulates Mammalian Infection and Sensitivity to Anti-Influenza Drug Treatment. *Dis. Model. Mech.* **2014**, *7*, 1227–1237. [CrossRef]
26. Van Dycke, J.; Ny, A.; Conceição-Neto, N.; Maes, J.; Hosmillo, M.; Cuvry, A.; Goodfellow, I.; Nogueira, T.C.; Verbeken, E.; Matthijnssens, J.; et al. A Robust Human Norovirus Replication Model in Zebrafish Larvae. *PLoS Pathog.* **2019**, *15*, e1008009. [CrossRef] [PubMed]
27. Laghi, V.; Rezelj, V.; Boucontet, L.; Frétaud, M.; Da Costa, B.; Boudinot, P.; Salinas, I.; Lutfalla, G.; Vignuzzi, M.; Levraud, J.-P. Exploring Zebrafish Larvae as a COVID-19 Model: Probable Abortive SARS-CoV-2 Replication in the Swim Bladder. *Front. Cell. Infect. Microbiol.* **2022**, *12*, 790851. [CrossRef] [PubMed]
28. Tyrkalska, S.D.; Candel, S.; Pedoto, A.; García-Moreno, D.; Alcaraz-Pérez, F.; Sánchez-Ferrer, Á.; Cayuela, M.L.; Mulero, V. Zebrafish Models of COVID-19. *FEMS Microbiol. Rev.* **2022**, *47*, fuac042. [CrossRef] [PubMed]
29. LaPatra, S.E.; Barone, L.; Jones, G.R.; Zon, L.I. Effects of Infectious Hematopoietic Necrosis Virus and Infectious Pancreatic Necrosis Virus Infection on Hematopoietic Precursors of the Zebrafish. *Blood Cells. Mol. Dis.* **2000**, *26*, 445–452. [CrossRef]
30. Langevin, C.; van der Aa, L.M.; Houel, A.; Torhy, C.; Briolat, V.; Lunazzi, A.; Harmache, A.; Bremont, M.; Levraud, J.-P.; Boudinot, P. Zebrafish ISG15 Exerts a Strong Antiviral Activity against RNA and DNA Viruses and Regulates the Interferon Response. *J. Virol.* **2013**, *87*, 10025–10036. [CrossRef]
31. Martín, V.; Mavian, C.; López Bueno, A.; de Molina, A.; Díaz, E.; Andrés, G.; Alcami, A.; Alejo, A. Establishment of a Zebrafish Infection Model for the Study of Wild-Type and Recombinant European Sheatfish Virus. *J. Virol.* **2015**, *89*, 10702–10706. [CrossRef] [PubMed]
32. Rakus, K.; Mojzesz, M.; Widziolek, M.; Pooranachandran, N.; Teitge, F.; Surachetpong, W.; Chadzinska, M.; Steinhagen, D.; Adamek, M. Antiviral Response of Adult Zebrafish (Danio Rerio) during Tilapia Lake Virus (TiLV) Infection. *Fish. Shellfish. Immunol.* **2020**, *101*, 1–8. [CrossRef] [PubMed]
33. Novoa, B.; Romero, A.; Mulero, V.; Rodríguez, I.; Fernández, I.; Figueras, A. Zebrafish (Danio Rerio) as a Model for the Study of Vaccination against Viral Haemorrhagic Septicemia Virus (VHSV). *Vaccine* **2006**, *24*, 5806–5816. [CrossRef]
34. Phelan, P.E.; Pressley, M.E.; Witten, P.E.; Mellon, M.T.; Blake, S.; Kim, C.H. Characterization of Snakehead Rhabdovirus Infection in Zebrafish (Danio Rerio). *J. Virol.* **2005**, *79*, 1842–1852. [CrossRef] [PubMed]
35. Sanders, G.E.; Batts, W.N.; Winton, J.R. Susceptibility of Zebrafish (*Danio rerio*) to a Model Pathogen, Spring Viremia of Carp Virus. *Comp. Med.* **2003**, *53*, 514–521.
36. López-Muñoz, A.; Roca, F.J.; Sepulcre, M.P.; Meseguer, J.; Mulero, V. Zebrafish Larvae Are Unable to Mount a Protective Antiviral Response against Waterborne Infection by Spring Viremia of Carp Virus. *Dev. Comp. Immunol.* **2010**, *34*, 546–552. [CrossRef]
37. Bello-Perez, M.; Pereiro, P.; Coll, J.; Novoa, B.; Perez, L.; Falco, A. Zebrafish C-Reactive Protein Isoforms Inhibit SVCV Replication by Blocking Autophagy through Interactions with Cell Membrane Cholesterol. *Sci. Rep.* **2020**, *10*, 566. [CrossRef]
38. Rakus, K.; Adamek, M.; Mojżesz, M.; Podlasz, P.; Chmielewska-Krzesińska, M.; Duk, K.; Kasica-Jarosz, N.; Kłak, K.; Rakers, S.; Way, K.; et al. Evaluation of Zebrafish (Danio Rerio) as an Animal Model for the Viral Infections of Fish. *J. Fish. Dis.* **2019**, *42*, 923–934. [CrossRef]
39. Boutier, M.; Ronsmans, M.; Rakus, K.; Jazowiecka-Rakus, J.; Vancsok, C.; Morvan, L.; Peñaranda, M.M.D.; Stone, D.M.; Way, K.; van Beurden, S.J.; et al. Cyprinid Herpesvirus 3: An Archetype of Fish Alloherpesviruses. In *Advances in Virus Research*; Elsevier: Amsterdam, The Netherlands, 2015; Volume 93, pp. 161–256; ISBN 978-0-12-802179-8.
40. Donohoe, O.; Zhang, H.; Delrez, N.; Gao, Y.; Suárez, N.M.; Davison, A.J.; Vanderplasschen, A. Genomes of Anguillid Herpesvirus 1 Strains Reveal Evolutionary Disparities and Low Genetic Diversity in the Genus Cyprinivirus. *Microorganisms* **2021**, *9*, 998. [CrossRef]

41. Delrez, N.; Zhang, H.; Lieffrig, F.; Mélard, C.; Farnir, F.; Boutier, M.; Donohoe, O.; Vanderplasschen, A. European Eel Restocking Programs Based on Wild-Caught Glass Eels: Feasibility of Quarantine Stage Compatible with Implementation of Prophylactic Measures Prior to Scheduled Reintroduction to the Wild. *J. Nat. Conserv.* **2021**, *59*, 125933. [CrossRef]
42. Thangaraj, R.S.; Nithianantham, S.R.; Dharmaratnam, A.; Kumar, R.; Pradhan, P.K.; Thangalazhy Gopakumar, S.; Sood, N. Cyprinid Herpesvirus-2 (CyHV-2): A Comprehensive Review. *Rev. Aquac.* **2021**, *13*, 796–821. [CrossRef]
43. Ueno, Y.; Shi, J.-W.; Yoshida, T.; Kitao, T.; Sakai, M.; Chen, S.-N.; Kou, G.H. Biological and Serological Comparisons of Eel Herpesvirus in Formosa (EHVF) and Herpesvirus Anguillae (HVA). *J. Appl. Ichthyol.* **1996**, *12*, 49–51. [CrossRef]
44. Driever, W.; Rangini, Z. Characterization of a Cell Line Derived from Zebrafish (*Brachydanio rerio*) Embryos. *In Vitro Cell. Dev. Biol. Anim.* **1993**, *29A*, 749–754. [CrossRef]
45. Chen, S.; Ueno, Y.; Kou, G. A Cell Line Derived from Japanese Eel (*Anguilla japonica*) Kidney. *Proc. Natl. Sci. Counc. Repub. China B* **1982**, *6*, 93–100.
46. Shibata, T.; Nanjo, A.; Saito, M.; Yoshii, K.; Ito, T.; Nakanishi, T.; Sakamoto, T.; Sano, M. In Vitro Characteristics of Cyprinid Herpesvirus 2: Effect of Kidney Extract Supplementation on Growth. *Dis. Aquat. Organ.* **2015**, *115*, 223–232. [CrossRef]
47. Neukirch, M.; Böttcher, K.; Bunnajirakul, S. Isolation of a Virus from Koi with Altered Gills. *Bull. Eur. Fish. Pathol.* **1999**, *19*, 221–224.
48. van Beurden, S.J.; Leroy, B.; Wattiez, R.; Haenen, O.L.; Boeren, S.; Vervoort, J.J.; Peeters, B.P.; Rottier, P.J.; Engelsma, M.Y.; Vanderplasschen, A.F. Identification and Localization of the Structural Proteins of Anguillid Herpesvirus 1. *Vet. Res.* **2011**, *42*, 105. [CrossRef]
49. Rakus, K.; Ronsmans, M.; Forlenza, M.; Boutier, M.; Piazzon, M.C.; Jazowiecka-Rakus, J.; Gatherer, D.; Athanasiadis, A.; Farnir, F.; Davison, A.J.; et al. Conserved Fever Pathways across Vertebrates: A Herpesvirus Expressed Decoy TNF-α Receptor Delays Behavioral Fever in Fish. *Cell. Host Microbe* **2017**, *21*, 244–253. [CrossRef]
50. Costes, B.; Raj, V.S.; Michel, B.; Fournier, G.; Thirion, M.; Gillet, L.; Mast, J.; Lieffrig, F.; Bremont, M.; Vanderplasschen, A. The Major Portal of Entry of Koi Herpesvirus in Cyprinus Carpio is the Skin. *J. Virol.* **2009**, *83*, 2819–2830. [CrossRef]
51. Ershov, D.; Phan, M.-S.; Pylvänäinen, J.W.; Rigaud, S.U.; Le Blanc, L.; Charles-Orszag, A.; Conway, J.R.W.; Laine, R.F.; Roy, N.H.; Bonazzi, D.; et al. TrackMate 7: Integrating State-of-the-Art Segmentation Algorithms into Tracking Pipelines. *Nat. Methods* **2022**, *19*, 829–832. [CrossRef]
52. Levraud, J.-P.; Colucci-Guyon, E.; Redd, M.J.; Lutfalla, G.; Herbomel, P. In Vivo Analysis of Zebrafish Innate Immunity. *Methods Mol. Biol. Clifton NJ* **2008**, *415*, 337–363. [CrossRef]
53. Kaufmann, A.; Mickoleit, M.; Weber, M.; Huisken, J. Multilayer Mounting Enables Long-Term Imaging of Zebrafish Development in a Light Sheet Microscope. *Dev. Camb. Engl.* **2012**, *139*, 3242–3247. [CrossRef]
54. Gagnon, J.A.; Valen, E.; Thyme, S.B.; Huang, P.; Akhmetova, L.; Ahkmetova, L.; Pauli, A.; Montague, T.G.; Zimmerman, S.; Richter, C.; et al. Efficient Mutagenesis by Cas9 Protein-Mediated Oligonucleotide Insertion and Large-Scale Assessment of Single-Guide RNAs. *PLoS ONE* **2014**, *9*, e98186. [CrossRef]
55. Jao, L.-E.; Wente, S.R.; Chen, W. Efficient Multiplex Biallelic Zebrafish Genome Editing Using a CRISPR Nuclease System. *Proc. Natl. Acad. Sci. USA* **2013**, *110*, 13904–13909. [CrossRef]
56. Varshney, G.K.; Pei, W.; LaFave, M.C.; Idol, J.; Xu, L.; Gallardo, V.; Carrington, B.; Bishop, K.; Jones, M.; Li, M.; et al. High-Throughput Gene Targeting and Phenotyping in Zebrafish Using CRISPR/Cas9. *Genome Res.* **2015**, *25*, 1030–1042. [CrossRef]
57. Labun, K.; Montague, T.G.; Krause, M.; Torres Cleuren, Y.N.; Tjeldnes, H.; Valen, E. CHOPCHOP v3: Expanding the CRISPR Web Toolbox beyond Genome Editing. *Nucleic Acids Res.* **2019**, *47*, W171–W174. [CrossRef]
58. Jobst-Schwan, T.; Schmidt, J.M.; Schneider, R.; Hoogstraten, C.A.; Ullmann, J.F.P.; Schapiro, D.; Majmundar, A.J.; Kolb, A.; Eddy, K.; Shril, S.; et al. Acute Multi-SgRNA Knockdown of KEOPS Complex Genes Reproduces the Microcephaly Phenotype of the Stable Knockout Zebrafish Model. *PLoS ONE* **2018**, *13*, e0191503. [CrossRef]
59. Ji, W.; Zhou, W.; Abruzzese, R.; Guo, W.; Blake, A.; Davis, S.; Davis, S.; Polejaeva, I. A Method for Determining Zygosity of Transgenic Zebrafish by TaqMan Real-Time PCR. *Anal. Biochem.* **2005**, *344*, 240–246. [CrossRef]
60. Livak, K.J.; Schmittgen, T.D. Analysis of Relative Gene Expression Data Using Real-Time Quantitative PCR and the 2(-Delta Delta C(T)) Method. *Methods* **2001**, *25*, 402–408. [CrossRef]
61. Pohlert, T. PMCMRplus: Calculate Pairwise Multiple Comparisons of Mean Rank Sums Extended. 2022. Available online: https://cran.r-project.org/web/packages/PMCMRplus/index.html (accessed on 15 February 2023).
62. R Core Team. *R: A Language and Environment for Statistical Computing*; R Foundation for Statistical Computing: Vienna, Austria, 2022.
63. Ogle, D. *FSA: Simple Fisheries Stock Assessment Methods*; R Foundation for Statistical Computing: Vienna, Austria, 2022.
64. Gao, Y.; Sridhar, A.; Bernard, N.; He, B.; Zhang, H.; Pirotte, S.; Desmecht, S.; Vancsok, C.; Boutier, M.; Suárez, N.M.; et al. Virus-Induced Interference as a Means for Accelerating Fitness-Based Selection of Cyprinid Herpesvirus 3 Single Nucleotide Variants in Vitro and in Vivo. *Virus Evol.* **2023**, *9*, vead003. [CrossRef]
65. Grinde, B. Herpesviruses: Latency and Reactivation—Viral Strategies and Host Response. *J. Oral. Microbiol.* **2013**, *5*, 22766. [CrossRef]
66. Bigalke, J.M.; Heldwein, E.E. Nuclear Exodus: Herpesviruses Lead the Way. *Annu. Rev. Virol.* **2016**, *3*, 387–409. [CrossRef]
67. Jorgensen, I.; Rayamajhi, M.; Miao, E.A. Programmed Cell Death as a Defence against Infection. *Nat. Rev. Immunol.* **2017**, *17*, 151–164. [CrossRef]

68. Orzalli, M.H.; Kagan, J.C. Apoptosis and Necroptosis as Host Defense Strategies to Prevent Viral Infection. *Trends Cell. Biol.* **2017**, *27*, 800–809. [CrossRef]
69. Shlomovitz, I.; Zargarian, S.; Erlich, Z.; Edry-Botzer, L.; Gerlic, M. Distinguishing Necroptosis from Apoptosis. *Methods Mol. Biol. Clifton NJ* **2018**, *1857*, 35–51. [CrossRef]
70. Zhang, Y.; Chen, X.; Gueydan, C.; Han, J. Plasma Membrane Changes during Programmed Cell Deaths. *Cell. Res.* **2018**, *28*, 9–21. [CrossRef]
71. Morgan, M.J.; Kim, Y.-S. Roles of RIPK3 in Necroptosis, Cell Signaling, and Disease. *Exp. Mol. Med.* **2022**, *54*, 1695–1704. [CrossRef]
72. Verdonck, S.; Nemegeer, J.; Vandenabeele, P.; Maelfait, J. Viral Manipulation of Host Cell Necroptosis and Pyroptosis. *Trends Microbiol.* **2022**, *30*, 593–605. [CrossRef]
73. Wang, W.; Asim, M.; Yi, L.; Hegazy, A.; Hu, X.; Zhou, Y.; Ai, T.; Lin, L. Abortive Infection of Snakehead Fish Vesiculovirus in ZF4 Cells Was Associated with the RLRs Pathway Activation by Viral Replicative Intermediates. *Int. J. Mol. Sci.* **2015**, *16*, 6235–6250. [CrossRef]
74. Davison, A.J.; Kurobe, T.; Gatherer, D.; Cunningham, C.; Korf, I.; Fukuda, H.; Hedrick, R.P.; Waltzek, T.B. Comparative Genomics of Carp Herpesviruses. *J. Virol.* **2013**, *87*, 2908–2922. [CrossRef]
75. van Beurden, S.J.; Bossers, A.; Voorbergen-Laarman, M.H.A.; Haenen, O.L.M.; Peters, S.; Abma-Henkens, M.H.C.; Peeters, B.P.H.; Rottier, P.J.M.; Engelsma, M.Y. Complete Genome Sequence and Taxonomic Position of Anguillid Herpesvirus 1. *J. Gen. Virol.* **2010**, *91*, 880–887. [CrossRef]
76. Waltzek, T.; Kelley, G.; Alfaro, M.; Kurobe, T.; Davison, A.; Hedrick, R. Phylogenetic Relationships in the Family Alloherpesviridae. *Dis. Aquat. Organ.* **2009**, *84*, 179–194. [CrossRef]
77. Ge, R.; Zhou, Y.; Peng, R.; Wang, R.; Li, M.; Zhang, Y.; Zheng, C.; Wang, C. Conservation of the STING-Mediated Cytosolic DNA Sensing Pathway in Zebrafish. *J. Virol.* **2015**, *89*, 7696–7706. [CrossRef]
78. Lama, R.; Pereiro, P.; Figueras, A.; Novoa, B. Zebrafish as a Vertebrate Model for Studying Nodavirus Infections. *Front. Immunol.* **2022**, *13*, 863096. [CrossRef]
79. Adamek, M.; Rakus, K.Ł.; Chyb, J.; Brogden, G.; Huebner, A.; Irnazarow, I.; Steinhagen, D. Interferon Type I Responses to Virus Infections in Carp Cells: In Vitro Studies on Cyprinid Herpesvirus 3 and Rhabdovirus Carpio Infections. *Fish. Shellfish. Immunol.* **2012**, *33*, 482–493. [CrossRef]
80. Zhang, C.; Liu, A.-Q.; Zhang, C.; Liu, L.-H.; Su, J.; Zhang, Y.-A.; Tu, J. MicroRNA MiR-722 Inhibits Cyprinid Herpesvirus 3 Replication via Targeting the Viral Immune Evasion Protein ORF89, Which Negatively Regulates IFN by Degrading IRF3. *J. Immunol.* **2022**, *209*, 1918–1929. [CrossRef]
81. Widziolek, M.; Janik, K.; Mojzesz, M.; Pooranachandran, N.; Adamek, M.; Pecio, A.; Surachetpong, W.; Levraud, J.-P.; Boudinot, P.; Chadzinska, M.; et al. Type I Interferon-Dependent Response of Zebrafish Larvae during Tilapia Lake Virus (TiLV) Infection. *Dev. Comp. Immunol.* **2021**, *116*, 103936. [CrossRef]
82. Lazarte, J.M.S.; Thompson, K.D.; Jung, T.S. Pattern Recognition by Melanoma Differentiation-Associated Gene 5 (Mda5) in Teleost Fish: A Review. *Front. Immunol.* **2019**, *10*, 906. [CrossRef]
83. Gong, X.-Y.; Zhang, Q.-M.; Zhao, X.; Li, Y.-L.; Qu, Z.-L.; Li, Z.; Dan, C.; Gui, J.-F.; Zhang, Y.-B. LGP2 is Essential for Zebrafish Survival through Dual Regulation of IFN Antiviral Response. *Iscience* **2022**, *25*, 104821. [CrossRef]
84. Nie, L.; Zhang, Y.; Dong, W.; Xiang, L.; Shao, J. Involvement of Zebrafish RIG-I in NF-KB and IFN Signaling Pathways: Insights into Functional Conservation of RIG-I in Antiviral Innate Immunity. *Dev. Comp. Immunol.* **2015**, *48*, 95–101. [CrossRef]
85. Kato, K.; Ahmad, S.; Zhu, Z.; Young, J.M.; Mu, X.; Park, S.; Malik, H.S.; Hur, S. Structural Analysis of RIG-I-like Receptors Reveals Ancient Rules of Engagement between Diverse RNA Helicases and TRIM Ubiquitin Ligases. *Mol. Cell.* **2021**, *81*, 599–613.e8. [CrossRef]
86. Jin, Y.; Jia, K.; Zhang, W.; Xiang, Y.; Jia, P.; Liu, W.; Yi, M. Zebrafish TRIM25 Promotes Innate Immune Response to RGNNV Infection by Targeting 2CARD and RD Regions of RIG-I for K63-Linked Ubiquitination. *Front. Immunol.* **2019**, *10*, 2805. [CrossRef]
87. Lamers, M.M.; van den Hoogen, B.G.; Haagmans, B.L. ADAR1: "Editor-in-Chief" of Cytoplasmic Innate Immunity. *Front. Immunol.* **2019**, *10*, 1763. [CrossRef]
88. Rothenburg, S.; Deigendesch, N.; Dey, M.; Dever, T.E.; Tazi, L. Double-Stranded RNA-Activated Protein Kinase PKR of Fishes and Amphibians: Varying the Number of Double-Stranded RNA Binding Domains and Lineage-Specific Duplications. *BMC Biol.* **2008**, *6*, 12. [CrossRef]
89. Rothenburg, S.; Deigendesch, N.; Dittmar, K.; Koch-Nolte, F.; Haag, F.; Lowenhaupt, K.; Rich, A. A PKR-like Eukaryotic Initiation Factor 2α Kinase from Zebrafish Contains Z-DNA Binding Domains Instead of DsRNA Binding Domains. *Proc. Natl. Acad. Sci. USA* **2005**, *102*, 1602–1607. [CrossRef]
90. Diallo, M.A.; Pirotte, S.; Hu, Y.; Morvan, L.; Rakus, K.; Suárez, N.M.; PoTsang, L.; Saneyoshi, H.; Xu, Y.; Davison, A.J.; et al. A Fish Herpesvirus Highlights Functional Diversities among Zα Domains Related to Phase Separation Induction and A-to-Z Conversion. *Nucleic Acids Res.* **2022**, *51*, 806–830. [CrossRef] [PubMed]
91. Chiang, D.C.; Li, Y.; Ng, S.K. The Role of the Z-DNA Binding Domain in Innate Immunity and Stress Granules. *Front. Immunol.* **2020**, *11*, 625504. [CrossRef] [PubMed]
92. Katibah, G.E.; Qin, Y.; Sidote, D.J.; Yao, J.; Lambowitz, A.M.; Collins, K. Broad and Adaptable RNA Structure Recognition by the Human Interferon-Induced Tetratricopeptide Repeat Protein IFIT5. *Proc. Natl. Acad. Sci. USA* **2014**, *111*, 12025–12030. [CrossRef]

93. Pichlmair, A.; Lassnig, C.; Eberle, C.-A.; Górna, M.W.; Baumann, C.L.; Burkard, T.R.; Bürckstümmer, T.; Stefanovic, A.; Krieger, S.; Bennett, K.L.; et al. IFIT1 Is an Antiviral Protein That Recognizes 5′-Triphosphate RNA. *Nat. Immunol.* **2011**, *12*, 624–630. [CrossRef]
94. Hartmann, G. Nucleic Acid Immunity. *Adv. Immunol.* **2017**, *133*, 121. [CrossRef]
95. Briolat, V.; Jouneau, L.; Carvalho, R.; Palha, N.; Langevin, C.; Herbomel, P.; Schwartz, O.; Spaink, H.P.; Levraud, J.-P.; Boudinot, P. Contrasted Innate Responses to Two Viruses in Zebrafish: Insights into the Ancestral Repertoire of Vertebrate IFN-Stimulated Genes. *J. Immunol.* **2014**, *192*, 4328–4341. [CrossRef]
96. Poynter, S.; Lisser, G.; Monjo, A.; DeWitte-Orr, S. Sensors of Infection: Viral Nucleic Acid PRRs in Fish. *Biology* **2015**, *4*, 460–493. [CrossRef]
97. Ma, J.; Li, J.; Fan, D.; Feng, W.; Lin, A.; Xiang, L.; Shao, J. Identification of DEAD-Box RNA Helicase DDX41 as a Trafficking Protein That Involves in Multiple Innate Immune Signaling Pathways in a Zebrafish Model. *Front. Immunol.* **2018**, *9*, 1327. [CrossRef]
98. Liu, Z.-F.; Ji, J.-F.; Jiang, X.-F.; Shao, T.; Fan, D.-D.; Jiang, X.-H.; Lin, A.-F.; Xiang, L.-X.; Shao, J.-Z. Characterization of CGAS Homologs in Innate and Adaptive Mucosal Immunities in Zebrafish Gives Evolutionary Insights into CGAS-STING Pathway. *FASEB J. Off. Publ. Fed. Am. Soc. Exp. Biol.* **2020**, *34*, 7786–7809. [CrossRef]
99. Schult, P.; Paeschke, K. The DEAH Helicase DHX36 and Its Role in G-Quadruplex-Dependent Processes. *Biol. Chem.* **2021**, *402*, 581–591. [CrossRef]
100. Chiang, J.J.; Sparrer, K.M.J.; van Gent, M.; Lässig, C.; Huang, T.; Osterrieder, N.; Hopfner, K.-P.; Gack, M.U. Viral Unmasking of Cellular 5S RRNA Pseudogene Transcripts Induces RIG-I Mediated Immunity. *Nat. Immunol.* **2018**, *19*, 53–62. [CrossRef] [PubMed]
101. Zhao, Y.; Ye, X.; Dunker, W.; Song, Y.; Karijolich, J. RIG-I like Receptor Sensing of Host RNAs Facilitates the Cell-Intrinsic Immune Response to KSHV Infection. *Nat. Commun.* **2018**, *9*, 4841. [CrossRef]
102. Chiu, Y.-H.; MacMillan, J.B.; Chen, Z.J. RNA Polymerase III Detects Cytosolic DNA and Induces Type-I Interferons Through the RIG-I Pathway. *Cell* **2009**, *138*, 576. [CrossRef] [PubMed]
103. Ablasser, A.; Bauernfeind, F.; Hartmann, G.; Latz, E.; Fitzgerald, K.A.; Hornung, V. RIG-I Dependent Sensing of Poly(DA-DT) via the Induction of an RNA Polymerase III Transcribed RNA Intermediate. *Nat. Immunol.* **2009**, *10*, 1065–1072. [CrossRef]
104. Rehwinkel, J.; Gack, M.U. RIG-I-like Receptors: Their Regulation and Roles in RNA Sensing. *Nat. Rev. Immunol.* **2020**, *20*, 537–551. [CrossRef] [PubMed]
105. Howe, K.; Schiffer, P.H.; Zielinski, J.; Wiehe, T.; Laird, G.K.; Marioni, J.C.; Soylemez, O.; Kondrashov, F.; Leptin, M. Structure and Evolutionary History of a Large Family of NLR Proteins in the Zebrafish. *Open. Biol.* **2016**, *6*, 160009. [CrossRef]
106. Krupovic, M.; Blomberg, J.; Coffin, J.M.; Dasgupta, I.; Fan, H.; Geering, A.D.; Gifford, R.; Harrach, B.; Hull, R.; Johnson, W.; et al. Ortervirales: New Virus Order Unifying Five Families of Reverse-Transcribing Viruses. *J. Virol.* **2018**, *92*, e00515-18. [CrossRef]
107. Wicker, T.; Sabot, F.; Hua-Van, A.; Bennetzen, J.L.; Capy, P.; Chalhoub, B.; Flavell, A.; Leroy, P.; Morgante, M.; Panaud, O.; et al. A Unified Classification System for Eukaryotic Transposable Elements. *Nat. Rev. Genet.* **2007**, *8*, 973–982. [CrossRef]
108. Macchietto, M.G.; Langlois, R.A.; Shen, S.S. Virus-Induced Transposable Element Expression up-Regulation in Human and Mouse Host Cells. *Life Sci. Alliance* **2020**, *3*, e201900536. [CrossRef]
109. Srinivasachar Badarinarayan, S.; Shcherbakova, I.; Langer, S.; Koepke, L.; Preising, A.; Hotter, D.; Kirchhoff, F.; Sparrer, K.M.J.; Schotta, G.; Sauter, D. HIV-1 Infection Activates Endogenous Retroviral Promoters Regulating Antiviral Gene Expression. *Nucleic Acids Res.* **2020**, *48*, 10890–10908. [CrossRef]
110. Gázquez-Gutiérrez, A.; Witteveldt, J.; Heras, S.R.; Macias, S. Sensing of Transposable Elements by the Antiviral Innate Immune System. *RNA* **2021**, *27*, 735–752. [CrossRef]
111. Chernyavskaya, Y.; Mudbhary, R.; Zhang, C.; Tokarz, D.; Jacob, V.; Gopinath, S.; Sun, X.; Wang, S.; Magnani, E.; Madakashira, B.P.; et al. Loss of DNA Methylation in Zebrafish Embryos Activates Retrotransposons to Trigger Antiviral Signaling. *Dev. Camb. Engl.* **2017**, *144*, 2925–2939. [CrossRef] [PubMed]
112. Zuo, W.; Wakimoto, M.; Kozaiwa, N.; Shirasaka, Y.; Oh, S.-W.; Fujiwara, S.; Miyachi, H.; Kogure, A.; Kato, H.; Fujita, T. PKR and TLR3 Trigger Distinct Signals That Coordinate the Induction of Antiviral Apoptosis. *Cell. Death Dis.* **2022**, *13*, 707. [CrossRef] [PubMed]
113. Thapa, R.J.; Nogusa, S.; Chen, P.; Maki, J.L.; Lerro, A.; Andrake, M.; Rall, G.F.; Degterev, A.; Balachandran, S. Interferon-Induced RIP1/RIP3-Mediated Necrosis Requires PKR and Is Licensed by FADD and Caspases. *Proc. Natl. Acad. Sci. USA* **2013**, *110*, E3109–E3118. [CrossRef] [PubMed]
114. Gal-Ben-Ari, S.; Barrera, I.; Ehrlich, M.; Rosenblum, K. PKR: A Kinase to Remember. *Front. Mol. Neurosci.* **2019**, *11*, 480. [CrossRef] [PubMed]
115. García, M.A.; Meurs, E.F.; Esteban, M. The DsRNA Protein Kinase PKR: Virus and Cell Control. *Biochimie* **2007**, *89*, 799–811. [CrossRef] [PubMed]
116. Dalet, A.; Gatti, E.; Pierre, P. Integration of PKR-Dependent Translation Inhibition with Innate Immunity Is Required for a Coordinated Anti-Viral Response. *FEBS Lett.* **2015**, *589*, 1539–1545. [CrossRef] [PubMed]
117. Williams, B.R. PKR; a Sentinel Kinase for Cellular Stress. *Oncogene* **1999**, *18*, 6112–6120. [CrossRef] [PubMed]
118. García, M.A.; Gil, J.; Ventoso, I.; Guerra, S.; Domingo, E.; Rivas, C.; Esteban, M. Impact of Protein Kinase PKR in Cell Biology: From Antiviral to Antiproliferative Action. Microbiol. *Mol. Biol. Rev.* **2006**, *70*, 1032–1060. [CrossRef] [PubMed]

119. Andreev, D.E.; O'Connor, P.B.F.; Fahey, C.; Kenny, E.M.; Terenin, I.M.; Dmitriev, S.E.; Cormican, P.; Morris, D.W.; Shatsky, I.N.; Baranov, P.V. Translation of 5′ Leaders Is Pervasive in Genes Resistant to EIF2 Repression. *eLife* **2015**, *4*, e03971. [CrossRef]
120. Ventoso, I.; Sanz, M.A.; Molina, S.; Berlanga, J.J.; Carrasco, L.; Esteban, M. Translational Resistance of Late Alphavirus MRNA to EIF2α Phosphorylation: A Strategy to Overcome the Antiviral Effect of Protein Kinase PKR. *Genes Dev.* **2006**, *20*, 87–100. [CrossRef]
121. Mokas, S.; Mills, J.R.; Garreau, C.; Fournier, M.-J.; Robert, F.; Arya, P.; Kaufman, R.J.; Pelletier, J.; Mazroui, R. Uncoupling Stress Granule Assembly and Translation Initiation Inhibition. *Mol. Biol. Cell.* **2009**, *20*, 2673–2683. [CrossRef]
122. Wen, X.; Huang, X.; Mok, B.W.-Y.; Chen, Y.; Zheng, M.; Lau, S.-Y.; Wang, P.; Song, W.; Jin, D.-Y.; Yuen, K.-Y.; et al. NF90 Exerts Antiviral Activity through Regulation of PKR Phosphorylation and Stress Granules in Infected Cells. *J. Immunol.* **2014**, *192*, 3753–3764. [CrossRef]
123. McCormick, C.; Khaperskyy, D.A. Translation Inhibition and Stress Granules in the Antiviral Immune Response. *Nat. Rev. Immunol.* **2017**, *17*, 647–660. [CrossRef]
124. Onomoto, K.; Onoguchi, K.; Yoneyama, M. Regulation of RIG-I-like Receptor-Mediated Signaling: Interaction between Host and Viral Factors. *Cell. Mol. Immunol.* **2021**, *18*, 539–555. [CrossRef] [PubMed]
125. Onomoto, K.; Jogi, M.; Yoo, J.-S.; Narita, R.; Morimoto, S.; Takemura, A.; Sambhara, S.; Kawaguchi, A.; Osari, S.; Nagata, K.; et al. Critical Role of an Antiviral Stress Granule Containing RIG-I and PKR in Viral Detection and Innate Immunity. *PLoS ONE* **2012**, *7*, e43031. [CrossRef]
126. Lawrence, T. The Nuclear Factor NF-KB Pathway in Inflammation. *Cold Spring Harb. Perspect. Biol.* **2009**, *1*, a001651. [CrossRef]
127. Donzé, O.; Deng, J.; Curran, J.; Sladek, R.; Picard, D.; Sonenberg, N. The Protein Kinase PKR: A Molecular Clock That Sequentially Activates Survival and Death Programs. *EMBO J.* **2004**, *23*, 564–571. [CrossRef] [PubMed]
128. Choy, M.S.; Yusoff, P.; Lee, I.C.; Newton, J.C.; Goh, C.W.; Page, R.; Shenolikar, S.; Peti, W. Structural and Functional Analysis of the GADD34:PP1 EIF2α Phosphatase. *Cell. Rep.* **2015**, *11*, 1885–1891. [CrossRef] [PubMed]
129. Su, Q.; Wang, S.; Baltzis, D.; Qu, L.-K.; Raven, J.F.; Li, S.; Wong, A.H.-T.; Koromilas, A.E. Interferons Induce Tyrosine Phosphorylation of the EIF2α Kinase PKR through Activation of Jak1 and Tyk2. *EMBO Rep.* **2007**, *8*, 265–270. [CrossRef]
130. Gil, J.; García, M.A.; Esteban, M. Caspase 9 Activation by the DsRNA-Dependent Protein Kinase, PKR: Molecular Mechanism and Relevance. *FEBS Lett.* **2002**, *529*, 249–255. [CrossRef]
131. Gil, J.; Esteban, M. The Interferon-Induced Protein Kinase (PKR), Triggers Apoptosis through FADD-Mediated Activation of Caspase 8 in a Manner Independent of Fas and TNF-α Receptors. *Oncogene* **2000**, *19*, 3665–3674. [CrossRef]
132. Tsuchiya, Y.; Nakabayashi, O.; Nakano, H. FLIP the Switch: Regulation of Apoptosis and Necroptosis by CFLIP. *Int. J. Mol. Sci.* **2015**, *16*, 30321–30341. [CrossRef] [PubMed]
133. Ram, D.R.; Ilyukha, V.; Volkova, T.; Buzdin, A.; Tai, A.; Smirnova, I.; Poltorak, A. Balance between Short and Long Isoforms of CFLIP Regulates Fas-Mediated Apoptosis in Vivo. *Proc. Natl. Acad. Sci. USA* **2016**, *113*, 1606–1611. [CrossRef]
134. Chukwurah, E.; Farabaugh, K.T.; Guan, B.-J.; Ramakrishnan, P.; Hatzoglou, M. A Tale of Two Proteins: PACT and PKR and Their Roles in Inflammation. *FEBS J.* **2021**, *288*, 6365–6391. [CrossRef]
135. Balachandran, S.; Kim, C.N.; Yeh, W.C.; Mak, T.W.; Bhalla, K.; Barber, G.N. Activation of the DsRNA-Dependent Protein Kinase, PKR, Induces Apoptosis through FADD-Mediated Death Signaling. *EMBO J.* **1998**, *17*, 6888–6902. [CrossRef] [PubMed]
136. Donzé, O.; Dostie, J.; Sonenberg, N. Regulatable Expression of the Interferon-Induced Double-Stranded RNA Dependent Protein Kinase PKR Induces Apoptosis and Fas Receptor Expression. *Virology* **1999**, *256*, 322–329. [CrossRef]
137. Xu, C.; Gamil, A.; Munang'andu, H.; Evensen, Ø. Apoptosis Induction by DsRNA-Dependent Protein Kinase R (PKR) in EPC Cells via Caspase 8 and 9 Pathways. *Viruses* **2018**, *10*, 526. [CrossRef] [PubMed]
138. Best, S.M. Viral Subversion of Apoptotic Enzymes: Escape from Death Row. *Annu. Rev. Microbiol.* **2008**, *62*, 171. [CrossRef]
139. Mocarski, E.S.; Upton, J.W.; Kaiser, W.J. Viral Infection and the Evolution of Caspase 8-Regulated Apoptotic and Necrotic Death Pathways. *Nat. Rev. Immunol.* **2011**, *12*, 79–88. [CrossRef]
140. Petrie, E.J.; Hildebrand, J.M.; Murphy, J.M. Insane in the Membrane: A Structural Perspective of MLKL Function in Necroptosis. *Immunol. Cell. Biol.* **2017**, *95*, 152–159. [CrossRef]
141. Vandenabeele, P.; Galluzzi, L.; Vanden Berghe, T.; Kroemer, G. Molecular Mechanisms of Necroptosis: An Ordered Cellular Explosion. *Nat. Rev. Mol. Cell. Biol.* **2010**, *11*, 700–714. [CrossRef] [PubMed]
142. Schilling, R.; Geserick, P.; Leverkus, M. Characterization of the Ripoptosome and Its Components: Implications for Anti-Inflammatory and Cancer Therapy. *Methods Enzymol.* **2014**, *545*, 83–102. [CrossRef] [PubMed]
143. Kalai, M.; Suin, V.; Festjens, N.; Meeus, A.; Bernis, A.; Wang, X.-M.; Saelens, X.; Vandenabeele, P. The Caspase-Generated Fragments of PKR Cooperate to Activate Full-Length PKR and Inhibit Translation. *Cell. Death Differ.* **2007**, *14*, 1050–1059. [CrossRef]
144. Tummers, B.; Green, D.R. Mechanisms of TNF-Independent RIPK3-Mediated Cell Death. *Biochem. J.* **2022**, *479*, 2049–2062. [CrossRef]
145. Cesaro, T.; Michiels, T. Inhibition of PKR by Viruses. *Front. Microbiol.* **2021**, *12*, 757238. [CrossRef]
146. Wu, C.; Zhang, Y.; Hu, C. PKZ, a Fish-Unique EIF2α Kinase Involved in Innate Immune Response. *Front. Immunol.* **2020**, *11*, 585. [CrossRef]
147. Liu, Z.-Y.; Jia, K.-T.; Li, C.; Weng, S.-P.; Guo, C.-J.; He, J.-G. A Truncated Danio Rerio PKZ Isoform Functionally Interacts with EIF2α and Inhibits Protein Synthesis. *Gene* **2013**, *527*, 292–300. [CrossRef]

148. Wu, C.; Hu, Y.; Fan, L.; Wang, H.; Sun, Z.; Deng, S.; Liu, Y.; Hu, C. Ctenopharyngodon Idella PKZ Facilitates Cell Apoptosis through Phosphorylating EIF2α. *Mol. Immunol.* **2016**, *69*, 13–23. [CrossRef] [PubMed]
149. Kim, D.; Hur, J.; Park, K.; Bae, S.; Shin, D.; Ha, S.C.; Hwang, H.-Y.; Hohng, S.; Lee, J.-H.; Lee, S.; et al. Distinct Z-DNA Binding Mode of a PKR-like Protein Kinase Containing a Z-DNA Binding Domain (PKZ). *Nucleic Acids Res.* **2014**, *42*, 5937–5948. [CrossRef]
150. Wu, C.-X.; Wang, S.-J.; Lin, G.; Hu, C.-Y. The Zα Domain of PKZ from Carassius Auratus Can Bind to d(GC)n in Negative Supercoils. *Fish. Shellfish. Immunol.* **2010**, *28*, 783–788. [CrossRef]
151. Bergan, V.; Jagus, R.; Lauksund, S.; Kileng, Ø.; Robertsen, B. The Atlantic Salmon Z-DNA Binding Protein Kinase Phosphorylates Translation Initiation Factor 2 Alpha and Constitutes a Unique Orthologue to the Mammalian DsRNA-Activated Protein Kinase R: Atlantic Salmon Z-DNA Binding Protein Kinase. *FEBS J.* **2008**, *275*, 184–197. [CrossRef]
152. Liu, T.-K.; Zhang, Y.-B.; Liu, Y.; Sun, F.; Gui, J.-F. Cooperative Roles of Fish Protein Kinase Containing Z-DNA Binding Domains and Double-Stranded RNA-Dependent Protein Kinase in Interferon-Mediated Antiviral Response. *J. Virol.* **2011**, *85*, 12769–12780. [CrossRef] [PubMed]
153. Hu, C.; Xie, Z.; Zhang, Y.; Chen, Y.; Deng, Z.; Jiang, J.; Gui, J. *Binding of the Zα Domain from a Carassius Auratus Protein Kinase PKR-like to Polyinosinic: Polycytidylic Acid*; Kunming Institute of Zoology, Chinese Academy of Sciences: Kunming, China, 2005.
154. Nailwal, H.; Chan, F.K.-M. Necroptosis in Anti-Viral Inflammation. *Cell. Death Differ.* **2019**, *26*, 4–13. [CrossRef]
155. Berghe, T.V.; Linkermann, A.; Jouan-Lanhouet, S.; Walczak, H.; Vandenabeele, P. Regulated Necrosis: The Expanding Network of Non-Apoptotic Cell Death Pathways. *Nat. Rev. Mol. Cell. Biol.* **2014**, *15*, 135–147. [CrossRef] [PubMed]
156. Land, W.G. (Ed.) Regulated Cell Death. In *Damage-Associated Molecular Patterns in Human Diseases: Volume 1: Injury-Induced Innate Immune Responses*; Springer International Publishing: Cham, Germany, 2018; pp. 427–466; ISBN 978-3-319-78655-1.
157. Zhou, X.; Jiang, W.; Liu, Z.; Liu, S.; Liang, X. Virus Infection and Death Receptor-Mediated Apoptosis. *Viruses* **2017**, *9*, 316. [CrossRef] [PubMed]
158. Gao, Y.; Suárez, N.M.; Wilkie, G.S.; Dong, C.; Bergmann, S.; Lee, P.-Y.A.; Davison, A.J.; Vanderplasschen, A.F.C.; Boutier, M. Genomic and Biologic Comparisons of Cyprinid Herpesvirus 3 Strains. *Vet. Res.* **2018**, *49*, 40. [CrossRef] [PubMed]
159. Vancsok, C.; Peñaranda, M.M.D.; Raj, V.S.; Leroy, B.; Jazowiecka-Rakus, J.; Boutier, M.; Gao, Y.; Wilkie, G.S.; Suárez, N.M.; Wattiez, R.; et al. Proteomic and Functional Analyses of the Virion Transmembrane Proteome of Cyprinid Herpesvirus 3. *J. Virol.* **2017**, *91*, e01209-17. [CrossRef] [PubMed]
160. Abramoff, M.D.; Magelhaes, P.J.; Ram, S.J. Image Processing with ImageJ. *Biophotonics Int.* **2004**, *11*, 36–42.
161. BBTools. Available online: https://jgi.doe.gov/data-and-tools/software-tools/bbtools/ (accessed on 5 October 2022).
162. Babraham Bioinformatics—FastQC A Quality Control Tool for High Throughput Sequence Data. Available online: https://www.bioinformatics.babraham.ac.uk/projects/fastqc/ (accessed on 5 October 2022).
163. Pertea, M.; Kim, D.; Pertea, G.M.; Leek, J.T.; Salzberg, S.L. Transcript-Level Expression Analysis of RNA-Seq Experiments with HISAT, StringTie and Ballgown. *Nat. Protoc.* **2016**, *11*, 1650–1667. [CrossRef]
164. Kim, D.; Paggi, J.M.; Park, C.; Bennett, C.; Salzberg, S.L. Graph-Based Genome Alignment and Genotyping with HISAT2 and HISAT-Genotype. *Nat. Biotechnol.* **2019**, *37*, 907–915. [CrossRef]
165. Danecek, P.; Bonfield, J.K.; Liddle, J.; Marshall, J.; Ohan, V.; Pollard, M.O.; Whitwham, A.; Keane, T.; McCarthy, S.A.; Davies, R.M.; et al. Twelve Years of SAMtools and BCFtools. *GigaScience* **2021**, *10*, giab008. [CrossRef] [PubMed]
166. Love, M.I.; Huber, W.; Anders, S. Moderated Estimation of Fold Change and Dispersion for RNA-Seq Data with DESeq2. *Genome Biol.* **2014**, *15*, 550. [CrossRef]
167. GitHub. Stringtie/PrepDE.Py at Master Gpertea/Stringtie. Available online: https://github.com/gpertea/stringtie/blob/master/prepDE.py (accessed on 5 October 2022).
168. GitHub. Kevinblighe/EnhancedVolcano: Publication-Ready Volcano Plots with Enhanced Colouring and Labeling. Available online: https://github.com/kevinblighe/EnhancedVolcano (accessed on 13 October 2022).
169. Shannon, P.; Markiel, A.; Ozier, O.; Baliga, N.S.; Wang, J.T.; Ramage, D.; Amin, N.; Schwikowski, B.; Ideker, T. Cytoscape: A Software Environment for Integrated Models of Biomolecular Interaction Networks. *Genome Res.* **2003**, *13*, 2498–2504. [CrossRef]
170. Doncheva, N.T.; Morris, J.H.; Gorodkin, J.; Jensen, L.J. Cytoscape StringApp: Network Analysis and Visualization of Proteomics Data. *J. Proteome Res.* **2019**, *18*, 623–632. [CrossRef]
171. Franz, M.; Rodriguez, H.; Lopes, C.; Zuberi, K.; Montojo, J.; Bader, G.D.; Morris, Q. GeneMANIA Update 2018. *Nucleic Acids Res.* **2018**, *46*, W60–W64. [CrossRef]
172. Chin, C.-H.; Chen, S.-H.; Wu, H.-H.; Ho, C.-W.; Ko, M.-T.; Lin, C.-Y. CytoHubba: Identifying Hub Objects and Sub-Networks from Complex Interactome. *BMC Syst. Biol.* **2014**, *8*, S11. [CrossRef]
173. Subramanian, A.; Tamayo, P.; Mootha, V.K.; Mukherjee, S.; Ebert, B.L.; Gillette, M.A.; Paulovich, A.; Pomeroy, S.L.; Golub, T.R.; Lander, E.S.; et al. Gene Set Enrichment Analysis: A Knowledge-Based Approach for Interpreting Genome-Wide Expression Profiles. *Proc. Natl. Acad. Sci. USA* **2005**, *102*, 15545–15550. [CrossRef]
174. Mootha, V.K.; Lindgren, C.M.; Eriksson, K.-F.; Subramanian, A.; Sihag, S.; Lehar, J.; Puigserver, P.; Carlsson, E.; Ridderstråle, M.; Laurila, E.; et al. PGC-1alpha-Responsive Genes Involved in Oxidative Phosphorylation Are Coordinately Downregulated in Human Diabetes. *Nat. Genet.* **2003**, *34*, 267–273. [CrossRef] [PubMed]
175. Data Formats. GeneSetEnrichmentAnalysisWiki. Available online: https://software.broadinstitute.org/cancer/software/gsea/wiki/index.php/Data_formats#Phenotype_Data_Formats (accessed on 13 October 2022).

176. Ashburner, M.; Ball, C.A.; Blake, J.A.; Botstein, D.; Butler, H.; Cherry, J.M.; Davis, A.P.; Dolinski, K.; Dwight, S.S.; Eppig, J.T.; et al. Gene Ontology: Tool for the Unification of Biology. The Gene Ontology Consortium. *Nat. Genet.* **2000**, *25*, 25–29. [CrossRef] [PubMed]
177. Gene Ontology Consortium the Gene Ontology Resource: Enriching a GOld Mine. *Nucleic Acids Res.* **2021**, *49*, D325–D334. [CrossRef] [PubMed]
178. Kanehisa, M.; Goto, S. KEGG: Kyoto Encyclopedia of Genes and Genomes. *Nucleic Acids Res.* **2000**, *28*, 27–30. [CrossRef]
179. Kanehisa, M. Toward Understanding the Origin and Evolution of Cellular Organisms. *Protein Sci. Publ. Protein Soc.* **2019**, *28*, 1947–1951. [CrossRef]
180. Kanehisa, M.; Furumichi, M.; Sato, Y.; Ishiguro-Watanabe, M.; Tanabe, M. KEGG: Integrating Viruses and Cellular Organisms. *Nucleic Acids Res.* **2021**, *49*, D545–D551. [CrossRef]
181. Geistlinger, L.; Csaba, G.; Zimmer, R. Bioconductor's EnrichmentBrowser: Seamless Navigation through Combined Results of Set- & Network-Based Enrichment Analysis. *BMC Bioinform.* **2016**, *17*, 45. [CrossRef]
182. Merico, D.; Isserlin, R.; Stueker, O.; Emili, A.; Bader, G.D. Enrichment Map: A Network-Based Method for Gene-Set Enrichment Visualization and Interpretation. *PLoS ONE* **2010**, *5*, e13984. [CrossRef] [PubMed]
183. Kucera, M.; Isserlin, R.; Arkhangorodsky, A.; Bader, G.D. AutoAnnotate: A Cytoscape App for Summarizing Networks with Semantic Annotations. *F1000Research* **2016**, *5*, 1717. [CrossRef] [PubMed]
184. Luo, W.; Brouwer, C. Pathview: An R/Bioconductor Package for Pathway-Based Data Integration and Visualization. Bioinforma. *Oxf. Engl.* **2013**, *29*, 1830–1831. [CrossRef] [PubMed]
185. Mark, A.; Thompson, R.; Afrasiabi, C.; Wu, C. Mygene: Access MyGene. Info Services. 2022. Available online: https://www.bioconductor.org/packages/release/bioc/html/mygene.html (accessed on 15 February 2023).

Experimental Section

3rd study

In vitro and *In vivo* Characterization of Novel *Cyprinid Herpesvirus 2* Strains from the Netherlands

Preamble

Cyprinid herpesvirus 2 (CyHV-2) is a pathogen responsible for significant losses in the global aquaculture industry, particularly in goldfish (*Carassius auratus*) gibel carp (*Carassius gibelio*) and Crucian carp (*Carassius carassius*) sectors. Despite the progress that has been made in the isolation and characterization of CyHV-2 strains in East Asia, there is a lack of information on strains isolated in Europe. Moreover, while there are CyHV-2 strains that are highly virulent when administered to hosts via immersion (an approach that best represents natural infection), notably, in previous challenge trials, we did not observe the same virulent phenotype in the context of any European host populations tested. This is despite the continuous highly virulent CyHV-2 outbreaks that occur in the field within European regions. To address this, our third study focused on isolating highly virulent CyHV-2 strains from outbreaks among European goldfish populations, with the aim of establishing a robust and highly virulent *in vivo* infection model based on inoculation via immersion. Ultimately, one of the CyHV-2 strains that we isolated from an outbreak among goldfish populations in The Netherlands, referred to as NL-2, exhibited high fitness *in vitro* and much more virulence than the CyHV-2 reference strain (ST-J1) during *in vivo* challenge trials involving inoculation by immersion. Thus, the NL-2 CyHV-2 strain represents a promising candidate for future experimental studies and will act as a crucial foundation for future research on virus-host interactions and vaccine development.

Experimental Section

3rd study

In vitro and *In vivo* Characterization of Novel *Cyprinid Herpesvirus 2* Strains from the Netherlands.

Preparing for Submission (formatted as per target journal)

He, B.; Sridhar, A.; Streiff, C.; Deketelaere, C.; Delrez, N.; Thiry, M.; Donohoe, O.; Vanderplasschen, A.

This research is one of my major topics. My contribution to this study consisted of the recruitment of experimental materials, experimental imaging, virus isolation, *in vitro* growth kinetics comparison, *in vivo* virulence characterization and data analysis. This manuscript is prepared for submission to an appropriate journal.

Abstract

Cyprinid herpesvirus 2 (CyHV-2) is the causative agent of herpesviral hematopoietic necrosis in goldfish (*Carassius auratus*) across many regions. It also infects gibel carp (*Carassius gibelio*) and Crucian carp (*Carassius carassius*) populations. Despite several CyHV-2 strains being isolated and fully sequenced, there is a lack of detailed characterization and consistent information on strains that exhibit high virulence in adult goldfish through the viral challenge by immersion, in particular in the context of European host populations. Strains that can cause highly virulent disease via this inoculation route are much more compatible with experimental designs that are representative of natural infection, thus their utilization provides greater biological relevance. Consequently, in this study, we isolated three novel strains of CyHV-2 which we refer to as NL-1, NL-2, and NL-3, originating from high mortality outbreaks in The Netherlands. Initial *in vivo* experiments in adult Shubunkin goldfish demonstrated that all three isolates exhibited inherent pathogenicity after inoculation via intraperitoneal (IP) injection and all were capable of transmission from infected fish to naive fish. Genome sequencing and phylogenetic analyses revealed that these newly isolated strains are distinct from known strains and from each other. Significant differences were observed between the strains, in terms of *in vitro* growth kinetics, with NL-2 exhibiting stable passaging and superior fitness *in vitro*. Importantly, challenge of adult Shubunkin goldfish with the NL-2 strain via immersion (2000 PFU/mL) induced an average mortality of ~40%, while parallel experiments with the CyHV-2 reference strain ST-J1 resulted in no mortality. In summary, this study revealed that the NL-2 strain is *(i)* compatible with stable passaging *in vitro*, and exhibiting acceptable replication kinetics in this environment, and *(ii)* highly virulent and capable of inducing CyHV-2 related mortality in adult Shubunkin goldfish when challenged via immersion. This resulted in the description of a new CyHV-2 *in vivo* infection model, much more compatible with experimental designs that are required to be representative of natural infection which will be extremely useful in many aspects of CyHV-2 research in the future.

Keywords: *Cyprinid herpesvirus 2*; *Alloherpesviridae*; Goldfish; Viral isolation; virus-host model

Introduction

Goldfish (*Carassius auratus*) are a species of freshwater cyprinid fish that are commonly kept as ornamental pets and are popular in many regions across the world. Through selective breeding, many different varieties have been created to meet the diverse aesthetic preferences that exist within the global market. Through this process, many distinct morphological and colour variations have emerged, resulting in the existence of over 180 unique goldfish varieties [1]. The practice of goldfish domestication and selective breeding extends back 1000 years to ancient China [2].

However, relative to their wild and cultured crucian carp (*Carassius carassius*) counterparts, the continuous artificial selection of goldfish based on aesthetic traits, has resulted in the introduction of many disadvantageous phenotypic alterations, prominently affecting attributes such as mobility and infectious disease resistance, [1,3] which presents a significant problem in this sector. Furthermore, in addition to goldfish aquaculture, in general, due to high stocking density and increased global movement of stock, modern intensive aquaculture environments are particularly prone to outbreaks of infectious disease caused by pathogenic bacteria, fungi, parasites, and viruses [4]. The prevalence of some types of viral disease in aquaculture settings may be due to the high susceptibility of teleost hosts during early developmental stages. This is likely to be compounded by the absence of effective therapeutics, the incomplete understanding of the pathogenesis of viral infections, and the limited understanding of the natural resistance mechanisms inherent in many teleost fish [5].

Among the viruses affecting widely cultivated freshwater fish such as goldfish, viral species from the genus *Cyprinivirus* (referred to as cyprinviruses), are among the most pathogenic, resulting in high mortality outbreaks. Cypriniviuses are part of the family *Alloherpesviridae*, in the order *Herpesvirales*, which consist of herpesviruses infecting fish and amphibians. Some cyprinivius species are relatively well studied, including Anguillid herpesvirus 1 (AngHV-1) with infect freshwater eels species of the genus *Anguilla*, *Cyprinid herpesvirus 1* (CyHV-1) and *Cyprinid herpesvirus 3* (CyHV-3), which both infect common carp (*Cyprinus carpio*) and related species [6]. However, within this genus, *Cyprinid herpesvirus 2* (CyHV-2), which infects goldfish, related species such as crucian carp and gibel carp (*Carassius gibelio*) as well as other *Carassius spp*. [7], remains less well understood. CyHV-2 is the causative agent of a disease referred to as herpesviral hematopoietic necrosis disease which is associated with elevated mortality rates. This represents a substantial threat to the sustainability of goldfish aquaculture and the culture of other economically important species such as gibel carp and crucian carp species, which are farmed for consumption, and thus also important in the context of food security [8]. This disease caused by CyHV-2 was initially documented in 1995, and since then, its global prevalence has increased substantially [8,9]. Documented instances CyHV-2 outbreaks goldfish span diverse geographic locations, encompassing Japan [9], the United States [10,11], Taiwan [12], Australia [13], New Zealand [14], the United Kingdom [15], India [16], Switzerland [17], France [18], Germany [19], Turkey [20], Poland [21], China [22], Korea [23], and Thailand [24]. Furthermore, susceptibility to the

CyHV-2 virus has been confirmed across all life stages of goldfish, including eggs, juveniles, and adults, with virulence reducing as development advances [11,25].

As with other emerging viruses, since the earliest reports, the isolation of CyHV-2 strains from infected hosts during clinical outbreaks, and subsequent *in vitro* culture has been a crucial first step towards gaining a better understanding of this virus. This is important, as many CyHV-2 isolates exhibit a finite capacity for stable propagation *in vivo* under experimental conditions, extending no more than 4-5 passages [9–11]. Some cell lines, such as KF-1, which is derived from koi (Cyprinus carpio koi, a relative of goldfish) has limited permissivity to CyHV-2, have been used for *in vitro* propagation of CyHV-2, but with limited success over multiple passages [7,15]. The first sustained and reproducible culture of CyHV-2 in vitro was achieved using a suitably permissive cell line derived from the fin of goldfish [26,27].

Among other advances, in vitro culture of CyHV-2 isolates has facilitated more in-depth characterization of CyHV-2, including full-length genome sequencing. According to NCBI Viral Genome Browser (https://www.ncbi.nlm.nih.gov/genome/viruses/), there are currently six full-length genome sequences of CyHV-2 publicly available, representing strains from various geographic regions. These are referred to as ST-J1 (JQ815364.1 or NC019495.1), SY-C1 (KM200722.1), SY (KT387800.1), CNDF-TB2015 (MN201961.1), YZ-01 (MK260012.1), YC-01 (MN593216.1). Among these, ST-J1 (which has been defined as the reference strain) is isolated from goldfish, while CNDF-TB2015 and YZ-01 are isolated from crucian carp and SY-C1, SY, and YC-01 are isolated from gibel carp. Early genetic comparisons between strains revealed that CyHV-2 isolates formed two main clades, which were designated the Japanese genotype (J Genotype) and the Chinese genotype (C Genotype) [28,29].

Notably, despite being isolated from goldfish undergoing clinical disease [7], we observed that the CyHV-2 ST-J1 reference strain exhibits very little virulence in populations of goldfish breeds that we sourced from European suppliers, including the popular Shubunkin goldfish breed. This lack of virulence was specifically observed when challanging adult subjects by immersion. We also observed a similar outcome using the YC-01 strain [25]. The Shubunkin goldfish is highly relevant as an economically important goldfish model. It is also relatively easy to breed, which is extremely useful in terms of sustaining a supply of hosts for experimental infection trials. However, the lack of a broadly virulent CyHV-2 strain that can be used with this model and others (for example those commonly traded globally, or intensively cultured), as part of immersion infection experiments, limits the study of CyHV-2 pathogenesis in the most useful biological contexts most relevant to disease mitigation and control. For example, this creates difficulties in designing suitable in vivo challenge trials with CyHV-2 vaccine prototypes. Despite the resistance that has emerged among some goldfish breeds (or at least some populations thereof) to certain CyHV-2 strains, newly emerged strains of CyHV-2 remain a problem for both domesticated and wild *Carassius spp*. [30,31]. Consequently, in the present study we sought to identify novel CyHV-2 strains that exhibited sufficient and consistent virulence in Shubunkin goldfish,

which would result in the establishment a more optimum CyHV-2 in vivo infection model to use in advancing our understanding of this virus.

As part of this process, we successfully prepared three novel CyHV-2 isolates from different internal organ samples originating from a high mortality CyHV-2 outbreak among goldfish and gibel carp in the Netherlands, which we designated NL-1, NL-2, and NL-3. We then compared their genetic characteristics to other sequenced strains, and in order to identify the optimum strain to use as part of a future CyHV-2 *in vivo* infection model, we compared their biological properties *in vitro* and *in vivo*. Through this process we selected the most suitable isolate for further comparison to the CyHV-2 ST-J1 reference strain. This revealed that NL-2 isolate was (*i*) much virulent in our CyHV-2 Shubunkin goldfish model compared to the reference strain, while (*ii*) also being highly compatible with long-term stable culture in vitro. These properties make the NL-2 isolate much more valuable for incorporation into our CyHV-2 -Shubunkin goldfish model. Importantly, the establishment of this new CyHV-2 *in vivo* infection model now greatly facilitates further avenues for research into CyHV-2 pathogenesis and disease mitigation.

Material and Methods

2.1 Sample Collection and Handling

Three independent pools of internal organs were collected from The Netherlands from diseased fish, including goldfish and gibel carp. Samples were designated the names NL-1 (unknown Goldfish breed; WBVR 16009271), NL-2 (Shubunkin Goldfish; WUR-NL-18015159-3), and NL-3 (Gibel carp; WUR-NL-16010689), respectively, according to the order in which samples were transferred to our laboratory. Each sample was processed separately. Samples were first homogenized with pestle and mortar and resuspended in 2 mL M199 medium (HEPES buffered; Sigma, Kawasaki, Japan), the suspension was clarified by centrifugation at 3000 ×g, 4 °C for 15 min (Allegra X-15R, Beckman, Brea, CA, USA). After centrifugation, the supernatant was separated from the tissue pellet. The supernatant was filtered twice using a cell strainer with a diameter of 100 µm, then filtered with a disposable needle filter with a pore size of 0.22 µm. Purified supernatant was then aliquoted and stored at –80 °C (designated as passage #0). DNA extraction was performed with the remaining tissue pellet using a commercial nucleic acid extraction kit (QIAamp DNA Mini Kit, QIAGEN, Germany). DNA samples were stored at -20 °C for further analysis.

2.2 *In vitro methods*

2.2.1 CyHV-2 PCR Detection

To confirm the presence of CyHV-2 in the samples, the DNA extracted from the tissue pellets was analyzed by PCR. Briefly, this was done using the High-Fidelity PCR Mix Buffer (New England Biolabs, USA) as per manufactures instructions, with a total reaction volume of 25 µl and 2 µl template. The forward and revers primers were 5'-GGACTTGCGAAGAGTTTGATTTCTAC-3', and 5'-CCATAGTCACCATCGTCTCATC-3', respectively (based on as described by [32]). The PCR cycling conditions included an initial denaturation at 98 °C for 2 min, followed by 35 cycles at 98 °C for 30 s, 60 °C for 45 s, 72 °C for 45 s, and a final extension at 72 °C for 10 min. The PCR products were loaded into electrophoresis gels and imaged by ImageQuan 800 CCD imagers (Cytiva, USA).

2.2.2 Cells and virus

The RyuF-2 cell line was used to propagate all viral isolates used in this study and was kindly provided by Prof. Sano (Tokyo University of Marine Science and Technology, Tokyo, Japan). Cells were cultured at 25 °C with no CO_2 using Medium 199 (HEPES buffered; Sigma, Kawasaki, Japan), supplemented with 10% fetal bovine serum (FBS; Gibco, Life Technologies, Carlsbad, CA, USA), penicillin (100 U/mL), streptomycin (100 µg/mL) and Amphotericin B (0.25 µg/mL). The CyHV-2 ST-J1 strain (GenBank: JQ815364.1 or NC019495.1) was used as the reference in this study. All isolates were cultured in RyuF-2 cells at 25 °C with no CO_2 using the cell culture media described above, supplemented with goldfish kidney extract (final concentration 0.2%, prepared as Shibata *et al*. described utilizing Shubunkin goldfish kidney) [33].

2.2.3 Initial *in vitro* culture and characterization of the isolates

Serial dilutions (10-fold) of the purified organ supernatant (NL-1 #0; NL-2 #0, and NL-3 #0), were prepared. Briefly, 100 µl supernatant was mixed with 900 µl serum-free medium, and repeated to create a dilution series ranging from 10^{-1} to 10^{-3}. Six-well plates with RyuF-2 fresh cells (100% confluent, approximately 24 hours post-seeding) were inoculated with 800 µl of diluted supernatant per well, and the cells were incubated for 2 hours at 25 °C. After this initial incubation, the initial inoculum was removed from each well and replaced with 2 mL complete cell culture medium (0.2% kidney extract added) containing 2% w/v carboxymethylcellulose (CMC) [33]. These plates were then incubated for 10 days at 25 °C. Viral plaques and CPE were visually inspected and imaged using an optical microscope (Olympus CKX41, Japan), followed by indirect immunofluorescence staining as we described previously (He et al., 2023). The stained samples were imaged using an epifluorescence microscope (Leica DM2000).

2.2.4 Plaque purification and Amplification

The earlier experimental procedure describing the initial *in vitro* culture and characterization of the isolates was replicated. At 10 dpi (days post inoculation), using an optical microscope, isolated viral plaques were identified in inoculated wells. Infectious material was collected by submerging a sterile pipette tip in the 2% CMC complete media,and allowing it to come into physical contact with the centre of the plaque and aspirating 10 µL of the serum-free culture medium and immediately collecting it again in the pipette tip. This 10 µL media was then transferred 90 µL of serum-free culture medium, as a means of collecting plaque-purified infectious material for later use. These 100 µL samples of plaque purified isolates were immediately stored at -80°C. Three independent viral plaques were purified for each isolate and designated as the first passage (#1). In order to amplify these plaque-purified sub-cultures, they were serially passaged in cell culture flasks. As part of this process, the 100 µL if each isolate was thawed, diluted in 900 µL complete media and used to inoculate 100% confluent cell culture flasks (175 cm^2). After two hours, add kidney extract to the culture medium to a final concentration of 0.2%. Once CPE became widespread (~10dpi; gentle shaking twice per day during the culture period to help the virus spread), viral culture media was collected, centrifuged at 300 x g for 5 minutes at 4°C and the viral supernatant was split into 1 mL aliquots. These aliquots were either immediately stored at -80°C or used to inoculate new cell culture flasks as part of serial viral passaging, with viral culture proceeding as described above.

2.2.5 Viral DNA Extraction and Restriction Fragment Length Polymorphism (RFLP) Analysis

Plaque purified sub-cultures were diluted in 1 mL complete culture medium, (NL-1 #1, NL-2 #1 and NL-3 #1) and used to inoculate 100% confluent cell culture flasks (175 cm^2), as described earlier. At 10 dpi viral culture media was collected and centrifuged at 3000 ×g, 4°C for 15 min (Allegra X-15R Centrifuge, Beckman, Brea, CA, USA) to remove cell debris. Viral supernatant (35 mL from each 175 cm^2 flask) was transferred to ultracentrifuge tubes and centrifuged at 100,000 ×g for 1 hour at 4°C. The supernatant was discarded after centrifugation and residual liquid drops on the tube borders were removed with a swab. The viral pellet was suspended in 1 mL TE buffer (0.1% NP40) and incubated in a

37°C water bath for 20 minutes, gently mixing every 5 minutes. It was then incubated at 56°C for an additional 10 minutes to accelerate pellet dissolution. 30 mL of cold TE buffer (4°C) was added to the tube after complete pellet dissolution. 5 mL of cold 30% sucrose was added to the the bottom of the tube using a glass Pasteur pipette. The tube was centrifuged at 100,000 ×g for 2 hours at 4°C. After this, the supernatant was discarded, and the pellet was resuspended in 450 µL of TE buffer. 50 µL of filtered 10% SDS and 20 µL of proteinase K (25 mg/mL) was added and mixed thoroughly. The tube was covered with a lid and incubated at 56°C water bath for 2 hours, shaking occasionally. After this, the sample was transferred to a 2 mL tube and mixed with 510 µL Phenol Chloroform (4°C). The mixture was agitated gently inverting the tube several times, and then centrifuged at 18,000 ×g for 15 minutes at 20°C. After centrifugation, the aqueous phase was carefully removed and transferred to a new 2 mL tube and the volume was topped up to 500 µL with ddH_2O. 1 mL of absolute ethanol and 50 µL of 3M AcNa (sodium acetate) was then added to the mixture. The sample was submerged in liquid nitrogen until frozen, then thawed by warming in a 37°C water bath until it formed a jelly-like consistency. At this point it was then centrifuged at 18,000 ×g for 15 minutes at 4°C. The supernatant was discarded and 600 µL of 70% ethanol was added followed by centrifugation again at 18,000 ×g for 15 minutes at 4°C. The pellet was air-dried at room temperature (RT) until transparent and then resuspended in 50 µL ddH_2O by incubating overnight at 4°C. After this the extracted and purified viral DNA was aliquoted and stored at -20°C for future use. The genomic diversity of the isolated strains was then investigated by SacI restriction RFLP analysis. Briefly, 3 µg of genomic DNA was digested using SacI (New England Biolabs). After 6 hours of digestion, fully digested DNA productions were separated in 0.8% electrophoresis agarose gel at 60 V for 18 h and imaged.

2.2.6 Genome Sequencing and Phylogenetic analysis

DNA was extracted from 3 independent plaque purified subcultures from NL-1, NL-2 and NL-3 (9 samples in total) as described earlier and full-length genome sequencing was performed. DNA samples were submitted for Illumina paired end sequencing (MiSeq Kit v3 600 cycles). Raw reads (in fastq format) were processed using BBduk (v38.26) [34] facilitating adaptor sequence removal and quality trimming. This was followed by an assessment of processed fastq files using FastQC (v0.11.8). Processed reads were used as input for reference guided assembly using an in house modified version of the popular de Bruijn graph based assembly tool “spades” v3.15.2 [35].

The modifications to the publicly available version of spades specifically involved increasing the maximum kmer size from a default of 127 to 251, thus utilizing larger portions of individual reads during assembly process, with the aim of improving the performance of spades, specifically the assembly of low-complexity regions, where ambiguous assembly (regarding the number of repeat units), reduced assembly scaffold contiguity. To achieve this, the following modifications were made to the publicly available source code: i) Line 224 in the spades_compile.sh script was replaced with “cmake -G "Unix Makefiles" -DCMAKE_INSTALL_PREFIX="$PREFIX" -DSPADES_MAX_K=251 $* "$BASEDIR/src”, ii) CMake (v3.15.3) was loaded in local Linux environment, and the modified

compilation script was run per standard installation instructions, iii) after compilation and the creation of the python script "options_storage.py" in /share/spades/spades_pipeline/, this new script was edited at line 59 to "MAX_K = 251" to ensure longer kmers would be tolerated when running spades, and line 74 was changed to "K_MERS_250 = [21, 33, 55, 77, 99, 127, 249]" to ensure that longer kmers were automatically included when spades generated combined assembly from different kmer sizes (note: for memory reasons, a value of 249 is used here as it is just under the new maximum limit of 251), and iv) as these modifications to utilize longer kmers caused run failure in initial testing due to memory issues, lines 69 and 70 of the python script "options_storage.py" were also changed to "THREADS = 32" and "MEMORY = 800" respectively, thus allowing assembly processes to successfully run to completion.

The assembly quality was assessed via QUAST [36] (v5.2.0), which revealed improved N50 metrics (measurement of contiguity of assembles) using the in-house version of the spades tool compared to the publicly available version. This also resulted in the assembly of low complexity regions (which were previously skipped, causing breaks in scaffolds when using the publicly version of spades). Elsewhere, the accuracy of low complexity region assembly using this in-house version of spades (i.e. regarding true number of repeat units present in these regions) was confirmed using PCR after *de novo* assembly of recombinant viral genomes generated in our lab. This in-house modified version of the spades tool is available to all Wallonia-based researchers via the Consortium des Équipements de Calcul Intensif (CECI).

Assembly graphs generated with the in-house version of spades with scaffold(s) in .gfa format were opened up using Bandage (v0.8.1) [37] for inspection, and alignment to local BLAST database representing the CyHV-2 reference strain, ST-J1 (NC019495.1). Individual scaffolds mapping to reference sequences, and thus collectively representing full-length assembled genome, were identified from inspection of the BLAST output in Bandage. Where multiple scaffolds matched the reference genome, full-length recombinant genomes were derived from concatenating these scaffolds based on overlaps at their terminals, this was done using SnapGene (v6.2.1) [38]. For isolates, NL-1, NL2 and NL-3, there were three reassembled genomes (each representing an independent plaque purified subculture). Taking each isolate separately, genome reassemblies of the three plaque purified subcultures were aligned to each other using MAFFT (v7) [39], and the output alignment was exported as a fasta file. This revealed little or no difference between plaque purified subcultures derived from the same isolates. The alignments of genomes from these subcultures were imported into SnapGene to generate consensus sequences for each isolate (>50% agreement).

Once the consensus sequences for NL-1 NL-2 and NL-3 were established as described earlier, we aligned these three sequences to other complete CyHV-2 genome sequences using MAFFT. Complete CyHV-2 genome sequences were compiled based on the accession numbers of fully sequenced CyHV-2 genomes listed in the NCBI Viral Genome Browser [40,41]. The alignment was exported in fasta format, imported in the MEGA (v11) [42] as an alignment and saved as MEGA format data file (.meg). This .meg format file was opened up in MEGA again, and used to generate a phylogenetic tree

using the UPGMA method, with topology confidence evaluated using bootstrapping (1000 iterations). The other complete genome sequences also used in analysis included an additional isolate that was sequenced in-house (YC-01) and the six available in full length CyHV-2 sequences in GenBank, which were CNDF-TB2015 (MN201961.1), YZ-01 (MK260012.1), SY (KT387800.1), SY-C1 (KM200722.1), ST-J1 (NC019495.1) and YC-01 Unverified (MN593216.1).

In order to understand the consequences of the differences between the newly assembled genomes of the isolates and the CyHV-2 ST-J1 reference genome, a list of differences relative to the reference genome were compiled and followed by inspection of their genomic context (i.e. coding/noncoding region etc.) and consequences (synonymous, non-synonymous amino acid change, frameshifts, ORFs impacted etc.). To achieve this, the consensus sequence for each fully assembled isolate was aligned to the CyHV-2 ST-J1 strain using MAFFT, and the resulting alignment was exported as a fasta file. All differences in the consensus relative to ST-J1 were summarized in variant call format (VCF) by converting the fasta alignment to a VCF file using the msa2vcf.jar tool [43,44]. The VCF file was opened in Excel, and each variant co-ordinate, which was in the context of the alignment only, was transformed to the corresponding coordinates in the ST-J1 reference strain. This was done by using an Excel formula to take into account the cumulative gaps in the ST-J1 and consensus sequence that had occurred prior to each variant call. The updated co-ordinates of these variants were verified by manually inspecting the raw read mapping data. This was done by building an index of the ST-J1 reference sequence and mapping processed reads to from each new isolate to the index using HISAT2 (v2.1.0) [45,46]. The mapping output was then converted from SAM to compressed BAM format using SAMTools (v1.9) [47], and finally raw mapping data (BAM format) was inspected using Integrative Genomics Viewer (IGV) (v2.8.0) [48]. Inspection involved sampling random variants described in the updated VCF file (co-ordinates and expected differences relative to ST-J1 reference) and using IGV to locate and verify the presence of these differences in reads from new isolates that were mapped to the ST-J1 reference by HISAT2.

The updated VCF files (with variant locations corresponding to the ST-J1 reference) were utilized to identify the consequence of each mutation in the consensus sequence relative to the ST-J1 reference strain using VEP (v107.0) [49]. To do this, the updated VCF, the ST-J1 sequence (fasta format) and ST-J1 feature co-ordinates (GFF format) were then used as input for VEP. Using a combination of grep, sort and bgzip tools in Linux, the first line of the GFF file was removed, contents were sorted by coordinates, and finally it was compressed in .gz format before being used as input for VEP.

Maps of each fully assembled genome were generated using Geneious Prime (v11.0.4+11) [50]. First, using SnapGene, the sequence of each assembled genome was annotated with the location of CyHV-2 ORFs and terminal repeats by importing features ($\geqslant$ 99% similarity) from a separate SnapGene file of the ST-J1 genome (initially downloaded as .gb file from GeneBank, opened in SnapGene and saved as SnapGene format .dna file). Using SnapGene, the annotated versions of each

newly assembled genome were saved as .gb files and imported into Geneious Prime. These maps were converted into GFF files and exported from Geneious Prime in GFF format, which were opened in Excel and modified to remove excess annotation. The fasta files for each assembly were then imported into Geneious Prime, along with the modified GFF files defining ORF annotations, and together they were used to generate a map of each fully assembled genome with ORFs. The locations or all mutations relative to the ST-J1 reference strain were also added these maps, by importing another GFF file defining the locations of each variant. This GFF file was generated by converting the same VCF file (with co-ordinates for each variant, and also used earlier as input for VEP) into GFF format using the python script vcf_gff.py [51,52]. After this, the GFF was opened in Excel and the locations of each variant, initially provided as ST-J1 co-ordinates, were converted to their corresponding co-coordinates for each newly assembled isolate using an Excel formula (described earlier). By calculating the lengths of each corresponding variant sequence which was stored in the "attributes" field (as a consequence of conversion from a VCF file) for each variant in the GFF, Excel formulas were used to classify each variant as an SNP or multiple-base-change / indel, and this information was added to the "type" field (column 3) for later utilization by Geneious Prime when generating a map. Feature names were also deleted from the attribute field of the GFF using Excel. This modified GFF was then imported Geneious Prime and used to update the maps with the location of each variant relative to the ST-J1 strain. Maps were then converted to PNG images.

All Linux based work on this project was conducted by our team via the NIC5 computing cluster which is part of the CECI and administered by ULiege.

2.2.7 Viral Growth Assay

Viral growth assays were conducted using the same inoculation method. CyHV-2 supernatant was diluted in serum-free media to achieve a specific multiplicity of infection (MOI) in each well. Triplicate cultures of RyuF-2 cells grown in 6-well plates were infected with 1 mL viral supernatant. After a 2-hour incubation period, the cells were washed with serum-free media and overlaid with complete cell culture medium supplemented with 0.2% kidney extract. At selected timepoints post infection, both viral supernatant and infected cells were collected from each well, the mixture was separated by centrifugation, and stored at −80°C. These samples were later thawed and analysed by viral titration using triplicate plaque assays in RyuF-2 cells. Different inoculum doses and sampling time points were used across various experiments (*i*) An MOI = 0.0001 was used for the comparison between NL-1 #10, NL-2 #10 and NL-2 #2, with time points at 8, 12, and 16 dpi. (*ii*) An MOI = 0.01 was used for the comparison between ST-J1 #10 and NL-2 #10, with time points at 4, 6, 8, and 10 dpi.

2.2.8 Viral Plaque Size Assay

RyuF-2 cells were cultured in six-well plates and inoculated with 100 PFU/well of virus, followed by a 2-hour incubation period. After incubation, the cells were washed with serum-free medium and then overlaid with culture medium supplemented with 1% (w/v) CMC and 0.2% kidney extract. At different time points, viral plaques were visualized by indirect immunofluorescent staining as described

in the CPE Imaging section. After a final wash with PBS, 20 randomly selected individual plaques were imaged using the Incucyte live cell analysis system (Sartorius, Germany), and their areas were measured manually using ImageJ software (Version 2.14).

2.3 *In vivo*

2.3.1 Fish

Two different sizes of Shubunkin goldfish (Carassius auratus) were utilized in this study, both at the adult developmental stage. The larger subjects had an average weight of 12 g (12 ± 1.4 g), while the smaller group averaged 6 g (5.84 ± 0.6 g). Mature Shubunkin goldfish were obtained from an accredited commercial company (Ruinemans Aquarium, Montfoort, The Netherlands). Microbiological, parasitic, and clinical examinations were conducted immediately upon arrival at the animal facility and then monthly to monitor fish health. PCR analysis of kidney homogenate confirmed that the adult goldfish from the colony were free of CyHV-2. Fish were maintained in 60 L freshwater recirculation tanks at 25°C until they were transferred to L2 facilities for infection experiments.

2.3.2 Infection of Fish with CyHV-2

Different modes of inoculation were used depending on the different test subjects and viral strains. *(i)* Basic evaluation of the inherent pathogenicity of NL-1, NL-2, and NL-3: The original supernatant of the three new isolates (NL-1 #0, NL-2 #0, and NL-3 #0) was diluted 10-fold using serum-free medium and kept on ice. Shubunkin goldfish (Big: average weight 12 ± 1.4 g; Small: 5.84 ± 0.6 g) were anesthetized by immersion in water containing benzocaine (25 mg/L). Once the fish were sluggish, the virus was injected intraperitoneally using a 300 µL syringe (BD Micro-Fine), with each fish receiving a dose of 100 µL (big) or 50 µL (small). After injection, the fish were placed in an aerated recovery bath for 10 minutes and then returned to the tank. Similarly, a mock group was injected with the same dose of culture medium. The experiment included 10 fish per group. Survival status and clinical manifestations were recorded daily, and the survival rate was calculated at the end of the experiment. On the 5th day post-injection (dpi), 10 sentinel goldfish were added to each tank as cohabitation fish. (*ii*) Comparison of *in vivo* pathogenicity of NL-2 strain and ST-J1 reference strain after 10 *in vitro* passages: The concentrations of NL-2 #10 and ST-J1 #10 were adjusted using culture medium to a final 2×10^4 PFU/mL. After administration of anesthesia as described above, inoculation was performed by intraperitoneal injection. Smaller Shubunkin goldfish (5.84 ± 0.6 g) were used, with three replicates of 10 fish for each virus strain. Each fish received a dose of 1000 PFU in 50 µL. The mock group underwent the same operation using the complete culture medium. Survival status and clinical manifestations were recorded daily, and the survival rate was calculated after 30 days post-injection. At 5dpi, two replicate groups for each virus strain were selected and placed with the same number of sentinel goldfish, and fish status was monitored as describe earlier for 30 days (*iii*) Comparison of virus pathogenicity under immersion infection: The subjects (5.84 ± 0.6 g) were inoculated by immersion in water containing the virus, thus simulating the natural infection route. ST-J1 #10 and NL-2 #10 were diluted ten-fold using

water at approximately 25°C to reach a final concentration of 2000 PFU/mL. After a 2-hour immersion (10 fish/L), the fish were returned to the 60 L tank. The mock group underwent the same process using the complete viral culture medium. Three replicates were included for each virus strain, with 10 fish in each replicate. Survival status and clinical symptoms were recorded daily, and the survival rate was calculated after 30 days post-injection.

2.3.3 Electron Microscopy

The kidney for the Electron microscopy exam was collected from moribund goldfish which was inoculated by IP injection 100 μL of NL-2 (p#0, 10-fold dilution). It was fixed for 2 h at room temperature in 2.5 % glutaraldehyde in 0.1 M Sörensen's buffer pH 7.4. After several washes in the same buffer, the samples were post-fixed for 60 min with 2 % osmium tetroxide in Sörensen's buffer, washed in deionized water, dehydrated at room temperature through a graded ethanol series (70, 96 and 100 %) and embedded in Epon for 48 h at 60 °C. Ultrathin sections (70 nm thick) were obtained utilizing an ultramicrotome (Reichert Ultracut E) equipped with a diamond knife (Diatome), were mounted on copper grids coated with collodion and were contrasted with uranyl acetate and lead citrate for 15 min each, and viewed by transmission electron microscopy (TEM) (Hitachi H-600 electron microscope operated at 75 kV).

2.4 Statistical Analysis

Two-way omnibus tests on data from the viral growth curve and plaque size experiments were conducted using two-way tests. First a two-way ANOVA model was generated using the anova function in R (v4.2.2) (part of the R core package) [53]. The residuals of this model were checked for normality using the Shapiro-Wilk test implemented using the shapiro.test function in R (part of the R core package). If normal distribution was observed, the significance of each variable on outcome was taken from the two-way ANOVA model, and multiple comparisons were conducted using a Tukey post hoc test implemented using the TukeyHSD function in R (part of the R core package). In the cases where normal distribution was not observed, analysis was performed using a generalized linear model (GLM) implemented using the glm function in R (part of the R core package), with Family option: "gamma", and Link option: "log". To determine the significance of each variable on outcome, the model was analysed using type III sum of squares test, implemented using the Anova tool from the R "car" package (v3.0–6) in R [54], with the default contrast coding in R adjusted appropriately prior to the use of the glm function to facilitate the use of type III sum of squares test. In such cases post hoc multiple comparisons tests were conducted on the same model using a least squares means test implemented using lsmeans tool from the "lsmeans" package (v2.3.0) in R [55], with BH correction. Survival curves were compared using the log-rank test implemented in GraphPad prism 8.0. All graphs were also generated using GraphPad 8.0. Only significant p-values (<0.05) are reported in the results section. For the purposes of visual clarity, only results from post hoc multiple comparisons are indicated in each corresponding figure and are represented using the following symbols: ns = not significant, * = $p < 0.05$; ** = $p < 0.01$; *** = $p < 0.001$.

2.5 Ethics Statement

The experiments, maintenance, and care of fish complied with the guidelines of the European Convention for the Protection of Vertebrate Animals used for Experimental and other Scientific Purposes (CETS No. 123). The animal studies were approved by the local ethics committee of the University of Liège, Belgium (Laboratory accreditation No. 1610008). All efforts were made to minimize suffering.

Results

3.1 Confirmation of CyHV-2 presence in pooled organ samples.

Three pooled organ samples from fish initially suspected of being infected with CyHV-2 were generously provided by Wageningen University in The Netherlands. We assigned them the names NL-1, NL-2 and NL-3 (see Materials and Methods section for details). Upon arrival in our lab, these samples were screened for the presence of CyHV-2 using a PCR assay targeting the CyHV-2 helicase gene. Through this process, we confirmed the presence of the virus, with the expected 366 bp PCR product forming in all three samples (Fig. 1 A).

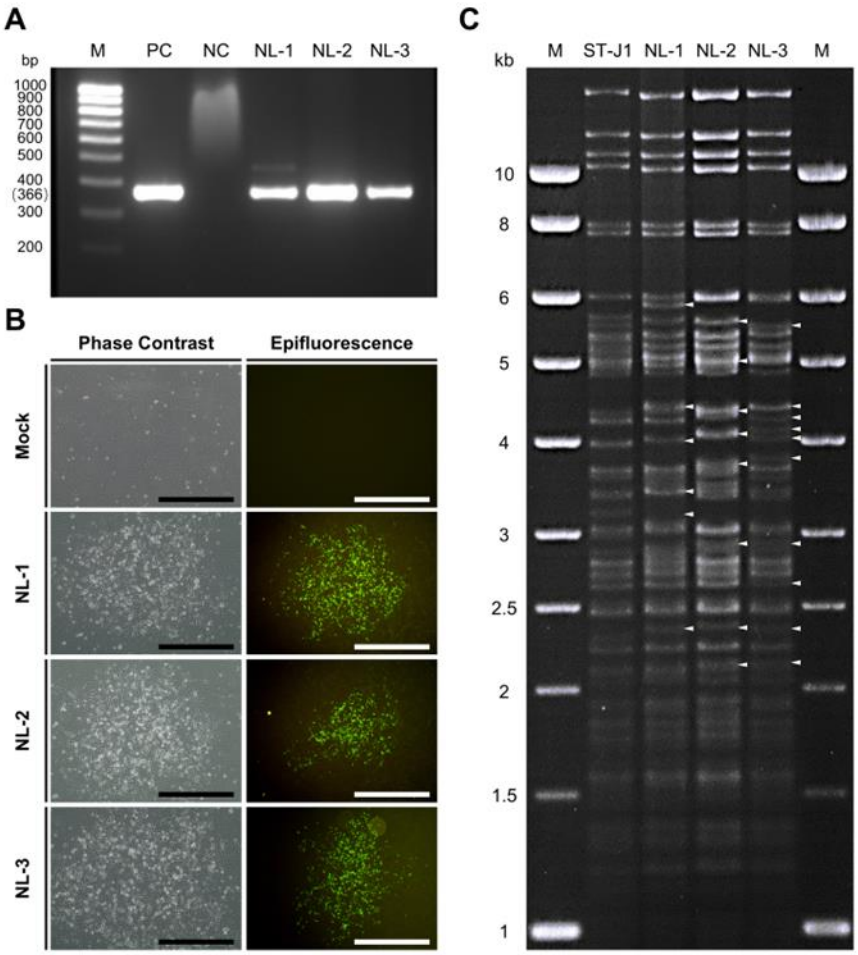

Figure 1. (A) PCR screening for CyHV-2 in three samples from The Netherlands. M: molecular weight marker (bp: base pair); PC: positive control (from ST-J1); NC: negative control; NL-1: NL-1 tissue DNA; NL-2: NL-2 tissue DNA; NL-3: NL-3 tissue DNA. (B) CPE imaging via microscopy at 10 dpi. The left and right panels represent the brightfield and epifluorescence channels respectively, with different representative plaques shown in each channel. CPE was only observed in RyuF-2 cells inoculated with purified the tissue supernatant from NL-1 #0, NL-2 #0, and NL-3 #0, and was entirely absent from the mock control. Black scale bar = 600 µm, white scale bar = 500 µm. (C) Genomic analysis of CyHV-2 strains. Viral DNA from plaque purified sub-cultures from ST-J1, NL-1, NL-2 and NL-3 (one from each) were compared by RFLP analysis after digestion using the SacI restriction enzyme. The white arrowhead indicates the most notable differences relative to the ST-J1 reference strain. M: molecular weight maker (kb: kilobase).

In parallel, RyuF-2 fresh cells were inoculated with dilutions of purified supernatant prepared from the NL-1, NL-2 and NL-3 pooled tissue samples (passage #0 or p#0, see Materials and Methods section) and incubated at 25°C. At 10 days post inoculation (dpi), the characteristic morphology of CyHV-2 associated CPE became visible via brightfield phase contrast microscopy and eventually formed plaques. The observed characteristics included focal areas of granulation, cell vacuolization, and the emergence of rounded phase-bright cells (Fig. 1 B left panel). By approximately 14 dpi, infected cells in these plaques began to detach, with this process starting from the central regions and radiating outwards as time progressed. The same CPE-like and plaque morphology was not observed in the mock group. Notably, no syncytial plaque formation was observed in cells infected with any of the three isolates.

These regions exhibiting signs of CyHV-2 induced CPE and plaque formation via brightfield phase contrast microscopy also stained positive for CyHV-2 via indirect immunofluorescent staining and epifluorescence microscopy (Fig. 1B right panel). This indicated i) that the p#0 supernatant samples prepared from the CyHV-2 PCR-positive samples contained viable CyHV-2 virus particles and ii) that these three CyHV-2 isolates, NL-1, NL-2 and NL-3 could be cultured *in vitro*.

3.2 Virus Isolation and Amplification

While the initial *in vitro* culture of the p#0 supernatant led to the formation of CPE and plaques, for any of these new isolates to be useful as part of future CyHV-2 *in vivo* infection models, it was crucial that they could be stably passaged in cell culture. Subsequent *in vitro* passaging of these three isolates revealed significant differences in the *in vitro* propagation of NL-1, NL-2, and NL-3 in RyuF-2 cells. Only NL-1 and NL-2 isolates could be consistently passaged successfully, reaching up to ten passages (#10). Conversely, the NL-3 isolate could not be passaged beyond p#3 in RyuF-2 cells, with cytopathic effects disappearing in the subsequent passages.

3.3 Genomic and Phylogenetic Analysis

At p#1, three independent plaques were sub-cultured from each isolate, amplified for one passage in cell culture flasks, generating p#2. At 10 dpi, viral culture media was used to prepare viral supernatant for subsequent virion purification and for extraction of pure viral DNA (i.e. free of host cell DNA), which would be suitable for genomic analysis. In addition, the CyHV-2 reference strain ST-J1 was used as a reference for comparative analysis.

Since the samples originated from distinct geographic regions and hosts, we hypothesized that the NL-1, NL-2, and NL-3 CyHV-2 isolates may represent genetically distinct CyHV-2 lineages. To investigate this further, used RFLP to conduct a quick preliminary analysis on one plaque purified subculture from each isolate. The results, are presented in Fig. 1 C. This indicated that the NL-1, NL2 and NL-3 exhibited major genetic differences relative to the ST-J1 strain. While some of these differences were common to two or more of these isolates, indicating that they were more closely related to each other than to the ST-J1 reference, the results also indicated notable differences between the three isolates, indicating that they were also somewhat genetically distinct from each other.

To determine the exact nature of the differences, viral DNA prepared from purified virions of each NL-1, NL-2 and NL-3 were also subject to genomic sequencing. As part of this process, three independent plaque purified sub-cultures (or replicates) were sequenced from each isolate. Genome assembly revealed little or no differences between the plaque purified sub-cultures of individual isolates. For each isolate, the sequences of the three purified sub-cultures were used to generate a single reprehensive consensus genome sequence, which was used in further analysis. The results of genome sequencing were in agreement with the RFLP analysis, indicating that each isolate exhibited many differences (each exhibiting >600 differences) relative to the ST-J-1 reference strain. These are presented in Fig. 2, described in detail in Tables S1-S6, and summarized in Table 1. Some of these included major changes such as frameshifts in several ORFs of unknown function, however, as expected, the majority of the changes consisted of single nucleotide polymorphisms (SNPs) (Fig. 3A Left) and Table 1) and either occurred outside of protein coding regions or were synonymous mutations with no impact on the amino acid sequence (Fig. 3 A Right).

Table 1. Genomic Variants Classification and Calculate Consequences. Variant classes are as defined as per https://www.ensembl.org/info/genome/variation/prediction/classification.html. Consequence types are as defined by the Sequence Ontology (SO) project and summarized here: https://www.ensembl.org/info/genome/variation/prediction/predicted_data.html.

		NL-1		NL-2		NL-3	
		Number	Proportion	Number	Proportion	Number	Proportion
Variants Class	Indel	13	2.2%	27	3.7%	23	3.1%
	Substitution	40	6.6%	45	6.1%	31	4.2%
	Insertion	117	19.4%	130	17.7%	153	20.5%
	Deletion	138	22.9%	179	24.4%	165	22.1%
	SNV	295	48.9%	353	48.1%	374	50.1%
Consequences	Stop gained	0	0%	0	0%	1	0.1%
	Frameshift*	5	0.8%	7	1%	8	1.1%
	Inframe insertion	29	4.8%	33	4.5%	41	5.5%
	Inframe deletion	48	8%	61	8.3%	55	7.4%
	Protein altering	2	0.3%	5	0.7%	5	0.7%
	Missenses	93	15.4%	118	16.1%	102	13.7
	Start retained	1	0.2%	0	0%	2	0.3%
	Stop retained	0	0%	1	0.1%	1	0.1%
	Synonymous	106	17.6%	125	17%	124	16.6%
	Coding sequence	1	0.2%	1	0.1%	2	0.3%
	Upstream gene	306	50.7%	358	48.8%	390	52.3%
	Downstream gene	9	1.5%	22	3%	11	1.5%
	Intergenic	3	0.5%	3	0.4%	4	0.5%

*This includes multiple frameshifts in the same ORF(s)

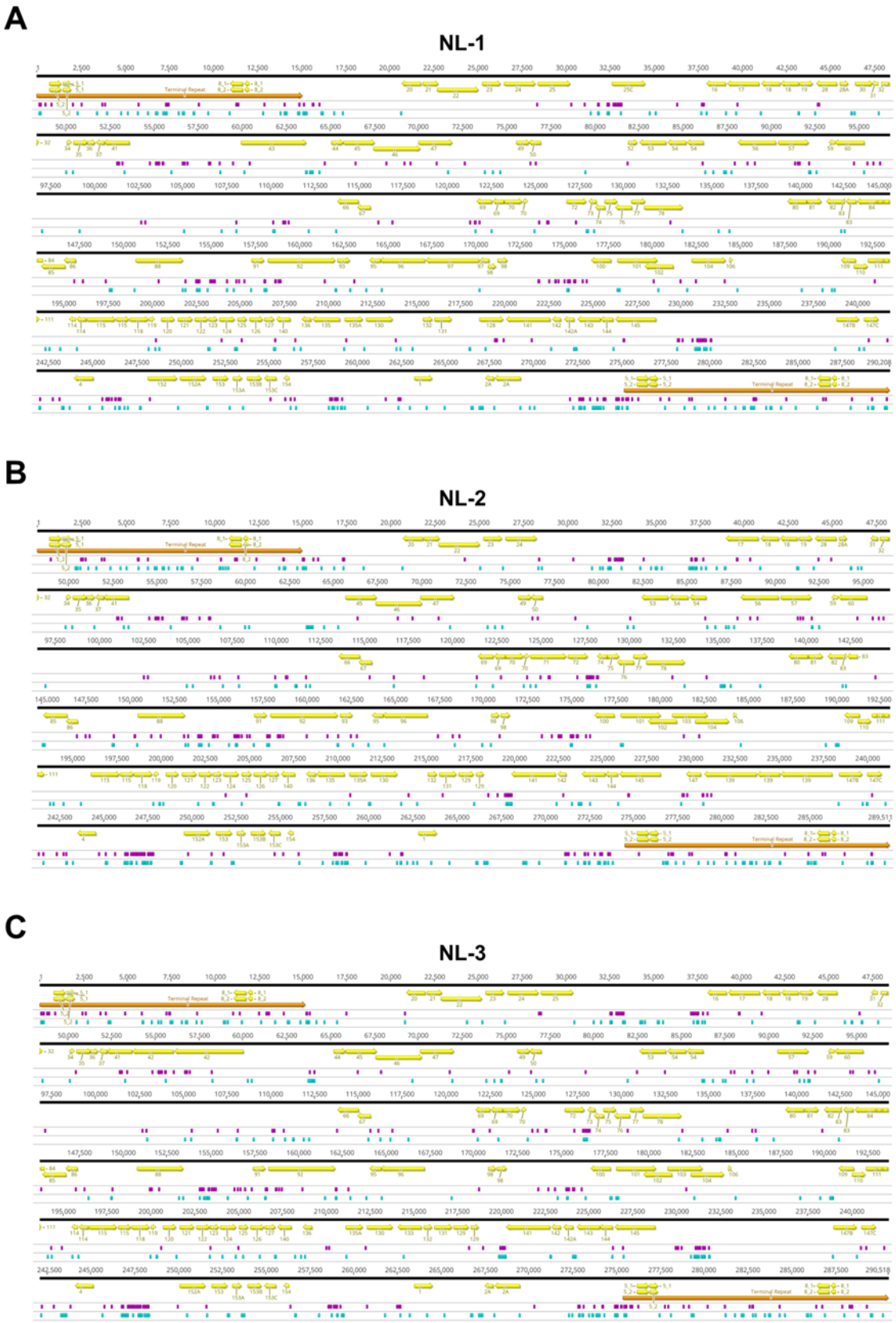

Figure 2. Schematic of (A) NL-1, (B) NL-2 and (C) NL-3 assembled genomes. Direct Terminal repeats are indicated in orange. ORFs with 99% sequence match to ORFs in CyHV-2 ST-J1 reference genome (NC_019495.1) are indicated in yellow and labelled by their corresponding ORF number in the reference genome. Single nucleotide polymorphisms (SNPs)

are indicated in purple. Substitutions involving more than one nucleotide, insertions or deletions are highlighted in turquoise. The locations of all variants are based on their starting point in each of their respective genomes, with feature lengths enlarged to ensure visualization on the map (co-ordinates correspond to the data in Tables S1, S2 and S3).

The high number of differences to the ST-J1 reference indicated that these newly sequenced isolates may not be as closely to the ST-J1 strain, while the commonalities observed in the RFLP analysis, indicated that they may be more related to each other than to the ST-J1 strain. To examine this further, a phylogenetic tree was constructed based on sequences of all known currently available CyHV-2 genomes and these newly sequenced isolates (Fig. 3B). This analysis indicated that, indeed, the new NL-1, NL-2 and NL-3 isolates were more closely related to each other than to the ST-J1 reference strain which represents the J Genotype (Fig. 3B). Notably the three new isolates are more related to the C Genotype strains (Fig. 3B). Within this large C Genotype clade, NL-1, NL-2 and NL-3 occupy separate sub-clades, indicating that they are indeed genetically distinct from each other. As a positive control for our genome assembly workflow, we also assembled the YC-01 genome. Our YC-01 assembly was almost identical to the publicly available YC-01 genome sequence, with notable genomic rearrangements and inversions relative to other strains [56], which is currently described as “Unverified” in GeneBank. Indeed, the YC-01 strain is more distantly related to all other fully sequenced strains (~96.7% vs >97% identity across the entire alignment length) and may represent a new distinct CyHV-2 genotype, which we provisionally propose to refer to as “Undefined” (Fig. 3B).

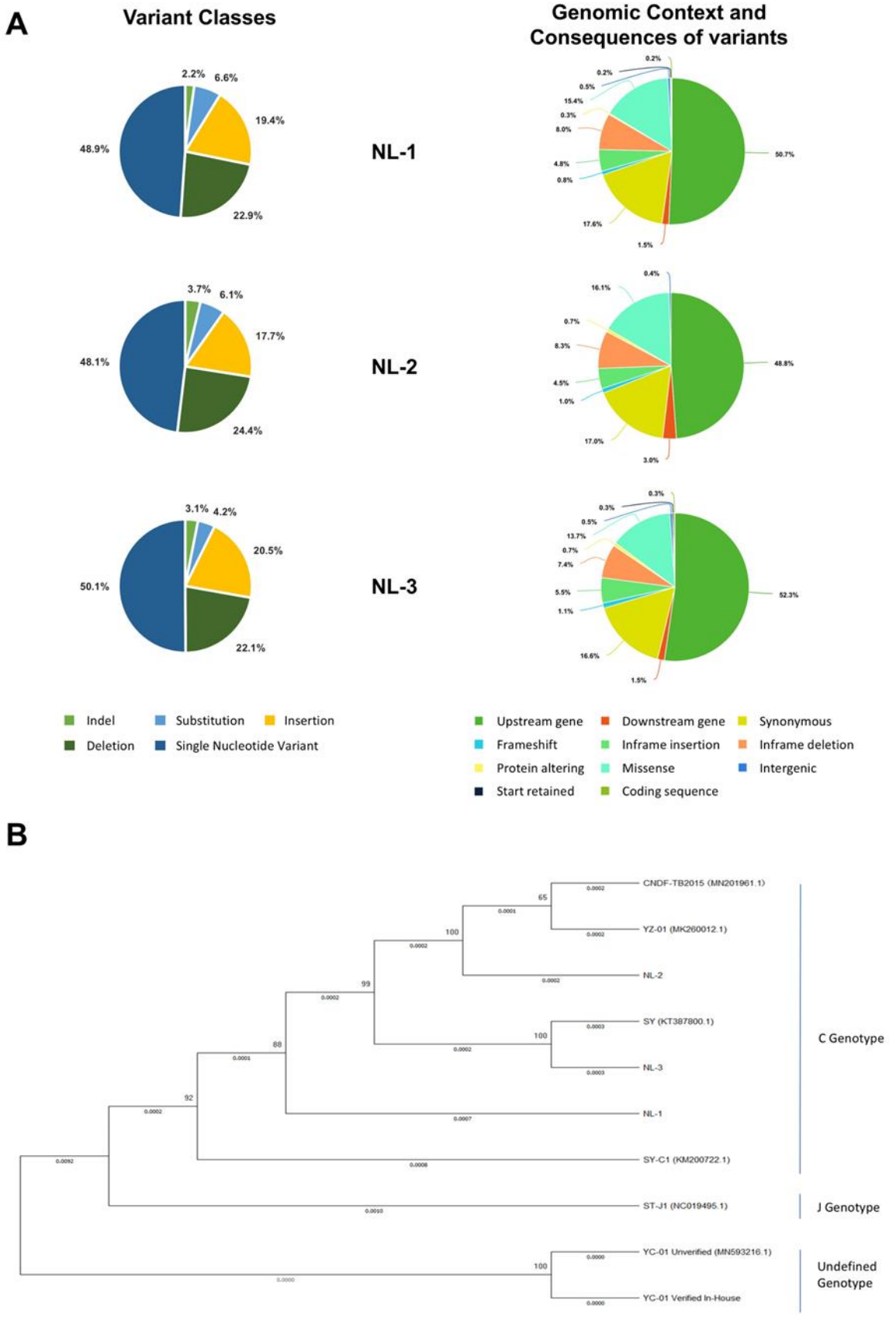

Figure 3. (A) (left) Pie charts indicating the breakdown of different variant classes that were identified in each of the newly sequenced isolates relative to the CyHV-2 ST-J1 reference strain. Variant classes are as defined as per here

https://www.ensembl.org/info/genome/variation/prediction/classification.html (Right) Pie charts indicating the breakdown of corresponding genomic context and consequences all variants identified. Mutation consequence are as defined by the Sequence Ontology (SO) project and summarized here: https://www.ensembl.org/info/genome/variation/prediction/predicted_data.html. (B) Phylogenetic tree based on complete genome sequences of CyHV-2 strains. Bootstrap values are shown at the nodes and the values below the branches represent number of substitutions per site.

3.4 The inherent pathogenicity of the three isolates

In order for any of the newly sequenced genotype isolates to useful in terms of utilization in a more virulent or robust CyHV-2 *in vivo* infection model, it was important to first determine if the p#0 inoculums we prepared were actually capable of causing clinical disease and mass mortality in commercially and economically relevant goldfish breeds. As part of this preliminary assessment of the virulence of these new isolates, we conducted *in vivo* challenge experiments using an in-house batch of adult Shubunkin goldfish, which previous to this, had exhibited substantial tolerance to the YC-01 and ST-J1 strains. In this trial, two sizes of adult Shubunkin goldfish were used. These were referred to as "small" and "big". Fish in the "big" group were twice the mean weight of the small group, and thus received a twice the volume of the non-tired p#0 inoculum relative to the small group. Subjects were inoculated either by intraperitoneal (IP) injection or by cohabitation with IP injected fish.

Mortality rates among the NL-1 and NL-2 group were similar, with both the IP and cohabitation groups showing high mortality, particularly in small fish. IP injected fish exhibited a more rapid onset of illness and clinical symptoms, with small fish mortality primarily occurring between 5 and 12 dpi (60% for NL-1, 70% for NL-2). Big fish had a longer disease course, higher survival rates and delayed death times, relative to small fish (Fig. 4A, C). Sentinel fish co-habituating with IP-injected fish exhibited lower mortality rates of 50% for NL-1 and 60% for NL-2 in small fish, both higher than the 40% seen in big fish, with NL-1 deaths concentrated between 9 and 16 dpi, and NL-2 between 11 and 20 dpi (Fig. 4B, D).

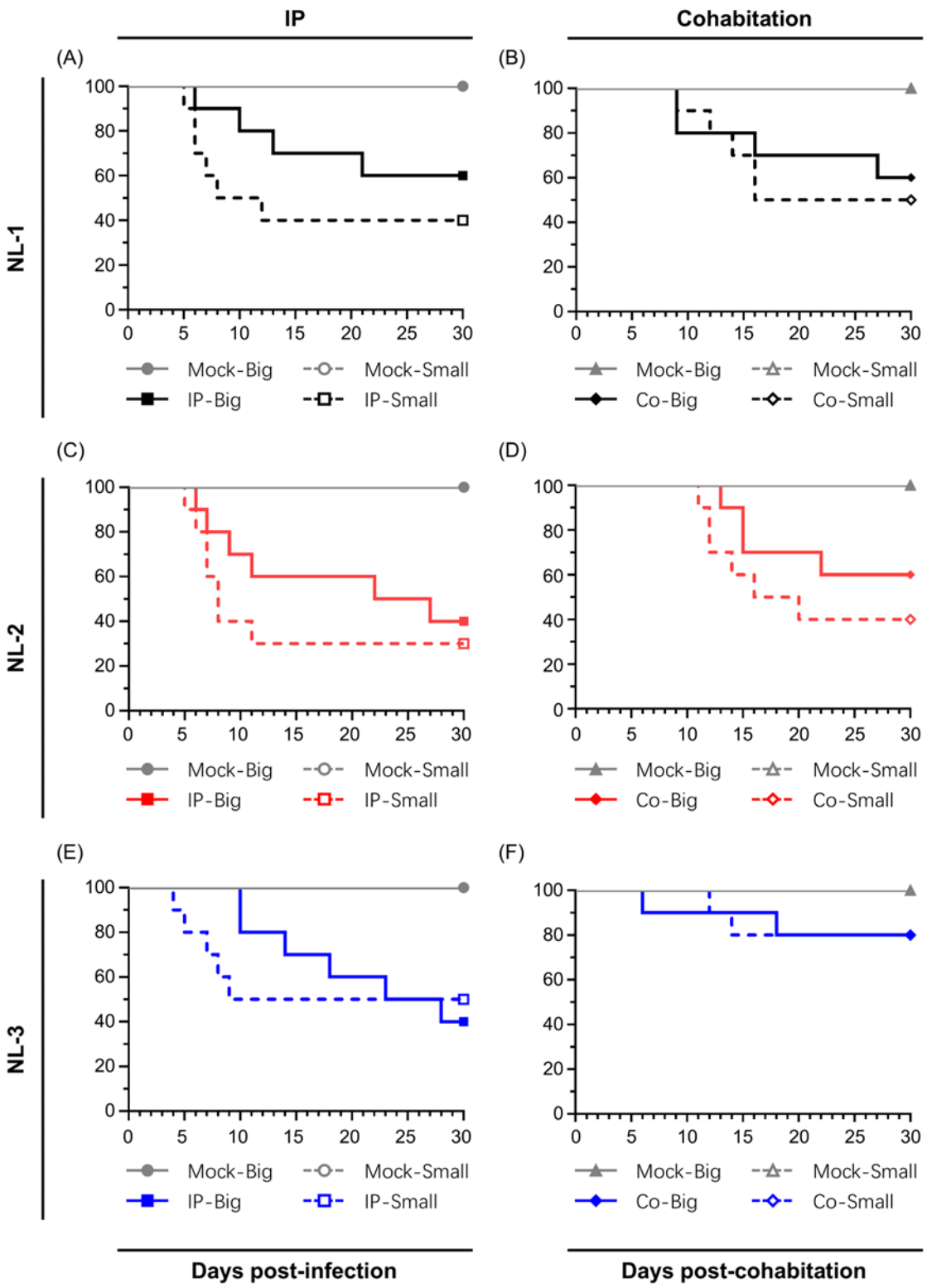

Figure 4. Primary comparison of inherent pathogenicity *in vivo* of the three isolates. The pathogenicity of the indicated strains was tested using the old adult Shubunkin goldfish (big, average weight 12 ± 1.4 g) and the young adult Shubunkin goldfish (small, average weight 5.84 ± 0.6 g). Each group consists of 10 subjects. Fish were either mock-infected or infected via IP injection with the respective strains (100 µL in big fish, 50 µL in small fish). For the cohabitation trial, 5 days post-injection, the same amount of fish was distributed into each tank. The fish were monitored daily for clinical signs of CyHV-

2 disease, and fish reaching the endpoints were euthanized. The mock-infected group is represented in gray, NL-1 in black, NL-2 in red, and NL-3 in blue.

The patterns observed in the NL-3 group were different to the NL-1 and NL-2 group. In big fish, the NL-3 inoculum induced slightly more mortality than the NL-1 and NL-2 inoculums. However, it induced similar mortality in small fish (Fig. 4 E). Furthermore, in contrast to NL-1 and NL-2, in co-habitation experiments with NL-3, limited mortality of 20% was observed among both small and big sentinel fish (Fig. 4 F). Moreover, even though one early mortality was recorded among the big sentinel fish, this mortality was not found to be attributed to CyHV-2 infection.

Overall, the results with NL-1 and NL-2 were consistent with our previous observations with the CyHV-2-Shubunkin goldfish model [25], which indicated that earlier developmental stages more permissive to CyHV-2 replication and exhibit higher mortality rates. However, again NL-3 was slightly different in this regard, while mortality certainly occurred earlier and faster in smaller fish in this group, it ceased very early. However, regardless of the isolate used, all IP infected groups fish exhibited classical clinical symptoms, including diminished appetite, lethargic swimming velocity, protruding eyeballs, distended abdomen, drooping dorsal fins, and loss of balance, with some instances of skin bleeding. Post-mortem examinations on subjects undergoing mortality during the experiment revealed severe ascites, enlarged spleen and kidneys, and white dot-like nodules within the kidneys, while the intestines were swollen with no food matter remaining, and no abnormalities were found in the gills (Supplementary Fig. 1). Sentinel fish from the co-habitation experiment exhibited similar but less severe clinical symptoms. No clinical symptoms. deaths or CyHV-2 PCR positive results were observed in the mock group.

Kidneys from subjects that underwent mortality were promptly sampled and stored at -80°C, whereas kidneys from survivors were collected at the end of the experiment. DNA was extracted from all kidneys, and subsequent PCR testing confirmed the presence of CyHV-2 in all infected subjects (data not shown). Separately, some kidney samples from fish infected with the NL-2 isolate by IP injection were immediately fixed after sampling for later analysis using high-magnification transmission electron microscopy. This provided clear evidence of CyHV-2 replication and assembly in kidney tissue (Fig. 5). Infected kidney cells exhibited nuclear changes characterized by central nucleoplasmic transparency and marginal chromatin aggregation. The nucleus contained aggregates of characteristic naked herpes-like virus nucleocapsids (90-100 nm), including incomplete particles with empty or partially complete cores, and capsids with a central electron-dense core. Potential organelle enveloped virus particles were also observed. These ultrastructural characteristics of the virus particles are consistent with those of CyHV-2 virions described in other reports [13,15,57]. Furthermore, the virus was successfully re-isolated from the kidneys in cohabitating goldfish.

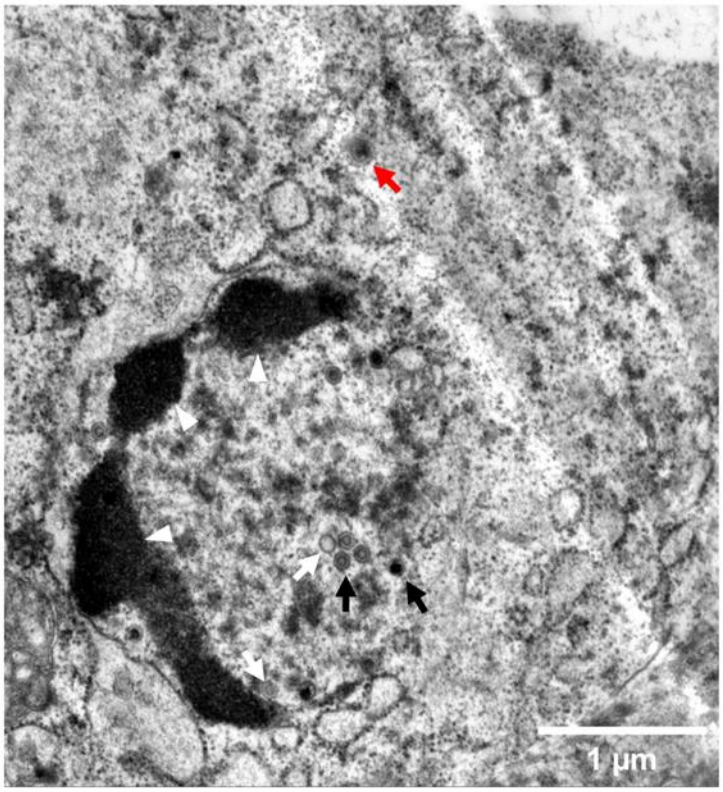

Figure 5. Ultrastructure of CyHV-2-infected cells in kidney viewed with high magnification. Marginal chromatin aggregation donated in white arrowheads. Virus particles at different stages of assembly include incomplete particles with empty or partially complete cores (white arrows), capsids with a central electron-dense core (black arrows), and some potential organelle enveloped virions (larger than nuclear viral particles), prior to egress from the cell (red arrows).

Taken together these experiments demonstrated that the p#0 inoculums prepared from NL-1, NL-2 and NL-3 tissue homogenates contained viable CyHV-2, capable of causing clinical disease and mass mortality in our Shubunkin goldfish model, and therefore we concluded that they may represent ideal candidates to replace CyHV-2 ST-J1 or YC-01 strains, which cause relatively little disease with this host model.

3.5 *In Vitro* Growth Kinetics comparison

All of the p#0 samples were shown to contain viable CyHV-2 capable of causing clinical disease in our Shubunkin goldfish model. However, to be useful in future studies, it was important that these isolates could also be easily cultured *in vitro* in order to be easily titred and to facilitate the sufficient expansion of viral stock for future *in vivo* studies. In general, the ability of a viral isolate to replicate *in vivo*, is not indicative of its ability replicate *in vitro*, or adapt quickly to this specific biological niche, and there are many factors that influence this. For example, while causing clinical disease *in vivo*, as described earlier, the passaging of the NL-3 isolate could not be sustained beyond p#3 *in vitro*, indicating that NL-3 was not practical for future use in a more robust CyHV-2 *in vivo* infection model. Therefore, we proceeded with further characterization of NL-1 and NL-2 only, which in contrast to NL-3, grew well *in vitro*, with viral titers increasing over several passages, thus providing sufficient viral

stock for further characterization. Notably, the NL-2 reached higher titers faster, indicating that it might be better adapted to *in vitro* culture. To investigate this further, we compared the *in vitro* growth kinetics of NL1 and NL-2. Importantly, to maximise the validity of the comparison, in addition to using the same dose of each isolate (MOI = 0.0001) for viral growth curves, we also compared them at the same passage number, in this case p#10, (referred to as NL-1 #10 and NL-2 #10, respectively). The results indicated that viral titers remained low initially from 8-12 dpi. However, from 12 dpi to 16 dpi, the titers of both isolates increased rapidly. At the end of the experiment, at 16 dpi, NL-2 reached titers close to 300 PFU/mL, nearly twice that of NL-1 #10, and we observed a significant difference in the growth kinetics of these two isolates at p#10, indicating that indeed NL-2 is better suited to *in vitro* culture compared NL-1 (Fig. 6A).

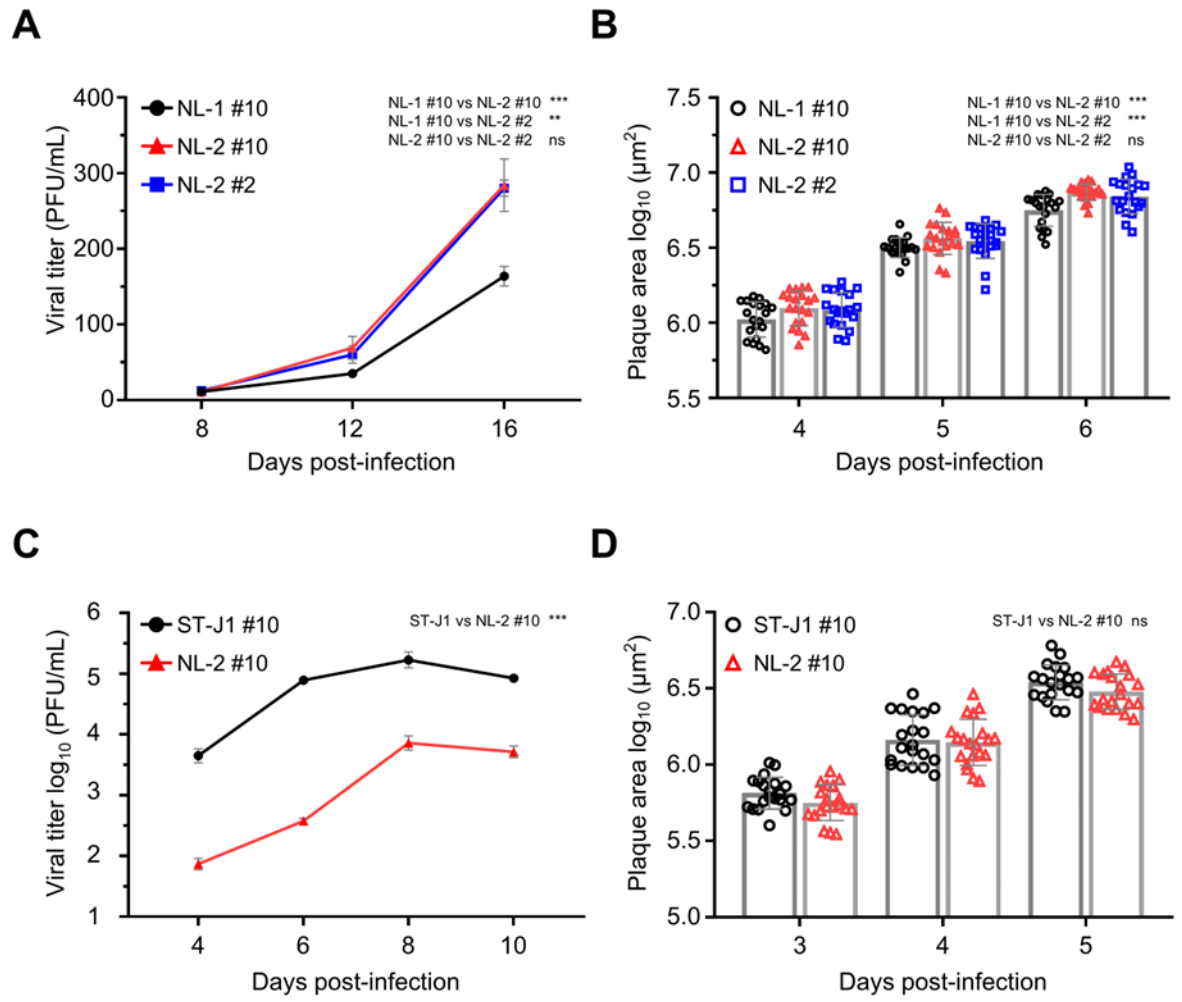

Figure 6. Comparison of *in vitro* growth kinetic and plaque sizes. (A) Viral growth curve comparison between NL-1 #10, NL-2 #10 and NL-2 #2. RyuF-2 cells were infected with the indicated strains (MOI=0.0001) and the $\log_{10}$ value of the titer (pfu/mL) in the supernatant was determined at the 8,12 and 16 dpi. Data represent the mean ± SEM of triplicate measurements. (B) Viral plaque size comparison between NL-1 #10, NL-2 #10 and NL-2 #2. RyuF-2 cells were infected with the respective strains, and plaque areas were measured at 4, 5, and 6 dpi. Data represent the mean ± SEM of 20 individual plaques. (C) Viral growth curve comparison between ST-J1 and NL-2. RyuF-2 cells were infected with the

indicated strains (MOI=0.01) and the $\log_{10}$ value of the titer (pfu/mL) in the supernatant was determined at the 4,6,8 and 10 dpi. Data represent the mean ± SEM of triplicate measurements. (D) Viral plaque size comparison in ST-J1 and NL-2. RyuF-2 cells were infected with the respective strains, and plaque areas were measured at 3, 4, and 5 dpi. Data represent the mean ± SEM of 20 individual plaques.

To explore the possibility that the superior growth kinetics of NL-2 may have been simply due to incremental adaptation to *in vitro* culture during the previous 10 passages, in parallel, we included a growth curve for NL-2 at passage #2. This indicated that there was no significant change growth kinetics of NL-2 between NL-2 between early (p#2) and later (p#10) passages (Fig. 6A). Similar patterns were also observed when comparing plaque size between the same isolates, with plaques from NL-2 #10 being slightly but significantly larger than NL-1 #10, with no difference between NL-2 #2 and NL-2 #10 in terms of plaque size. (Fig 6. B). Taken together, these experiments indicated that out of the three new isolates, the biological properties of NL-2 made it intrinsically better suited to stable and efficient culture *in vitro* and therefore potentially represented a more useful candidate for utilization in a more robust CyHV-2 *in vivo* infection model.

Next, we compared the *in vitro* growth kinetics NL-2 #10 with the CyHV-2 reference strain ST-J1, also at p#10, using an MOI of 0.01 for both. At this MOI, the progression of the viral growth curve over time was similar for both strains with viral titers increasing over the first three timepoints, peaking at 8 dpi, and decreasing by 10 dpi (Fig. 6 C). However, the viral titre of ST-J1 was higher than NL-2 at each timepoint, resulting in a significant difference between the two strains overall, demonstrating that relative to NL-2, the ST-J1 strain exhibits superior replication kinetics *in vitro*. Despite this, the comparison of viral plaque size at early timepoints in the infection (3, 4, and 5 dpi) revealed no consistent difference between the two strains, with no statistically significant difference overall (Fig. 6 D).

Taken together, these experiments indicated that NL-2 was better suited to *in vitro* culture compared to NL-1 and NL-3, and furthermore, its properties remained stable over multiple passages. While the ST-J1 reference strain exhibited superior *in vitro* replication properties, the replication kinetics of the NL-2 isolate was sufficient to build up enough virla stocks to facilitate its use in subsequent *in vivo* experiments.

3.6 Comparison of *in vivo* pathogenicity of NL-2 strain and reference strain ST-J1

After examining the *in vitro* growth kinetics, we compared the virulence of the NL-2 strain to the CyHV-2 reference strain ST-J1 *in vivo*. In this experiment, young adult subjects inoculated with the same dose of each strain via IP injection allowing a valid comparison between both strains. Infected fish exhibited a wide range of mortality rates, which was dependent on the strain used (Fig. 7 A). NL-2 induced more intense and faster-developing clinical symptoms associated with CyHV-2 disease compared to ST-J1. Symptoms in the NL-2 group began at 4 dpi, with mortality starting at 5 dpi, rapidly increasing after and finally ceasing approximately two weeks post-infection, with an average mortality rate of 76.6%. In contrast, the ST-J1 group exhibited only mild symptoms and a short recovery period,

with mortality events limited to between 6 and 9 dpi and a significantly lower average mortality rate of 20%. No mortality was observed in the mock infected groups.

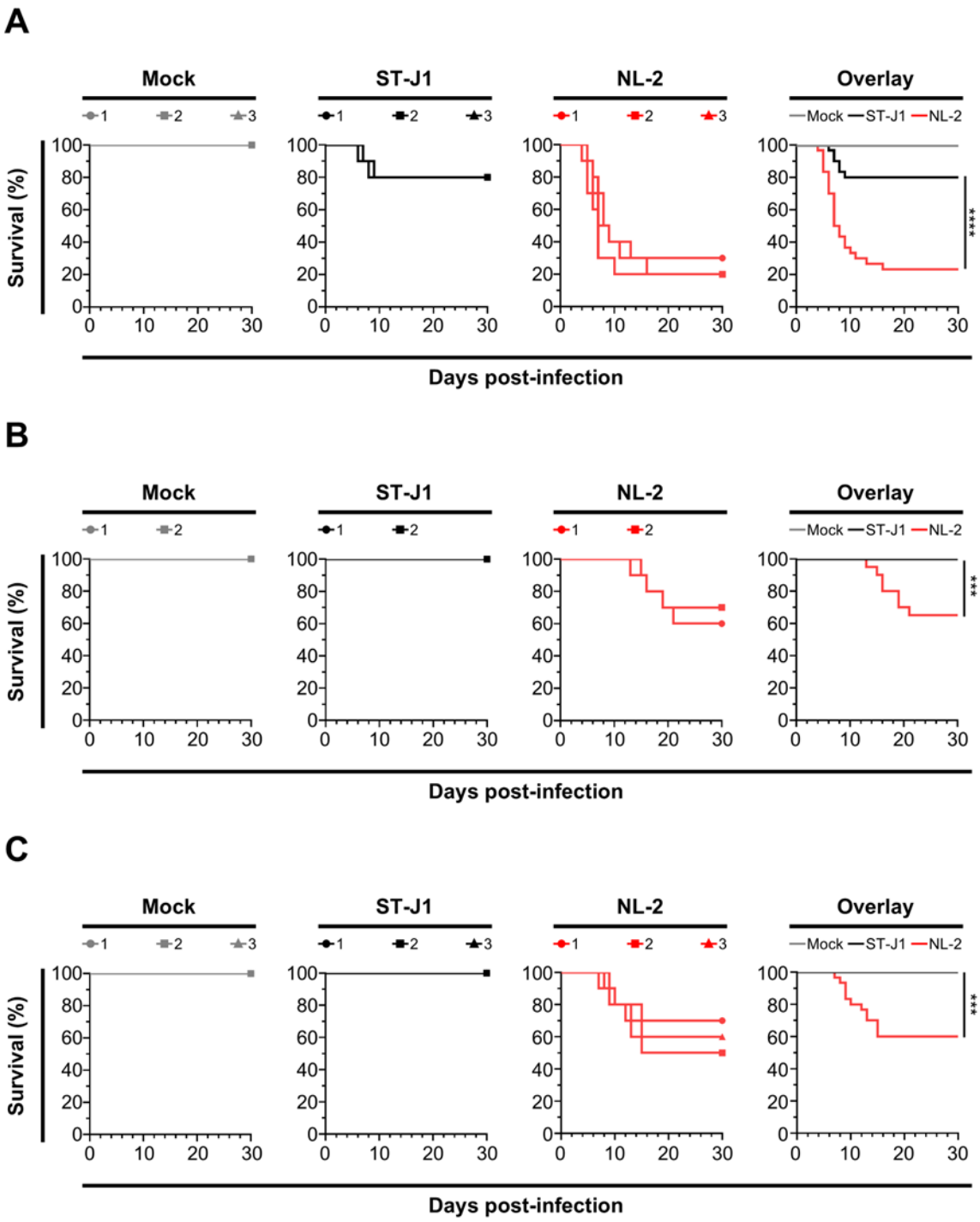

Figure 7. (A) Comparison of pathogenicity *in vivo* of the ST-J1 and isolated NL-2 strains by IP. The pathogenicity of the two strains (both were in ten passages, #10) was tested in the young adult Shubunkin goldfish (triplicate groups each consisting of 10 subjects, average weight 5.84 ± 0.6 g). Fish were mock-infected or infected by IP injection with the indicated strains, and each subject received a 50 µL injection volume (1000 PFU/fish). The fish were monitored daily for clinical signs of CyHV-2 disease, and fish reaching the endpoints were euthanized. In the overlay graph, the mean survival results were compared. (B) Monitoring the mortality of cohabitation fish in ST-J1 and NL-2 injection. The same number of goldfish

were placed as sentinel fish in the first two replicates after injection infection. (C) Survival curves of young adult Shubunkin goldfish following infection by immersion with the indicated strain were monitored. Three independent replicates of young adult Shubunkin goldfish, each group consisting of 10 subjects, were infected by immersion in water containing the virus at a final concentration of 2000 PFU/mL, with 10 fish sharing 1L of infectious water. Fish were examined daily, and those reaching the endpoints were euthanized. The overlay graph shows the mean survival curves based on the three replicates.

The cohabitation experiment also revealed a striking contrast between the two CyHV-2 strains, with only sentinel fish in the NL-2 group exhibiting mortality after co-habitation with IP injected fish. Mortality among sentinel fish occurred mainly between 2- and 3-weeks post-cohabitation, (Fig. 7 B), leading to an overall mortality rate of approximately 35% which was lower than the IP inoculated group. Notably, this this pattern, including mortality window, was consistent with the earlier NL-2 co-habitation experiment (Fig. 4 D), but the mortality rates were slightly lower in this later co-habitation experiment. In stark contrast to this, no mortality or clinical disease was observed in the ST-J1 co-habitation group, or the mock group (Fig. 7 B).

We observed a similar contrast between the two strains in an additional experiment which involved inoculation by immersion in water containing virus. This involved the immersion 10 subjects in 1L of water counting 2000 PFU/mL of each strain, for a period of 2 hours, before being returned to 60L tanks. Unlike IP injection, it is more representative of the natural waterborne infection route. Using this inoculation strategy, NL-2 exhibited a mortality average rate approximately 40%, which occurred during one to two weeks post-infection (Fig. 7 C). As per earlier experiments, the typical clinical symptoms such as abdominal swelling, severe skin lesions were observed in the NL-2 infection group. Moribund subjects exhibited multiple skin hemorrhages and enlarged kidneys (Supplementary Fig. 2 A). In contrast to the earlier experiments, a white necrosis appeared on the tail fins of all goldfish three days after infection, with some fish experiencing tail fin structure destruction and impaired swimming posture in the later stages of infection (Supplementary Fig. 2 B). In contrast, no mortality or clinical disease was observed within the ST-J1 group.

Collectively, these results demonstrate that the NL-2 strain is much more virulent and pathogenic with our adult Shubunkin goldfish model, which, despite being relatively easy to breed, had also up to this point, been quite resistant to CyHV-2 in experiments with the ST-J1 CyHV-2 reference strain and previous experiments with the CyHV-2 YC-01 strain [25].

Supplementary materials

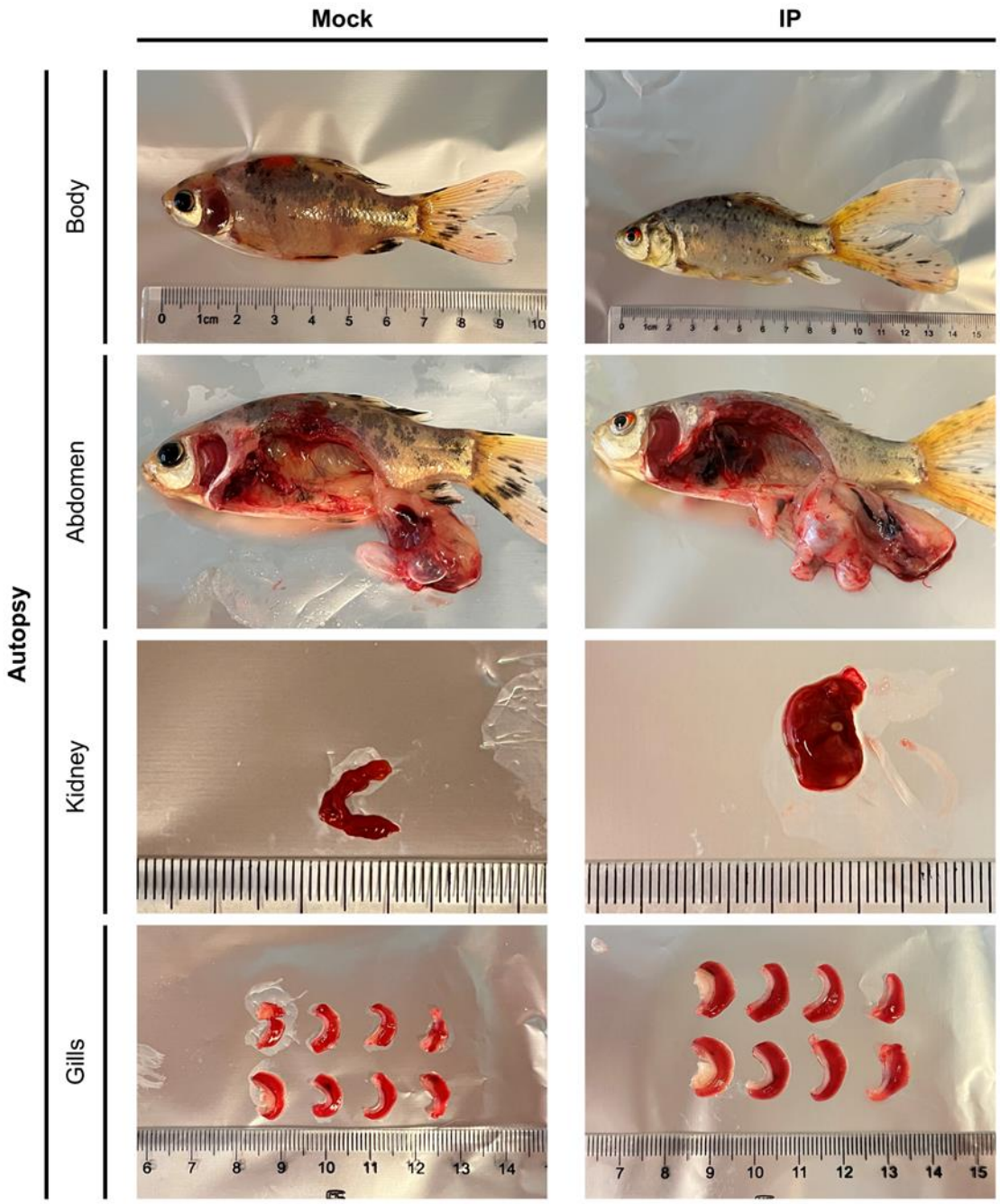

Supplementary Figure 1. Comparison of autopsy conditions. External examination: No obvious hemorrhagic areas were found on the skin of the whole body. However, abdominal swelling. Internal examination: Abdomen: The attacked fish exhibited a large amount of fluid in the abdominal cavity, indicating severe ascites. There was notable enlargement of internal organs. Intestines were severely swollen. Kidneys: The kidneys were congested and swollen, with white nodules, which could indicate a localized necrosis. Gills: No obvious lesions were observed in the gills upon naked-eye examination.

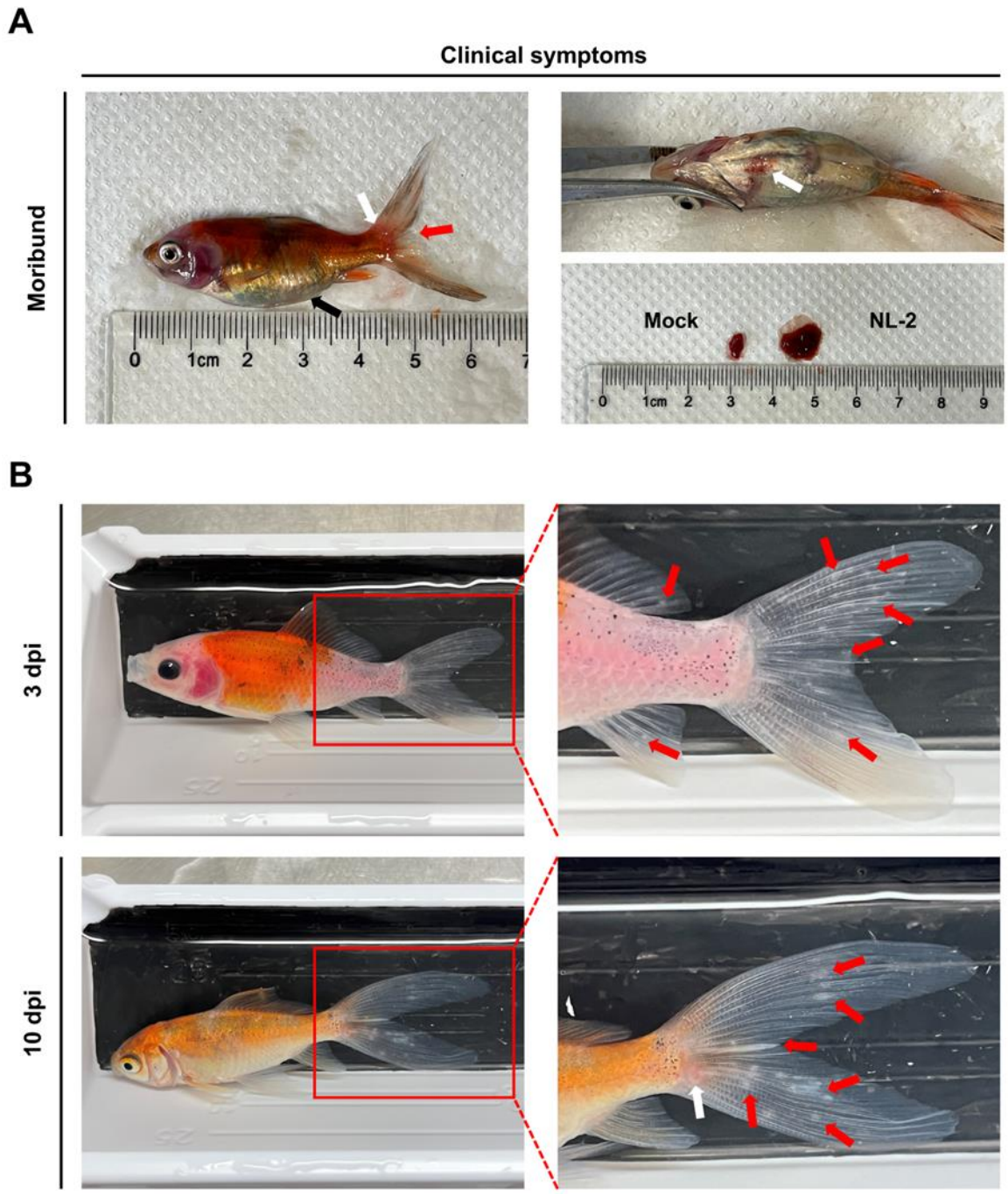

Supplementary Figure 2. (A) Clinical symptoms of moribund goldfish were observed. The left panel displays severe abdominal swelling (black arrow), severe skin lesions with hemorrhagic spots (white arrow), and significant damage to the tail fin structure (red arrow). The right panel highlights hemorrhagic lesions on the abdominal skin (white arrow). Upon dissection, a comparison of kidneys from the mock group and the NL-2 infected group reveals that the kidneys of NL-2 infected fish are significantly enlarged. (B) Clinical symptoms at the early stage (3 dpi) and late stage (10 dpi) of immersion infection were distinct. In the upper panel, white lesions (red arrows) can be observed at 3 dpi, scattered on the caudal fin and occasionally on other fins such as the dorsal fin and pelvic fin. At the peak period of mortality (10 dpi), about two weeks after infection, the lesion area increased (red arrows), and the structure of the caudal fin was destroyed. Obvious hemorrhagic areas appeared, usually at the junction of the body and the caudal fin (white arrows).

Table S1. Summary of NL-1 Variants. In this table, the location of each variant in NL-1 relative to the CyHV-2 ST-J1 reference genome (NC_019495.1) is listed along with the sequence of the variant. In addition, the corresponding location in the CyHV-2 reference genome is listed along with the reference sequence at this location.

Table S2. Summary of NL-2 Variants. In this table, the location of each variant in NL-2 relative to the CyHV-2 ST-J1 reference genome (NC_019495.1) is listed along with the sequence of the variant. In addition, the corresponding location in the CyHV-2 reference genome is listed along with the reference sequence at this location.

Table S3. Summary of NL-3 Variants. In this table, the location of each variant in NL-3 relative to the CyHV-2 ST-J1 reference genome (NC_019495.1) is listed along with the sequence of the variant. In addition, the corresponding location in the CyHV-2 reference genome is listed along with the reference sequence at this location.

Table S4. Summary of NL-1 Variant Effects. Based on annotations in CyHV-2 ST-J1 reference genome (NC_019495.1)

Table S5. Summary of NL-2 Variant Effects. Based on annotations in CyHV-2 ST-J1 reference genome (NC_019495.1)

Table S6. Summary of NL-3 Variant Effects. Based on annotations in CyHV-2 ST-J1 reference genome (NC_019495.1)

Discussion

A crucial element in the study of any virus is the identification of a suitable virus-host model for *in vivo* experimental infection. Being able to study a virus in its natural host allows us to make more biologically relevant insights into many aspects of virus-host interaction. Like all known members of the genus *Cyprinivirus*, CyHV-2 can be easily studied in its natural host, the goldfish, making them interesting models to use in the study of herpesvirus infection, with strong relevance to other vertebrate species. Indeed, this process is greatly facilitated by the availability of a host that can be easily maintained under controlled conditions, and easily bred to allow a consistent and sufficient supply of subjects for experiments.

With regard to CyHV-2, there are many breeds of goldfish that meet this criteria, including Shubunkin goldfish. In addition to being susceptible to CyHV-2, Shubunkin goldfish are heavily associated with international trade [30], which is likely to be a key epidemiological factor in the global spread of CyHV-2, making them very relevant host models in the context of research into disease control, and mitigation. While the ST-J1, (also referred to in the literature as the Saitama-1, or SaT-1 or Saitama Japan-1 [7,58]) can induce mortality in some goldfish strains by immersion, as outlined earlier, adult European sourced Shubunkin goldfish populations exhibit no virulence when challenged with ST-J1 CyHV-2 reference strain (Fig. 7), and the YC-01 strain in challenge by immersion [25]. However, it also remains possible that ORF disruptions in these CyHV-2 strains - that may or may not have emerged during passaging [7,56], may also be responsible for this lack of virulence, which we will discuss later. Regardless of whether this is due to host or viral factors, this renders these CyHV-2 strains sub-optimum to use with these a wide range of economically and epidemiologically relevant cohorts. At the same time, outbreaks of CyHV-2 among European populations of Shubunkin goldfish, indicate that they remain susceptible to new and uncharacterized CyHV-2 variants [30]. We therefore sought to identify and characterize some of these new CyHV-2 isolates, in order to assess their usefulness in future CyHV-2 studies utilizing the Shubunkin goldfish infection model.

In Europe, where CyHV-2 has a wide geographical distribution, CyHV-2 outbreaks are frequently described in goldfish and gibel carp populations in both aquaculture facilities and in the wild [15,17–19,59,60]. Within these regions, The Netherlands, has experienced outbreaks as early as 2011, with repeated occurrences since then [61], as is the case elsewhere, these represent a mixture of cases in domesticated and wild fish [30,31,62]. It was from one of these outbreaks in The Netherlands that we were able to obtain high quality tissue samples from diseased fish for further investigation, leading to the isolation of three new isolates NL-1, NL-2 and NL-3. Further *in vitro* and *in vivo* characterisation established that the NL-2 isolate *(i)* could be stably cultured cells, leading to the generation high titer viral stock, and *(ii)* exhibits much greater virulence in adult Shubunkin goldfish relative to the CyHV-2 reference strain ST-J1. Given their properties, the use of this CyHV-2 NL-2 isolate in combination

with Shubunkin goldfish, represents a much more optimum *in vivo* infection model to use in future research into CyHV-2 disease mitigation, control and viral host interaction.

Whole genome sequencing of the NL-1, NL-2 and NL-3 isolates and genetic comparison of these strains to existing strains, indicated that they were distantly related to the CyHV-2 ST-J1 reference strain and the CyHV-2 YC-01 strain, both of which cause limited or no mortality in adult Shubunkin goldfish when exposed to virus by co-habitation and/or immersion (see [25] and Fig. 7). Instead, these new isolates are more related to other CyHV-2 strains that occupy the C Genotype clade (Fig. 3B). Notably, all of the isolates were different to each other. Occupying separate sub-clades of the C Genotype clade, and these genetic differences between and new isolates and the ST-J1 reference strain, may provide some interesting insights into phenotypic differences observed in further characterization.

The initial *in vivo* characterization of these new CyHV-2 isolates revealed that they could all cause clinical disease associated with CyHV-2 in adult Shubunkin goldfish using IP inoculation. In all cases, this also led to subsequent transmission of virus to co-habiting fish (Fig. 4). While this experiment was conducted using unknown titers of each isolate, making it difficult to make a valid comparison of virulence between the strains, importantly, it did indicate that they were capable of inducing mass mortality in adult Shubunkin goldfish.

However, in addition to causing virulence *in vivo*, for these new viral isolates to be useful it was equally important that they could be stably and efficiently passaged *in vitro*. The initial *in vitro* culture of the three CyHV-2 isolates revealed slow lesion development in cells post-inoculation (#0 to #1), with virus plaques identified after approximately 10 days (Fig. 1B). This was similar across the three isolates and consistent with the previous isolation of other CyHV-2 strains [15,26,63,64]. However, differences between the isolates emerged during continuous passage. Most notably, we observed that CPE caused by NL-3 could not be observed beyond the third passage. Similar instances of instability of CyHV-2 isolates *in vitro* have been observed using KF-1 cell lines [15,64] and goldfish-derived cell lines GFSe and GFKf [65]. This suggests that the NL-3 isolate is intrinsically less fit *in vitro* compared to the other isolates. Alternatively, while could not be passaged continuously in RyuF-2 cells, it may be fit in other cells that are permissive to CyHV-2 replication. For example, some CyHV-2 isolates were observed to causing CPE in EPC cells, while others have not [8], however it is also important to consider experimental differences between these studies that may also cause this. In contrast to NL-3, the NL-1 and NL-2 isolates could be passaged more stably in RyuF-2 cells, with NL-2 exhibiting superior replication kinetics relative to NL-1 in this cell line. However, the CyHV-2 ST-J1 reference strain, exhibited much higher replication kinetics, compared to NL-2. Taken together, these observations allow us to infer a simple ranking system in terms of replication kinetics or fitness in RyuF-2 cells, i.e. “ST-J1 > NL-2 > NL-1 > NL-3”.

The genetic determinants of these different phenotypes are unclear as each isolate exhibits hundreds of differences to the reference strain (Fig. 2, Table S1 S2 and S3). Many of these are SNPs, that occur either outside of ORFs or result in synonymous changes with in ORFs, with no impact on protein

sequences (Fig. 3). However, other mutations, such as insertions and deletions, can cause frameshifts within ORFs leading to much more substantial changes in protein sequences, and hence these are much more likely to result in phenotypic impacts (Tables S4, S5 and S6). Notably, all of the new isolates have frameshifts in ORF138, ORF151A, ORF25B and ORF156, relative to ST-J1. The frameshifts in ORF138 and ORF25B are identical in all of the new isolates, and are also present in other CyHV-2 strains. The frameshifts in ORF156 is identical in NL-1 and NL-3, and a similar frameshift is present in NL-2 ORF156, leading to a similar ORF156 truncation. Indeed, these common mutations point towards a common monophyletic origin of these tree new isolates separate to the J Genotype. Conversely, the frameshifts in the NL-1, NL-2 and NL-3 encoded ORF151A relative to the ST-J1 reference are all different, and only the ORF151A frameshift in NL-2 is found in other CyHV-2 strains. Nonetheless, the ORF151A proteins encoded by the three isolates are all different from the ST-J1 ORF151A. It is possible that the ST-J1 proteome is more optimum for CyHV-2 fitness *in vitro*. Outside of these four major differences that are common to all three isolates, additional changes relative to this "optimum proteome", may further reduce fitness *in vitro*. Consistent with this, it is notable that NL-3, which exhibited the least fitness *in vitro*, has more frameshifts (a total of eight, including frameshifts in ORF28A, ORF30, ORF89 and ORF90) relative to ST-J1 than that other two isolates. Thus, the NL-3 proteome, which is predicted to be more divergent from that of ST-J1 than the other two isolates, may be less optimum for CyHV-2 fitness *in vitro*. It also raises the possibility that the ORFs disrupted in NL-3 may be important for facilitating stable passaging of CyHV-2 *in vitro*, and it may be interesting to investigate this further in future studies. However, it is important to note, that outside of highly disruptive changes such as frameshifts, it remains possible that the smaller protein changes such as single nucleotide changes leading to non-synonymous amino acid substitutions may also impact fitness *in vitro*, as we described recently in a closely related virus *Cyprinid herpesvirus 3* (CyHV-3) [66].

The direct comparisons between the NL-2 isolate and the CyHV-2 reference strain ST-J1 *in vitro* and *in vivo*, also yielded some intriguing results. Despite the ST-J1 being more fit *in vitro*, it was less fit *in vivo*, and vice versa for NL-2. This is similar to our previous observations with different CyHV-3 strains [66,67]. This may occur as a consequence of continuous passaging *in vitro*, which introduces a selective pressure that favours variants that are adapted to *in vitro* conditions. In the absence of any selective pressure to retain *in vivo* fitness, these *in vitro* adapted strains may develop an attenuated phenotype *in vivo*, as we described previously with CyHV-3 variants [66]. It is unclear if the same has occurred with ST-J1, leading to an attenuated phenotype in some goldfish breeds (or populations thereof) or if it has facilitated the emergence of CyHV-2 resistance. Notably, in comparisons between ST-J1 and NL-2, both strains were at the 10^{th} passage. However, as we demonstrated with CyHV-3, selective pressure *in vitro* may cause *in vitro* adapted strains to dominate viral cultures in as few as five passages [66].

Interestingly, a total of six frameshifted ORFs exist in NL-2 relative to the ST-J1 strain (ORF16, ORF25B, ORF52 ORF138, ORF151A, ORF156 - Table S5). Given that these represent the biggest

differences in their respective proteomes, it may be interesting to determine if ST-J1 virulence *in vivo* may be improved through replacement of one or more of these with the equivalent NL-2 allele(s). With the exception of ORF156, the functions of the proteins encoded by these CyHV-2 ORFs have been predicted based on homology with other proteins in related viruses such as CyHV-3 [7], which may allow us to hypothesize which of these changes are more likely to be responsible for these differences in phenotype between ST-J1 and NL-2 *in vivo*.

Some of these frameshifts result in truncation of predicted proteins in NL-2, relative to ST-J1 and other CyHV-2 strains, some of which may be responsible for reduced fitness of NL-2 relative to ST-J1 in vitro. For example, ORF52 is predicted to encode a signal peptide, which truncated in NL-2 relative to ST-J1 and most other fully sequenced strains, however the potential impact of this on NL-2 fitness relative to ST-J1 in vitro is unclear. In the case of other frameshift mutations causing truncated predicted protein products in NL-2, the potential impact in vitro may be more apparent. For example, in NL-2 ORF16 and ORF138 are both predicted to encode truncated proteins relative to ST-J1 and other fully sequenced CyHV-2 strains. ORF16 and ORF138 are predicted to encode Class III and Class I viral membrane proteins respectively, both of which are important for herpesvirus viral entry and egress [68,69]. Although potentially important for viral entry and egress, these viral membrane protein truncations in the NL-2 isolate do not prevent host cell entry or egress in vitro, but it remains possible that they may reduce fitness relative to ST-J1 in this environment (Fig 6C). However, the same truncated membrane proteins did not prevent NL-2 from exhibiting much higher virulence and transmission in vivo relative to ST-J1 (Fig 7).

Conversely, other frameshifts in NL-2 relative to ST-J1, such as those in ORF25B and ORF151A, actually represent truncations of these protein products in ST-J1 relative to other fully sequenced CyHV-2 strains. As per ORF138, ORF25B is also a Class I viral membrane protein, and may therefore be important for viral entry and egress. Notably, this ORF25B truncation in ST-J1 does not reduce its fitness in vitro relative to NL-2 (Fig 6C). While we observe a lack of virulence and transmission when ST-J1 is delivered by immersion in vivo (Fig 7), it is unclear if this is directly connected to this ORF25B truncation. However, in CyHV-3, we previously provided evidence that mutations in class I membrane proteins, can impact virion viability in extracellular environments such as mucosal surfaces [66], and it would be interesting to investigate this possibility in the future in a similar manner. In contrast to other major gene disruptions between NL-2 and ST-J1, the in vivo impact of the truncation of ORF151A in ST-J1 may be more readily apparent. ORF151A encodes a protein that is predicted to be a viral receptor for Tumour Necrosis factor (TNF) and is a member of a Tumour Necrosis Factor receptor (TNFR) family of proteins that are encoded by CyHV-1, CyHV-2 and CyHV-3 [67]. TNF is an important element of the innate immune response, and is produced in the early stages of viral infection in response to the nuclear factor-κB (NF-κB) inflammatory pathway. Through interaction with its natural cellular receptors (cellular TNFRs), TNF stimulates signalling that leads to an inflammatory response in order to help recruitment of immune cells to the site of infection, stimulate their activation,

and also cause fever [70–73], all of which are important for rapid clearance of viral infections. However, virally encoded TNFRs can act as "decoy" TNFR receptors, preventing interaction with the cellular TNFR and thus reducing the antiviral effects of cellular TNF [70,73]. Indeed, we previously demonstrated that a soluble decoy TNFR expressed by CyHV-3, can interfere with behavioural fever response during infection [74]. However, ST-J1 encodes a truncated from of ORF151A (129AA) in which the TNFR domain is missing. Conversely, unlike ST-J1, NL-2 and other CyHV-2 strains encode a full-length protein that includes the TNFR domain (324 AA) (InterProScan analysis, data not shown). Therefore, it is possible that the ability of the ST-J1 strain to counteract host cell TNF during infection is compromised due to the lack of this decoy TNF receptor encoded by the full-length ORF151A. Given the roles that TNF plays during viral infection, this deficiency may have a greater impact in vivo than in vitro, leading to ST-J1 to exhibit an attenuated phenotype in vivo, relative to NL-2. This may partially account for the opposite patterns we observed between ST-J1 and NL-2 in terms of in vitro and in vivo fitness. Notably, ST-J1 is the only fully sequenced CyHV-2 strain that has been observed to encode truncations in both ORF25B and ORF151A, and it is possible that the attenuation in vitro bay be caused by the combined impact of both of these frameshifts. Taken together, the genomic and biological comparisons of CyHV-2 from this study have allowed us to build some interesting hypotheses on some potential determinants of CyHV-2 virulence in vivo and provides plenty of scope for further investigation in future studies.

According to the literature, laboratory challenges with CyHV-2 are primarily conducted via intraperitoneal (IP) injection of infected tissue homogenates or cell culture fluid containing the virus, which can rapidly induce clinical symptoms and high mortality [63,75–78]. However, this highly artificial challenge method has significant drawbacks. It amplifies the pathogenicity and virulence of the virus, fails to represent the series of events that occur during a natural infection, and it does not reflect the natural immune response of the host during a CyHV-2 infection. In fish, mucosal surfaces, including the skin, gills and gastrointestinal mucosa, serve as the primary entry routes for viruses [79] and previously we identified that the skin is a major entry portal for CyHV-2 [25]. Therefore, identifying an *in vivo* infection model that will allow us to simulate this natural infection process via the mucosal surfaces is crucial in order to have biologically relevant experiment designs. In this study, inoculation of adult goldfish with NL-2 by immersion using final concentration of 2000 PFU/mL led to 40% mortality in goldfish (Fig. 7). Notably this dose is 50 times lower than the dose we used in equivalent experiments previously with the YC-01 strain (1×10^5 PFU/mL) [25], which, despite the higher dose, led to little or no mortality in adult Shubinkin goldfish. This would indicate that the NL-2-Shubunkin goldfish model is ideal for the future study of CyHV-2, maximizing the biological relevance of observations, and thus it also represents a useful tool to the wider CyHV-2 research community.

Conclusion:

Three isolates of CyHV-2 NL-1, NL-2, and NL-3 that were characterized in this study. They were found to be genetically distinct from the ST-J1 reference strain and from each other. They were all found to cause disease associated with CyHV-2 in experiments that involved infection by of adult Shubunkin goldfish by IP injection and co-habitation. Among these, NL-2 could be stably passaged *in vitro* and also exhibited the most efficient replication *in vitro*. NL-2 was also capable of inducing CyHV-2 related mortality in adult Shubunkin goldfish through inoculation by immersion. These two properties make the NL-2 -Shubunkin model an optimum *in vivo* infection model to use in future studies, as it facilitates both stable maintenance and generation of viral stock *in vitro*, and the infection of hosts in a way that is more representative of natural infection, which will be of interest to the wider field. Due to their distinct genetic characteristics and biological properties, we formally refer to these isolates as the NL-1, NL-2 and NL-3 strains respectively.

References

1. Chen, D.; Zhang, Q.; Tang, W.; Huang, Z.; Wang, G.; Wang, Y.; Shi, J.; Xu, H.; Lin, L.; Li, Z.; et al. The Evolutionary Origin and Domestication History of Goldfish (Carassius Auratus). Pr oc. Natl. Acad. Sci. 2020, 117, 29775–29785, doi:10.1073/pnas.2005545117.
2. Omori, Y.; Kon, T. Goldfish: An Old and New Model System to Study Vertebrate Developmen t, Evolution and Human Disease. J. Biochem. (Tokyo) 2019, 165, 209–218, doi:10.1093/jb/mv y076.
3. Li, J. Swimming in Four Goldfish (Carassius Auratus) Morphotypes: Understanding Function al Design and Performance through Artificial Selection, University of British Columbia, 2007.
4. McLoughlin, M. Fish Vaccination—a Brief Overview. 2014.
5. Kibenge, F.S.B.; Godoy, M.G.; Fast, M.; Workenhe, S.; Kibenge, M.J.T. Countermeasures aga inst Viral Diseases of Farmed Fish. Antiviral Res. 2012, 95, 257–281, doi:10.1016/j.antiviral.2 012.06.003.
6. Donohoe, O.; Zhang, H.; Delrez, N.; Gao, Y.; Suárez, N.M.; Davison, A.J.; Vanderplasschen, A. Genomes of Anguillid Herpesvirus 1 Strains Reveal Evolutionary Disparities and Low Gen etic Diversity in the Genus Cyprinivirus. Microorganisms 2021, 9, 998, doi:10.3390/microorg anisms9050998.
7. Davison, A.J.; Kurobe, T.; Gatherer, D.; Cunningham, C.; Korf, I.; Fukuda, H.; Hedrick, R.P.; Waltzek, T.B. Comparative Genomics of Carp Herpesviruses. J. Virol. 2013, 87, 2908–2922, d oi:10.1128/jvi.03206-12.
8. Thangaraj, R.S.; Nithianantham, S.R.; Dharmaratnam, A.; Kumar, R.; Pradhan, P.K.; Thangala zhy Gopakumar, S.; Sood, N. Cyprinid Herpesvirus-2 (CyHV-2): A Comprehensive Review. R ev. Aquac. 2021, 13, 796–821, doi:10.1111/raq.12499.
9. Jung, S.J.; Miyazaki, T. Herpesviral Haematopoietic Necrosis of Goldfish, Carassius Auratus (L.). J. Fish Dis. 1995, 18, 211–220, doi:10.1111/j.1365-2761.1995.tb00296.x.
10. Goodwin, A.E.; Khoo, L.; LaPatra, S.E.; Bonar, C.; Key, D.W.; Garner, M.; Lee, M.V.; Hanso n, L. Goldfish Hematopoietic Necrosis Herpesvirus (Cyprinid Herpesvirus 2) in the USA: Mol ecular Confirmation of Isolates from Diseased Fish. J. Aquat. Anim. Health 2006, 18, 11–18, d oi:10.1577/H05-007.1.
11. Groff, J.M.; LaPatra, S.E.; Munn, R.J.; Zinkl, J.G. A Viral Epizootic in Cultured Populations o f Juvenile Goldfish Due to a Putative Herpesvirus Etiology. J. Vet. Diagn. Invest. 1998, 10, 37 5–378, doi:10.1177/104063879801000415.
12. Chang, P.H.; Lee, S.H.; Chiang, H.C.; Jong, M.H. Epizootic of Herpes-like Virus Infection in Goldfish, Carassius Auratus in Taiwan. Fish Pathol. 1999, 34, 209–210, doi:10.3147/jsfp.34.2 09.
13. Stephens, F.J.; Raidal, S.R.; Jones, B. Haematopoietic Necrosis in a Goldfish (Carassius Aurat us) Associated with an Agent Morphologically Similar to Herpesvirus. Aust. Vet. J. 2004, 82, 167–169.
14. Matthew, S. Quarterly Report of Investigations of Suspected Exotic Diseases. Minist. Prim. In d. 2005, 32, 32–35.
15. Jeffery, K.R.; Bateman, K.; Bayley, A.; Feist, S.W.; Hulland, J.; Longshaw, C.; Stone, D.; Woo lford, G.; Way, K. Isolation of a Cyprinid Herpesvirus 2 from Goldfish, Carassius Auratus (L.), in the UK. J. Fish Dis. 2007, 30, 649–656, doi:10.1111/j.1365-2761.2007.00847.x.
16. Sahoo, P.K.; Swaminathan, T.R.; Abraham, T.J.; Kumar, R.; Pattanayak, S.; Mohapatra, A.; Ra th, S.S.; Patra, A.; Adikesavalu, H.; Sood, N.; et al. Detection of Goldfish Haematopoietic Nec rosis Herpes Virus (Cyprinid Herpesvirus-2) with Multi-Drug Resistant Aeromonas Hydrophil a Infection in Goldfish: First Evidence of Any Viral Disease Outbreak in Ornamental Freshwa ter Aquaculture Farms in India. Acta Trop. 2016, 161, 8–17, doi:10.1016/j.actatropica.2016.05. 004.
17. Giovannini, S.; Bergmann, S.M.; Keeling, C.; Lany, C.; Schütze, H.; Schmidt-Posthaus, H. He rpesviral Hematopoietic Necrosis in Goldfish in Switzerland: Early Lesions in Clinically Nor mal Goldfish (Carassius Auratus). Vet. Pathol. 2016, 53, 847–852, doi:10.1177/030098581561 4974.

18. Boitard, P.-M.; Baud, M.; Labrut, S.; de Boisséson, C.; Jamin, M.; Bigarré, L. First Detection of Cyprinid Herpesvirus 2 (CyHV-2) in Goldfish (Carassius Auratus) in France. J. Fish Dis. 20 16, 39, 673–680, doi:10.1111/jfd.12400.
19. Adamek, M.; Hellmann, J.; Jung-Schroers, V.; Teitge, F.; Steinhagen, D. CyHV-2 Transmissio n in Traded Goldfish Stocks in Germany—A Case Study. J. Fish Dis. 2018, 41, 401–404, doi:1 0.1111/jfd.12734.
20. Kalayci, G.; Ozkan, B.; Pekmez, K.; Kaplan, M.; Mefut, A.; Cagirgan, A. First Detection of C yprinid Herpesvirus-2 (CyHV-2) Followed by Screening and Monitoring Studies in Goldfish (Carassius Auratus) in Turkey. Bull. Eur. Assoc. Fish Pathol. 2018, 38, 94–103.
21. Panicz, R.; Sadowski, J.; Eljasik, P. Detection of Cyprinid Herpesvirus 2 (CyHV-2) in Sympto matic Ornamental Types of Goldfish (Carassius Auratus) and Asymptomatic Common Carp (C yprinus Carpio) Reared in Warm-Water Cage Culture. 2019, doi:10.1016/j.aquaculture.2019.0 1.065.
22. Jiang, N.; Yuan, D.; Zhang, M.; Luo, L.; Wang, N.; Xing, W.; Li, T.; Huang, X.; Ma, Z. Diagn ostic Case Report: Disease Outbreak Induced by CyHV-2 in Goldfish in China. Aquaculture 2 020, 523, 735156, doi:10.1016/j.aquaculture.2020.735156.
23. Jung, M.-H.; Ryu, J.-W.; Nikapitiya, C.; Jung, S.-J. Detection of Herpesviral Hematopoietic N ecrosis Virus (Cyprinid Herpesvirus 2, CyHV-2) from Goldfish, Carassius Auratus (L.) in Kor ea. Fish. Aquat. Sci. 2022, 25, 403–408, doi:10.47853/FAS.2022.e36.
24. Piewbang, C.; Wardhani, S.W.; Sirivisoot, S.; Surachetpong, W.; Sirimanapong, W.; Kasantiku l, T.; Techangamsuwan, S. First Report of Natural Cyprinid Herpesvirus-2 Infection Associate d with Fatal Outbreaks of Goldfish (Carassius Auratus) Farms in Thailand. Aquaculture 2024, 581, 740481, doi:10.1016/j.aquaculture.2023.740481.
25. He, B.; Sridhar, A.; Streiff, C.; Deketelaere, C.; Zhang, H.; Gao, Y.; Hu, Y.; Pirotte, S.; Delrez, N.; Davison, A.J.; et al. In Vivo Imaging Sheds Light on the Susceptibility and Permissivity o f Carassius Auratus to Cyprinid Herpesvirus 2 According to Developmental Stage. Viruses 202 3, 15, 1746, doi:10.3390/v15081746.
26. Ito, T.; Kurita, J.; Ozaki, A.; Sano, M.; Fukuda, H.; Ototake, M. Growth of Cyprinid Herpesvir us 2 (CyHV-2) in Cell Culture and Experimental Infection of Goldfish Carassius Auratus. Dis. Aquat. Organ. 2013, 105, 193–202, doi:10.3354/dao02627.
27. Li, X.; Fukuda, H. In Vitro Culture of Goldfish Cell Sensitive to Goldfish Herpes Virus. CABI Databases 2003, 12, 12–18.
28. Li, L.; Luo, Y.; Gao, Z.; Huang, J.; Zheng, X.; Nie, H.; Zhang, J.; Lin, L.; Yuan, J. Molecular Characterisation and Prevalence of a New Genotype of Cyprinid Herpesvirus 2 in Mainland C hina. Can. J. Microbiol. 2015, 61, 381–387, doi:10.1139/cjm-2014-0796.
29. Wang, F.; Xu, Y.; Zhou, Y.; Ding, C.; Duan, H. Isolation and Characterization of a Cyprinid H erpesvirus Strain YZ01 from Apparently Healthy Goldfish after Rising Water Temperature 202 1, 2021.07.05.451087.
30. Ito, T.; Kurita, J.; Haenen, O.L.M. Importation of CyHV-2-Infected Goldfish into the Netherla nds. Dis. Aquat. Organ. 2017, 126, 51–62, doi:10.3354/dao03157.
31. Kurobe, T.; Kurita, J.; Haenen, O.; Voorbergen-Laarman, M.; Ito, T. Mass Mortality Events As sociated with Cyprinid Herpesvirus 2 (CyHV-2) Infection in Wild Prussian Carp Carassius Gi belio in the Netherlands, and Molecular Biology of Virus Strains. J. Fish Dis. 2024, 47, e1386 8, doi:10.1111/jfd.13868.
32. Waltzek, T.B.; Kurobe, T.; Goodwin, A.E.; Hedrick, R.P. Development of a Polymerase Chain Reaction Assay to Detect Cyprinid Herpesvirus 2 in Goldfish. J. Aquat. Anim. Health 2009, 2 1, 60–67, doi:10.1577/H08-045.1.
33. Shibata, T.; Nanjo, A.; Saito, M.; Yoshii, K.; Ito, T.; Nakanishi, T.; Sakamoto, T.; Sano, M. In Vitro Characteristics of Cyprinid Herpesvirus 2: Effect of Kidney Extract Supplementation on Growth. Dis. Aquat. Organ. 2015, 115, 223–232, doi:10.3354/dao02885.
34. BBTools Available online: https://jgi.doe.gov/data-and-tools/software-tools/bbtools/ (accessed on 5 October 2022).
35. Antipov, D.; Korobeynikov, A.; McLean, J.S.; Pevzner, P.A. hybridSPAdes: An Algorithm for Hybrid Assembly of Short and Long Reads. Bioinformatics 2016, 32, 1009–1015, doi:10.1093 /bioinformatics/btv688.

36. Mikheenko, A.; Prjibelski, A.; Saveliev, V.; Antipov, D.; Gurevich, A. Versatile Genome Assembly Evaluation with QUAST-LG. Bioinforma. Oxf. Engl. 2018, 34, i142–i150, doi:10.1093/bioinformatics/bty266.
37. Wick, R.R.; Schultz, M.B.; Zobel, J.; Holt, K.E. Bandage: Interactive Visualization of de Novo Genome Assemblies. Bioinformatics 2015, 31, 3350–3352, doi:10.1093/bioinformatics/btv383.
38. LLC, G.B. SnapGene | Software for Everyday Molecular Biology Available online: https://www.snapgene.com/ (accessed on 7 May 2024).
39. Katoh, K.; Rozewicki, J.; Yamada, K.D. MAFFT Online Service: Multiple Sequence Alignment, Interactive Sequence Choice and Visualization. Brief. Bioinform. 2019, 20, 1160–1166, doi:10.1093/bib/bbx108.
40. Complete Genomes: Alloherpesviridae Available online: https://www.ncbi.nlm.nih.gov/genomes/GenomesGroup.cgi?taxid=548682 (accessed on 7 August 2024).
41. Viral Genomes Available online: https://www.ncbi.nlm.nih.gov/genome/viruses/ (accessed on 7 August 2024).
42. Kumar, S.; Stecher, G.; Li, M.; Knyaz, C.; Tamura, K. MEGA X: Molecular Evolutionary Genetics Analysis across Computing Platforms. Mol. Biol. Evol. 2018, 35, 1547–1549, doi:10.1093/molbev/msy096.
43. Lindenbaum, P. JVarkit: Java-Based Utilities for Bioinformatics. 2015, doi:10.6084/m9.figshare.1425030.v1.
44. MsaToVcf Available online: http://lindenb.github.io/jvarkit/MsaToVcf.html (accessed on 27 June 2024).
45. Kim, D.; Paggi, J.M.; Park, C.; Bennett, C.; Salzberg, S.L. Graph-Based Genome Alignment and Genotyping with HISAT2 and HISAT-Genotype. Nat. Biotechnol. 2019, 37, 907–915, doi:10.1038/s41587-019-0201-4.
46. Pertea, M.; Kim, D.; Pertea, G.M.; Leek, J.T.; Salzberg, S.L. Transcript-Level Expression Analysis of RNA-Seq Experiments with HISAT, StringTie and Ballgown. Nat. Protoc. 2016, 11, 1650–1667, doi:10.1038/nprot.2016.095.
47. Danecek, P.; Bonfield, J.K.; Liddle, J.; Marshall, J.; Ohan, V.; Pollard, M.O.; Whitwham, A.; Keane, T.; McCarthy, S.A.; Davies, R.M.; et al. Twelve Years of SAMtools and BCFtools. Gigascience 2021, 10, giab008, doi:10.1093/gigascience/giab008.
48. Robinson, J.T.; Thorvaldsdóttir, H.; Winckler, W.; Guttman, M.; Lander, E.S.; Getz, G.; Mesirov, J.P. Integrative Genomics Viewer. Nat. Biotechnol. 2011, 29, 24–26, doi:10.1038/nbt.1754.
49. McLaren, W.; Gil, L.; Hunt, S.E.; Riat, H.S.; Ritchie, G.R.S.; Thormann, A.; Flicek, P.; Cunningham, F. The Ensembl Variant Effect Predictor. Genome Biol. 2016, 17, 122, doi:10.1186/s13059-016-0974-4.
50. Geneious | Bioinformatics Software Available online: https://www.geneious.com/ (accessed on 4 July 2024).
51. Baldwin, S.; Revanna, R.; Thomson, S.; Pither-Joyce, M.; Wright, K.; Crowhurst, R.; Fiers, M.; Chen, L.; Macknight, R.; McCallum, J.A. A Toolkit for Bulk PCR-Based Marker Design from next-Generation Sequence Data: Application for Development of a Framework Linkage Map in Bulb Onion (Allium Cepa L.). BMC Genomics 2012, 13, 637, doi:10.1186/1471-2164-13-637.
52. McCallum, J. Cfljam/Galaxy-Pcr-Markers 2022.
53. R Core Team R: A Language and Environment for Statistical Computing. R Foundation for Statistical Computing 2022.
54. John, F.; Sanford, W. An R Companion to Applied Regression; Los Angeles, 2018; ISBN 978-1-5443-3647-3.
55. Lenth, R.V. Least-Squares Means: The R Package Lsmeans. J. Stat. Softw. 2016, 69, 1–33, doi:10.18637/jss.v069.i01.
56. Yang, J.; Xiao, S.; Lu, L.; Wang, H.; Jiang, Y. Genomic and Molecular Characterization of a Cyprinid Herpesvirus 2 YC-01 Strain Isolated from Gibel Carp. Heliyon 2024, 10, e32811, doi:10.1016/j.heliyon.2024.e32811.

57. Luo, Y.Z.; Lin, L.; Liu, Y.; Wu, Z.X.; Gu, Z.M.; Li, L.J.; Yuan, J.F. Haematopoietic Necrosis o f Cultured Prussian Carp, Carassius Gibelio (Bloch), Associated with Cyprinid Herpesvirus 2. J. Fish Dis. 2013, 36, 1035–1039, doi:10.1111/jfd.12110.
58. Saito, H.; Minami, S.; Yuguchi, M.; Shitara, A.; Kondo, H.; Kato, G.; Sano, M. Effect of Temp erature on the Protective Efficacy of a Live Attenuated Vaccine against Herpesviral Haematop oietic Necrosis in Goldfish. J. Fish Dis. 2024, 47, e13906, doi:10.1111/jfd.13906.
59. Daněk, T.; Kalous, L.; Vesel, T.; Krásová, E.; Reschová, S.; Rylková, K.; Kulich, P.; L, M.P.; P okorová, D.; Knytl, M. Massive Mortality of Prussian Carp Carassius Gibelio in the Upper Elb e Basin Associated with Herpesviral Hematopoietic Necrosis (CyHV-2). Dis. Aquat. Organ. 20 12, 102, 87–95, doi:10.3354/dao02535.
60. Doszpoly, A.; Benkő, M.; Csaba, G.; Dán, Á.; Lang, M.; Harrach, B. Introduction of the Famil y Alloherpesviridae: The First Molecular Detection of Herpesviruses of Cyprinid Fish in Hung ary. Magy. Allatorvosok Lapja 2011, 133, 174–181.
61. Haenen, O.; Way, K.; Gorgoglione, B.; Ito, T.; Paley, R.; Bigarré, L.; Waltzek, T. Novel Viral I nfections Threatening Cyprinid Fish. Bull. Eur. Assoc. Fish Pathol. 2016, 36, 11–23.
62. Schiphouwer, M.; Kessel, N.; Matthews, J.; Leuven, R.S.E.W.; Koppel, S.; Kranenbarg, J.; Ha enen, O.; Lenders, H.; Nagelkerke, L.; Van der Velde, G.; et al. Risk Analysis of Exotic Fish S pecies Included in the Dutch Fisheries Act and Their Hybrids. 2014.
63. Xiao, Z.; Xue, M.; Xu, C.; Jiang, N.; Luo, X.; Li, Y.; Fan, Y.; Meng, Y.; Liu, W.; Zeng, L.; et a l. First Report of Cyprinid Herpesvirus 2 Isolated from the Golden Crucian Carp in China. Aq uaculture 2022, 558, 738361, doi:10.1016/j.aquaculture.2022.738361.
64. Xu, J.; Zeng, L.; Zhang, H.; Zhou, Y.; Ma, J.; Fan, Y. Cyprinid Herpesvirus 2 Infection Emerg ed in Cultured Gibel Carp, Carassius Auratus Gibelio in China. Vet. Microbiol. 2013, 166, 138 –144, doi:10.1016/j.vetmic.2013.05.025.
65. Jing, H.; Gao, L.; Zhang, M.; Wang, N.; Lin, X.; Zhang, L.; Wu, S. Establishment from the Sn out and Kidney of Goldfish, Carassius Auratus, of Two New Cell Lines and Their Susceptibili ty to Infectious Pancreatic Necrosis Virus. Fish Physiol. Biochem. 2016, 42, 303–311, doi:10. 1007/s10695-015-0138-6.
66. Gao, Y.; Sridhar, A.; Bernard, N.; He, B.; Zhang, H.; Pirotte, S.; Desmecht, S.; Vancsok, C.; B outier, M.; Suárez, N.M.; et al. Virus-Induced Interference as a Means for Accelerating Fitness -Based Selection of Cyprinid Herpesvirus 3 Single Nucleotide Variants in Vitro and in Vivo. V irus Evol. 2023, vead003, doi:10.1093/ve/vead003.
67. Gao, Y.; Suárez, N.M.; Wilkie, G.S.; Dong, C.; Bergmann, S.; Lee, P.-Y.A.; Davison, A.J.; Van derplasschen, A.F.C.; Boutier, M. Genomic and Biologic Comparisons of Cyprinid Herpesviru s 3 Strains. Vet. Res. 2018, 49, 40, doi:10.1186/s13567-018-0532-z.
68. Ahmad, I.; Wilson, D.W. HSV-1 Cytoplasmic Envelopment and Egress. Int. J. Mol. Sci. 2020, 21, 5969, doi:10.3390/ijms21175969.
69. Jambunathan, N.; Clark, C.M.; Musarrat, F.; Chouljenko, V.N.; Rudd, J.; Kousoulas, K.G. Two Sides to Every Story: Herpes Simplex Type-1 Viral Glycoproteins gB, gD, gH/gL, gK, and Ce llular Receptors Function as Key Players in Membrane Fusion. Viruses 2021, 13, 1849, doi:10. 3390/v13091849.
70. Al Rumaih, Z.; Tuazon Kels, Ma.J.; Ng, E.; Pandey, P.; Pontejo, S.M.; Alejo, A.; Alcamí, A.; C haudhri, G.; Karupiah, G. Poxvirus-Encoded TNF Receptor Homolog Dampens Inflammation and Protects from Uncontrolled Lung Pathology during Respiratory Infection. Proc. Natl. Aca d. Sci. 2020, 117, 26885–26894, doi:10.1073/pnas.2004688117.
71. Charles A Janeway, J.; Travers, P.; Walport, M.; Shlomchik, M.J. Induced Innate Responses to Infection. In Immunobiology: The Immune System in Health and Disease. 5th edition; Garlan d Science, 2001.
72. Netea, M.G.; Kullberg, B.J.; Van der Meer, J.W.M. Circulating Cytokines as Mediators of Fev er. Clin. Infect. Dis. 2000, 31, S178–S184, doi:10.1086/317513.
73. Rahman, M.M.; Lucas, A.R.; McFadden, G. Viral TNF Inhibitors as Potential Therapeutics. In Madame Curie Bioscience Database [Internet]; Landes Bioscience, 2013.
74. Rakus, K.; Ronsmans, M.; Forlenza, M.; Boutier, M.; Piazzon, M.C.; Jazowiecka-Rakus, J.; G atherer, D.; Athanasiadis, A.; Farnir, F.; Davison, A.J.; et al. Conserved Fever Pathways across

Vertebrates: A Herpesvirus Expressed Decoy TNF-α Receptor Delays Behavioral Fever in Fis h. Cell Host Microbe 2017, 21, 244–253, doi:10.1016/j.chom.2017.01.010.
75. Chai, W.; Qi, L.; Zhang, Y.; Hong, M.; Jin, L.; Li, L.; Yuan, J. Evaluation of Cyprinid Herpesv irus 2 Latency and Reactivation in Carassius Gibel. Microorganisms 2020, 8, 445, doi:10.3390 /microorganisms8030445.
76. Liang, L. -G.; Xie, J.; Chen, K.; Bing, X. Pathogenicity and Biological Characteristics of CyH V-2. Fish Pathol. 2015, 35, 85–93.
77. Ouyang, P.; Zhou, Y.; Wang, K.; Geng, Y.; Lai, W.; Huang, X.; Chen, D.; Guo, H.; Fang, J.; Ch en, Z.; et al. First Report of Cyprinid Herpesvirus 2 Outbreak in Cultured Gibel Carp, Carassiu s Auratus Gibelio at Low Temperature. J. World Aquac. Soc. 2020, 51, 1208–1220, doi:10.111 1/jwas.12681.
78. Wen, J.; Xu, Y.; Su, M.; Lu, L.; Wang, H. Susceptibility of Goldfish to Cyprinid Herpesvirus 2 (CyHV-2) SH01 Isolated from Cultured Crucian Carp. Viruses 2021, 13, 1761, doi:10.3390/v 13091761.
79. Løkka, G.; Gamil, A.A.A.; Evensen, Ø.; Kortner, T.M. Establishment of an In Vitro Model to Study Viral Infections of the Fish Intestinal Epithelium. Cells 2023, 12, 1531, doi:10.3390/cell s12111531.

Discussion - Perspectives

Viral infections pose significant threats to animal welfare and sustainable development within the aquaculture industry. Among these, some herpesviruses have been identified as representing significant threats to global aquaculture (Pearson, 2004). Indeed, currently, several herpesviruses have been identified as causative agents of disease during high mortality outbreaks, yet numerous others remain to be characterized (Bergmann et al., 2024; Hanson et al., 2011; Kennedy et al., 2016). *Cyprinid herpesvirus 2* (CyHV-2) is the causative agent of frequent high mortality outbreaks in the aquaculture sector and is now the most frequently detected virus in goldfish (Ito et al., 2017). Besides its impact on ornamental goldfish, CyHV-2 also infects other economically important species in the genus *Carassius*, including gibel carp and crucian carp, both of which are significant in the food sector, with production reaching as high as 2,748.6 thousand tonnes in 2020, accounting for 5.6% of the world's total production of major finfish (FAO, 2022).

Prior to this present study, scientific knowledge regarding this disease was fragmentary, and the pathogenesis remained inadequately understood. The primary aim of this thesis was to bridge these knowledge gaps and provide some insights into CyHV-2 pathogenesis. In the first study, CyHV-2 pathogenesis was explored in its natural host utilizing an In Vivo Bioluminescent Imaging System (IVIS) in conjunction with a recombinant viral strain expressing the luciferase (Luc) and copepod GFP (copGFP) reporter genes. This recombinant construct enabled the investigation of relative susceptibility (the ability to support CyHV-2 entry) and permissivity (the ability to support CyHV-2 replication) across different developmental stages, as well as the route of viral entry into the host. The experiments yielded the following findings: *(i)* In goldfish, earlier developmental stages exhibit lower susceptibility but higher permissivity to CyHV-2 infection compared to later developmental stages, resulting in increased mortality in the former. *(ii)* Across all developmental stages, the skin exhibits a higher viral load than other organs during the early stages of infection by immersion, suggesting that the skin is the primary portal of viral entry into the host, as opposed to other mucosal surfaces in constant contact with environmental water such as gills and gastrointestinal tract. Although notably, the CyHV-2 strain that was used did not cause much mortality in adult hosts when challenged by immersion.

In the second study, a zebrafish model was tested to determine its susceptibility and permissivity to CyHV-2. This was done in order to explore the possibility of establishing, through genetic engineering, new zebrafish strains, with increased susceptibility and permissivity to CyHV-2 and other Cyprinivirus species. In theory, with the correct modifications, mutant zebrafish strains may have facilitated the study of these viruses in the zebrafish model. Importantly, given that this host can be easily genetically modified further, this may have facilitated studies on the importance of various evolutionarily conserved host factors during CyHV-2 infection. Therefore, the generation of a CyHV-2-zebrafish infection model may have been useful for exploratory studies before further investigation in the natural hosts of CyHV-2. Initial *in vitro* investigations revealed that zebrafish embryonic fibroblast cells (ZF4) were susceptible and transiently permissive to CyHV-2 replication, but that this was followed by rapid

clearance of infection. Similarly, *in vivo* experiments employing microinjections demonstrated that while zebrafish larvae displayed susceptibility to CyHV-2, these infections were also rapidly cleared. A related *Cyprinivirus*, CyHV-3, exhibited slightly more fitness in these *in vitro* and *in vivo* zebrafish model, and was thus used to test genetically engineered immunodeficient zebrafish strains. Considering the strong host specificity exhibited by Cyprinivirus, and the results with both CyHV-2 and CyHV-3, we concluded that the zebrafish model offered only limited applicability in terms of the study of Cyprinivirus.

Given the lack of mortality observed with the YC-01 and ST-J1 strains when adult fish were challenged by immersion, in the third study we aimed to identify novel strains of CyHV-2 that were *(i)* compatible with stable culture *in vitro*, and *(ii)* capable of causing disease and mortality in adult hosts after vial challenge by immersion. As a result, we isolated and characterized three new CyHV-2 strains originating from high mortality CyHV-2 outbreaks in the field. These were isolated from CyHV-2 outbreaks in the Netherlands, thus we denoted these NL-1, NL-2, and NL-3. Genome sequencing revealed many differences relative to the ST-J1 CyHV-2 reference strain. Additionally, distinct *in vitro* growth kinetics were observed among these strains. NL-2 exhibited the highest fitness *in vitro* and, unlike the ST-J1 CyHV-2 reference strain, it was demonstrated to induce high mortality in adult Shubunkin goldfish after viral challenge by immersion. Overall, this NL-2 Shubunkin-goldfish model was found to represent a much more appropriate model for future investigations into CyHV-2 pathogenesis and CyHV-2 challenge trials as part of vaccine development. Furthermore, the identification of gene disruptions in the ST-J1 reference strain relative to the NL-2 strain, provided insights into what viral genes may be important for CyHV-2 fitness *in vivo*.

This section provides further discussion of the results from these three earlier studies described in the experimental sections of this thesis, together with future perspectives. Rather than repeating points from these earlier discussions, in this final discussion section the results from the three studies are discussed collectively with the added benefit of additional retrospective insights gained after their completion. Furthermore, additional data and context that were outside the scope of the three experimental sections of this thesis are also provided in this final discussion section.

Design and rationale behind the first CyHV-2 recombinant and future perspectives

One of the earliest contributions to the field of CyHV-2 research that was made as part of this Ph.D. project was the development of the first recombinant CyHV-2 strain, expressing both bioluminescent (Firefly luciferase) and fluorescent (copGFP) reporter genes (Experimental Section 1) (He et al., 2023). The Luc and copGFP proteins represent widely employed molecular reporters that can be noninvasively detected in living cells. (Li et al., 2021; Gould and Subramani, 1988; Wilmann et al., 2006; Shokrollahi et al., 2016). Firefly luciferase (Luc) is a member of the acyl-adenylate/thioester-forming superfamily of enzymes and catalyzes the oxidation of firefly luciferin with molecular oxygen

to emit light (Inouye, 2010). As the detection of signal from Luc does not require any excitation light source, non-specific background signal is eliminated. CopGFP, also known as ppluGFP2, is a basic (constitutively fluorescent) green fluorescent protein described in 2004, derived from *Pontellina plumate* (Shagin et al., 2004). Unlike bioluminescent reporters, fluorescent reporters like CopGFP do require an excitation light source. As many biomolecules may absorb and emit light in the same part of the spectrum as CopGFP, this may result in a lot of background signals in some circumstances. However, fluorescent reporters such as CopGFP are much more suited to microscopic imaging processes. Therefore having both bioluminescent and fluorescent reporters in a single recombinant allowed us to exploit both of these useful properties (Day et al., 1998; Molina et al., 2002). Furthermore, in the construct used in this project we linked the Luc and copGFP ORFs using an in-frame T2A self-cleaving peptide signal, therefore both reporter proteins could be expressed from a single constitutively active EF1α promotor, generating a single mRNA encoding a single large ORF, thus requiring less space in the CyHV-2 recombinant genome. Briefly, the presence of the T2A signal between the two genes results in the generation of two independent peptides, one representing the coding sequence prior to the T2A signal and one representing the coding sequence after the T2A signal. More specifically, after the first gene is translated, due to the absence of a stop codon, the ribosome proceeds with translation of the downstream T2A sequence, but fails form a peptide link between the upstream and downstream proteins due to the specific properties of the T2A signal. This results in the generation of two separate proteins rather than a single fused protein after translation, despite the fact that they are essentially encoded in a single ORF (Szymczak-Workman et al., 2012). In the context of the reporter construct employed in this project, this design resulted in a CyHV-2 recombinant capable of simultaneous constitutive expression of fully functional Luc and CopGFP reporter proteins, while requiring minimum space in the CyHV-2 genome, thus minimizing any phenotypic impact of the construct insertion. It was also important to choose an insertion site that would minimize disruption to adjacent genes. In order to achieve this, after a survey of the CyHV-2 genome, it was decided to place the reporter construct in a region downstream of the polyadenylation signal for CyHV-2 ORF64 and upstream of the polyadenylation signal for CyHV-2 ORF66 (which is transcribed on the opposite orientation to ORF64, thus avoiding disruption of promoters for genes downstream of ORF64). Furthermore, this location was also chosen as it should represent a region where transcription from both of these ORFs should cease given that it is flanked by polyadenylation signals in opposite "head-to-head" orientations. We verified this using publicly available CyHV-2 transcriptome data (Discussion Fig. S1). This rational approach to insertion site selection resulted in the generation a recombinant that retained the transcriptional, *in vitro* and *in vivo* phenotype of the parental strain (Experimental Section 1 Fig. 1C, and Fig. 2), allowing us to use it to make valid biological inferences about the parental strain.

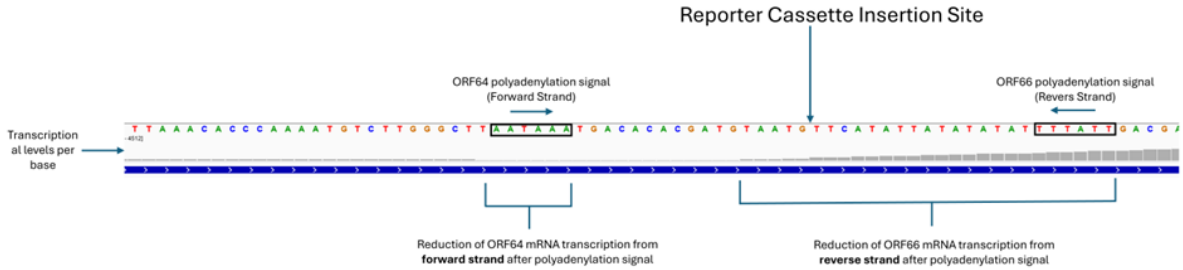

Discussion Figure S1 - Transcriptomic data from CyHV-2 ORF64 (forward strand) and ORF66 (reverse strand) confirming that for both ORF64 and ORF66 mRNAs, the per-base transcription reduces after the polyadenylation signals. This indicates that the insertion of the reporter cassette at the indicated site (which is flanked by polyadenylation signals) should have minimum impact on ORF64 and ORF66 mRNA sequences during CyHV-2 infection.

Regarding the choice of parental strain for the recombinant, it was important to select a strain that exhibited high fitness *in vitro*. This was not only important to facilitate the continuous generation of any resulting recombinant viral stock *in vitro* in the future, but also important in order to maximise the chances of success in generating a recombinant CyHV-2 strain to begin with. This was because the process we used to generate the recombinant relied on homologous recombination between the parental strain and the reporter construct on a donor plasmid (see Experimental Section 1). These recombination events are rare in cells. Furthermore, this requires cells to be simultaneously transfected with plasmid and infected with actively replicating virus. Given the low plasmid transfection efficiency in goldfish cells in general, cells that are both infected with CyHV-2 and transfected with a donor plasmid are also rare. Furthermore, cells transfected with donor plasmids were much more likely to enter an antiviral state due to stimulation of innate immune receptors by incoming plasmid with non-methylated CpG motifs (Reyes-Sandoval and Ertl, 2004). Therefore, it was important to maximise the number of infected cells, and this necessitated the use of a CyHV-2 strain that exhibited high fitness *in vitro*. While the ST-J1 CyHV-2 reference strain exhibits a high degree of fitness *in vitro* compared to other strains (Experimental Section 3 Fig. 6), earlier experiments revealed that the YC-01 exhibits an even higher fitness *in vitro* than that of the ST-J1 strain (Discussion Fig. S2). Therefore, in order to maximise the chances of success, the YC-01 strain was chosen as the parental strain for the CyHV-2 recombinant.

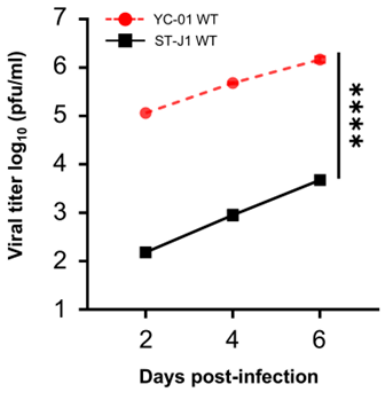

Discussion Figure S2 - Viral growth curve comparison between YC-01 and ST-J1. RyuF-2 cells were infected with the indicated strains (MOI=0.01) and the log10 value of the titer (pfu/mL) in the supernatant was determined at the 2, 4 and 6 dpi. Data represents the mean of the triplicate measurements.

The generation of this CyHV-2 recombinant expressing these two reporter genes represented an important advance beyond the current state of the art in the field of CyHV-2 research. Prior to this, in the absence of any virally expressed bioluminescent reporters, there was no way to easily follow the progression of CyHV-2 infections *in vivo* and quantify the extent of viral replication over time. Although, in theory, this can be achieved by qPCR or immunostaining, these approaches require several sample processing and analysis steps in order to measure viral load. Furthermore, at adult developmental stages, results obtained from such methods will be greatly impacted by the random nature of tissue sampling, especially for large organs, particularly in the case of the skin, where subsamples of tissue need to be taken rather than the entire organ. Conversely, given that in the case of bioluminescence, subsampling of organs is not required, this eliminates any such experimental sampling artifacts and facilitates a non-biased measurement of viral load in entire organs, or across the entire external surface of subjects, in the case of the skin. Also, viral loads can be directly measured in samples without the need for any additional tissue processing or molecular or immunostaining analysis (He et al., 2023) thus reducing experimental error.

In Experimental Section 1, the combined use of the Luc and CopGFP reporters to follow and measure CyHV-2 replication *in vivo* was a crucial factor in allowing us to establish that at all developmental stages, the virus initially enters hosts via the skin, and this recombinant will continue to be very valuable research tool in this field. However, as with the CyHV-2 ST-J1 reference strain (Experimental Section 3 Fig. 7 B), the YC-01 recombinant strain exhibited an attenuated phenotype in adult subjects when challenged by immersion, causing little or no mortality (Experimental Section 1, Fig. 9 B). This is in stark contrast to the newly described NL-2 strain (Experimental Section 3 Fig. 7 B). Notably, the NL-2 strain also exhibits reasonably good fitness *in vitro* and is compatible with stable passaging in this environment (Experimental Section 3 Fig. 6). Thus, as part of future CyHV-2 research projects, it may be valuable to generate a similar CyHV-2 recombinant using NL-2 as the parental strain, which may facilitate the study of disease caused by highly pathogenic strains in adults after viral challenge by immersion, which may be more representative of natural infection routes. Although the generation of a recombinant using NL-2 may be more cumbersome than YC-01 given the formers lower fitness *in vitro* (Compare Experimental Section 3 Fig. 6 with Discussion Fig. S2, with ST-J1 as common reference), this process will benefit greatly from the knowledge gained and output from the generation of the YC-01 recombinant in terms of reporter protein selection, recombination protocols, pre-existing donor plasmids, and pre-existing optimum insertion sites. Furthermore, the generation of an NL-2 recombinant may be extremely useful in future fundamental research into CyHV-2 and vaccine challenge trials (discussed in more detail later), in the same way that similar CyHV-3 recombinants have facilitated major

advances in the fundamental understanding and vaccine development with this closely related virus (Boutier et al., 2015a; Costes et al., 2009; Fournier et al., 2012; Ronsmans et al., 2014).

It is acknowledged that this tracing method carries the risk of producing false negatives, where the virus may be actively replicating in an organ but remains undetected. Several factors could account for this. During viral replication, mutations in the viral genome could alter the reporter gene sequence, potentially preventing its proper expression. Additionally, the timing of detection is crucial. Certain tissues inherently produce bioluminescent or fluorescent signals, which can increase background noise, thereby complicating the detection of weak luciferase signals. Thus, detection must be timed to occur when viral replication is sufficiently advanced and reporter gene expression exceeds the detection threshold. Moreover, the signal may not be detected if there is insufficient contact between the substrate and the enzyme. This is a common issue, as the intensity of the bioluminescent signal depends on the quantity of luciferase produced by the virus in infected cells. For instance, an inaccurate microinjection site failure to deliver the substrate into the heart can prevent it from reaching the infected tissue, consequently diminishing signal intensity. Despite these potential challenges, the strategy we have employed remains highly feasible and offers distinct advantages.

The "fine-tuning" of the CyHV-2 *in vivo* infection model throughout this Ph.D. project and future perspectives

One of the overarching themes, particularly in Experimental Sections 2 and 3, was the identification of a suitable *in vivo* experimental infection model for CyHV-2. Ideally, experimental infection conditions, including viral and host strain selection, should be adequate to facilitate robust and reproducible high mortality disease among subjects after viral challenge by immersion, as this infection route is more representative of natural infections. Whether or not this can be achieved may depend on *(i)* the viral strains used, as changes in key virulence factors may determine the phenotype *in vivo*, and *(ii)* host factors, given that various genetic or epigenetic circumstances may impact resistance to viral challenge. Given that it was best to produce the CyHV-2 recombinant using YC-01 as a parental strain, (for reasons described earlier) we sought to determine which goldfish breed may be the most susceptible to the YC-01 WT strain before proceeding further. As part of this process, we conducted initial challenge trials using different goldfish breeds. We selected goldfish breeds that were reported to be susceptible to CyHV-2 including Common goldfish (Hedrick et al., 2006), Ryukin goldfish (Ito et al., 2017), Wakin goldfish (Panicz et al., 2019), Shubunkin goldfish (Ito et al., 2017), and two additional breeds that had not been tested yet in terms of CyHV-2 susceptibility namely, Comet goldfish and Sarasa goldfish. In all cases, subjects were at the adult stage of development or approaching adulthood. Mortality was observed after viral challenge by IP injection with a high viral load, but there were differences between goldfish breeds. However, even after IP injection, mortality caused by the YC-01 strain was still absent or low in all goldfish breeds, with the exception of Shubunkin goldfish which exhibited almost 80% mortality, indicating that it was the most susceptible to mortality induced by the CyHV-2 YC-01 strain

(Discussion Fig. S3). Thus, we chose to use Shubunkin goldfish as part of the YC-01 recombinant *in vivo* infection model in further experiments. Even though this goldfish breed was very resistant to YC-01 induced mortality via challenge by immersion at the adult stage, these subjects were still extremely susceptible to infection (Experimental Section 1, Fig. 9 C), allowing us to identify the skin as the primary portal of entry in this development stage, which was consistent with other developmental stages. These comparisons between developmental stages also indicated that the YC-01 strain was indeed capable of inducing mortality in Shubinkin goldfish via challenge by immersion, but this decreased as development progressed, ultimately leading to little or no mortality at the adult stage.

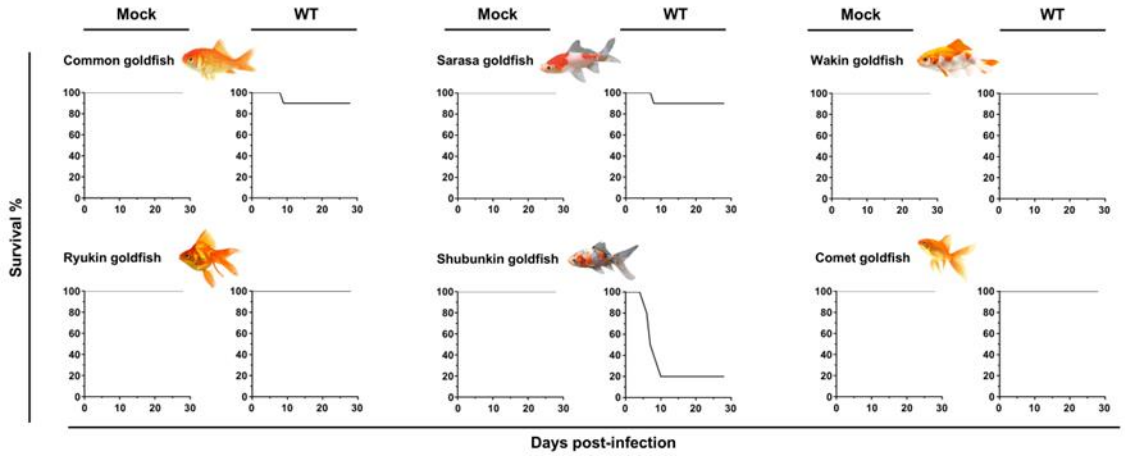

Discussion Figure S3 - Primary comparison of various goldfish breeds. Each group consists of 10 subjects challenged by IP and the same number of fish as Mock. Common goldfish (average weight 7.3g), Ryukin goldfish (average weight 7.07g), Wakin goldfish (average weight 4.25g), Shubunkin goldfish (average weight 3.44g), Comet goldfish (average weight 8.6g) and Sarasa goldfish (average weight 4.02g).

The YC-01 recombinant strain was extremely useful in determining these differences in CyHV-2 susceptibility and permissively across different developmental stages, and allowing us to identify the portal of entry in Experimental Section 1. Although this recombinant strain was an extremely valuable tool, given that it exhibited an attenuated phenotype in adults when challenged by immersion, it was clearly not representative of highly pathogenic CyHV-2 strains responsible for high mortality outbreaks in the field, including strains responsible for outbreaks within adult Shubinkin goldfish populations (Ito et al., 2017). Consequently, we reasoned that the YC-01 recombinant may not be suitable for future studies on viral host interaction during acute high mortality outbreaks in adults involving viral challenge by immersion. Furthermore, we also reasoned that this YC-01 recombinant may not be optimum for incorporation into challenge trials to determine vaccine efficacy. This is because it cannot reliably cause mortality in naive adult subjects after challenge by immersion. Therefore, if using the YC-01 recombinant as a challenge strain in future vaccine trials, it will only be possible to demonstrate differences in viral load or clearance times in vaccinated adults. This may not necessarily be indicative of the extent of protection against highly virulent strains responsible for mass mortality in the field.

Therefore, in order to improve our CyHV-2 *in vivo* infection model, rather than focusing on identifying less resistant goldfish breeds, we chose to change our approach and instead worked towards isolating and characterizing novel highly pathogenic CyHV-2 strains from outbreaks in the field, in order to replace the YC-01 strain and ST-J1 reference strains that we predominantly used in our CyHV-2 *in vivo* infection models. We also reasoned that it would be useful to retain the use of Shubunkin goldfish breed as a host, as they were the most sensitive to the CyHV-2 strains that we had used up to that point and were sensitive to highly pathogenic field strains (Ito et al., 2017). Furthermore, we could easily breed Shubunkin goldfish in our facility. This change of approach ultimately led to the isolation and characterization of the NL-2 CyHV-2 strain. In contrast to the ST-J1 and YC-01 strain, this strain was much more virulent in Shubunkin adult goldfish in experiments involving viral challenge by immersion causing high mortality among subjects.

This process of "fine tuning" the CyHV-2 *in vivo* infection model over the course of this Ph.D. project by testing different combinations of CyHV-2 strains and goldfish breeds revealed differences in CyHV-2 resistance between these breeds, as observed elsewhere (Ito et al., 2013). However, it also revealed that the biggest factor in establishing a high virulence CyHV-2 *in vivo* infection model was possibly the choice of viral strain. This ultimately led to the establishment of the much more virulent NL-2-Shubunkin CyHV-2 *in vivo* infection model. As mentioned earlier, it may also represent an ideal parental strain for the generation of a new CyHV-2 recombinant expressing the same reporter genes, which would be an ideal recombinant for challenge trials in future projects aimed at developing CyHV-2 vaccines. Furthermore, it is also possible an NL-2 recombinant may be more virulent than the YC-01 strain in the WT or immunodeficient mutant zebrafish model that was described in Experimental Section 2, which may be very interesting to test. If the NL-2 strain could be found to be more virulent in these zebrafish models, or if it can facilitate the establishment of infection by immersion, it would allow us to revisit the possibility of using genetically modified zebrafish to identify important evolutionary conserved innate immune factors that are important for CyHV-2 clearance in survivors. This would be extremely valuable for building hypotheses and providing new insights into key viral host interaction processes that may also take place during CyHV-2 infections in its natural host species.

It is important to note that in this context, although zebrafish and goldfish belong to the same family (*Cyprinidae*) and that closely related cyprinviruses can establish infections in both species, it is essential to recognize that zebrafish is a highly specialized laboratory species. As a tropical freshwater organism, zebrafish exhibits significant differences from commercially valuable aquaculture species in terms of size, physiology, reproductive strategy, and environmental tolerance (Sofyantoro et al., 2024; Tsang et al., 2017). Commercial aquaculture primarily targets larger, temperate species such as carp, goldfish, catfish, and salmon, which have distinct growth requirements, stress responses, and disease profiles that zebrafish cannot adequately model. For instance, zebrafish have markedly different metabolic rates, growth efficiencies, and feed conversion ratios compared to species cultivated on a

commercial scale for human consumption (Gonzales and Law, 2013). Furthermore, zebrafish thrive in controlled laboratory environments, which differ significantly from the complex, pathogen-rich conditions found in aquaculture systems, such as ponds or recirculating aquaculture systems (RAS). For instance, *Aeromonas hydrophila* is commonly present in aquaculture environments, where it typically does not cause severe outbreaks or high mortality. Research has also demonstrated that CyHV-2 can interact with *A. hydrophila* in antagonistic or synergistic ways, depending on the timing of infection (Ren et al., 2021). However, in zebrafish, *A. hydrophila* often leads to high mortality rates, highlighting the species' susceptibility to this pathogen under experimental conditions (Rodríguez et al., 2008). While zebrafish serve as a valuable model for basic biological research, their direct application to enhancing aquaculture production remains limited. Therefore, for any insights that may be gained from zebrafish, a follow-up with species-specific research will always remain essential if such insights are to be exploited in addressing the challenges faced by commercially important fish species in aquaculture.

Future prospectives regarding CyHV-2 vaccine development arising from this Ph.D. Project.

Over the course of this Ph.D., we encountered challenges in terms of establishing a highly virulent *in vivo* infection model compatible challenge by immersion. However, these challenges have given us a greater appreciation for the huge phenotypic differences that exist between different CyHV-2 strains. A key example of this is the differences between the two attenuated CyHV-2 strains, YC-01 and ST-J1 and our newly characterized NL-2 strain. Adaptation to *in vitro* culture conditions can often lead to the development of an attenuated phenotype *in vivo*, and we have shown this to be the case with strains of CyHV-3 (Gao et al., 2023, 2018), which is the closest known relative to CyHV-2 (Donohoe et al., 2021). In the case of one of these CyHV-2 attenuated strains, ST-J1, it is worth noting that it has been passaged *in vivo* and *in vitro* since 1992. It is unclear if the ORF disruptions that it exhibits have occurred during adaptation *in vitro* passaging or not [3] or if additional changes have emerged during its use in this Ph.D. project. Notably, we have demonstrated that, with CyHV-3 at least, that *in vitro* adaptation, leading to *in vivo* attenuation can occur over very few passages *in vitro*. In the case of the other attenuated strain, YC-01, while it was isolated much more recently than ST-J1, it exhibits many genomic differences to all other CyHV-2 strains (Experimental Section 3, Fig. 3B), particularly genomic inversions (Yang et al., 2024). However, again, it is unclear if such changes were also present in the field or if they emerged during passaging *in vitro*. Interestingly, attenuation through serial passaging *in vitro* has been used as a method of generating live attenuated CyHV-2 vaccine candidates (Saito et al., 2022; Y. Sun et al., 2023) and given the attenuated phenotype exhibited by the ST-J1 or YC-01 strains passaged in our laboratory, it may be interesting to see if subjects challenged with these strains by immersion (which cause little or no disease or mortality), exhibit resistance to the more virulent NL-2 strain. Interestingly in the case of the YC-01 recombinant, the Luc reporter would be very useful to robustly determine how long it takes for the attenuated YC-01 infection to be completely cleared after vaccination. Once this is established, the same fish could then be challenged with a NL-2 recombinant after this initial vaccination with the

YC-01 recombinant. Interestingly, in such a study, it may be useful if the NL-2 recombinant was designed to express a different bioluminescent reporter than the YC-01 recombinant, and ideally one that relies on a different substrate. This would facilitate specific detection of the NL-2 challenge strain replication in subjects already vaccinated with the YC-01 (Luc-expressing) recombinant. A bioluminescent reporter that may be compatible with this is nano-luciferase (NLuc). This is a very sensitive bioluminescent reporter that relies on a different substrate than Luc (England et al., 2016). However, as emission from NLuc is at a lower wavelength than Luc, it may not penetrate tissue as easily. Interestingly, this problem may be overcome using modified versions of NLuc that are fused to fluorescent proteins. In these cases, NLuc emission is immediately absorbed by the fused fluorescent protein, through a process known as bioluminescence resonance energy transfer (BRET). This allows NLuc emission to act as a highly efficient excitation source for the fluorescent protein. This leads to highly intense emission from the fluorescent protein at higher wavelengths that can penetrate tissue much more easily than the initial light emitted from NLuc (Schaub et al., 2015; Suzuki et al., 2016). This multiplex *in vivo* imaging approach (using Luc and NLuc-BRET reporters) to vaccine challenge trials would allow us to further exploit and build on the CyHV-2 genetic engineering, *in vivo* infection and *in vivo* imaging platforms that we have established and refined throughout the course of this Ph.D project, allowing us to continue progress towards CyHV-2 vaccine development and continue to push CyHV-2 research beyond the current state of the art in the future.

References

Abram, Q.H., Dixon, B., Katzenback, B.A., 2017. Impacts of Low Temperature on the Teleost Immun e System. Biology 6, 39. https://doi.org/10.3390/biology6040039

Ackermann, M., 2004. Herpesviruses, in: Zhao, S., Stodolsky, M. (Eds.), Bacterial Artificial Chromos omes: Volume 2 Functional Studies. Humana Press, Totowa, NJ, pp. 199–219. https://doi.org/ 10.1385/1-59259-753-X:199

Adamek, M., Hellmann, J., Jung-Schroers, V., Teitge, F., Steinhagen, D., 2018. CyHV-2 transmission in traded goldfish stocks in Germany—A case study. J. Fish Dis. 41, 401–404. https://doi.org/ 10.1111/jfd.12734

Ahmad, I., Wilson, D.W., 2020. HSV-1 Cytoplasmic Envelopment and Egress. Int. J. Mol. Sci. 21, 59 69. https://doi.org/10.3390/ijms21175969

Akimenko, M.-A., Marí-Beffa, M., Becerra, J., Géraudie, J., 2003. Old questions, new tools, and some answers to the mystery of fin regeneration. Dev. Dyn. 226, 190–201. https://doi.org/10.1002/ dvdy.10248

Aoki, T., Hirono, I., Kurokawa, K., Fukuda, H., Nahary, R., Eldar, A., Davison, A.J., Waltzek, T.B., B ercovier, H., Hedrick, R.P., 2007. Genome sequences of three koi herpesvirus isolates represe nting the expanding distribution of an emerging disease threatening koi and common carp wor ldwide. J. Virol. 81, 5058–65.

Aswad, A., Katzourakis, A., 2017. A novel viral lineage distantly related to herpesviruses discovered within fish genome sequence data. Virus Evol. 3, vex016. https://doi.org/10.1093/ve/vex016

Atmar, R.L., Ramani, S., 2020. Immunologic Detection and Characterization, in: Kaslow, R.A., Stanb erry, L.R., Powers, A.M. (Eds.), Viral Infections of Humans: Epidemiology and Control. Spri nger US, New York, NY, pp. 1–30. https://doi.org/10.1007/978-1-4939-9544-8_3-1

Bergmann S.M., Wang Y., Li Y., Wang Q., Klafack S., Jin Y., Hofmann A.C., Kielpinska J., Becker A.M., Zeng W., 2024. Occurrence of herpesvirus in fish. J. Vet. Res. 0.

Beurden S.J., Engelsma M.Y., Roozenburg I., Voorbergen-Laarman M.A., Tulden P.W., Kerkhoff S., Nieuwstadt A.P., Davidse A., Haenen O.L.M., 2012. Viral diseases of wild and farmed Europ ean eel Anguilla anguilla with particular reference to the Netherlands. Dis. Aquat. Organ. 101, 69–86. https://doi.org/10.3354/dao02501

Beurden, S. van, Engelsma, M., Beurden, S. van, Engelsma, M., 2012. Herpesviruses of Fish, Amphib ians and Invertebrates, in: Herpesviridae - A Look Into This Unique Family of Viruses. Intech Open. https://doi.org/10.5772/29575

Blanco, A.M., Sundarrajan, L., Bertucci, J.I., Unniappan, S., 2018. Why goldfish? Merits and challeng es in employing goldfish as a model organism in comparative endocrinology research. Gen. C omp. Endocrinol., Proceedings of the 8th International Symposium on Fish Endocrinology 20 16 257, 13–28. https://doi.org/10.1016/j.ygcen.2017.02.001

Blanco, A.M., Unniappan, S., 2022. Chapter 15 - Goldfish (Carassius auratus): biology, husbandry, an d research applications, in: D'Angelo, L., de Girolamo, P. (Eds.), Laboratory Fish in Biomedi cal Research. Academic Press, pp. 373–408. https://doi.org/10.1016/B978-0-12-821099-4.000 12-2

Bo, A., Po, O., Okonko, I., 2012. Immune Response of Fish to Viral Infection. Nat. Sci. 10, 70–76.

Boitard, P.-M., Baud, M., Labrut, S., de Boisséson, C., Jamin, M., Bigarré, L., 2016. First detection of Cyprinid Herpesvirus 2 (CyHV-2) in goldfish (Carassius auratus) in France. J. Fish Dis. 39, 6 73–680. https://doi.org/10.1111/jfd.12400

Boutier, M., Morvan, L., Delrez, N., Origgi, F., Doszpoly, A., Vanderplasschen, A., 2021. Fish and A mphibian Alloherpesviruses (Herpesviridae), in: Bamford, D.H., Zuckerman, M. (Eds.), Ency clopedia of Virology (Fourth Edition). Academic Press, Oxford, pp. 306–315. https://doi.org/1 0.1016/B978-0-12-809633-8.20931-X

Boutier, M., Ronsmans, M., Ouyang, P., Fournier, G., Reschner, A., Rakus, K., Wilkie, G.S., Farnir, F ., Bayrou, C., Lieffrig, F., Li, H., Desmecht, D., Davison, A.J., Vanderplasschen, A., 2015a. R ational Development of an Attenuated Recombinant Cyprinid Herpesvirus 3 Vaccine Using Pr okaryotic Mutagenesis and In Vivo Bioluminescent Imaging. PLOS Pathog 11, e1004690. htt ps://doi.org/10.1371/journal.ppat.1004690

Boutier, M., Ronsmans, M., Rakus, K., Jazowiecka-Rakus, J., Vancsok, C., Morvan, L., Peñaranda, M .M.D., Stone, D.M., Way, K., van Beurden, S.J., Davison, A.J., Vanderplasschen, A., 2015b. Cyprinid Herpesvirus 3: An Archetype of Fish Alloherpesviruses. Adv. Virus Res. 93, 161–25 6. https://doi.org/10.1016/bs.aivir.2015.03.001

Brenden, R.A., Huizinga, H.W., 1986. Pathophysiology of experimental Aeromonas hydrophila infect ion in goldfish, Carassius auratus (L.). J. Fish Dis. 9, 163–167. https://doi.org/10.1111/j.1365-2761.1986.tb00999.x

Bretzinger, A., Fischer-Scherl, T., Oumouna, M., Hoffmann, R., Truyen, U., 1999. Mass mortalities in Koi carp, Cyprinus carpio, associated with gill and skin disease. Bull. Eur. Assoc. Fish Pathol .

Brown, J.C., 2017. Herpes Simplex Virus Latency: The DNA Repair-Centered Pathway. Adv. Virol. 2 017, 7028194. https://doi.org/10.1155/2017/7028194

Brunner, B., 2005. The ocean at home : an illustrated history of the aquarium. New York : Princeton A rchitectural Press.

Cao, Z., Liu, S., Nan, H., Zhao, K., Xu, X., Wang, G., Ji, H., Chen, H., 2019. Immersion immunizatio n with recombinant baculoviruses displaying cyprinid herpesvirus 2 membrane proteins induc ed protective immunity in gibel carp. Fish Shellfish Immunol. 93, 879–887. https://doi.org/10. 1016/j.fsi.2019.08.036

Cassedy, A., Parle-McDermott, A., O'Kennedy, R., 2021. Virus Detection: A Review of the Current a nd Emerging Molecular and Immunological Methods. Front. Mol. Biosci. 8.

Chai, W., Qi, L., Zhang, Y., Hong, M., Jin, L., Li, L., Yuan, J., 2020. Evaluation of Cyprinid Herpesvi rus 2 Latency and Reactivation in Carassius gibel. Microorganisms 8, 445. https://doi.org/10.3 390/microorganisms8030445

Chang, J.P., Johnson, J.D., Sawisky, G.R., Grey, C.L., Mitchell, G., Booth, M., Volk, M.M., Parks, S. K., Thompson, E., Goss, G.G., Klausen, C., Habibi, H.R., 2009. Signal transduction in multifa ctorial neuroendocrine control of gonadotropin secretion and synthesis in teleosts—studies on the goldfish model. Gen. Comp. Endocrinol., International Fish Endocrine Symposium Specia l Issue 161, 42–52. https://doi.org/10.1016/j.ygcen.2008.09.005

Chang, P.H., Lee, S.H., Chiang, H.C., Jong, M.H., 1999. Epizootic of Herpes-like Virus Infection in G oldfish, Carassius auratus in Taiwan. Fish Pathol. 34, 209–210. https://doi.org/10.3147/jsfp.34 .209

Charnov, E.L., Gillooly, J.F., 2004. Size and Temperature in the Evolution of Fish Life Histories1. Int egr. Comp. Biol. 44, 494–497. https://doi.org/10.1093/icb/44.6.494

Chen, D., Zhang, Qing, Tang, W., Huang, Z., Wang, G., Wang, Yongjun, Shi, J., Xu, H., Lin, L., Li, Z ., Chi, W., Huang, L., Xia, J., Zhang, X., Guo, L., Wang, Yuanyuan, Ma, P., Tang, J., Zhou, G ., Liu, M., Liu, F., Hua, X., Wang, B., Shen, Q., Jiang, Q., Lin, J., Chen, X., Wang, H., Dou, M., Liu, L., Pan, H., Qi, Y., Wu, B., Fang, J., Zhou, Y., Cen, W., He, W., Zhang, Qiujin, Xue, T., Lin, G., Zhang, W., Liu, Z., Qu, L., Wang, A., Ye, Q., Chen, J., Zhang, Y., Ming, R., Van Montagu, M., Tang, H., Van de Peer, Y., Chen, Y., Zhang, J., 2020. The evolutionary origin a nd domestication history of goldfish (Carassius auratus). Proc. Natl. Acad. Sci. 117, 29775–29 785. https://doi.org/10.1073/pnas.2005545117

Chen, P., Zhang, M., Zhang, Y., Li, J., Wan, X., Lv, T., Chen, Y., Zhao, Z., Ma, Z., Zhu, Z., Chen, L., Li, Z., Wang, Z., Qiao, G., 2023. Cyprinid herpesvirus 2 infection changes microbiota and me

tabolites in the gibel carp (Carassius auratus gibelio) midgut. Front. Cell. Infect. Microbiol. 12
.

Chen, S.C., 1956. A history of the domestication and the factors of the varietal formation of the comm on goldfish, Carassius auratus. Sci. Sin. 6, 89.

Cheng, A.Z., Moraes, S.N., Shaban, N.M., Fanunza, E., Bierle, C.J., Southern, P.J., Bresnahan, W.A., Rice, S.A., Harris, R.S., 2021. APOBECs and Herpesviruses. Viruses 13, 390. https://doi.org/ 10.3390/v13030390

Cheng, W., Chen, Q., Ren, Y., Zhang, Y., Lu, L., Gui, L., Xu, D., 2023. The identification of viral rib onucleotide reductase encoded by ORF23 and ORF141 genes and effect on CyHV-2 replicatio n. Front. Microbiol. 14.

Conroy, D.A., 1961. A study of the bacterium associated with an outbreak of oedema amongst goldfis h (Carassius carassius var. auratus). Microbiol. Esp. 14, 73–105.

Corbeil, S., 2020. Abalone Viral Ganglioneuritis. Pathogens 9, 720. https://doi.org/10.3390/pathogens 9090720

Corbeil, S., Kurath, G., Lapatra, S.E., 2000. Fish DNA vaccine against infectious hematopoietic necro sis virus: efficacy of various routes of immunisation. Fish Shellfish Immunol. 10, 711–723. ht tps://doi.org/10.1006/fsim.2000.0286

Costes, B., Fournier, G., Michel, B., Delforge, C., Raj, V.S., Dewals, B., Gillet, L., Drion, P., Body, A ., Schynts, F., Lieffrig, F., Vanderplasschen, A., 2008. Cloning of the koi herpesvirus genome as an infectious bacterial artificial chromosome demonstrates that disruption of the thymidine kinase locus induces partial attenuation in Cyprinus carpio koi. J. Virol. 82, 4955–64.

Costes, B., Raj, V.S., Michel, B., Fournier, G., Thirion, M., Gillet, L., Mast, J., Lieffrig, F., Bremont, M., Vanderplasschen, A., 2009. The Major Portal of Entry of Koi Herpesvirus in Cyprinus car pio Is the Skin. J. Virol. 83, 2819–2830. https://doi.org/10.1128/JVI.02305-08

Culture, P., n.d. China Fishery Statistical Yearbook 2016 [WWW Document]. Purple Cult. URL https: //www.purpleculture.net/china-fishery-statistical-yearbook-2016-p-23930/ (accessed 10.15.24).

Daněk, T., Kalous, L., Vesel, T., Krásová, E., Reschová, S., Rylková, K., Kulich, P., L, M.P., Pokorov á, D., Knytl, M., 2012. Massive mortality of Prussian carp Carassius gibelio in the upper Elbe basin associated with herpesviral hematopoietic necrosis (CyHV-2). Dis. Aquat. Organ. 102, 8 7–95. https://doi.org/10.3354/dao02535

Das, S., Dharmaratnam, A., Ravi, C., Kumar, R., Swaminathan, T.R., 2021. Immune gene expression i n cyprinid herpesvirus-2 (CyHV-2)–sensitized peripheral blood leukocytes (PBLs) co-culture d with CyHV-2-infected goldfish fin cell line. Aquac. Int. 29, 1925–1934. https://doi.org/10.1 007/s10499-021-00721-6

Davison, A.J., 2007. Comparative analysis of the genomes, in: Arvin, A., Campadelli-Fiume, G., Moc arski, E., Moore, P.S., Roizman, B., Whitley, R., Yamanishi, K. (Eds.), Human Herpesviruses : Biology, Therapy, and Immunoprophylaxis. Cambridge University Press, Cambridge.

Davison, A.J., 2002. Evolution of the herpesviruses. Vet. Microbiol., Importance of Veterinary Herpes viruses in the Context of Pathogenesis, Immunology and Gene Therapy 86, 69–88. https://doi. org/10.1016/S0378-1135(01)00492-8

Davison, A.J., 1998. The Genome of Salmonid Herpesvirus 1. J. Virol. 72, 1974–1982. https://doi.org/ 10.1128/jvi.72.3.1974-1982.1998

Davison, A.J., 1992. Channel catfish virus: A new type of herpesvirus. Virology 186, 9–14. https://doi .org/10.1016/0042-6822(92)90056-U

Davison, A.J., Eberle, R., Ehlers, B., Hayward, G.S., McGeoch, D.J., Minson, A.C., Pellett, P.E., Roizman, B., Studdert, M.J., Thiry, E., 2009. The order Herpesvirales. Arch. Virol. 154, 171–177. https://doi.org/10.1007/s00705-008-0278-4

Davison, A.J., Kurobe, T., Gatherer, D., Cunningham, C., Korf, I., Fukuda, H., Hedrick, R.P., Waltzek, T.B., 2013. Comparative Genomics of Carp Herpesviruses. J. Virol. 87, 2908–2922. https://doi.org/10.1128/jvi.03206-12

Davison, A.J., Trus, B.L., Cheng, N., Steven, A.C., Watson, M.S., Cunningham, C., Deuff, R.-M.L., Renault, T., 2005. A novel class of herpesvirus with bivalve hosts. J. Gen. Virol. 86, 41–53. https://doi.org/10.1099/vir.0.80382-0

Dawson, A.J., Meyer, R.L., 2008. Growth dynamics and morphology of regenerating optic fibers in tectum are altered by injury conditions: An in vivo imaging study in goldfish. Exp. Neurol. 210, 592–601. https://doi.org/10.1016/j.expneurol.2007.12.006

Day, R.N., Kawecki, M., Berry, D., 1998. Dual-Function Reporter Protein for Analysis of Gene Expression in Living Cells. BioTechniques 25, 848–856. https://doi.org/10.2144/98255bt02

Dharan, V., Khoo, L., Phelps, N.B.D., Kumar, G., Steadman, J., Bosworth, B., Aarattuthodi, S., 2022. An investigation into the pathogenesis of blue catfish alloherpesvirus in ictalurid catfish. J. World Aquac. Soc. 53, 384–400. https://doi.org/10.1111/jwas.12850

Dharmaratnam, A., Kumar, R., Valaparambil, B.S., Sood, N., Pradhan, P.K., Das, S., Swaminathan, T. R., 2020. Establishment and characterization of fantail goldfish fin (FtGF) cell line from goldfish, Carassius auratus for in vitro propagation of Cyprinid herpes virus-2 (CyHV-2). PeerJ 8, e 9373. https://doi.org/10.7717/peerj.9373

Dharmaratnam, A., Sudhagar, A., Das, S., Nair, R.R., Nithianantham, S.R., Preena, P.G., Lekshmi, N., Swaminathan, T.R., 2022. Immune gene expression and protective effects in goldfish (Carassius auratus L.) immunized with formalin-inactivated cyprinid herpesvirus-2 (CyHV-2) vaccine. Microb. Pathog. 164, 105452. https://doi.org/10.1016/j.micpath.2022.105452

Dharmaratnam, A., Sudhagar, A., Swaminathan, T.R., 2023. Evaluation of protective effects of heat-inactivated cyprinid herpesvirus-2 (CyHV-2) vaccine against herpesviral hematopoietic necrosis disease (HVHND) in goldfish (Carassius auratus). Fish Shellfish Immunol. 132, 108460. https://doi.org/10.1016/j.fsi.2022.108460

Diallo, M.A., Pirotte, S., Hu, Y., Morvan, L., Rakus, K., Suárez, N.M., PoTsang, L., Saneyoshi, H., Xu, Y., Davison, A.J., Tompa, P., Sussman, J.L., Vanderplasschen, A., 2022. A fish herpesvirus highlights functional diversities among Zα domains related to phase separation induction and A-to-Z conversion. Nucleic Acids Res. gkac761. https://doi.org/10.1093/nar/gkac761

Ding, Z., Xia, S., Zhao, Z., Xia, A., Shen, M., Tang, J., Xue, H., Geng, X., Yuan, S., 2014. Histopathological characterization and fluorescence in situ hybridization of Cyprinid herpesvirus 2 in cultured Prussian carp, Carassius auratus gibelio in China. J. Virol. Methods 206, 76–83. https://doi.org/10.1016/j.jviromet.2014.05.011

Dishon, A., Perelberg, A., Bishara-Shieban, J., Ilouze, M., Davidovich, M., Werker, S., Kotler, M., 2005. Detection of Carp Interstitial Nephritis and Gill Necrosis Virus in Fish Droppings. Appl. Environ. Microbiol. 71, 7285–7291. https://doi.org/10.1128/AEM.71.11.7285-7291.2005

Dong, Z.-R., Mu, Q.-J., Kong, W.-G., Qin, D.-C., Zhou, Y., Wang, X.-Y., Cheng, G.-F., Luo, Y.-Z., Ai, T.-S., Xu, Z., 2022. Gut mucosal immune responses and protective efficacy of oral yeast Cyprinid herpesvirus 2 (CyHV-2) vaccine in Carassius auratus gibelio. Front. Immunol. 13.

Donohoe, O., Zhang, H., Delrez, N., Gao, Y., Suárez, N.M., Davison, A.J., Vanderplasschen, A., 2021. Genomes of Anguillid Herpesvirus 1 Strains Reveal Evolutionary Disparities and Low Genetic Diversity in the Genus Cyprinivirus. Microorganisms 9, 998. https://doi.org/10.3390/microorganisms9050998

Doszpoly, A., Benkő, M., Csaba, G., Dán, Á., Lang, M., Harrach, B., 2011. Introduction of the family Alloherpesviridae: The first molecular detection of herpesviruses of cyprinid fish in Hungary. Magy. Allatorvosok Lapja 133, 174–181.

Du, M., Chen, M., Shen, H., Wang, Wei, Li, Z., Wang, Weiyi, Huang, J., Chen, J., 2015. CyHV-2 ORF104 activates the p38 MAPK pathway. Fish Shellfish Immunol. 46, 268–273. https://doi.org/10.1016/j.fsi.2015.06.011

England, C.G., Ehlerding, E.B., Cai, W., 2016. NanoLuc: A Small Luciferase is Brightening up the Field of Bioluminescence. Bioconjug. Chem. 27, 1175–1187. https://doi.org/10.1021/acs.bioconjchem.6b00112

FAO, 2022. The State of World Fisheries and Aquaculture 2022: Towards Blue Transformation, The State of World Fisheries and Aquaculture (SOFIA). FAO, Rome, Italy. https://doi.org/10.4060/cc0461en

Fichi, G., Cardeti, G., Cocumelli, C., Vendramin, N., Toffan, A., Eleni, C., Siemoni, N., Fischetti, R., Susini, F., 2013. Detection of Cyprinid herpesvirus 2 in association with an Aeromonas sobria infection of Carassius carassius (L.), in Italy. J. Fish Dis. 36, 823–830. https://doi.org/10.1111/jfd.12048

Fournier, G., Boutier, M., Stalin Raj, V., Mast, J., Parmentier, E., Vanderwalle, P., Peeters, D., Lieffrig, F., Farnir, F., Gillet, L., Vanderplasschen, A., 2012. Feeding Cyprinus carpio with infectious materials mediates cyprinid herpesvirus 3 entry through infection of pharyngeal periodontal mucosa. Vet. Res. 43, 6. https://doi.org/10.1186/1297-9716-43-6

Fu, Y., Zhang, J., Cheng, W., Cheng, X., Lu, L., Gui, L., Jiang, Y., Zhang, Y., Xu, D., 2023. miR-124 mediates the expression of ccBax to regulate Cyprinid herpesvirus 2 (CyHV-2)-induced apoptosis and viral replication. J. Fish Dis. 46, 743–749. https://doi.org/10.1111/jfd.13783

Gandar, F., Wilkie, G.S., Gatherer, D., Kerr, K., Marlier, D., Diez, M., Marschang, R.E., Mast, J., Dewals, B.G., Davison, A.J., Vanderplasschen, A.F.C., 2015. The Genome of a Tortoise Herpesvirus (Testudinid Herpesvirus 3) Has a Novel Structure and Contains a Large Region That Is Not Required for Replication In Vitro or Virulence In Vivo. J. Virol. 89, 11438–11456. https://doi.org/10.1128/jvi.01794-15

Gao, T., Cui, B., Kong, X., Bai, Z., Zhuang, X., Qian, Z., 2019. Investigation of bacterial diversity and pathogen abundances in gibel carp (Carassius auratus gibelio) ponds during a cyprinid herpesvirus 2 outbreak. MicrobiologyOpen 8, e907. https://doi.org/10.1002/mbo3.907

Gao, W., Wen, H., Wang, H., Lu, J., Lu, L., Jiang, Y., 2020. Identification of structure proteins of cyprinid herpesvirus 2. Aquaculture 523, 735184. https://doi.org/10.1016/j.aquaculture.2020.735184

Gao, W., Zhao, L., Zheng, Y., Wu, K., Xu, F., Wang, H., Lu, L., Jiang, Y., 2022. Generation and application of a monoclonal antibody specific for the ORF121 of cyprinid herpesvirus 2. J. Fish Dis. 45, 387–394. https://doi.org/10.1111/jfd.13566

Gao, Y., Sridhar, A., Bernard, N., He, B., Zhang, H., Pirotte, S., Desmecht, S., Vancsok, C., Boutier, M., Suárez, N.M., Andrew, J.D., Donohoe, O., Vanderplasschen, A.F.C., 2023. Virus-induced interference as a means for accelerating fitness-based selection of cyprinid herpesvirus 3 single nucleotide variants in vitro and in vivo. Virus Evol. vead003. https://doi.org/10.1093/ve/vead003

Gao, Y., Suárez, N.M., Wilkie, G.S., Dong, C., Bergmann, S., Lee, P.-Y.A., Davison, A.J., Vanderplasschen, A.F.C., Boutier, M., 2018. Genomic and biologic comparisons of cyprinid herpesvirus 3 strains. Vet. Res. 49, 40. https://doi.org/10.1186/s13567-018-0532-z

Garofalo, F., Imbrogno, S., Tota, B., Amelio, D., 2012. Morpho-functional characterization of the goldfish (Carassius auratus L.) heart. Comp. Biochem. Physiol. A. Mol. Integr. Physiol. 163, 215–222. https://doi.org/10.1016/j.cbpa.2012.05.206

George, M.R., John, K.R., Mansoor, M.M., Saravanakumar, R., Sundar, P., Pradeep, V., 2015. Isolatio n and characterization of a ranavirus from koi, Cyprinus carpio L., experiencing mass mortalit ies in India. J. Fish Dis. 38, 389–403. https://doi.org/10.1111/jfd.12246

Gilad, O., Yun, S., Adkison, M.A., Way, K., Willits, N.H., Bercovier, H., Hedrick, R.P., 2003. Molec ular comparison of isolates of an emerging fish pathogen, koi herpesvirus, and the effect of wa ter temperature on mortality of experimentally infected koi. J. Gen. Virol. 84, 2661–2667. http s://doi.org/10.1099/vir.0.19323-0

Gilad, O., Yun, S., Zagmutt-Vergara, F.J., Leutenegger, C.M., Bercovier, H., Hedrick, R.P., 2004. Co ncentrations of a Koi herpesvirus (KHV) in tissues of experimentally infected Cyprinus carpio koi as assessed by real-time TaqMan PCR. Dis. Aquat. Organ. 60, 179–187. https://doi.org/1 0.3354/dao060179

Giovannini, S., Bergmann, S.M., Keeling, C., Lany, C., Schütze, H., Schmidt-Posthaus, H., 2016. Her pesviral Hematopoietic Necrosis in Goldfish in Switzerland: Early Lesions in Clinically Norm al Goldfish (Carassius auratus). Vet. Pathol. 53, 847–852. https://doi.org/10.1177/0300985815 614974

Gonzales, J.M., Law, S.H.W., 2013. Feed and Feeding Regime Affect Growth Rate and Gonadosomat ic Index of Adult Zebrafish (Danio Rerio). Zebrafish 10, 532–540. https://doi.org/10.1089/zeb .2013.0891

Goodwin, A.E., Khoo, L., LaPatra, S.E., Bonar, C., Key, D.W., Garner, M., Lee, M.V., Hanson, L., 20 06a. Goldfish Hematopoietic Necrosis Herpesvirus (Cyprinid Herpesvirus 2) in the USA: Mol ecular Confirmation of Isolates from Diseased Fish. J. Aquat. Anim. Health 18, 11–18. https:// doi.org/10.1577/H05-007.1

Goodwin, A.E., Merry, G.E., Sadler, J., 2006b. Detection of the herpesviral hematopoietic necrosis dis ease agent (Cyprinid herpesvirus 2) in moribund and healthy goldfish: validation of a quantita tive PCR diagnostic method. Dis. Aquat. Organ. 69, 137–143. https://doi.org/10.3354/dao069 137

Goodwin, A.E., Sadler, J., Merry, G.E., Marecaux, E.N., 2009. Herpesviral haematopoietic necrosis vi rus (CyHV-2) infection: case studies from commercial goldfish farms. J. Fish Dis. 32, 271–27 8. https://doi.org/10.1111/j.1365-2761.2008.00988.x

Gould, S.J., Subramani, S., 1988. Firefly luciferase as a tool in molecular and cell biology. Anal. Bioc hem. 175, 5–13. https://doi.org/10.1016/0003-2697(88)90353-3

Groff, J.M., LaPatra, S.E., Munn, R.J., Zinkl, J.G., 1998. A Viral Epizootic in Cultured Populations of Juvenile Goldfish Due to a Putative Herpesvirus Etiology. J. Vet. Diagn. Invest. 10, 375–378. https://doi.org/10.1177/104063879801000415

Gui, J.-F., 2024. Chinese wisdom and modern innovation of aquaculture. Water Biol. Secur. 3, 100271 . https://doi.org/10.1016/j.watbs.2024.100271

Guo, B., Wei, C., Luan, L., Zhang, J., Li, Q., 2022. Production and application of monoclonal antibodi es against ORF66 of cyprinid herpesvirus 2. J. Virol. Methods 299, 114342. https://doi.org/10. 1016/j.jviromet.2021.114342

Haenen, O., Dijkstra, S.G., van Tulden, P., Davidse, A., Nieuwstadt, Wagenaar, F., Wellenberg, G.J., 2002. Herpesvirus anguillae (HVA) isolations from disease outbreaks in cultured European ee l, Anguilla anguilla in The Netherlands since 1996. Bull. Eur. Assoc. Fish Pathol. 22 247-257 22.

Hänfling, B., Bolton, P., Harley, M., Carvalho, G.R., 2005. A molecular approach to detect hybridisati on between crucian carp (Carassius carassius) and non-indigenous carp species (Carassius spp . and Cyprinus carpio). Freshw. Biol. 50, 403–417. https://doi.org/10.1111/j.1365-2427.2004. 01330.x

Hanson, L., Dishon, A., Kotler, M., 2011. Herpesviruses that Infect Fish. Viruses 3, 2160–2191. https://doi.org/10.3390/v3112160

Hanson, L., Doszpoly, A., van Beurden, S.J., de Oliveira Viadanna, P.H., Waltzek, T., 2016. Chapter 9 - Alloherpesviruses of Fish, in: Kibenge, F.S.B., Godoy, M.G. (Eds.), Aquaculture Virology . Academic Press, San Diego, pp. 153–172. https://doi.org/10.1016/B978-0-12-801573-5.00009-7

Hanson, L.A., Doszpoly, A., van Beurden, S., Viadanna, P.H. de O., Waltzek, T., 2024. Chapter 8 - Alloherpesviruses of fish, in: Kibenge, F.S.B., Godoy, M.G. (Eds.), Aquaculture Virology (Second Edition). Academic Press, pp. 165–189. https://doi.org/10.1016/B978-0-323-91169-6.00013-3

Harkness, J.M., Kader, M., DeLuca, N.A., 2014. Transcription of the Herpes Simplex Virus 1 Genome during Productive and Quiescent Infection of Neuronal and Nonneuronal Cells. J. Virol. 88, 6847–6861. https://doi.org/10.1128/JVI.00516-14

He, B., Sridhar, A., Streiff, C., Deketelaere, C., Zhang, H., Gao, Y., Hu, Y., Pirotte, S., Delrez, N., Davison, A.J., Donohoe, O., Vanderplasschen, A.F.C., 2023. In Vivo Imaging Sheds Light on the Susceptibility and Permissivity of Carassius auratus to Cyprinid Herpesvirus 2 According to Developmental Stage. Viruses 15, 1746. https://doi.org/10.3390/v15081746

He, J., Shi, X., Yu, L., Zheng, X., Lan, W., Jia, P., Wang, J., Liu, H., 2013. Development and evaluation of a loop-mediated isothermal amplification assay for diagnosis of Cyprinid herpesvirus 2. J. Virol. Methods 194, 206–210. https://doi.org/10.1016/j.jviromet.2013.08.028

Heath, J.R., Dembowski, J.A., 2022. Fashionably late: Temporal regulation of HSV-1 late gene transcription. PLOS Pathog. 18, e1010536. https://doi.org/10.1371/journal.ppat.1010536

Hedrick, R.P., Gilad, O., Yun, S., Spangenberg, J.V., Marty, G.D., Nordhausen, R.W., Kebus, M.J., Bercovier, H., Eldar, A., 2000. A Herpesvirus Associated with Mass Mortality of Juvenile and Adult Koi, a Strain of Common Carp. J. Aquat. Anim. Health 12, 44–57. https://doi.org/10.1577/1548-8667(2000)012<0044:AHAWMM>2.0.CO;2

Hedrick, R.P., Waltzek, T.B., McDowell, T.S., 2006. Susceptibility of Koi Carp, Common Carp, Goldfish, and Goldfish × Common Carp Hybrids to Cyprinid Herpesvirus-2 and Herpesvirus-3. J. Aquat. Anim. Health 18, 26–34. https://doi.org/10.1577/H05-028.1

Helfman, G.S., Collette, B.B., Facey, D.E., Bowen, B.W., 2009. The Diversity of Fishes: Biology, Evolution, and Ecology. John Wiley & Sons.

Heming, J.D., Conway, J.F., Homa, F.L., 2017. Herpesvirus capsid assembly and DNA packaging. Adv. Anat. Embryol. Cell Biol. 223, 119–142. https://doi.org/10.1007/978-3-319-53168-7_6

Hervey, G., 1950. The Goldfish of China in the XVIII Century. By George Hervey, Etc. [The French Text and English Translation of “Kin-yu, Ou Poisson Doré Dorade de Chine” Attributed to Aloysius Kô, Together with a Reproduction of a Chinese Scroll of 1772 Depicting 92 Goldfish; with the Text and English Translation of the “Histoire Naturelle Des Dorades de la Chine” by L.E. Billardon de Sauvigny. Edited, Translated, and with an Introduction by G. Hervey.]. London.

Honess, R.W., Roizman, B., 1974. Regulation of Herpesvirus Macromolecular Synthesis I. Cascade Regulation of the Synthesis of Three Groups of Viral Proteins 1. J. Virol. 14, 8–19.

Hossain, S., De Silva, B.C.J., Wimalasena, S.H.M.P., Pathirana, H.N.K.S., Dahanayake, P.S., Heo, G.-J., 2018. Distribution of Antimicrobial Resistance Genes and Class 1 Integron Gene Cassette Arrays in Motile Aeromonas spp. Isolated from Goldfish (Carassius auratus). Microb. Drug Resist. 24, 1217–1225. https://doi.org/10.1089/mdr.2017.0388

Houalla, T., Levine, R.L., 2003. The isolation and culture of microglia-like cells from the goldfish brain. J. Neurosci. Methods 131, 121–131. https://doi.org/10.1016/j.jneumeth.2003.08.004

Huang, X., Liu, S., Zuo, F., Luo, L., Chen, D., Ou, Y., Geng, Y., Zhang, Y., Lin, G., Yang, S., Luo, W ., Yin, L., He, Z., 2022. cMOS enhanced the mucosal immune function of skin and gill of gold fish (Carassius auratus Linnaeus) to improve the resistance to *Ichthyophthirius multifiliis* infec tion. Fish Shellfish Immunol. 126, 1–11. https://doi.org/10.1016/j.fsi.2022.05.024

Hubbard, P.C., Barata, E.N., Canário, A.V.M., 2003. Olfactory Sensitivity to Catecholamines and thei r Metabolites in the Goldfish. Chem. Senses 28, 207–218. https://doi.org/10.1093/chemse/28. 3.207

Huo, X., Fan, C., Ai, T., Su, J., 2020. The Combination of Molecular Adjuvant CCL35.2 and DNA Va ccine Significantly Enhances the Immune Protection of Carassius auratus gibelio against CyH V-2 Infection. Vaccines 8, 567. https://doi.org/10.3390/vaccines8040567

Huo, X., Yan, Y., Chang, J., Su, J., 2023. Astragalus polysaccharide or β-glucan combined with inacti vated vaccine markedly prevent CyHV-2 infection in Carassius auratus gibelio. Aquac. Fish. h ttps://doi.org/10.1016/j.aaf.2022.12.004

ICTV, 2023. ICTV [WWW Document]. URL https://ictv.global/taxonomy (accessed 9.5.24).

ICTV 9th Report (2011) | ICTV [WWW Document], n.d. URL https://ictv.global/report_9th (accessed 1.10.24).

Ilouze, M., Dishon, A., Kotler, M., 2012. Coordinated and sequential transcription of the cyprinid herp esvirus-3 annotated genes. Virus Res. 169, 98–106. https://doi.org/10.1016/j.virusres.2012.07. 015

Inoue, Y., Kumagai, M., Zhang, X., Saga, T., Wang, D., Koga, A., Takeda, H., 2018. Fusion of piggy Bac-like transposons and herpesviruses occurs frequently in teleosts. Zool. Lett. 4, 6. https://d oi.org/10.1186/s40851-018-0089-8

Inoue, Y., Saga, T., Aikawa, T., Kumagai, M., Shimada, A., Kawaguchi, Y., Naruse, K., Morishita, S., Koga, A., Takeda, H., 2017. Complete fusion of a transposon and herpesvirus created the Ter atorn mobile element in medaka fish. Nat. Commun. 8, 551. https://doi.org/10.1038/s41467-0 17-00527-2

Inouye, S., 2010. Firefly luciferase: an adenylate-forming enzyme for multicatalytic functions. Cell. M ol. Life Sci. 67, 387–404. https://doi.org/10.1007/s00018-009-0170-8

Iqbal, Z., Sheikh, U., Mughal, R., 2012. Fungal infections in some economically important freshwater fishes. Pak. Vet. J.

Ito, T., Kurita, J., Haenen, O.L.M., 2017. Importation of CyHV-2-infected goldfish into the Netherlan ds. Dis. Aquat. Organ. 126, 51–62. https://doi.org/10.3354/dao03157

Ito, T., Kurita, J., Ozaki, A., Sano, M., Fukuda, H., Ototake, M., 2013. Growth of cyprinid herpesvirus 2 (CyHV-2) in cell culture and experimental infection of goldfish Carassius auratus. Dis. Aqu at. Organ. 105, 193–202. https://doi.org/10.3354/dao02627

Ito, T., Maeno, Y., 2014a. Susceptibility of Japanese Cyprininae fish species to cyprinid herpesvirus 2 (CyHV-2). Vet. Microbiol. 169, 128–134. https://doi.org/10.1016/j.vetmic.2014.01.002

Ito, T., Maeno, Y., 2014b. Effects of experimentally induced infections of goldfish Carassius auratus with cyprinid herpesvirus 2 (CyHV-2) at various water temperatures. Dis. Aquat. Organ. 110, 193–200. https://doi.org/10.3354/dao02759

Ito, T., Ototake, M., 2013. Vaccination against cyprinid herpesvirus 2 (CyHV-2) infection in goldfish Carassius auratus. Bull. Eur. Assoc. Fish Pathol. 33, 158–164.

Jeffery, K.R., Bateman, K., Bayley, A., Feist, S.W., Hulland, J., Longshaw, C., Stone, D., Woolford, G., Way, K., 2007. Isolation of a cyprinid herpesvirus 2 from goldfish, Carassius auratus (L.), in the UK. J. Fish Dis. 30, 649–656. https://doi.org/10.1111/j.1365-2761.2007.00847.x

Jeong, Y.J., Jeon, Y.G., Choi, H.J., Baek, E.J., Kim, G.H., Yang, Y.J., Kim, M.J., Min, J.G., Kim, K.I. , 2023. Genetic characterization of alloherpesvirus (cyprinid herpesvirus-2 and koi herpesviru

s) and poxvirus (carp edema virus) identified from domestic and imported cyprinids in Korea. Fish. Aquat. Sci. 26, 437–446. https://doi.org/10.47853/FAS.2023.e36

Jiang, N., Xu, J., Ma, J., Fan, Y., Zhou, Y., Liu, W., Zeng, L., 2015. Histopathology and ultrastructura l pathology of cyprinid herpesvirus II (CyHV-2) infection in gibel carp, Carassius auratus gibe lio. Wuhan Univ. J. Nat. Sci. 20, 413–420. https://doi.org/10.1007/s11859-015-1114-9

Jiang, N., Yuan, D., Zhang, M., Luo, L., Wang, N., Xing, W., Li, T., Huang, X., Ma, Z., 2020. Diagno stic case report: Disease outbreak induced by CyHV-2 in goldfish in China. Aquaculture 523, 735156. https://doi.org/10.1016/j.aquaculture.2020.735156

Jing, H., Gao, L., Zhang, M., Wang, N., Lin, X., Zhang, L., Wu, S., 2016. Establishment from the sno ut and kidney of goldfish, Carassius auratus, of two new cell lines and their susceptibility to in fectious pancreatic necrosis virus. Fish Physiol. Biochem. 42, 303–311. https://doi.org/10.100 7/s10695-015-0138-6

Joardar, S.N., 2018. Lymphocystis infection in an uncommon host: Goldfish (Carassius auratus, Linn.). 10.5958/0974-0147.2018.00010.7 39, 45–48. https://doi.org/10.5958/0974-0147.2018.0001 0.7

Jose Priya, T.A., Kappalli, S., 2022. Modern biotechnological strategies for vaccine development in aq uaculture – Prospects and challenges. Vaccine 40, 5873–5881. https://doi.org/10.1016/j.vaccin e.2022.08.075

Jung, M.-H., Ryu, J.-W., Nikapitiya, C., Jung, S.-J., 2022. Detection of herpesviral hematopoietic necr osis virus (Cyprinid herpesvirus 2, CyHV-2) from goldfish, Carassius auratus (L.) in Korea. F ish. Aquat. Sci. 25, 403–408. https://doi.org/10.47853/FAS.2022.e36

Jung, S.J., Miyazaki, T., 1995. Herpesviral haematopoietic necrosis of goldfish, Carassius auratus (L.) . J. Fish Dis. 18, 211–220. https://doi.org/10.1111/j.1365-2761.1995.tb00296.x

Kajishima, T., 1960. The normal developmental stages of the goldfish, Carassius auratus. Jpn. J. Ichth yol. 8, 20–28. https://doi.org/10.11369/jji1950.8.20

Kalayci, G., Ozkan, B., Pekmez, K., Kaplan, M., Mefut, A., Cagirgan, A., 2018. First detection of Cyp rinid herpesvirus-2 (CyHV-2) followed by screening and monitoring studies in Goldfish (Cara ssius Auratus) in Turkey. Bull. Eur. Assoc. Fish Pathol. 38, 94–103.

Kaneko, A., Suzuki, S., Pinto, L.H., Tachibana, M., 1991. Membrane currents and pharmacology of re tinal bipolar cells: A comparative study on goldfish and mouse. Comp. Biochem. Physiol. Part C Comp. Pharmacol. 98, 115–127. https://doi.org/10.1016/0742-8413(91)90188-Y

Katakura, F., Katzenback, B.A., Belosevic, M., 2015. Recombinant goldfish thrombopoietin up-regula tes expression of genes involved in thrombocyte development and synergizes with kit ligand A to promote progenitor cell proliferation and colony formation. Dev. Comp. Immunol. 49, 15 7–169. https://doi.org/10.1016/j.dci.2014.11.001

Kempter, J., M, K., Panicz, R., Sadowski, J., Bartosz, M., Bergmann, S.M., 2012. Horizontaltransmiss ion of koi herpes virus (KHV) from potential vector species to common carpHorizontal transm ission of koi herpes virus (KHV) from potential vector species to common carp. Bull. Eur. As soc. Fish Pathol. 32, 212–219.

Kennedy, D.A., Kurath, G., Brito, I.L., Purcell, M.K., Read, A.F., Winton, J.R., Wargo, A.R., 2016. P otential drivers of virulence evolution in aquaculture. Evol. Appl. 9, 344–354. https://doi.org/1 0.1111/eva.12342

Kielpinski, M., Kempter, J., Panicz, R., Sadowski, J., Schütze, H., Ohlemeyer, S., Bergmann, S.M., 20 10. Detection of KHV in Freshwater Mussels and Crustaceans from Ponds with KHV History in Common Carp (Cyprinus carpio). Isr. J. Aquac. - Bamidgeh 62. https://doi.org/10.46989/00 1c.20576

King, A.M.Q., Adams, M.J., Carstens, E.B., Lefkowitz, E.J. (Eds.), 2012a. Family - Herpesviridae, in: Virus Taxonomy. Elsevier, San Diego, pp. 111–122. https://doi.org/10.1016/B978-0-12-384684-6.00007-0

King, A.M.Q., Adams, M.J., Carstens, E.B., Lefkowitz, E.J. (Eds.), 2012b. Family - Alloherpesviridae, in: Virus Taxonomy. Elsevier, San Diego, pp. 108–110. https://doi.org/10.1016/B978-0-12-384684-6.00006-9

King, A.M.Q., Adams, M.J., Carstens, E.B., Lefkowitz, E.J. (Eds.), 2012c. Order - Herpesvirales, in: Virus Taxonomy. Elsevier, San Diego, pp. 99–107. https://doi.org/10.1016/B978-0-12-384684-6.00005-7

Knytl, M., Forsythe, A., Kalous, L., 2022. A Fish of Multiple Faces, Which Show Us Enigmatic and Incredible Phenomena in Nature: Biology and Cytogenetics of the Genus Carassius. Int. J. Mol. Sci. 23, 8095. https://doi.org/10.3390/ijms23158095

Komiyama, T., Kobayashi, H., Tateno, Y., Inoko, H., Gojobori, T., Ikeo, K., 2009. An evolutionary origin and selection process of goldfish. Gene 430, 5–11. https://doi.org/10.1016/j.gene.2008.10.019

Kong, S.Y., Jiang, Y.S., Wang, Q., Lu, J.F., Xu, D., Lu, L.Q., 2017. Detection methods of Cyprinid herpesvirus 2 infection in silver crucian carp (Carassius auratus gibelio) via a pORF72 monoclonal antibody. J. Fish Dis. 40, 1791–1798. https://doi.org/10.1111/jfd.12648

Kucuktas, H., Brady, Y.J., 1999. Molecular biology of channel catfish virus. Aquaculture 172, 147–161. https://doi.org/10.1016/S0044-8486(98)00442-6

Kurobe, T., Kurita, J., Haenen, O., Voorbergen-Laarman, M., Ito, T., 2024. Mass mortality events associated with cyprinid herpesvirus 2 (CyHV-2) infection in wild Prussian carp Carassius gibelio in the Netherlands, and molecular biology of virus strains. J. Fish Dis. 47, e13868. https://doi.org/10.1111/jfd.13868

Le Morvan, C., Deschaux, P., Troutaud, D., 1996. Effects and mechanisms of environmental temperature on carp (Cyprinus carpio) anti-DNP antibody response and non-specific cytotoxic cell activity: a kinetic study. Dev. Comp. Immunol. 20, 331–40.

Le Morvan, C., Troutaud, D., Deschaux, P., 1998. Differential effects of temperature on specific and nonspecific immune defences in fish. J. Exp. Biol. 201, 165–8.

Lefkowitz, E.J., Dempsey, D.M., Hendrickson, R.C., Orton, R.J., Siddell, S.G., Smith, D.B., 2018. Virus taxonomy: the database of the International Committee on Taxonomy of Viruses (ICTV). Nucleic Acids Res. 46, D708–D717. https://doi.org/10.1093/nar/gkx932

Li, I.-J., Chang, C.-J., Liu, S.-C., Abe, G., Ota, K.G., 2015. Postembryonic staging of wild-type goldfish, with brief reference to skeletal systems. Dev. Dyn. 244, 1485–1518. https://doi.org/10.1002/dvdy.24340

Li, K., Yuan, R., Zhang, M., Zhang, T., Gu, Y., Zhou, Y., Dai, Y., Fang, P., Feng, Y., Hu, X., Cao, G., Xue, R., Chen, H., Gong, C., 2019. Recombinant baculovirus BacCarassius-D4ORFs has potential as a live vector vaccine against CyHV-2. Fish Shellfish Immunol. 92, 101–110. https://doi.org/10.1016/j.fsi.2019.05.065

Li, L., Luo, Y., Gao, Z., Huang, J., Zheng, X., Nie, H., Zhang, J., Lin, L., Yuan, J., 2015. Molecular characterisation and prevalence of a new genotype of Cyprinid herpesvirus 2 in mainland China. Can. J. Microbiol. 61, 381–387. https://doi.org/10.1139/cjm-2014-0796

Li, S., Ruan, Z., Zhang, H., Xu, H., 2021. Recent achievements of bioluminescence imaging based on firefly luciferin-luciferase system. Eur. J. Med. Chem. 211, 113111. https://doi.org/10.1016/j.ejmech.2020.113111

Li, X., Fukuda, H., 2003. In vitro culture of goldfish cell sensitive to goldfish herpes virus. CABI Databases 12, 12–18.

Li, Z., Wang, Z.-W., Wang, Y., Gui, J.-F., 2018. Crucian Carp and Gibel Carp Culture, in: Aquaculture in China. John Wiley & Sons, Ltd, pp. 149–157. https://doi.org/10.1002/9781119120759.ch2_4

Liang, L. -G., Xie, J., Chen, K., Bing, X., 2015. Pathogenicity and biological characteristics of CyHV-2. Fish Pathol. 35, 85–93.

Liang, L. -G., Xie, J., Luo, D., 2014. Development of a rapid cyprinid herpesvirus 2 detection method by loop-mediated isothermal amplification. Lett. Appl. Microbiol. 59, 432–437. https://doi.org/10.1111/lam.12296

Liu, B., Zhou, Y., Li, K., Hu, X., Wang, C., Cao, G., Xue, R., Gong, C., 2018. The complete genome of Cyprinid herpesvirus 2, a new strain isolated from Allogynogenetic crucian carp. Virus Res. 256, 6–10. https://doi.org/10.1016/j.virusres.2018.07.016

Loch, T.P., Faisal, M., 2015. Emerging flavobacterial infections in fish: A review. J. Adv. Res., Editors and International Board Member collection 6, 283–300. https://doi.org/10.1016/j.jare.2014.10.009

Lovy, J., Friend, S.E., 2014. Cyprinid herpesvirus-2 causing mass mortality in goldfish: applying electron microscopy to histological samples for diagnostic virology. Dis. Aquat. Organ. 108, 1–9. https://doi.org/10.3354/dao02698

Lu, C., Tang, R., Su, M., Zou, J., Lu, L., 2022. Induction of Reactive Oxygen Species Is Necessary for Efficient Onset of Cyprinid Herpesvirus 2 Replication: Implications for Novel Antiviral Strategy With Antioxidants. Front. Microbiol. 12.

Lu, J., Shen, Z., Lu, L., Xu, D., 2019. Cyprinid Herpesvirus 2 miR-C12 Attenuates Virus-Mediated Apoptosis and Promotes Virus Propagation by Targeting Caspase 8. Front. Microbiol. 10.

Lu, J., Xu, D., Jiang, Y., Kong, S., Shen, Z., Xia, S., Lu, L., 2017. Integrated analysis of mRNA and viral miRNAs in the kidney of Carassius auratus gibelio response to cyprinid herpesvirus 2. Sci. Rep. 7, 13787. https://doi.org/10.1038/s41598-017-14217-y

Lu, J., Xu, D., Lu, L., 2018. A novel cell line established from caudal fin tissue of Carassius auratus gibelio is susceptible to cyprinid herpesvirus 2 infection with the induction of apoptosis. Virus Res. 258, 19–27. https://doi.org/10.1016/j.virusres.2018.09.010

Lu, Z., Wang, J., Li, M., Liu, Q., Wei, D., Yang, M., Kong, L., 2014. 1H NMR-based metabolomics study on a goldfish model of Parkinson's disease induced by 1-methyl-4-phenyl-1,2,3,6-tetrahydropyridine (MPTP). Chem. Biol. Interact. 223, 18–26. https://doi.org/10.1016/j.cbi.2014.09.006

Luo, Y.Z., Lin, L., Liu, Y., Wu, Z.X., Gu, Z.M., Li, L.J., Yuan, J.F., 2013. Haematopoietic necrosis of cultured Prussian carp, Carassius gibelio (Bloch), associated with Cyprinid herpesvirus 2. J. Fish Dis. 36, 1035–1039. https://doi.org/10.1111/jfd.12110

Lussignol, M., Esclatine, A., 2017. Herpesvirus and Autophagy: "All Right, Everybody Be Cool, This Is a Robbery!" Viruses 9, 372. https://doi.org/10.3390/v9120372

Ma, J., Jiang, N., LaPatra, S.E., Jin, L., Xu, J., Fan, Y., Zhou, Y., Zeng, L., 2015. Establishment of a novel and highly permissive cell line for the efficient replication of cyprinid herpesvirus 2 (CyHV-2). Vet. Microbiol. 177, 315–325. https://doi.org/10.1016/j.vetmic.2015.04.006

MacLachlan, N.J., Dubovi, E.J. (Eds.), 2011. Chapter 8 - Asfarviridae and Iridoviridae, in: Fenner's Veterinary Virology (Fourth Edition). Academic Press, San Diego, pp. 167–177. https://doi.org/10.1016/B978-0-12-375158-4.00008-0

Madavaraju, K., Koganti, R., Volety, I., Yadavalli, T., Shukla, D., 2021. Herpes Simplex Virus Cell Entry Mechanisms: An Update. Front. Cell. Infect. Microbiol. 10. https://doi.org/10.3389/fcimb.2020.617578

Marchant, T.A., Chang, J.P., Nahorniak, C.S., Peter, R.E., 1989. Evidence That Gonadotropin-Releasi ng Hormone Also Functions as a Growth Hormone-Releasing Factor in the Goldfish. Endocri nology 124, 2509–2518. https://doi.org/10.1210/endo-124-5-2509

Matsui Y., 1935. Kagaku to shumi kara mita kingyo no kenkyū.

Mayer, J., Donnelly, T.M. (Eds.), 2013. Flukes (Monogenean Parasites), in: Clinical Veterinary Advis or. W.B. Saunders, Saint Louis, pp. 22–24. https://doi.org/10.1016/B978-1-4160-3969-3.0001 6-0

McGeoch, D.J., Dolan, A., Ralph, A.C., 2000. Toward a Comprehensive Phylogeny for Mammalian a nd Avian Herpesviruses. J. Virol. 74, 10401–10406. https://doi.org/10.1128/jvi.74.22.10401-1 0406.2000

McGeoch, D.J., Gatherer, D., 2005. Integrating Reptilian Herpesviruses into the Family Herpesviridae . J. Virol. 79, 725–731. https://doi.org/10.1128/jvi.79.2.725-731.2005

McGeoch, D.J., Rixon, F.J., Davison, A.J., 2006. Topics in herpesvirus genomics and evolution. Virus Res., Comparative Genomics and Evolution of Complex Viruses 117, 90–104. https://doi.org /10.1016/j.virusres.2006.01.002

McKinnell, R.G., Tarin, D., 1984. Temperature-dependent metastasis of the Lucke renal carcinoma an d its significance for studies on mechanisms of metastasis. Cancer Metastasis Rev. 3, 373–386 . https://doi.org/10.1007/BF00051461

Mettenleiter, T.C., 2004. Budding events in herpesvirus morphogenesis. Virus Res., Mechanisms of E nveloped Virus Release 106, 167–180. https://doi.org/10.1016/j.virusres.2004.08.013

Mettenleiter, T.C., Klupp, B.G., Granzow, H., 2009. Herpesvirus assembly: An update. Virus Res., Vi rus Research - 25th Anniversary Issue 143, 222–234. https://doi.org/10.1016/j.virusres.2009.0 3.018

Michel, B., Fournier, G., Lieffrig, F., Costes, B., Vanderplasschen, A., 2010. Cyprinid Herpesvirus 3. Emerg. Infect. Dis. 16, 1835–1843. https://doi.org/10.3201/eid1612.100593

Minarovits, J., Gonczol, E., Valyi-Nagy, T. (Eds.), 2007. Latency Strategies of Herpesviruses. Springe r US, Boston, MA. https://doi.org/10.1007/978-0-387-34127-9

Molina, A., Carpeaux, R., Martial, J.A., Muller, M., 2002. A transformed fish cell line expressing a gr een fluorescent protein-luciferase fusion gene responding to cellular stress. Toxicol. In Vitro 1 6, 201–207. https://doi.org/10.1016/S0887-2333(01)00106-0

Mora-Ferrer, C., Neumeyer, C., 2009. Neuropharmacology of vision in goldfish: A review. Vision Re s., From Retinal and Cortical Circuitry to Clinical Application In memory of Henk Spekreijse - a life dedicated to Vision Research 49, 960–969. https://doi.org/10.1016/j.visres.2008.08.004

Mulertt, H., 1883. The goldfish and its systematic culture with a view to profit. A practical treatise on the fish, its propagation, enemies, diseases, and care of the fish in captivity .. Cincinnati [McD onald & Eick, print.].

Nagahama, Y., 1983. 6 The Functional Morphology of Teleost Gonads, in: Hoar, W.S., Randall, D.J., Donaldson, E.M. (Eds.), Fish Physiology, Reproduction. Academic Press, pp. 223–275. https: //doi.org/10.1016/S1546-5098(08)60290-3

Nanjo, A., Shibata, T., Saito, M., Yoshii, K., Tanaka, M., Nakanishi, T., Fukuda, H., Sakamoto, T., Ka to, G., Sano, M., 2017a. Susceptibility of isogeneic ginbuna Carassius auratus langsdorfii Tem minck et Schlegel to cyprinid herpesvirus-2 (CyHV-2) as a model species. J. Fish Dis. 40, 157 –168. https://doi.org/10.1111/jfd.12500

Nanjo, A., Shibata, T., Yoshii, K., Shibasaki, Y., Nakanishi, T., Tanaka, M., Kato, G., Sano, M., 2017 b. Passive immunisation of goldfish with the serum of those surviving a cyprinid herpesvirus 2 infection after high temperature water treatment. Bull. Eur. Assoc. Fish Pathol. 37, 62–69.

Nevels, M., Nitzsche, A., Paulus, C., 2011. How to control an infectious bead string: nucleosome-base d regulation and targeting of herpesvirus chromatin. Rev. Med. Virol. 21, 154–180. https://doi .org/10.1002/rmv.690

Nguyen Thuc, T., Kempter, J., Panicz, R., 2016. Monitoring of herpesvirus anguillae (AngHV-1) infec tions in the European eel in north-west Poland. Med. Weter. 72, 564–566. https://doi.org/10.2 1521/mw.5560

Nicoll, M.P., Proença, J.T., Efstathiou, S., 2012. The molecular basis of herpes simplex virus latency. Fems Microbiol. Rev. 36, 684–705. https://doi.org/10.1111/j.1574-6976.2011.00320.x

Nieuwstadt, A.P. van, Dijkstra, S.G., Haenen, O.L.M., 2001. Persistence of herpesvirus of eel Herpesv irus anguillae in farmed European eel Anguilla anguilla. Dis. Aquat. Organ. 45, 103–107. http s://doi.org/10.3354/dao045103

Nightingale, C.H., Gibaldi, M., 1971. Kinetics of Drug Absorption in Goldfish. J. Pharm. Sci. 60, 136 0–1363. https://doi.org/10.1002/jps.2600600915

Omori, Y., Kon, T., 2019. Goldfish: an old and new model system to study vertebrate development, ev olution and human disease. J. Biochem. (Tokyo) 165, 209–218. https://doi.org/10.1093/jb/mv y076

Ota, K.G., Abe, G., 2016. Goldfish morphology as a model for evolutionary developmental biology. WIREs Dev. Biol. 5, 272–295. https://doi.org/10.1002/wdev.224

Otani, S., Maegawa, S., Inoue, K., Arai, K., Yamaha, E., 2002. The Germ Cell Lineage Identified by v as-mRNA during the Embryogenesis in Goldfish. Zoolog. Sci. 19, 519–526. https://doi.org/10 .2108/zsj.19.519

Ouyang, P., Rakus, K., Boutier, M., Reschner, A., Leroy, B., Ronsmans, M., Fournier, G., Scohy, S., Costes, B., Wattiez, R., Vanderplasschen, A., 2013. The IL-10 homologue encoded by cyprini d herpesvirus 3 is essential neither for viral replication in vitro nor for virulence in vivo. Vet. Res. 44, 53. https://doi.org/10.1186/1297-9716-44-53

Ouyang, P., Zhou, Y., Wang, K., Geng, Y., Lai, W., Huang, X., Chen, D., Guo, H., Fang, J., Chen, Z., Tang, L., Huang, C., Liu, W., Yin, L., 2020. First report of Cyprinid herpesvirus 2 outbreak i n cultured gibel carp, Carassius auratus gibelio at low temperature. J. World Aquac. Soc. 51, 1 208–1220. https://doi.org/10.1111/jwas.12681

Panicz, R., Sadowski, J., Eljasik, P., 2019. Detection of Cyprinid herpesvirus 2 (CyHV-2) in symptom atic ornamental types of goldfish (Carassius auratus) and asymptomatic common carp (Cyprin us carpio) reared in warm-water cage culture. https://doi.org/10.1016/j.aquaculture.2019.01.06 5

Payne, S., 2017. Chapter 34 - Family Herpesviridae, in: Payne, S. (Ed.), Viruses. Academic Press, pp. 269–278. https://doi.org/10.1016/B978-0-12-803109-4.00034-9

Pearson, H., 2004. Carp virus crisis prompts moves to avert global spread. Nature 427, 577. https://doi .org/10.1038/427577a

Pellett, P., Davison, A.J., Eberle, R., Ehlers, B., Hayward, G.S., Lacoste, V., Minson, A.C., Nicholas, J., Roizman, B., Studdert, M., Wang, F., 2011. Herpesvirales. Virus Taxon. 9th Rep. Int. Com m. Taxon. Viruses 99–107.

Pellett, P.E., Bernard, R., 2013. Herpesviridae, in: Fields Virology 6th Ed. pp. 1802–1822.

Peng, C., Chang, J.P., Yu, K.L., Wong, A.O., Van Goor, F., Peter, R.E., Rivier, J.E., 1993. Neuropepti de-Y stimulates growth hormone and gonadotropin-II secretion in the goldfish pituitary: invol vement of both presynaptic and pituitary cell actions. Endocrinology 132, 1820–1829. https:// doi.org/10.1210/en.132.4.1820

Piewbang, C., Wardhani, S.W., Sirivisoot, S., Surachetpong, W., Sirimanapong, W., Kasantikul, T., T echangamsuwan, S., 2024. First report of natural Cyprinid herpesvirus-2 infection associated

with fatal outbreaks of goldfish (Carassius auratus) farms in Thailand. Aquaculture 581, 740481. https://doi.org/10.1016/j.aquaculture.2023.740481

Podlesnykh, A.V., Brykov, V.A., Skurikhina, L.A., 2015. Polyphyletic Origin of Ornamental Goldfish. Food Nutr. Sci. 06, 1005. https://doi.org/10.4236/fns.2015.611104

Pollard, H.B., Adeyemo, M., Dhariwal, K., Levine, M., Caohuy, H., Markey, S., Markey, C.J., Youdim, M.B.H., 1993. The Goldfish as a Drug Discovery Vehicle for Parkinson's Disease and Other Neurodegenerative Disorders. Ann. N. Y. Acad. Sci. 679, 317–320. https://doi.org/10.1111/j.1749-6632.1993.tb18314.x

Popesku, J.T., Martyniuk, C.J., Mennigen, J., Xiong, H., Zhang, D., Xia, X., Cossins, A.R., Trudeau, V.L., 2008. The goldfish (Carassius auratus) as a model for neuroendocrine signaling. Mol. Cell. Endocrinol., Non-Mammalian Models of Endocrine Signalling 293, 43–56. https://doi.org/10.1016/j.mce.2008.06.017

Puzdrowski, R.L., 2008. Peripheral Distribution and Central Projections of the Lateral-Line Nerves in Goldfish, Carasius auratus (Part 1 of 2). Brain. Behav. Evol. 34, 110–120. https://doi.org/10.1159/000116496

Qian, M., Xiao, S., Yang, Y., Yu, F., Wen, J., Lu, L., Wang, H., 2023. Screening and identification of cyprinid herpesvirus 2 (CyHV-2) ORF55-interacting proteins by phage display. Virol. J. 20, 66. https://doi.org/10.1186/s12985-023-02026-x

Radosavljevic, V., Adamek, M., Milicevic, V., Maksimovic-Zoric, J., Steinhagen, D., 2018. Occurrence of two novel viral pathogens (CEV and CyHV-2) affecting Serbian cyprinid aquaculture and ichthyofauna. J. Fish Dis. 41, 851–854. https://doi.org/10.1111/jfd.12789

Raj, V.S., Fournier, G., Rakus, K., Ronsmans, M., Ouyang, P., Michel, B., Delforges, C., Costes, B., Farnir, F., Leroy, B., Wattiez, R., Melard, C., Mast, J., Lieffrig, F., Vanderplasschen, A., 2011. Skin mucus of Cyprinus carpio inhibits cyprinid herpesvirus 3 binding to epidermal cells. Vet. Res. 42, 92. https://doi.org/10.1186/1297-9716-42-92

Rakus, K., Ouyang, P., Boutier, M., Ronsmans, M., Reschner, A., Vancsok, C., Jazowiecka-Rakus, J., Vanderplasschen, A., 2013. Cyprinid herpesvirus 3: an interesting virus for applied and fundamental research. Vet. Res. 44, 85. https://doi.org/10.1186/1297-9716-44-85

Rakus, K., Ronsmans, M., Forlenza, M., Boutier, M., Piazzon, M.C., Jazowiecka-Rakus, J., Gatherer, D., Athanasiadis, A., Farnir, F., Davison, A.J., Boudinot, P., Michiels, T., Wiegertjes, G.F., Vanderplasschen, A., 2017. Conserved Fever Pathways across Vertebrates: A Herpesvirus Expressed Decoy TNF-α Receptor Delays Behavioral Fever in Fish. Cell Host Microbe 21, 244–253. https://doi.org/10.1016/j.chom.2017.01.010

Reed, A.N., Izume, S., Dolan, B.P., LaPatra, S., Kent, M., Dong, J., Jin, L., 2014. Identification of B Cells as a Major Site for Cyprinid Herpesvirus 3 Latency. J. Virol. 88, 9297–9309. https://doi.org/10.1128/jvi.00990-14

Reimschuessel, R., 2001. A Fish Model of Renal Regeneration and Development. ILAR J. 42, 285–291. https://doi.org/10.1093/ilar.42.4.285

Ren, W., Pan, X., Dai, C., Shu, T., Li, L., Yuan, J., 2021. Investigation of Cyprinid herpesvirus 2 and bacterial coinfection in Carassius gibel. Aquaculture 537, 736521. https://doi.org/10.1016/j.aquaculture.2021.736521

Renault, T., 2016. Chapter 37 - Malacoherpesviruses of Mollusks, in: Kibenge, F.S.B., Godoy, M.G. (Eds.), Aquaculture Virology. Academic Press, San Diego, pp. 513–524. https://doi.org/10.1016/B978-0-12-801573-5.00037-1

Reyes-Sandoval, A., Ertl, H.C.J., 2004. CpG Methylation of a Plasmid Vector Results in Extended Transgene Product Expression by Circumventing Induction of Immune Responses. Mol. Ther. 9, 249–261. https://doi.org/10.1016/j.ymthe.2003.11.008

Rixon, F.J., Schmid, M.F., 2014. Structural similarities in DNA packaging and delivery apparatuses in Herpesvirus and dsDNA bacteriophages. Curr. Opin. Virol., Emerging viruses / Virus structu re and function 5, 105–110. https://doi.org/10.1016/j.coviro.2014.02.003

Rodríguez, I., Novoa, B., Figueras, A., 2008. Immune response of zebrafish (Danio rerio) against a ne wly isolated bacterial pathogen Aeromonas hydrophila. Fish Shellfish Immunol. 25, 239–249. https://doi.org/10.1016/j.fsi.2008.05.002

Ronen, A., Perelberg, A., Abramowitz, J., Hutoran, M., Tinman, S., Bejerano, I., Steinitz, M., Kotler, M., 2003. Efficient vaccine against the virus causing a lethal disease in cultured *Cyprinus car pio*. Vaccine 21, 4677–4684. https://doi.org/10.1016/S0264-410X(03)00523-1

Ronsmans, M., Boutier, M., Rakus, K., Farnir, F., Desmecht, D., Ectors, F., Vandecan, M., Lieffrig, F. , Mélard, C., Vanderplasschen, A., 2014. Sensitivity and permissivity of Cyprinus carpio to cy prinid herpesvirus 3 during the early stages of its development: importance of the epidermal m ucus as an innate immune barrier. Vet. Res. 45, 100. https://doi.org/10.1186/s13567-014-0100 -0

Rougée, L., Ostrander, G.K., Richmond, R.H., Lu, Y., 2007. Establishment, characterization, and viral susceptibility of two cell lines derived from goldfish Carassius auratus muscle and swim blad der. Dis. Aquat. Organ. 77, 127–135. https://doi.org/10.3354/dao01802

Rupp, B., Reichert, H., Wullimann, M.F., 1996. The zebrafish brain: a neuroanatomical comparison w ith the goldfish. Anat. Embryol. (Berl.) 194, 187–203. https://doi.org/10.1007/BF00195012

Rylková, K., Kalous, L., Bohlen, J., Lamatsch, D.K., Petrtýl, M., 2013. Phylogeny and biogeographic history of the cyprinid fish genus Carassius (Teleostei: Cyprinidae) with focus on natural and anthropogenic arrivals in Europe. Aquaculture 380–383, 13–20. https://doi.org/10.1016/j.aqua culture.2012.11.027

Sahoo, P.K., Swaminathan, T.R., Abraham, T.J., Kumar, R., Pattanayak, S., Mohapatra, A., Rath, S.S. , Patra, A., Adikesavalu, H., Sood, N., Pradhan, P.K., Das, B.K., Jayasankar, P., Jena, J.K., 20 16. Detection of goldfish haematopoietic necrosis herpes virus (Cyprinid herpesvirus-2) with multi-drug resistant Aeromonas hydrophila infection in goldfish: First evidence of any viral di sease outbreak in ornamental freshwater aquaculture farms in India. Acta Trop. 161, 8–17. htt ps://doi.org/10.1016/j.actatropica.2016.05.004

Saito, H., Minami, S., Yuguchi, M., Shitara, A., Kondo, H., Kato, G., Sano, M., 2024a. Efficient show ering vaccination with a live attenuated vaccine against herpesviral hematopoietic necrosis in goldfish. Aquaculture 578, 740140. https://doi.org/10.1016/j.aquaculture.2023.740140

Saito, H., Minami, S., Yuguchi, M., Shitara, A., Kondo, H., Kato, G., Sano, M., 2024b. Effect of temp erature on the protective efficacy of a live attenuated vaccine against herpesviral haematopoiet ic necrosis in goldfish. J. Fish Dis. 47, e13906. https://doi.org/10.1111/jfd.13906

Saito, H., Okamura, T., Shibata, T., Kato, G., Sano, M., 2022. Development of a live attenuated vacci ne candidate against herpesviral hematopoietic necrosis of goldfish. Aquaculture 552, 737974. https://doi.org/10.1016/j.aquaculture.2022.737974

Sampour, M., 2008. The study of adrenal chromaffin of fish, Carassius auratus (Toleostei). Pak. J. Bio l. Sci. 11, 1032–1036. https://doi.org/10.3923/pjbs.2008.1032.1036

Sano, M., Fukuda, H., Sano, T., 1990. Isolation and characterization of a new Herpesvirus from eel, in : Perkins, F.O., Cheng, T.C. (Eds.), Pathology in Marine Science. Academic Press, San Diego, pp. 15–31. https://doi.org/10.1016/B978-0-12-550755-4.50008-2

Sarbahi, D.S., 1951. Studies of the digestive tracts and the digestive enzymes of the goldfish, carassius auratus (linnaeus) and the largemouth black bass, micropterus salmoides (lacépède). Biol. Bu ll. 100, 244–257. https://doi.org/10.2307/1538534

Savin, K.W., Cocks, B.G., Wong, F., Sawbridge, T., Cogan, N., Savage, D., Warner, S., 2010. A neur otropic herpesvirus infecting the gastropod, abalone, shares ancestry with oyster herpesvirus a

nd a herpesvirus associated with the amphioxus genome. Virol. J. 7, 308. https://doi.org/10.1186/1743-422X-7-308

Scharsack, J.P., Franke, F., 2022. Temperature effects on teleost immunity in the light of climate change. J. Fish Biol. 101, 780–796. https://doi.org/10.1111/jfb.15163

Schaub, F.X., Reza, M.S., Flaveny, C.A., Li, W., Musicant, A.M., Hoxha, S., Guo, M., Cleveland, J.L., Amelio, A.L., 2015. Fluorophore-NanoLuc BRET Reporters Enable Sensitive In Vivo Optical Imaging and Flow Cytometry for Monitoring Tumorigenesis. Cancer Res. 75, 5023–5033. https://doi.org/10.1158/0008-5472.CAN-14-3538

Shagin, D.A., Barsova, E.V., Yanushevich, Y.G., Fradkov, A.F., Lukyanov, K.A., Labas, Y.A., Semenova, T.N., Ugalde, J.A., Meyers, A., Nunez, J.M., Widder, E.A., Lukyanov, S.A., Matz, M.V., 2004. GFP-like Proteins as Ubiquitous Metazoan Superfamily: Evolution of Functional Features and Structural Complexity. Mol. Biol. Evol. 21, 841–850. https://doi.org/10.1093/molbev/msh079

Shaheena, A., Asely, A.E., Latif, A., Moustafa, M., Elsaied, H., 2015. Saprolegniosis in goldfish (Carassius auratus) associated with novel strain ; molecular characterization and electron scanning .

Sharma, M., Shrivastav, A.B., Sahni, Y.P., Pandey, G., 2012. Overviews of the treatment and control of common fish diseases.

Sharma, S.C., Ungar, F., 1980. Histogenesis of the goldfish retina. J. Comp. Neurol. 191, 373–382. https://doi.org/10.1002/cne.901910305

She, R., Li, T.-T., Luo, D., Li, J.-B., Yin, L.-Y., Li, H., Liu, Y.-M., Li, X.-Z., Yan, Q., 2017. Changes in the Intestinal Microbiota of Gibel Carp (Carassius gibelio) Associated with Cyprinid herpesvirus 2 (CyHV-2) Infection. Curr. Microbiol. 74, 1130–1136. https://doi.org/10.1007/s00284-017-1294-y

Shen, Z., Jiang, Y., Lu, J., Sano, M., Xu, D., Lu, L., 2018. Application of a monoclonal antibody specific for the ORF92 capsid protein of Cyprinid herpesvirus 2. J. Virol. Methods 261, 22–27. https://doi.org/10.1016/j.jviromet.2018.07.012

Shibata, T., Nanjo, A., Saito, M., Yoshii, K., Ito, T., Nakanishi, T., Sakamoto, T., Sano, M., 2015. In vitro characteristics of cyprinid herpesvirus 2: effect of kidney extract supplementation on growth. Dis. Aquat. Organ. 115, 223–232. https://doi.org/10.3354/dao02885

Shokrollahi, N., Shahbazzadeh, D., Pooshang-Bagheri, K., Habibi-Anbouhi, M., Jahanian-Najafabadi, A., Behdani, M., 2016. A Model to Study the Phenotypic Changes of Insect Cell Transfection by Copepod Super Green Fluorescent Protein (cop-GFP) in Baculovirus Expression System. Iran. Biomed. J. 20, 182–186. https://doi.org/10.7508/ibj.2016.03.008

Sin, Y.M., Ling, K. h., Lam, T.J., 1992. Protection against velvet disease in goldfish recovered from ichthyophthiriasis. Aquaculture 102, 187–191. https://doi.org/10.1016/0044-8486(92)90301-Z

Sivron, T., Eitan, S., Schreyer, D.J., Schwartz, M., 1993. Astrocytes play a major role in the control of neuronal proliferation in vitro. Brain Res. 629, 199–208. https://doi.org/10.1016/0006-8993(93)91321-I

Smartt, J., 2001. Goldfish Varieties and Genetics: Handbook for Breeders | Wiley [WWW Document]. Wiley.com. URL https://www.wiley.com/en-sg/Goldfish+Varieties+and+Genetics%3A+Handbook+for+Breeders-p-9780470999783 (accessed 12.23.23).

Sofyantoro, F., Priyono, D.S., Septriani, N.I., Putri, W.A., Mamada, S.S., Ramadaningrum, W.A., Wijayanti, N., Frediansyah, A., Nainu, F., 2024. Zebrafish as a model organism for virus disease research: Current status and future directions. Heliyon 10. https://doi.org/10.1016/j.heliyon.2024.e33865

Stephens, F.J., Raidal, S.R., Jones, B., 2004. Haematopoietic necrosis in a goldfish (Carassius auratus) associated with an agent morphologically similar to herpesvirus. Aust. Vet. J. 82, 167–169.

Steward, G.F., Culley, A.I., Wood-Charlson, E.M., 2013. Marine Viruses, in: Levin, S.A. (Ed.), Encyc lopedia of Biodiversity (Second Edition). Academic Press, Waltham, pp. 127–144. https://doi. org/10.1016/B978-0-12-384719-5.00401-9

St-Hilaire, S., Beevers, N., Way, K., Le Deuff, R.M., Martin, P., Joiner, C., 2005. Reactivation of koi herpesvirus infections in common carp Cyprinus carpio. Dis. Aquat. Organ. 67, 15–23. https:/ /doi.org/10.3354/dao067015

Su, M., Tang, R., Wang, H., Lu, L., 2021. Suppression effect of plant-derived berberine on cyprinid he rpesvirus 2 proliferation and its pharmacokinetics in Crucian carp (Carassius auratus gibelio). Antiviral Res. 186, 105000. https://doi.org/10.1016/j.antiviral.2020.105000

Sun, B.-Y., Kou, H.-Y., Jian, P.-Y., Kong, L.-J., Fang, J., Meng, P.-K., Wu, K., Yang, C.-G., Yang, G. , Song, X.-H., 2023. Protective effects of egg yolk immunoglobulins (IgY) against CyHV-2 in fection in gibel carp (*Carassius gibelio*). Aquaculture 569, 739371. https://doi.org/10.1016/j.a quaculture.2023.739371

Sun, Y., Xu, C., Wang, H., Qiao, G., Wang, Z., Li, Z., Li, Q., Wei, C., 2023. An attenuated strain of c yprinid herpesvirus 2 as a vaccine candidate against herpesviral hematopoietic necrosis diseas e in gibel carp, Carassius auratus gibelio. Fish Shellfish Immunol. 138, 108826. https://doi.org /10.1016/j.fsi.2023.108826

Sunarto, A., Liongue, C., McColl, K.A., Adams, M.M., Bulach, D., Crane, M.S.J., Schat, K.A., Slobe dman, B., Barnes, A.C., Ward, A.C., Walker, P.J., 2012. Koi herpesvirus encodes and express es a functional interleukin-10. J. Virol. 86, 11512–11520. https://doi.org/10.1128/JVI.00957-1 2

Suzuki, K., Kimura, T., Shinoda, H., Bai, G., Daniels, M.J., Arai, Y., Nakano, M., Nagai, T., 2016. Fi ve colour variants of bright luminescent protein for real-time multicolour bioimaging. Nat. Co mmun. 7, 13718. https://doi.org/10.1038/ncomms13718

Szymczak-Workman, A.L., Vignali, K.M., Vignali, D.A.A., 2012. Design and Construction of 2A Pep tide-Linked Multicistronic Vectors. Cold Spring Harb. Protoc. 2012, pdb.ip067876. https://doi .org/10.1101/pdb.ip067876

Takada, M., Tachihara, K., Kon, T., Yamamoto, G., Iguchi, K., Miya, M., Nishida, M., 2010. Biogeog raphy and evolution of the Carassius auratus-complex in East Asia. BMC Evol. Biol. 10, 7. htt ps://doi.org/10.1186/1471-2148-10-7

Tang, R., Lu, L., Wang, B., Yu, J., Wang, H., 2020. Identification of the Immediate-Early Genes of C yprinid Herpesvirus 2. Viruses 12, 994. https://doi.org/10.3390/v12090994

Thangaraj, R.S., Nithianantham, S.R., Dharmaratnam, A., Kumar, R., Pradhan, P.K., Thangalazhy Go pakumar, S., Sood, N., 2021. Cyprinid herpesvirus-2 (CyHV-2): a comprehensive review. Rev . Aquac. 13, 796–821. https://doi.org/10.1111/raq.12499

Thilakaratne, I.D.S.I.P., Rajapaksha, G., Hewakopara, A., Rajapakse, R.P.V.J., Faizal, A.C.M., 2003. Parasitic infections in freshwater ornamental fish in Sri Lanka. Dis. Aquat. Organ. 54, 157–16 2. https://doi.org/10.3354/dao054157

Thompson, D.J., Khoo, L.H., Wise, D.J., Hanson, L.A., 2005. Evaluation of Channel Catfish Virus La tency on Fingerling Production Farms in Mississippi. J. Aquat. Anim. Health 17, 211–215. htt ps://doi.org/10.1577/H04-048.1

Tombácz, D., Tóth, J.S., Petrovszki, P., Boldogkői, Z., 2009. Whole-genome analysis of pseudorabies virus gene expression by real-time quantitative RT-PCR assay. BMC Genomics 10, 491. https ://doi.org/10.1186/1471-2164-10-491

Torrealba, D., Thomson, C., Barreda, D., 2018. Fever improves the response of goldfish to in vivo aer omonas veronii challenge.

Tsai, H.-Y., Chang, M., Liu, S.-C., Abe, G., Ota, K.G., 2013. Embryonic development of goldfish (Carassius auratus): A model for the study of evolutionary change in developmental mechanisms by artificial selection. Dev. Dyn. 242, 1262–1283. https://doi.org/10.1002/dvdy.24022

Tsang, B., Zahid, H., Ansari, R., Lee, R.C.-Y., Partap, A., Gerlai, R., 2017. Breeding Zebrafish: A Review of Different Methods and a Discussion on Standardization. Zebrafish 14, 561–573. https://doi.org/10.1089/zeb.2017.1477

Underwood, W.L., 1901. Goldfish as Destroyers of Mosquito Larvæ. Science 14, 1017–1018. https://doi.org/10.1126/science.14.365.1017

van Beurden, S.J., Bossers, A., Voorbergen-Laarman, M.H.A., Haenen, O.L.M., Peters, S., Abma-Henkens, M.H.C., Peeters, B.P.H., Rottier, P.J.M., Engelsma, M.Y., 2010. Complete genome sequence and taxonomic position of anguillid herpesvirus 1. J. Gen. Virol. 91, 880–887. https://doi.org/10.1099/vir.0.016261-0

Vanamala, P., Sindhura, P., Sultana, U., Vasavilatha, T., Gul, M.Z., 2022. Chapter 14 - Common bacterial pathogens in fish: An overview, in: Dar, G.H., Bhat, R.A., Qadri, H., Al-Ghamdy, K.M., Hakeem, K.R. (Eds.), Bacterial Fish Diseases. Academic Press, pp. 279–306. https://doi.org/10.1016/B978-0-323-85624-9.00010-5

Wafer, L.N., Whitney, J.C., Jensen, V.B., 2015. Fish Lice (Argulus japonicus) in Goldfish (Carassius auratus). Comp. Med. 65, 93–95.

Walker, L., Subramaniam, K., Viadanna, P.H.O., Vann, J.A., Marcquenski, S., Godard, D., Kieran, E., Jr, S.F., Popov, V.L., Kerr, K., Davison, A.J., Waltzek, T.B., 2022. Characterization of an alloherpesvirus from wild lake sturgeon Acipenser fulvescens in Wisconsin (USA). Dis. Aquat. Organ. 149, 83–96. https://doi.org/10.3354/dao03661

Waltzek, T.B., Kelley, G.O., Alfaro, M.E., Kurobe, T., Davison, A.J., Hedrick, R.P., 2009a. Phylogenetic relationships in the family Alloherpesviridae. Dis. Aquat. Organ. 84, 179–194. https://doi.org/10.3354/dao02023

Waltzek, T.B., Kelley, G.O., Stone, D.M., Way, K., Hanson, L., Fukuda, H., Hirono, I., Aoki, T., Davison, A.J., Hedrick, R.P., 2005. Koi herpesvirus represents a third cyprinid herpesvirus (CyHV-3) in the family Herpesviridae. J. Gen. Virol. 86, 1659–1667. https://doi.org/10.1099/vir.0.80982-0

Waltzek, T.B., Kurobe, T., Goodwin, A.E., Hedrick, R.P., 2009b. Development of a Polymerase Chain Reaction Assay to Detect Cyprinid Herpesvirus 2 in Goldfish. J. Aquat. Anim. Health 21, 60–67. https://doi.org/10.1577/H08-045.1

Wang, H., Xu, L., Lu, L., 2016. Detection of cyprinid herpesvirus 2 in peripheral blood cells of silver crucian carp, Carassius auratus gibelio (Bloch), suggests its potential in viral diagnosis. J. Fish Dis. 39, 155–162. https://doi.org/10.1111/jfd.12340

Wang, L., He, J., Liang, L., Zheng, X., Jia, P., Shi, X., Lan, X., Xie, J., Liu, H., Xu, P., 2012. Mass mortality caused by Cyprinid Herpesvirus 2 (CyHV-2) in Prussian carp (Carassius gibelio) in China. Bull. Eur. Assoc. Fish Pathol. 32, 164–173.

Wang, Q., Lin, F., He, Q., Liu, X., Xiao, S., Zheng, L., Yang, H., Zhao, H., 2019a. Assessment of the Effects of Bisphenol A on Dopamine Synthesis and Blood Vessels in the Goldfish Brain. Int. J. Mol. Sci. 20, 6206. https://doi.org/10.3390/ijms20246206

Wang, Q., Yang, H., Yang, M., Yu, Y., Yan, M., Zhou, L., Liu, X., Xiao, S., Yang, Y., Wang, Y., Zheng, L., Zhao, H., Li, Y., 2019b. Toxic effects of bisphenol A on goldfish gonad development and the possible pathway of BPA disturbance in female and male fish reproduction. Chemosphere 221, 235–245. https://doi.org/10.1016/j.chemosphere.2019.01.033

Wang S.-Y., Luo J., Murphy R.W., Wu S.-F., Zhu C.-L., Gao Y., Zhang Y.-P., 2013. Origin of Chinese Goldfish and Sequential Loss of Genetic Diversity Accompanies New Breeds. PLOS ONE 8, e59571. https://doi.org/10.1371/journal.pone.0059571

Wei, C., Iida, H., Chuah, Q., Tanaka, M., Kato, G., Sano, M., 2019. Persistence of cyprinid herpesviru s 2 in asymptomatic goldfish Carassius auratus (L.) that survived an experimental infection. J. Fish Dis. 42, 913–921. https://doi.org/10.1111/jfd.12996

Wei, C., Kakazu, T., Chuah, Q.Y., Tanaka, M., Kato, G., Sano, M., 2020. Reactivation of cyprinid her pesvirus 2 (CyHV-2) in asymptomatic surviving goldfish Carassius auratus (L.) under immun osuppression. Fish Shellfish Immunol. 103, 302–309. https://doi.org/10.1016/j.fsi.2020.05.02 0

Wei, C., Xu, C., Sun, Y., Li, J., Sano, M., Li, Q., 2023. Investigation of the latency of Cyprinid herpes virus 2 in apparently healthy farmed gibel carp, Carassius auratus gibelio. Aquaculture 562, 7 38854. https://doi.org/10.1016/j.aquaculture.2022.738854

Wei, Y.-J., Pan, X.-Y., Lin, L.-Y., Yao, J.-Y., Hao, G.-J., Cao, Z., Xia, Y.-C., Yin, W.-L., Liu, Y.-H., Shen, J.-Y., 2020. Establishment of spinal cord cell line of Carassius auratus gibelio and its se nsitivity to CyHV-2. Oceanol. Limnol. Sin. 51, 1232–1238. https://doi.org/10.11693/hyhz202 00300071

Wen, J., Xu, Y., Su, M., Lu, L., Wang, H., 2021. Susceptibility of Goldfish to Cyprinid Herpesvirus 2 (CyHV-2) SH01 Isolated from Cultured Crucian Carp. Viruses 13, 1761. https://doi.org/10.33 90/v13091761

Wilmann, P.G., Battad, J., Petersen, J., Wilce, M.C.J., Dove, S., Devenish, R.J., Prescott, M., Rossjoh n, J., 2006. The 2.1 Å Crystal Structure of copGFP, a Representative Member of the Copepo d Clade Within the Green Fluorescent Protein Superfamily. J. Mol. Biol. 359, 890–900. https:/ /doi.org/10.1016/j.jmb.2006.04.002

Wu, H., Liu, F., Du, H.-Y., He, Y.-G., Bao, C.-H., Wei, Z., Zhu, R., 2022. Establishment and suscepti bility to cyprinid herpesvirus 2 of Carassius carassius gill cell line. Aquac. Rep. 27, 101382. h ttps://doi.org/10.1016/j.aqrep.2022.101382

Wu, R., Shen, J., Lai, X., He, T., Li, Y., 2020a. Development of monoclonal antibodies against serum immunoglobulins from gibel carp (Carassius auratus gibelio) and their applications in serodia gnosis of inapparent infection and evaluation of vaccination strategies. Fish Shellfish Immuno l. 96, 69–77. https://doi.org/10.1016/j.fsi.2019.11.059

Wu, R., Xue, Y., Huang, J., Ozdemir, E., Li, Y., Ding, S., 2021. Development and evaluation of a con venient immunochromatographic strip test for rapid detection of cyprinid herpesvirus 2 (CyH V-2). Dis. Aquat. Organ. 143, 195–203. https://doi.org/10.3354/dao03561

Wu, R., Zhang, Q., Li, Y., 2020b. Development, characterization of monoclonal antibodies specific fo r the ORF25 membrane protein of Cyprinid herpesvirus 2 and their applications in immunodia gnosis and neutralization of virus infection. Aquaculture 519, 734904. https://doi.org/10.1016/ j.aquaculture.2019.734904

Wu, T., Ding, Z., Ren, M., An, L., Xiao, Z., Liu, P., Gu, W., Meng, Q., Wang, W., 2013. The histo- an d ultra-pathological studies on a fatal disease of Prussian carp (Carassius gibelio) in mainland China associated with cyprinid herpesvirus 2 (CyHV-2). Aquaculture 412–413, 8–13. https://d oi.org/10.1016/j.aquaculture.2013.07.004

Xia, S., Wang, H., Hong, X., Lu, J., Xu, D., Jiang, Y., Lu, L., 2018. Identification and characterization of a type I interferon induced by cyprinid herpesvirus 2 infection in crucian carp Carassius au ratus gibelio. Fish Shellfish Immunol. 76, 35–40. https://doi.org/10.1016/j.fsi.2018.02.043

Xiao, Z., Xue, M., Xu, C., Jiang, N., Luo, X., Li, Y., Fan, Y., Meng, Y., Liu, W., Zeng, L., Zhou, Y., 2 022. First report of cyprinid herpesvirus 2 isolated from the golden crucian carp in China. Aqu aculture 558, 738361. https://doi.org/10.1016/j.aquaculture.2022.738361

Xie, Y., Shui, D., Wu, P., 2019. Study on cyprinid herpesvirus II (cyHV-2) detection techniques based on the different PCR methods. Genomics Appl. Biol. 38, 1018–1025.

Xing, L., Venables, M.J., Trudeau, V.L., 2017. Role of aromatase and radial glial cells in neurotoxin-induced dopamine neuron degeneration and regeneration. Gen. Comp. Endocrinol., International Symposium on Reproductive Biology and Comparative Endocrinology 241, 69–79. https://doi.org/10.1016/j.ygcen.2016.02.011

Xu, J., Zeng, L., Zhang, H., Zhou, Y., Ma, J., Fan, Y., 2013. Cyprinid herpesvirus 2 infection emerged in cultured gibel carp, Carassius auratus gibelio in China. Vet. Microbiol. 166, 138–144. https://doi.org/10.1016/j.vetmic.2013.05.025

Xu, L., Podok, P., Xie, J., Lu, L., 2014. Comparative analysis of differential gene expression in kidney tissues of moribund and surviving crucian carp (Carassius auratus gibelio) in response to cyprinid herpesvirus 2 infection. Arch. Virol. 159, 1961–1974. https://doi.org/10.1007/s00705-014-2011-9

Xu, Y., Zhou, Y., Wang, F., Ding, C., Cao, J., Duan, H., 2019. Development of two brain cell lines from goldfish and silver crucian carp and viral susceptibility to Cyprinid herpesivirus-2. Vitro Cell. Dev. Biol. - Anim. 55, 749–755. https://doi.org/10.1007/s11626-019-00402-y

Yamaha, E., Mizuno, T., Matsushita, K., Hasebe, Y., 1999. Developmental Staging in Goldfish during the Pre-gastrula Stage. Nippon Suisan Gakkaishi 65, 709–717. https://doi.org/10.2331/suisan.65.709

Yan, W., Nie, P., Lu, Y., 2011. Establishment, characterization and viral susceptibility of a new cell line derived from goldfish, Carassius auratus (L.), tail fin. J. Fish Dis. 34, 757–768. https://doi.org/10.1111/j.1365-2761.2011.01292.x

Yan, Y., Huo, X., Ai, T., Su, J., 2020. β-glucan and anisodamine can enhance the immersion immune efficacy of inactivated cyprinid herpesvirus 2 vaccine in Carassius auratus gibelio. Fish Shellfish Immunol. 98, 285–295. https://doi.org/10.1016/j.fsi.2020.01.025

Yang, J., Wen, J., Xiao, S., Wei, C., Yu, F., Roengjit, P., Lu, L., Wang, H., 2022. Complete Genome and Molecular Characterization of a New Cyprinid Herpesvirus 2 (CyHV-2) SH-01 Strain Isolated from Cultured Crucian Carp. Viruses 14, 2068. https://doi.org/10.3390/v14092068

Yang, J., Xiao, S., Lu, L., Wang, H., Jiang, Y., 2024. Genomic and molecular characterization of a cyprinid herpesvirus 2 YC-01 strain isolated from gibel carp. Heliyon 10, e32811. https://doi.org/10.1016/j.heliyon.2024.e32811

Yang, Z.X., Li, G.L., Wang, Y., Yao, X.P., Wang, K.Y., Peng, S.Z., Wang, B., Ya, H.X., Ren, R.Y., 2014. Primary Establishment of LAMP Method for Cyprinid Herpesvirus 2 Detection. Appl. Mech. Mater. 602–605, 1823–1828. https://doi.org/10.4028/www.scientific.net/AMM.602-605.1823

Yanong, R.P.E., 2003. Fungal diseases of fish. Vet. Clin. Exot. Anim. Pract. 6, 377–400. https://doi.org/10.1016/S1094-9194(03)00005-7

Yuan, X., Shen, J., Pan, X., Yao, J., Lyu, S., Liu, L., Zhang, H., 2020. Screening for protective antigens of Cyprinid herpesvirus 2 and construction of DNA vaccines. J. Virol. Methods 280, 113877. https://doi.org/10.1016/j.jviromet.2020.113877

Zeng, X.-T., Chen, Z.-Y., Deng, Y.-S., Gui, J.-F., Zhang, Q.-Y., 2016. Complete genome sequence and architecture of crucian carp Carassius auratus herpesvirus (CaHV). Arch. Virol. 161, 3577–3581. https://doi.org/10.1007/s00705-016-3037-y

Zhang, H., Zeng, L., Fan, Y., Zhou, Y., Xu, J., Ma, J., 2014. A Loop-Mediated Isothermal Amplification Assay for Rapid Detection of Cyprinid Herpesvirus 2 in Gibel Carp (Carassius auratus gibelio). Sci. World J. 2014, e716413. https://doi.org/10.1155/2014/716413

Zhang, J., Cui, Z., Hu, G., Jiang, X., Wang, J., Qiao, G., Li, Q., 2020. Transcriptome analysis provides insights into the antiviral response in the spleen of gibel carp (Carassius auratus gibelio) after poly I: C treatment. Fish Shellfish Immunol. 102, 13–19. https://doi.org/10.1016/j.fsi.2020.03.065

Zhang, J., Sun, S., Mao, Y., Qiao, G., Li, Q., 2023. Identification and analysis of differentially expressed microRNAs in gibel carp Carassius auratus gibelio responding to polyinosinic-polycytidylic acid (poly I:C) stimulation. Fish Shellfish Immunol. Rep. 4, 100083. https://doi.org/10.1016/j.fsirep.2023.100083

Zhang, L., Ma, J., Fan, Y., Zhou, Y., Xu, J., Liu, W., Gu, Z., Zeng, L., 2016. Immune response and protection in gibel carp, Carassius gibelio, after vaccination with *β*-propiolactone inactivated cyprinid herpesvirus 2. Fish Shellfish Immunol. 49, 344–350. https://doi.org/10.1016/j.fsi.2016.01.003

Zhang, P., Lu, G., Liu, J., Yan, Z., Wang, Y., 2020. Toxicological responses of Carassius auratus induced by benzophenone-3 exposure and the association with alteration of gut microbiota. Sci. Total Environ. 747, 141255. https://doi.org/10.1016/j.scitotenv.2020.141255

Zhang, T., Gu, Y., Liu, X., Yuan, R., Zhou, Y., Dai, Y., Fang, P., Feng, Y., Cao, G., Chen, H., Xue, R., Hu, X., Gong, C., 2021. Incidence of Carassius auratus Gibelio Gill Hemorrhagic Disease Caused by CyHV-2 Infection Can Be Reduced by Vaccination with Polyhedra Incorporating Antigens. Vaccines 9, 397. https://doi.org/10.3390/vaccines9040397

Zhao, L., Gao, W., Zheng, Y., Lu, L., Li, Q., Jiang, Y., 2022. Development and characterization of monoclonal antibodies specific for cyprinid herpesvirus 2. J. Fish Dis. 45, 1673–1681. https://doi.org/10.1111/jfd.13689

Zhao, R., Geng, Y., Yu, Z., Wang, K., OuYang, P., Chen, D., Huang, X., He, C., Peng, G., Lai, W., 2019. New detection of Cyprinid herpesvirus 2 associated with mass mortality in colour crucian carp (Carassius auratus), in China. Aquac. Res. 50, 1705–1709. https://doi.org/10.1111/are.14054

Zhou, Y., Jiang, N., Ma, J., Fan, Y., Zhang, L., Xu, J., Zeng, L., 2015. Protective immunity in gibel carp, Carassius gibelio of the truncated proteins of cyprinid herpesvirus 2 expressed in Pichia pastoris. Fish Shellfish Immunol. 47, 1024–1031. https://doi.org/10.1016/j.fsi.2015.11.012

Zhu, M., Dai, Y., Tong, X., Zhang, Y., Zhou, Y., Cheng, J., Jiang, Y., Yang, R., Wang, X., Cao, G., Xue, R., Hu, X., Gong, C., 2022. Circ-Udg Derived from Cyprinid Herpesvirus 2 Promotes Viral Replication. Microbiol. Spectr. 10, e00943-22. https://doi.org/10.1128/spectrum.00943-22

Zhu, M., Li, K., Xuan, Y., Sun, Z., Liu, B., Kumar, D., Jiang, M., Pan, Y., Zhang, Y., Gong, Y., Lu, X., Yu, D., Hu, X., Cao, G., Xue, R., 2019. Host Range and Vertical Transmission of Cyprinid herpesvirus 2. Turk. J. Fish. Aquat. Sci. 19, 645–652.

Zhu, M., Liu, B., Cao, G., Hu, X., Wei, Y., Yi, J., Zhou, Y., Pan, G., Wang, J., Xue, R., Gong, C., 2015. Identification and rapid diagnosis of the pathogen responsible for haemorrhagic disease of the gill of Allogynogenetic crucian carp. J. Virol. Methods 219, 67–74. https://doi.org/10.1016/j.jviromet.2015.03.019

List of publications

1. **He, B**.; Sridhar, A.; Streiff, C.; Deketelaere, C.; Zhang, H.; Gao, Y.; Hu, Y.; Pirotte, S.; Delrez, N.; Davison, A.J.; et al. In Vivo Imaging Sheds Light on the Susceptibility and Permissivity of *Carassius auratus* to *Cyprinid herpesvirus 2* According to Developmental Stage. Viruses 2023, 15, 1746. https://doi.org/10.3390/v15081746

2. Streiff, C.; **He, B**.; Morvan, L.; Zhang, H.; Delrez, N.; Fourrier, M.; Manfroid, I.; Suárez, N.M.; Betoulle, S.; Davison, A.J.; et al. Susceptibility and Permissivity of Zebrafish (*Danio rerio*) Larvae to Cypriniviruses. Viruses 2023, 15, 768. https://doi.org/10.3390/v15030768

3. Yuan Gao, Arun Sridhar, Noah Bernard, **Bo He**, Haiyan Zhang, Sébastien Pirotte, Salomé Desmecht, Catherine Vancsok, Maxime Boutier, Nicolás M Suárez, Andrew J Davison, O wen Donohoe, Alain F C Vanderplasschen, Virus-induced interference as a means for acce lerating fitness-based selection of *Cyprinid herpesvirus 3* single-nucleotide variants *in vitr o* and *in vivo*, Virus Evolution, Volume 9, Issue 1, 2023, vead003, https://doi.org/10.1093/ve/vead003

4. **He, B**.; Sridhar, A.; Delrez, N.; Deketelaere, C.; Gao, Y.; Thiry, M.; Donohoe, O.; Vanderplasschen, A. *In vitro* and *In vivo* Characterization of New Isolated *Cyprinid herpesvirus 2* Strains from Netherlands. (Preparing for Submission)

5. Zhang, H., Sridhar, A., Delrez, N., **He, B.,** Fourny, S., Donohoe, O., Vanderplasschen, A. Development of an attenuated recombinant *in vivo* defective *Anguillid herpesvirus-1* vaccine using bioluminescence imaging. (Preparing for Submission)